PHARMACEUTICAL COCRYSTAL EUTECTIC ANALYSIS: STUDY OF THERMODYNAMIC STABILITY, SOLUBILITY, AND PHASE BEHAVIOR

by

David John Good

A dissertation submitted in partial fulfillment
of the requirements for the degree of
Doctor of Philosophy
(Pharmaceutical Sciences)
in The University of Michigan
2010

Doctoral Committee:

Associate Professor Naír Rodríguez-Hornedo, Chair
Professor Gordon L. Amidon
Professor Vincent L. Pecoraro
Research Professor Gregory E. Amidon

To my wife, Jessica, and my parents, Kathleen and David

ACKNOWLEDGEMENTS

I wish to thank the many individuals who have helped and supported me in the pursuit of my graduate studies and made these years such a rich and enjoyable experience. First and foremost, I would like to express my sincerest gratitude to Dr. Naír Rodríguez-Hornedo. The challenges and excitement of this research have been immensely rewarding because of your enthusiasm, encouragement, and excellence. It has been a great privilege to work in your laboratory and benefit from your instruction. I will forever cherish the experiences of being your student and the enormous influences you have had on my scientific interests and my personal development. Thank you to my dissertation committee members, Dr. Gordon Amidon, Dr. Gregory Amidon, and Dr. Vincent Pecoraro for your valuable insights, guidance, and suggestions.

This doctoral research was made possible by financial contributions from the American Foundation for Pharmaceutical Education Fellowship, and the Gordon and Pamela Amidon, Fred W. Lyons, Jr., Warner Lambert/Parke Davis and Upjohn Endowment Fellowships from The University of Michigan College of Pharmacy. Funding from the Purdue-Michigan Consortium on Supramolecular Assemblies and Solid State Properties and a research gift from Boehringer Ingelheim are also acknowledged. Thank you to all who gave financial support to this research and my education.

Special thanks to past and present members of the Rodríguez laboratory including Sarah Bethune, Adivaraha (Jay) Jayasankar, Neal Huang, Chinmay Maheshwari, Lilly Roy, Sreenivas Reddy, and Phil Zocharski as well as Crystal Miranda and Toshiro Fukami who spent time studying with the group. I greatly appreciate all of your assistance including many contributions and discussions that enabled aspects of this work. We have had some good fun amidst the hard work and I am lucky to be surrounded with such great people to share the experiences of graduate school.

I would like to acknowledge the extensive support of my family and friends for which I am truly grateful. Thank you to my parents, Kathleen and David, who have always supported my interests and education and given me all the encouragement and guidance I could ever hope for. Your perspective and advice give me strength, cheer, and helped me focus on the important things in life. Thank you to my sisters Rebecca and Rachel and my brother Dan for your thoughts and encouragement. To Dorothea, Bill, and Katherine Henry as well as Bert, Vickie, Andrew and Becky Steck and the Ivie family, thank you for making Michigan feel like home since we arrived.

Above all, I thank Jessica, my wife, for your patience, support, and for changing your career path so I could pursue my studies. I cannot possibly recount all the support you have provided since our first visit to Ann Arbor, and the ways you have sacrificed for me to achieve my goals. You are my constant joy and inspiration.

TABLE OF CONTENTS

LIST OF FIGURES

LIST OF TABLES

ABSTRACT

Pharmaceutical Cocrystal Eutectic Analysis: Study of Thermodynamic Stability, Solubility, and Phase Behavior

by

David John Good

Chair: Naír Rodríguez-Hornedo

Cocrystals are an emerging solid-state form to change physicochemical and biopharmaceutical drug properties. This dissertation focuses on the thermodynamic stability and solubility of pharmaceutical cocrystals. Specifically, the objectives are to: (i) develop methods to measure the thermodynamic solubility of metastable cocrystals, (ii) provide models that describe the equilibrium phase behavior of cocrystals based on component and cocrystal properties, (iii) explain the effect of temperature on cocrystal thermodynamic stability, (iv) estimate solubility and stability for different solvents based on component activity coefficients and measured cocrystal solubility in one solvent, and

(v) identify mechanisms by which hygroscopic additives affect the stability of mixtures of solid cocrystal components.

Cocrystal solubilities were calculated from eutectic concentration measurements where solution is in equilibrium with solid drug and cocrystal. Cocrystal solubility was directly proportional to coformer eutectic concentration and to the solubility of cocrystal components for carbamazepine, caffeine, and theophylline cocrystals. Cocrystal eutectic constants (K_{eu}), the ratio of solution activities of cocrystal components at the eutectic, are fundamental indicators of phase behavior and are a function of the cocrystal to drug solubility ratio (α) in pure solvent. More than forty eutectic constants are presented that demonstrate K_{eu} dependence on i) solvent, ii) complexation, and iii) ionization, as does the solubility of cocrystals. Applications of these findings to the discovery and phase stability of carbamazepine-sarcosine anhydride cocrystals are presented. A solution-mediated mechanism of cocrystal formation is shown for cocrystal components mixed with hygroscopic additives that sorbed moisture. More cocrystal formation occurred for additives that lowered the K_{eu}.

K_{eu} temperature dependence is explained by thermodynamic models based on cocrystal and component enthalpies of solution, which are solvent specific. The K_{eu} and α values of carbamazepine-nicotinamide in water decreased with temperature, but for several organic solvents K_{eu} was temperature independent (4-47˚C). Cocrystal solubility and stability was also shown to depend on the component activity coefficients, which

were estimated using the component solubilities. The models developed based on component and cocrystal properties combined with methods to estimate cocrystal solubilities from eutectic concentrations provide a useful guide for cocrystal design, synthesis, and selection.

CHAPTER 1

INTRODUCTION

Research in the design and utility of pharmaceutical cocrystals has received interest in recent years from a variety of disciplines including crystal engineering, chemistry, material sciences and the pharmaceutical sciences. Cocrystals are able to alter the physicochemical properties of active drug substances through combining drugs and additional components (i.e. coformers) in the same crystal structure thereby altering solid-state properties and solution behavior without modifying chemical structure. Coformers are substances that are solids at ambient conditions in their pure form and in the presence of drug can form crystalline solids that exhibit non-ionic intermolecular interactions and contain both components. Cocrystals are a single homogenous crystalline phase containing multiple distinct molecules; they are not physical blends of pure components. Cocrystal physical and chemical properties are a function of the unique solid-state crystalline arrangement and interaction of the multiple components. All properties that have a basis in crystal structure can be affected to some degree when a cocrystal is formed.[1-4]

For the systematic design, screening, synthesis, and selection of effective pharmaceutical cocrystals there is a need for fundamental descriptions of their physicochemical properties. This is especially true for the solution behavior and stability of cocrystals because of their potential to address poor aqueous solubility issues that persist for at least one-third of current and new drug substances.[5, 6] Alternatively, solubility control is sought for sustained and controlled release dosage forms, as well as to address chemical stability concerns and for taste masking of certain drugs.

The bioavailability of oral drug substances is a function of their solubility and dissolution in gastric/intestinal fluids as well as the drugs ability to permeate cellular membranes if efficacy requires distribution away from the gastric/intestinal fluids. Together solubility and permeability are the basis for the biopharmaceutical classification system (BCS) that segments drugs into four classifications based on these two properties.[7] Solubility improvements are particularly desirable for BCS class II compounds that have low solubility and high permeability. Class II drugs exhibit solubility limited oral adsorption and bioavailability. Numerous cocrystals and other multi-component crystals of class II drugs have been identified and several examples are listed in Table 1.1. Selecting a suitable coformer from many options requires effective material sparing methods for determining solubility and stability. Furthermore, indentifying correlations between cocrystal, coformer, and drug physicochemical properties is essential to the efficient design of new cocrystals.

Table 1.1: Examples of multi-component crystals containing BCS class II drugs.

Drug	Coformers (acids)	Reference
Piroxicam	L-tartaric, citric, fumaric, adipic acid succinic, L-malic, glutaric, DL-malic, oxalic, (+)-camphoric, ketoglutaric, benzoic, 4-hydroxybenzoic, malonic, salicylic, glycolic, 1-hydroxy-2-naphthoic, gentisic, DL-tartaric, maleic, caprylic, hippuric, L-pyroglutamic acid	8
Carbamazepine	succinic, benzoic, ketoglutaric, maleic, glutaric, malonic, oxalic, adipic, (+)-camphoric, 4-hydroxybenzoic, salicylic, 1-hydroxy-2-naphthoic, DL-tartaric, L-tartaric, glycolic, fumaric, DL-malic, L-malic, acetic, butyric, 5-nitroisophthalic, formic, 4-aminobenzoic, trifluoroacetic, 2,6-pyridinedicarboxylic, trimesic, adamantane-1,3,5,7-tetracarboxylic	9, 10
Itraconazole	succinic, fumaric, L-malic, L-tartaric, D-tartaric, DL-tartaric	11
Sulfamethazine	2-aminobenzoic, 4-aminobenzoic, 4-aminosalicylic, acetylsalicylic, benzoic, anthranilic, o-phthalic, p-chlorbenzoic, 2-hydroxybenzoic	12-14

Cocrystals are unique relative to current options for altering physicochemical drug properties in pharmaceutical development because of the number of suitable drugs and possible coformers as well as the large number of intramolecular associations and supramolecular structures that can lead to cocrystal formation. However, there are few commercial examples of cocrystal drug products and therefore a presumed risk associated with cocrystal drug products.[4] A more established practice to improve physicochemical drug properties is modification of the chemical structure. These structural changes also typically alter activity and toxicology and can adversely affect drug performance. Various solid-state forms of drugs including salts, polymorphs, and solvates or hydrates are familiar to pharmaceutical scientists and offer some valuable but limited options for

physicochemical property changes. Only drugs with ionizable groups are candidates for salt formation and successful salt formation is in part a function of the drug pKa value(s) and the properties of the limited group of pharmaceutically acceptable counterions. Using amorphous solids can significantly change the solubility of a drug by eliminating crystal lattice energy as a barrier to dissolution, however thermodynamic stability issues limit their applications. Crystallization of the stable thermodynamic form is a major risk for amorphous drugs and formulation additives or solid dispersions are used to improve amorphous form stability.[15-21] Cocrystals expand the options for drugs with challenging physicochemical properties by offering a large number of suitable coformers to change solution and solid-state chemistry. Furthermore cocrystals afford the preferred solid-state stability of a crystalline solid form for oral delivery. An overview of the classification and nomenclature of solid forms relevant to pharmaceutical development presented in Figure 1.1 includes multi-component crystalline forms and cocrystals.

This chapter introduces background related to the structure, design, synthesis, and properties of cocrystals. Established solution phase behavior of other multi-component crystalline solids such as racemates, salts, solvates and hydrates are included because of their relevance toward understanding cocrystal behavior. The model compounds considered throughout the work are too numerous to address and therefore the reader is referred to relevant descriptions included in introduction and materials sections of

subsequent chapters. This chapter concludes with a statement of the dissertation research that summarizes the scope and results of all subsequent chapters.

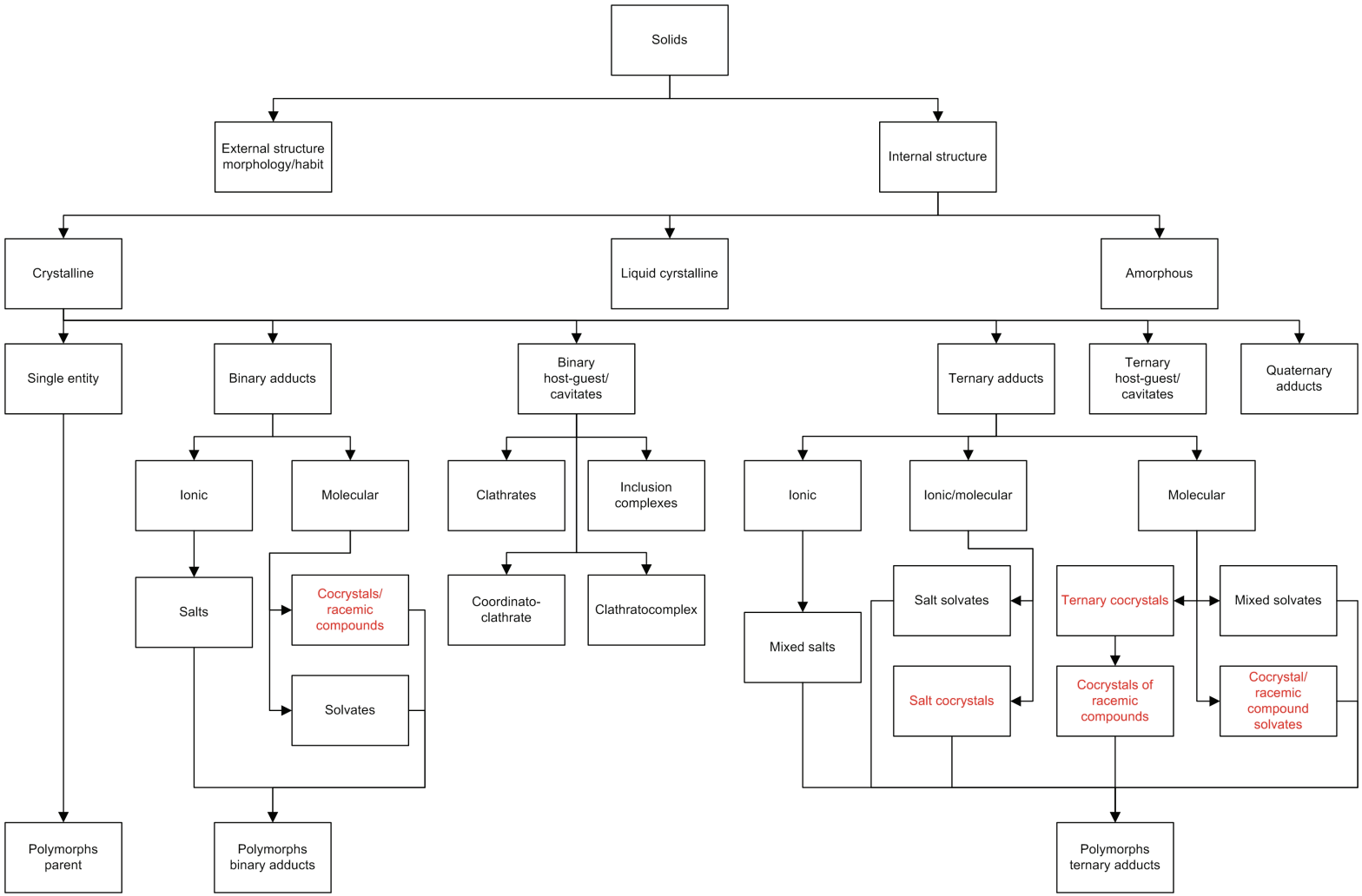

Figure 1.1: Classification/nomenclature of solids and crystalline phases with multiple components. Adapted in part from Weber *et al.*, Stahl *et al.*, and Qiu *et al.*, and Halebian.[22-25]

1.1. BACKGROUND

1.1.1. Cocrystal Design

The fields of crystal engineering and supramolecular chemistry have sought to discover and design novel intermolecular interactions, extended molecular architectures, and recognition phenomena relevant to crystal packing. The nature of noncovalent intermolecular interactions between cocrystal components can be used to control the three-dimensional ordered cocrystal structure. Supramolecular retrosynthetic analysis of intermolecular units for a target cocrystal structure can be readily preformed using the Cambridge Structural Database (CSD). This process can identify suitable coformer attributes based on preferred orientations and geometries of specific known instances of intermolecular interactions from this database. The use of favorable and frequently occurring substructural units and geometric considerations from the CSD enable identification of reasonable candidate components for cocrystallization. Many solid-state cocrystal design considerations focus on hydrogen bonding associations because of their strength and directionality. Often coformers are selected based on functional groups capable of complimentary hydrogen bonding with the drug substance.

Hydrogen bond synthons are intermolecular arrangements of functional groups resulting in one or more hydrogen bonds. Synthons formed between two identical functional moieties, such as synthons I and II in Figure 1.2, are called homosynthons. The other synthons II-X are between different functional moieties and are classified as

heterosynthons. Both homosnthons and heterosythons are important interactions in the design and structure of cocrystals. Further classification of intermolecular associations distinguishes whether the interacting molecules are the same (homomer) or different (heteromer).[26-31]

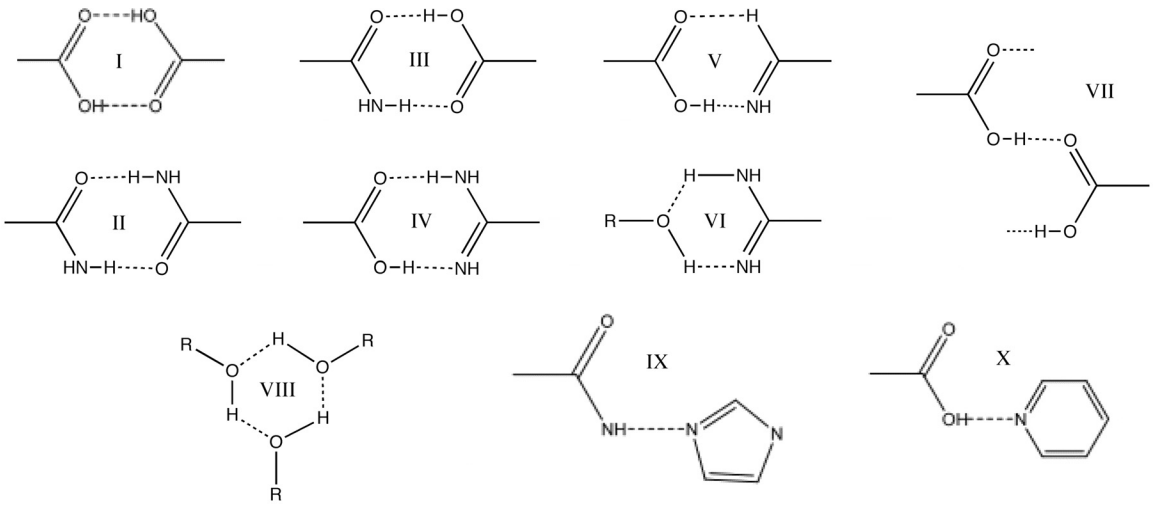

Figure 1.2: Schematic examples of synthon arrangements including homosynthon (I-II) and hetersynthons (III-X) interactions.

The types of hydrogen-bond synthons and molecular aggregates likely to form between cocrystals components can be predicted by several general rules developed by Donohue and Etter.[32-35] The first rule states that all available acidic hydrogen atoms will be incorporated in hydrogen bonds in the crystal structure. Additionally, all good hydrogen-bond acceptors form bonds if an adequate number of donors exist. A third rule suggests that the best donor (most acidic) will preferentially form a hydrogen bond with the best acceptor (most basic). [26-31] Hydrogen bonds with six member intramolecular rings have also been indicated to preferentially form with respect to intermolecular

hydrogen bonds. While these rules are good general considerations they do not predict crystal structure, molecules capable of cocrystallizing with each other, conditions that promote cocrystallization, or the properties of cocrystals that might form.[36] Exceptions to these guidelines often occur due to competition of multiple hydrogen bonding, dipole, or ionic sites as well as steric or conformational limitations.

For selecting complementary drug and coformer components, hydrogen bond guidelines are good considerations, however they do not alone indicate cocrystal formation or structure. Considerations of van der Waals interactions and stereochemistry of the components are also relevant for cocrystal design and coformer selection.[36] Symmetry elements and conformational energies of molecules play essential roles in determining crystal structures. The formation of stable crystal structures is additionally based on minimizing electrostatic energies (e.g. bond or molecular dipoles) and minimizing free volume (i.e. maximizing density). Kitaigorodskii's Principle of Close Packing is considered the primary rule for crystal packing and states that void space is always unfavorable.[36, 37] Recent analysis of coformers published in the CSD indicated that shape, polarity, and available synthons were key parameters for designing cocrystals, however the number of hydrogen bond donors and acceptor was not statistically significant.[38] Together all these structural considerations of the crystalline state influence the design and stability of cocrystals.

1.1.2. Cocrystal Synthesis

Reaction crystallization method (RCM) was recently established for the synthesis and screening of cocrystals and was carried out by slurrying cocrystal component(s) in a nonstoichiometric solution of the components. RCM has been used to create conditions favorable for cocrystal formation by maintaining one component at or near saturation in solution while slurrying the other component.[39] The RCM is based on nonstoichiometric solution conditions where cocrystal is typically the most stable solid phase (i.e. least soluble) that could exist in equilibrium with solution based on cocrystal solubility product behavior. This method does not require an exhaustive use of various solvents to find conditions suitable for cocrystal formation.[9, 40] The solubility product behavior of cocrystals described by Nehm and Rodríguez-Hornedo *et al.* provided the basis for their development of RCM wherein cocrystal had lowest solubility, was thermodynamically stable, in solutions containing excess of one of the cocrystal components.[41]

RCM has been carried out in many solvents, however green solvents are favored including water and alcohols. Also, because RCM is based on thermodynamically stable cocrystal conditions it is an attractive process for any reaction scale. *In situ* monitoring of cocrystal formation by RCM has recently been demonstrated for carbamazepine-nicotinamide cocrystals and can be used to effectively control and scale cocrystallization processes.[42, 43]

Other solution processes have been used wherein stoichiometric ratios of the components were dissolved in solvent that was subsequently evaporated or was heated to facilitate dissolution then cooled (solvo-thermal). These empirically based methods have an inherent risk of crystallizing one or more undesirable phases including pure components and often require the screening of many solvents and or experimental conditions. Difficulties could be encountered when attempting different size crystallization processes due to variability in evaporation or temperature changes.

Solid-state cocrystal synthesis methods have been used in which the crystalline or amorphous components are combined. Mechanical activation by grinding cocrystal components together is a common method to form cocrystals.[9, 33-35, 44-49] Cocrystal components have been shown to proceed through and intermediate amorphous phases in some cases.[50] The glass transition temperature (Tg) and melt temperature of components are important material properties for any mechanochemical methods that induce phase transformations and therefore should be considered along with process temperature in the synthetic outcome. The addition of solvent drops to grinding reactions often impacts the synthetic outcome and cocrystal formation can occur through solution and/or solid phases.

A recent screening of twenty-seven carbamazepine cocrystals by four different methods including RCM identified all of the forms generated by grinding of components were also found by at least one of the other solution methods.[9] While grinding

experiments are attractive because of small requisite quantities of components and rapid synthesis some limitations include the difficulty of readily discerning the formation mechanism or pathway, the chemical stability of components subjected to high kinetic energy process, purity of products (i.e. extent of transformation), empirical nature, and challenges regarding scalability.

Less common synthetic methods include melt processes such as the Kofler mixed fusion method and differential scanning calorimetry (DSC) of components in physical blends. Kofler's methods have been used to efficiently determine the formation and phase behavior of many multicomponent crystals and their polymorphs.[51-57] A recent example is the work of Berry *et al.* who screened for cocrystals of seven drugs with nicotinamide and determined the structures of three novel cocrystals including that of R/S-ibuprofen-nicotinamide.[58] DSC was also shown as an efficient thermal method for screening cocrystals of carbamazepine, theophylline, caffeine, and sulfamethazine. Sixteen of twenty cocrystals were resolved from thermal analysis of physical blends and confirmed by variable temperature X-ray diffraction.[59] In addition to these thermal methods cocrystal synthesis has also been demonstrated from supercritical fluids and vapor phase mediated crystallizations.[60, 61]

1.1.3. Cocrystal Properties

The structure and properties of cocrystals are distinct from that of their individual components. Cocrystals have been shown to change the hygroscopicity, melt temperature, chemical stability, morphology, solubility, dissolution rate, bioavailability, thermal stability, hydrate/solvate formation, mechanical properties, and many others. Any chemical or physical properties that are a function of the supramolecular structure are potentially modified by cocrystal formation. The design and formation of a cocrystal to change a particular physicochemical drug property will likely change additional properties since the structure and supramolecular chemistry are not exclusive to any one physicochemical property. If designing a cocrystal for improved drug solubility one should anticipate changes to many other properties, such as possibly the crystal density or habit, that are dependent on supramolecular structure.

Bioavailability and dissolution

Increased bioavailability or maximum plasma concentration (C_{max}) has been demonstrated for several drug substances. McNamera *et al.* showed the 1:1 glutaric acid cocrystal of 2-[4-(4-chloro-2-fluorophenoxy)phenyl]pyrimidine-4-carboxamide, a developmental sodium channel blocker, had greater C_{max} and AUC levels in beagle dogs given equivalent doses of cocrystal and drug at both 5 and 50mg/kg levels.[62] These *in vivo* studies were in agreement with aqueous rotating disk intrinsic dissolution results that indicated significant improvement for the cocrystal (~18-fold increase) over the pure

drug at 37˚C. Similarly, reports of an Amgen investigational drug (AMG 517) cocrystallized with sorbic acid (1:1) exhibited faster powder dissolution in fasted simulated intestinal fluids and improved bioavailability in rats.[63] A 10mg/kg dose of cocrystal was shown to produce similar C_{max} values and about half the AUC of a 500mg/kg dose of the free drug substance. Normalizing these results by the dose indicates the cocrystal had approximately a 50 and 25-fold increase in C_{max} and AUC, respectively. Additionally a cocrystal of Merck L-883555, a developmental phosphodiesterase-IV inhibitor, and L-tartaric acid (0.5:1) showed more than 10 and 20-fold increase of C_{max} and AUC, respectively, for 3mg/kg dose given orally in methocel to rhesus monkeys.[64]

Carbamazepine-saccharin (1:1) cocrystal has exhibited higher average cocrystal C_{max} and AUC values relative to the marketed form III of carbamazepine in beagle dogs. Despite these higher average observed pharmacokinetic parameters corresponding high error levels indicated no statistically significance differences between the cocrystal and drug forms.[65] Three different cocrystals of lamotrigine-nicotinamide were shown to have powder dissolution rates that were improved or equivalent to free lamotrigine at acidic and neutral pH conditions, respectively. However, the two nicotinamide cocrystal forms administered to rats demonstrated lower serum concentrations.[66] This discrepancy could be caused by several factors such as the influence of the coformer on oral absorption or the oral suspension vehicle (PEG400 and methyl cellulose) that could change the

thermodynamic stability or solubility of the cocrystal. Whatever the case, future animal experiments should carefully consider the thermodynamic solubility of cocrystals and the relevant solubility equilibrium associated with excipients and *in vivo* or biorelevant conditions.

Remenar *et al.* showed itraconazole cocrystals of various carboxylic acids had much improved aqueous powder dissolution rates. The itraconalzole-(L)malic acid cocrystal had a dissolution profile similar to that of the marketed amorphous form. The three cocrystals studied achieved sustained (>400 minutes) dissolution concentrations from 4 to 20-fold of the crystalline itraconazole level.[11] Remenar also showed for the celecoxib-nicotinamide cocrystal that formulation with surfactant (SDS) and polymer (PVP) provided similar dissolution rates as amorphous blends of drug and PVP. Here the cocrystal formulation produced an amorphous/crystalline blend with small particulates (~380nm) of a metastable drug polymorph (celecoxib IV).[67] This study demonstrated formulation methods to exploit the high cocrystal solubility relative to celecoxib to design rapidly dissolving drug products.

Hygroscopicity

The interaction of water with drugs and pharmaceutical dosage forms is critically important to the stability, efficacy, and safety of these materials. Pharmaceutical drug products may come into contact with water during production and formulation or at any point through exposure to humid environmental conditions. Drug

products that incorporate materials containing water have the potential to transfer it to other components, subject to water sensitive stability.[68] Water can interact with crystals through adsorption on the surface of particles, absorption or capillary condensation, hydrate formation, and deliquescence. The structure, form, composition, and material properties of a crystalline phase contribute to its hygroscopic nature. Studies of carbamazepine cocrystals each showed no hydrate formation and less than 0.2% weight change after either two or three weeks storage at 98% and 100% relative humidity for saccharin and nicotinamide coformers, respectively. However, anhydrous carbamazepine readily formed dihydrate at these humidity levels.[69] These studies confirmed that cocrystal formation could change hygroscopic drug properties. Numerous theophylline and caffeine cocrystals have also shown similar results wherein the cocrystals do not transform under conditions that pure drugs form hydrates.[70, 71]

Deliquescent and hygroscopic cocrystal components or excipients have been shown to facilitate solution-mediated formation of cocrystals. Deliquescent excipients including sucrose, fructose, and citric acid led to cocrystal formation for various components listed in Table 1.2.[72] The mechanism indicated consisted of deliquescence of the excipient, followed by dissolution of the cocrystal components in the sorbed moisture, then subsequent crystallization of cocrystal from solution. In this solution mediated mechanism supersaturation with respect to cocrystal was generated from dissolution of components in the sorbed moisture. Cocrystal nucleation was observed near the surface

of undissolved carbamazepine crystals presumably due to the high drug concentrations at this boundary producing the greatest supersaturation in the concentrated nicotinamide/sucrose solution. The formation of cocrystal depends on the deliquescent material and its potency for moisture uptake as well as its ability to modify the mode and rate of nucleation. Chapter 7 presents the stability and solubility of carbamazepine cocrystals in the presence of the hygroscopic additive polyvinylpyrrolidone (PVP).

Table 1.2: Drug and corresponding coformers that formed cocrystals by both slurrying and deliquescence.[72]

Drug	Carbamazepine	Caffeine	Theophylline	Sulfamethazine
Coformers	Nicotinamide	Oxalic acid	Oxalic acid	Salicylic acid
	Saccharin	Maleic acid	Maleic acid	Anthranilic acid
		Glutaric acid	Glutaric acid	
		Malonic acid	Malonic acid	

Mechanical properties

The mechanical properties of drug substances determine the formulation and processing methods required to make drug products. The crystalline structural properties influence these mechanical properties. Four new cocrystals of paracetamol and two known polymorphs demonstrated mechanical properties differences in relation to the crystallographic structural features.[73] Tablet formation and associated mechanical properties (tensile strength, breaking force, etc.) of each tablet form were studied and each of the four cocrystals improved over the two polymorphs. Three of the four

cocrystals exhibited arrangement of drug and coformer layers in the crystal structures and corresponding weak shear planes nearly parallel these molecular layers. It was suggested these shear planes contributed to the improved elasticity and tabletability. Similarly, slip planes in the 1:1 caffeine-methyl gallate cocrystal have also been correlated with improved tabletability.[74] The caffeine cocrystal produced higher tensile strength than pure caffeine and pure methyl gallate across all compaction pressures (~40-400 MPa). These studies demonstrated the feasibility of using cocrystals and molecular level design of synthons to create structural features that improve the mechanical properties of drug substances for pharmaceutical processing of oral solid dosage forms.

Chemical stability

Chemical stability changes have been demonstrated for solid-state reactions that involve cocrystals of carbamazepine or 1,4,5,8-naphthalenetetracarboxylic dianhydride (NTCDA). Carbamazepine cocrystals of saccharin and nicotinamide do not have azepine ring distances (<4.1 Å) and alignment that facilitate formation of the cyclobutyl dimer by photodegradation. In comparison the known polymorphs of carbamazepine do undergo photodegredation due to their azepine ring distances.[69] Cocrystals of NTCDA with 3-aminobenzoic acid or 2-methyl-4-nitroaniline have solid-state alignment of the anhydride carbonyl carbon atom and the coformer amino nitrogen atom sufficient to facilitate condensation reactions and formation of the diimide NTCDA derivative upon heating.[75] In this example the cocrystal formation altered the chemical stability of the components

by aligning reactive functional groups to produce specific high yield products through solid-sate topochemical synthesis.

Fusion properties

The fusion properties reported for cocrystals can vary significantly from that of their components due to the differences in the nature and extent of intra and intermolecular interactions associated with the new crystal structure. Thermal analysis of twenty-seven carbamazepine cocrystals showed melt temperatures (Tm) that are less than, between, and greater than those of the pure components.[9] Since the intermolecular interactions present in the pure components are no indicator of the cocrystal interactions it is reasonable that fusion temperature will not be described solely by the components. Indeed several studies have indicated correlations between coformer and cocrystal melt temperatures for a given drug substance. Regression values for large cocrystal sets (>10) with the same drug and various coformers have indicated approximately 80% of the cocrystal Tm is explained by the coformer Tm.[9, 76, 77] A set of five hexamethylenebisacetamide cocrystals with dicarboxylic acid coformers of sequential chain lengths showed nearly linear correlations between cocrystal and coformer Tm.[78] This high correlation could in part be due to the limited diversity and size of the data set. The design of low melting cocrystals could be desired for thermally labile drugs where melt processing is needed. Additionally low Tm is typically associated with greater

solubility, however the reported aqueous solubilities in these studies did not confirm such behavior.

1.2. SOLUBILITY AND SOLUTION CHEMISTRY OF MULTICOMPONENT CRYSTALS

1.2.1. Cocrystals

Higuchi, Connors, and coworkers examined the solution chemistry of cocrystals as early as the 1950's, however the majority of this work related to the solution complexation of components.[79-86] The methodology presented and the determination of stability constants (i.e. solution complexation constants) for a variety of pharmaceutical substances was valuable to advancing the understanding of solubilization phenomena and its utility for drug delivery and formulation. Recently published work has described detailed equilibrium solution behavior of cocrystals and demonstrated solubility product (K_{sp}) and solution complexation behavior for carbamazepine-nicotinamide in several organic solvents.[41] This work established the fundamental solution behavior of cocrystals wherein cocrystal solubility was dependent on the component concentrations. Higher solution coformer concentrations were shown to decrease cocrystal solubility and corresponding drug concentrations. Figure 1.3 represents the reported carbamazepine-nicotinamide (CBZ-NCT) cocrystal solubility as a function of nicotinamide concentration in several organic solvents.[41]

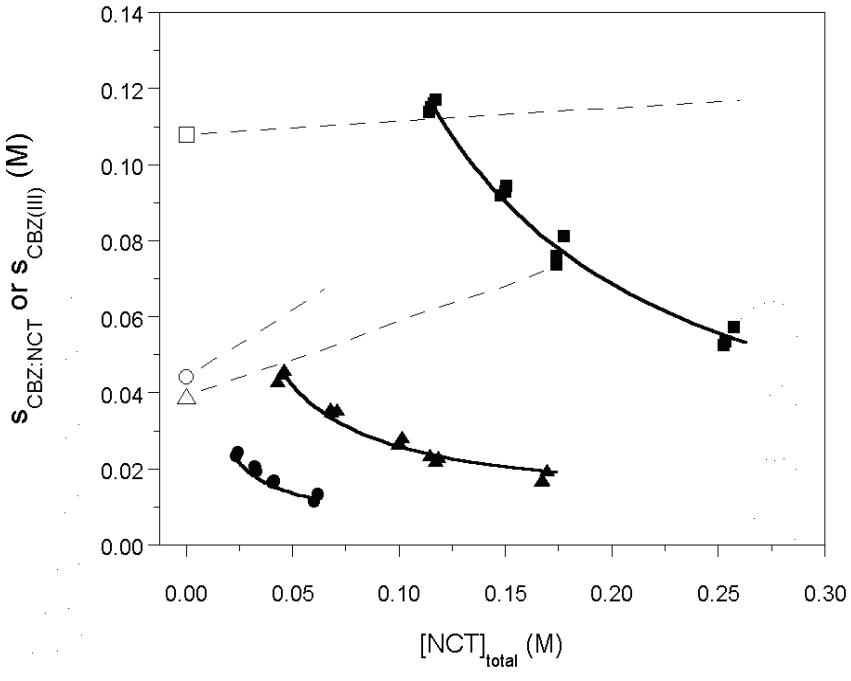

Figure 1.3: Solubility of 1:1 CBZ-NCT cocrystal (solid points) and CBZ(III) (open points) at 25˚C as a function of total NCT concentration in ethanol (squares), 2-propanol (tiangles), and ethyl acetate (circles). The solid lines represent the predicted solubility behavior from the solubility product and solution complexation.[41]

Cocrystal solubilities have been commonly expressed using a variety of equilibrium and kinetic measurements. Kinetic solubility measurements reported are typically powder dissolution or intrinsic rotating disk dissolution. Both equilibrium and kinetic experiments present valuable information on the solution properties and performance of cocrystals relative to the components. Several examples of cocrystal dissolution results are listed in section 1.1.3. Crystallization of other drug forms can occur in kinetic studies particularly when cocrystal is highly soluble relative to the components. Stanton *et al.* performed powder dissolution on 14 cocrystals of Amgen

investigational drugs (TRPV1 antagonsits) and observed conversion to the free base drug form in 12 of the 14 cases.[77] All cases indicated maximum dissolution concentrations above that of the free base. These supersaturated drug levels depend on cocrystal dissolution and free base crystallization and related parameters including particle size, powder wetability, supersaturation, nucleation and growth rates. Since many parameters influence the observed maximum concentration there is a need for equilibrium measurements that can be used to calculate the thermodynamic solubility of highly soluble cocrystals.

The measurement of an equilibrium or steady state drug concentration from a cocrystal placed in solution does not always reflect the actual stoichiometric solubility depending on the final solid phase(s) that persist at equilibrium point. Isolation and analysis of solid phase(s) is critical in describing solubility because the final solid form is associated with the measured concentration(s). Only when the initial cocrystal form is observed as the single solid phase after equilibration with pure solvent are the equilibrium concentrations descriptive of the true stoichiometric solubility. In this case the concentration ratio of the two components in solution should equal the stoichiometric cocrystal ratio. The true stoichiometric solubility of a cocrystal is often difficult to measure directly because of purity issues, unknown or complex solubility phase behavior, and potential transformations to other solid forms such as components or other cocrystal stoichiometries or solvates. When a solid phase other than the starting cocrystal is

observed, the corresponding steady state drug concentration is not the true cocrystal solubility. In these instances both component concentrations should be recorded to best describe solubility behavior of the solid phase(s) in equilibrium with the solution. If one of the stable equilibrium solid phases is a cocrystal of known stoichiometry, the K_{sp} can be calculated and reported to describe the thermodynamic cocrystal solubility.

Ionizable coformers have been used to design pH dependent cocrystal solubility. Solution models and solubilities of cocrystals with ionizable components have been determined. Examples of pH dependent cocrystal solubility were provided for neutral drug (carbamazepine) with acidic and amphoteric coformers (saccharin, salicylic acid, and 4-aminobenzoic acid).[87] Additionally, the solubility data and models for gabapentin (zwiterionic) and 3-hydroxybenzoic acid (diprotic acid) were reported.[88] Figure 1.4 contains the predicted pH dependent cocrystal aqueous solubility and the measured solubilities for pH conditions where cocrystal was the stable phase in equilibrium with solution. These models, and several other recent reports, have described how pH dependent solubility can be designed for neutral or ionizable drugs using cocrystals.[88, 89]

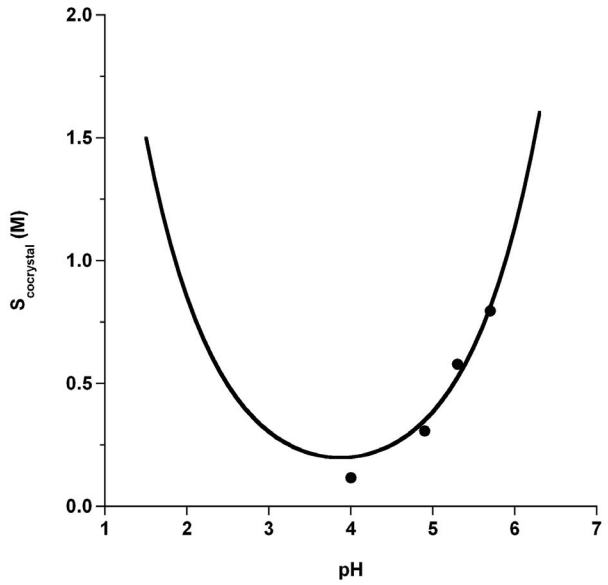

Figure 1.4: Gabapentin-(3-hydroxybenzoic acid) solubility dependence on pH. Symbols represent experimental data. Predicted solubility curve was based on measured K_{sp}.[88]

1.2.2. Pharmaceutical Salts

The principles of salt solubility and the relevant solution equilibria have been well established and widely used in the successful design of commercial drug products. Numerous texts and reviews have been written to establish the appropriate solubility considerations for developing and screening new salt forms.[24, 90, 91] The solubility of a salt is described by solubility product behavior and the salt solubility is lower when counterion concentration is increased. For this reason hydrochloride salts are often studied to determine the extent *in vivo* solubility will be affected by chloride ion concentrations. Because salts are ionizable they also display pH dependent solubility. The solubility of salts have been shown in some cases to depend on the counterion

hydrophobicity or the melting point of the salt, which is related to the strength and nature of the solid-state interactions.[92, 93]

The maximum solubility of a salt (pH_{max}) is the pH value where the free acid or base and its corresponding salt form are equally soluble. pH_{max} is dependent on the intrinsic solubility and pKa value(s) of the ionizable drug as well as the salt K_{sp}. The calculation of salt solubility profiles and K_{sp} values according to ideal behavior can be achieved by *in situ* screening in solutions of the target counterion acid or base (e.g. maleic acid, ammonia).[94]

Salt solubility behavior is relevant to the descriptions of cocrystal solubility, despite the absence of cocrystal proton transfer/ionic interactions, because solution phase equilibria apply to these two dissociable crystal forms. Furthermore cocrystals can form salts with one component having ionic interactions (e.g. fluoxetine-benzoic acid HCl) or the components can be ionizable in solution and salt conversion can occur and affect the solution behavior of the cocrystal.[95]

1.2.3. Racemic Compounds

The resolution, phase behavior, and solubility of racemates have been the subject of considerable work and therefore serve as good references for the solubility behavior of cocrystals. Racemic compounds are a specific subset of cocrystals wherein the two crystal components differ only in their stereochemistry. For achiral solvents both individual enantiomers have equal solubility and the thermodynamic stability of the

racemate is greater or equal to the enantiomers in pure solvent. Since racemic compounds are stable and do not transform to the individual enantiomers in pure achiral solvent they have a lower chemical potential. The thermodynamic equilibrium solubility of racemic compounds in pure achiral solvent is equal or lower than that of the pure enantiomers and therefore dissolution of racemic compound does not produce supersaturation with respect to the enantiomers (i.e. congruently saturating). In contrast cocrystals are often comprised of components with different solubilities/activities and can be thermodynamically unstable or stable in pure solvent. Cocrystals that are unstable (i.e. incongruently saturating) in pure solvent have a higher chemical potential and higher thermodynamic solubility relative to the more stable phase that is formed. The solubility and activity differences of cocrystal components account for their disparate solution behavior relative to racemic compounds. The solubility of cocrystals presented in Chapters 3 and 4 reveal several important differences relative to the solubility behavior of racemic compounds.

Despite being the thermodynamically stable phase in solution racemic compounds are commonly reported as more soluble than either pure enantiomer. Of course this is not possible and merely reflects the standard practice of adding the concentration of each enantiomer in a saturated racemate solution to indicate the racemic compound solubility. These reported solubilities are not the thermodynamic solubility of the racemic compound and are based on the definition of one *total* mole of the two enantiomers

forming one mole of the racemate. That is, one mole of a racemate represents a total of one mole of the two enantiomers. However, a 1:1 cocrystal AB is defined as comprising one mole of component A and one mole of component B (i.e. 2 total moles of components).

The Meyerhoffer double solubility rule that states the sum of the two equal enantiomer solubilities should reflect the solubility of a racemic conglomerate is based on the common description of racemate solubility as the additive enantiomer concentrations. Therefore conglomerates, blends of crystals of the two pure enantiomers, ideally exhibit twice the solubility of a single enantiomer.[96] Figure 1.5 shows an isothermal triangular phase diagram (TPD) corresponding to a conglomerate that exhibits ideal solubility for enantiomers are not salt forms. The solubility lines of each enantiomer run parallel to the sides of the phase diagram. A 50/50 blend of the ideal conglomerate racemate demonstrates double the solubility of either pure enantiomer. For dissociable enantiomers (e.g. salts of the two eantiomers) the solution equilibrium behavior for conglomerates can be extended to show the ideal solubility is that of the enantiomer salt times the square root of two. Reported values for free and salt forms (i.e. dissociable and nondissociable) of enantiomers that are conglomerates have shown close agreement to their predicted solubilities.[97]

The practical limit for the ideal solubility of racemic compounds, which are homogeneous solid phase addition compounds of the components, is the sum of the

solubility of each enantiomer in pure solvent. In other words the equilibrium solubility of a stable racemic compound can not exceed the conglomerate solubility.[97] Racemic compound solubility diagrams include an additional region in the center where racemic compound is the stable phase. The curved boundary of this phase region is defined by the solubility product (i.e. equilibrium constant for racemic compound dissociation) and indicates solution concentrations that are saturated with respect to the racemic compound. Racemic compound phase solubility diagrams are similar to those of two component cocrystals, however enantiomers have equal solubility and their triangular phase diagrams have vertical symmetry. This is often not the case for cocrystals where the components are unlikely to have identical solubilities.

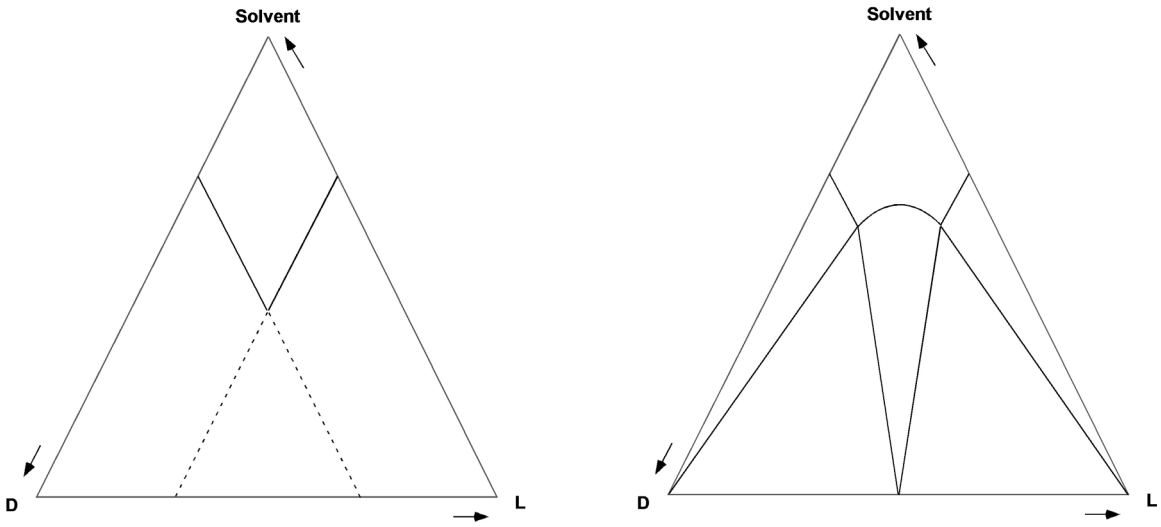

Figure 1.5: Schematic triangular phase diagram (TPD) of conglomerate (left) and racemic compound (right). D and L represent enantiomers and each apex represents a pure phase corresponding to the label.

1.3. STATEMENT OF DISSERTATION RESEARCH

The purpose of this dissertation is to investigate the physicochemical properties of pharmaceutical cocrystals and provide fundamental descriptions of their thermodynamic stability and solubility. Emphasis is placed on determining cocrystal properties in relation to their structure and components in order to improve the systematic methods for cocrystal design, synthesis, screening, selection, and formulation. Phase behavior and solution equilibria are considered to provide general and robust descriptions of the stoichiometric solubility of cocrystals that are either thermodynamically stable or unstable in pure solvent. Cocrystal solubility can be influenced by solid-state chemistry and solution chemistry including solute-solvent and solute-solute interactions as well as ionization. The chapters presented describe important aspects of both solution and solid-state chemistry of cocrystals.

Chapter 2 introduces the concept of eutectic points (i.e. isothermal invariant points) for calculating the stoichiometric solubility of cocrystals in pure solvent. This theoretical framework enables the same measurement to be used in determining the solubility of cocrystals that are thermodynamically stable or unstable in pure solvent. Methods are developed to measure cocrystal eutectic points from conditions that are undersaturated or saturated with respect to the cocrystal. Together these eutectic concentrations are used to calculate cocrystal solubilities, which are further analyzed in the context of the cocrystal component solubilities. It is shown that cocrystal solubility is

proportional to the solubility of the coformer for a set of carbamazepine cocrystals. Likewise the solubility of several nicotinamide cocrystals show a direct correlation to the drug component solubility. Thermal analysis and ideal solubility calculations show that crystal melt temperature is a fair indicator of cocrystal solubility in the organic solvents studied, but are poor indicators of aqueous solubility. This chapter presents the fundamental solubility and phase behavior of cocrystals as well as the eutectic measurements used throughout this research.

Chapter 3 presents a thermodynamic cocrystal eutectic constant (K_{eu}) which is the activity ratio of coformer to drug at the eutectic. K_{eu} is derived from a series of relevant cocrystal solution equilibrium expressions. K_{eu} is a function of cocrystal solubility behavior including ionization and complexation and was demonstrated for more than forty cocrystal and solvent combinations.

Chapter 4 describes the thermodynamic relationships for K_{eu} as a function of temperature. The stability and solubility of cocrystals relative to their components is shown to be temperature dependent. These thermodynamic expressions make it possible to predict thermal conditions where cocrystal or its components are the most stable phase in equilibrium with solution. The carbamazepine-nicotinamide cocrystal is considered in various organic solvents along with enthalpies of solution for the components.

Cocrystal activity coefficients that account for non-ideal solution behavior are derived from experimental and ideal solubility values in Chapter 5. Together ideal

solubility values and activity coefficients represent the solid-state and solution contributions to cocrystal solubility, respectively.

The synthesis and solubility of three new carbamazepine-sarcosine anhydride cocrystals are presented in Chapter 6. The phase behavior and solubility of these cocrystals are examined as well as the crystal structure of one of the 2:1 cocrystals.

In Chapter 7 hygroscopic and deliquescent excipients are shown to induce cocrystal phase transformations. The moisture sorbed by these excipients facilitates the solution-mediated transformation from crystalline components to cocrystal. Dissolution of components in the sorbed moisture creates supersaturation and subsequent crystallization of cocrystal based on known solubility product and phase behavior.

Finally, the conclusions and future work of this dissertation research are provided in Chapter 8. Future challenges include those associated with determining solubility for cocrystal and solvent combinations where cocrystal does not follow solubility product behavior, solution behavior is dominated by complexation, or is not readily stabilized.

Several of these chapters have been published. Cocrystal solubility and eutectic point relationships described in Chapters 2 and 3 are the subject of two publications in *Crystal Growth and Design* (1) 2009 vol. 9 pp. 2252-2264 and (2) 2010 vol. 10 pp. 1028-1032. Chapter 7 is part of a publication that presents the mechanisms by which moisture leads to cocrystal formation in *Molecular Pharmaceutics* 2007 vol. 4 pp. 360-372.

1.4. REFERENCES

(1) Childs, S. L.; Zaworotko, M. J., The Reemergence of Cocrystals: The Crystal Clear Writing Is on the Wall Introduction to Virtual Special Issue on Pharmaceutical Cocrystals. *Cryst Growth Des* **2009,** 9, (10), 4208-4211.

(2) Rodríguez-Hornedo, N.; Nehm, S. J.; Jayasankar, A., Cocrystals: Design, Properties and Formation Mechanisms. In *Encyclopedia of Pharmaceutical Technology*, Swarbrick, J., Ed. Taylor & Francis Group: London, 2006.

(3) Shan, N.; Zaworotko, M. J., The role of cocrystals in pharmaceutical science. *Drug Discovery Today* **2008,** 13, (9-10), 440-446.

(4) Stahly, G. P., A Survey of Cocrystals Reported Prior to 2000. *Cryst Growth Des* **2009,** 9, (10), 4212-4229.

(5) Lipinski, C., Poor aqueous solubility: an industry wide problem in drug discovery. *American Pharmaceutical Reviews* **2002,** 5, 82-85.

(6) Takagi, T.; Ramachandran, C.; Bermejo, M.; Yamashita, S.; Yu, L. X.; Amidon, G. L., A Provisional Biopharmaceutical Classification of the Top 200 Oral Drug Products in the United States, Great Britain, Spain, and Japan. *Mol Pharm* **2006,** 3, (6), 631-643.

(7) Amidon, G. L.; Lennernas, H.; Shah, V. P.; Crison, J. R., A theoretical basis for a biopharmaceutic drug classification: the correlation of in vitro drug product dissolution and in vivo bioavailability. *Pharm Res* **1995,** 12, (3), 413-20.

(8) Childs, S. L.; Hardcastle, K. I., Cocrystals of piroxicam with carboxylic acids. *Cryst Growth Des* **2007,** 7, 1291-1304.

(9) Childs, S. L.; Rodriguez-Hornedo, N.; Reddy, L. S.; Jayasankar, A.; Maheshwari, C.; McCausland, L.; Shipplett, R.; Stahly, B. C., Screening strategies based on solubility

and solution composition generate pharmaceutically acceptable cocrystals of carbamazepine. *Crystal Engineering Communications* **2008,** 10, 856-864.

(10) Fleischman, S. G.; Kuduva, S. S.; McMahon, J. A.; Moulton, B.; Walsh, R. D. B.; Rodriguez-Hornedo, N.; Zaworotko, M. J., Crystal Engineering of the Composition of Pharmaceutical Phases: Multiple-Component Crystalline Solids Involving Carbamazepine. *Cryst Growth Des* **2003,** 3, 909-919.

(11) Remenar, J. F.; Morissette, S. L.; Peterson, M. L.; Moulton, B.; MacPhee, J. M.; Guzman, H. R.; Almarsson, O., Crystal Engineering of Novel Cocrystals of a Triazole Drug with 1,4-Dicarboxylic Acids. *J Am Chem Soc* **2003,** 125, 8456-8457.

(12) Caira, M. R., Molecular complexes of sulfonamides. Part 1. 1:1 complexes between sulfadimidine [4-amino-N-(4,6-dimethyl-2-pyrimidinyl)benzenesulfonamide] and 2- and 4-aminobenzoic acids. *Journal of Crystallographic and Spectroscopic Research* **1991,** 21, 641-648.

(13) Caira, M. R., Molecular complexes of sulfonamides. 2. 1:1 complexes between drug molecules: sulfadimidine-acetylsalicylic acid and sulfadimidine-4-aminosalicylic acid. *Journal of Crystallographic and Spectroscopic Research* **1992,** 22, 193-200.

(14) Caira, M. R., Sulfa drugs as model cocrystal formers. *Molecular Pharmaceutics* **2007,** 4, (3), 310-6.

(15) Bhugra, C.; Shmeis, R.; Krill, S. L.; Pikal, M. J., Prediction of onset of crystallization from experimental relaxation times. II. Comparison between predicted and experimental onset times. *Journal of Pharmaceutical Sciences* **2008,** 97, (1), 455-472.

(16) Hancock, B. C.; Christensen, K.; Shamblin, S. L., Estimating the critical molecular mobility temperature (T(K)) of amorphous pharmaceuticals. *Pharmaceutical Research* **1998,** 15, (11), 1649-1651.

(17) Hancock, B. C.; Zografi, G., Characteristics and Significance of the Amorphous State in Pharmaceutical Systems. *Journal of Pharmaceutical Sciences* **1997,** 86, (1).

(18) Korhonen, O.; Bhugra, C.; Pikal, M. J., Correlation between molecular mobility and crystal growth of amorphous phenobarbital and Phenobarbital with polyvinylpyrrolidone and L-proline. *Journal of Pharmaceutical Sciences* **2008,** 97, (9), 3830-3841.

(19) Luthra, S. A.; Hodge, I. M.; Utz, M.; Pikal, M. J., Correlation of annealing with chemical stability in lyophilized pharmaceutical glasses. *Journal of Pharmaceutical Sciences* **2008,** 97, (12), 5240-5251.

(20) Shamblin, S. L.; Hancock, B. C.; Dupuis, Y.; Pikal, M. J., Interpretation of relaxation time constants for amorphous pharmaceutical systems. *Journal of Pharmaceutical Sciences* **2000,** 89, (3), 417-427.

(21) Shekunov, B. Y.; York, P., Crystallization processes in pharmaceutical technology and drug delivery design. *Journal of Crystal Growth* **2000,** 211, (1), 122-136.

(22) Haleblian, J. K., Characterization of habits and crystalline modification of solids and their pharmaceutical applications. *Journal of Pharmaceutical Sciences* **1975,** 64, (8), 1269-1288.

(23) Qiu, Y.; Liu, L.; Chen, Y.; Zhang, G. Z.; Porter, W., *Developing Solid Oral Dosage Forms: Pharmaceutical Theory and Practice*. First ed.; Academic Press: 2009; p 943.

(24) Stahl, P. H.; Wermuth, C. G., *Handbook of Pharmaceutical Salts*. Wiley, John & Sons: Hoboken, NJ, 2001.

(25) Weber, E.; Josel, H. P., A proposal for the classification and nomenclature of host-guest-type compounds. *Journal of Inclusion Phenomena and Macrocyclic Chemistry* **1983,** 1, (1), 79-85.

(26) Desiraju, G. R., Supramolecular Synthons in Crystal Engineering--A New Organic Synthesis. *Angewandte Chemie International Edition in English* **1995,** 34, 2311-2327.

(27) Desiraju, G. R., Designer crystals: intermolecular interactions, network structures and supramolecular synthons. *Chemical Communications* **1997**, 1475-1482.

(28) Desiraju, G. R., Crystal engineering: solid state supramolecular synthesis. *Current Opinion in Solid State & Materials Science* **1997,** 2, 451-454.

(29) Desiraju, G. R., Hydrogen Bridges in Crystal Engineering: Interactions without Borders. *Accounts of Chemical Research* **2002,** 35, 565-573.

(30) Nangia, A.; Desiraju, G. R., Supramolecular Synthons and Pattern Recognition. *Topics in Current Chemistry* **1998,** 198, 57-95.

(31) Thalladi, V. R.; Goud, B. S.; Hoy, V. J.; Allen, F. H.; Howard, J. A. K.; Desiraju, G. R., Supramolecular synthons in crystal engineering. Structure simplification, synthon robustness and supramolecular retrosynthesis. *Chemical Communications* **1996**, 401-402.

(32) Donohue, J., The Hydrogen Bond in Organic Crystals. *J Phys Chem-Us* **1952,** 56, (4), 502-510.

(33) Etter, M. C., Encoding and Decoding Hydrogen-Bond Patterns of Organic Compounds. *Accounts of Chemical Research* **1990,** 23, 120-126.

(34) Etter, M. C., Hydrogen Bonds as Design Elements in Organic Chemistry. *J Phys Chem-Us* **1991,** 95, 4601-4610.

(35) Etter, M. C.; Reutzel, S. M., Hydrogen Bond Directed Cocrystallization and Molecular Recognition Properties of Acyclic Imides. *J Am Chem Soc* **1991,** 113, 2586-2598.

(36) Brock, C. P.; Dunitz, J. D., Towards a Grammar of Crystal Packing. *Chem Mater* **1994,** 6, (8), 1118-1127.

(37) Kitaigorodskii, A. I., *Organic chemical crystallography*. ed.; Consultants Bureau: New York, 1961; p 541 p.

(38) Fábián, L., Cambridge Structural Database Analysis of Molecular Complementarity in Cocrystals. *Cryst Growth Des* **2009,** 9, (3), 1436-1443.

(39) Rodríguez-Hornedo, N.; Nehm, S. J.; Seefeldt, K. F.; Pagán-Torres, Y.; Falkiewicz, C. J., Reaction Crystallization of Pharmaceutical Molecular Complexes. *Molecular Pharmaceutics* **2006,** 3, 362-367.

(40) Weyna, D. R.; Shattock, T.; Vishweshwar, P.; Zaworotko, M. J., Synthesis and Structural Characterization of Cocrystals and Pharmaceutical Cocrystals: Mechanochemistry vs Slow Evaporation A from Solution. *Cryst Growth Des* **2009,** 9, (2), 1106-1123.

(41) Nehm, S.; Rodriguez-Spong, B.; Rodriguez-Hornedo, N., Phase Solubility Diagrams of Cocrystals Are Explained by Solubility Product and Solution Complexation. *Cryst Growth Des* **2006,** 6, 592-600.

(42) Gagniere, E.; Mangin, D.; Puel, F. o.; Bebon, C.; Klein, J.-P.; Monnier, O.; Garcia, E., Cocrystal Formation in Solution: In Situ Solute Concentration Monitoring of the Two Components and Kinetic Pathways. *Cryst Growth Des* **2009,** 9, (8), 3376-3383.

(43) Gagniere, E.; Mangin, D.; Puel, F.; Rivoire, A.; Monnier, O.; Garcia, E.; Klein, J. P., Formation of co-crystals: Kinetic and thermodynamic aspects. *Journal of Crystal Growth* **2009,** 311, (9), 2689-2695.

(44) Friscic, T.; Childs, S. L.; Rizvi, S. A. A.; Jones, W., The role of solvent in mechanochemical and sonochemical cocrystal formation: a solubility-based approach for predicting cocrystallisation outcome. *Crystal Engineering Communications* **2009**, (published online Dec. 2008).

(45) Friscic, T.; Jones, W., Recent Advances in Understanding the Mechanism of Cocrystal Formation via Grinding. *Cryst Growth Des* **2009,** 9, (3), 1621-1637.

(46) Karki, S.; Friscic, T.; Jones, W., Control and interconversion of cocrystal stoichiometry in grinding: stepwise mechanism for the formation of a hydrogen bonded cocrystal. *Crystal Engineering Communications* **2009**, (published online Nov 2008).

(47) Shan, N.; Toda, F.; Jones, W., Mechanochemistry and co-crystal formation: effect of solvent on reaction kinetics. *Chemical Communications* **2002**, 2372-2373.

(48) Trask, A., V.; Motherwell, W. D. S.; Jones, W., Solvent-drop grinding: green polymorph control of cocrystallisation. *Chemical Communications* **2004**, 890-891.

(49) Trask, A. V.; Jones, W., Crystal Engineering of Organic Cocrystals by the Solid-State Grinding Approach. *Topics in Current Chemistry* **2005,** 254, 41-70.

(50) Jayasankar, A.; Somwangthanaroj, A.; Shao, Z. J.; Rodriguez-Hornedo, N., Cocrystal formation during cogrinding and storage is mediated by amorphous phase. *Pharmaceutical Research* **2006,** 23, 2381-2392.

(51) Kofler, L., Mikroskopische Methoden in Der Mikrochemie. *Angew Chem-Ger Edit* **1950,** 62, (23-2), 579-579.

(52) Kofler, A., Quasi-eutectic syn-crystallisation on organic mixtures. (II Announcement). *Ber Dtsch Chem Ges* **1944,** 77, (2), 110-118.

(53) Kofler, A., Micro-thermal analysis of organic two-substance systems. *Naturwissenschaften* **1943,** 31, 553-557.

(54) Kofler, A., Thermal analysis in the temperable Microscope IV Report - Contact method in binary systems with unhomogeneous, melting compounds and miscibility gaps of the fluid phases. *Z Phys Chem a-Chem T* **1942,** 190, (5), 287-306.

(55) Kofler, A., Thermic analysis in heatable microscopes III Announcement Polimorphism and isomorphism phenomena in trinitro benzoyl, picric acid and alpha-trinitrotoluol. *Z Phys Chem a-Chem T* **1941,** 188, (4), 201-228.

(56) Kofler, A., Thermal analysis in heated microscopes II Announcement - Analysis of contact zones. *Z Phys Chem a-Chem T* **1940,** 187, (6), 363-373.

(57) Kofler, L.; Kofler, A., The meltingpoint of mixtures under the microscope. *Angew Chem-Ger Edit* **1940,** 53, 434-435.

(58) Berry, D. J.; Seaton, C. C.; Clegg, W.; Harrington, R. W.; Coles, S. J.; Horton, P. N.; Hursthouse, M. B.; Storey, R.; Jones, W.; Friscic, T.; Blagden, N., Applying hot-stage microscopy to co-crystal screening: A study of nicotinamide with seven active pharmaceutical ingredients. *Cryst Growth Des* **2008,** 8, (5), 1697-1712.

(59) Lu, E.; Rodríguez-Hornedo, N.; Suryanarayanan, R., A rapid thermal method for cocrystal screening. *Crystal Engineering Communications* **2008,** 10, 665-668.

(60) Braga, D.; Giaffreda, S. L.; Rubini, K.; Grepioni, F.; Chierotti, M. R.; Gobetto, R., Making crystals from crystals: three solvent-free routes to the hydrogen bonded co-crystal between 1,1 '-di-pyridyl-ferrocene and anthranilic acid. *Crystengcomm* **2007,** 9, (1), 39-45.

(61) Padrela, L.; Rodrigues, M. A.; Velaga, S. R.; Matos, H. A.; de Azevedo, E. G., Formation of indomethacin-saccharin cocrystals using supercritical fluid technology. *Eur J Pharm Sci* **2009,** 38, (1), 9-17.

(62) McNamara, D. P.; Childs, S. L.; Giordano, J.; Iarriccio, A.; Cassidy, J.; Shet, M. S.; Mannion, R.; O'Donnell, E.; Park, A., Use of a glutaric acid cocrystal to improve oral bioavailability of a low solubility API. *Pharmaceutical Research* **2006,** 23, 1888-1897.

(63) Bak, A.; Gore, A.; Yanez, E.; Staton, M.; Tufekcic, S.; Syed, R.; Akrami, A.; Rose, M.; Surapaneni, S.; Bostick, T.; King, A.; Neervannan, S.; Ostovic, D.; Koparkar, A., The co-crystal approach to improve the exposure of a water insoluble compound: AMG 517 sorbic acid cocrystal characterization and pharmacokinetics. *Journal of Pharmaceutical Sciences* **2008,** 97, 3942-3956.

(64) Variankaval, N.; Wenslow, R.; Murry, J.; Hartman, R.; Helmy, R.; Kwong, E.; Clas, S. D.; Dalton, C.; Santos, I., Preparation and solid-state characterization of nonstoichiometric cocrystals off a phosphodiesterase-IV inhibitor annul L-tartaric acid. *Cryst Growth Des* **2006,** 6, (3), 690-700.

(65) Hickey, M. B.; Peterson, M. L.; Scoppettuolo, L. A.; Morrisette, S. L.; Vetter, A.; Guzman, H.; Remenar, J. F.; Zhang, Z.; Tawa, M. D.; Haley, S.; Zaworotko, M. J.;

Almarsson, O., Performance comparison of a co-crystal of carbamazepine with marketed product. *Eur J Pharm Sci* **2006,** 67, 112-119.

(66) Cheney, M. L.; Shan, N.; Healey, E. R.; Hanna, M.; Wojtas, L.; Zaworotko, M. J.; Sava, V.; Song, S.; Sanchez-Ramos, J. R., Effects of Crystal Form on Solubility and Pharmacokinetics: A Crystal Engineering Case Study of Lamotrigine. *Cryst Growth Des* **2009,** 10, (1), 394-405.

(67) Remenar, J. F.; Peterson, M. L.; Stephens, P. W.; Zhang, Z.; Zimenkov, Y.; Hickey, M. B., Celecoxib:Nicotinamide Dissociation: Using excipients to capture the cocrystal's potential. *Molecular Pharmaceutics* **2007,** 4, 386-400.

(68) Zografi, G.; Grandolfi, G. P.; Kontny, M. J.; Mendenhall, D. W., Prediction of Moisture Transfer in Mixtures of Solids - Transfer Via the Vapor-Phase. *Int J Pharm* **1988,** 42, (1-3), 77-88.

(69) Rodríguez-Spong, B. Enhancing the Pharmaceutical Behavior of Poorly Soluble Drugs Through the Formation of Cocrystals and Mesophases, Ph.D. Thesis. University of Michigan, 2005.

(70) Trask, A.; Motherwell, W. D. S.; Jones, W., Physical Stability Enhancement of Theophylline Via Cocrystallization. *Int J Pharm* **2006,** 320, 114-123.

(71) Trask, A. V.; Motherwell, W. D. S.; Jones, W., Pharmaceutical Cocrystallization: Engineering a Remedy for Caffeine Hydration. *Cryst Growth Des* **2005,** 5, 1013-1021.

(72) Jayasankar, A.; Good, D. J.; Rodríguez-Hornedo, N., Mechanisms by which moisture generates cocrystals. *Molecular Pharmaceutics* **2007,** 4, 360-372.

(73) Karki, S.; Friscic, T.; Fabian, L.; Laity, P. R.; Day, G. M.; Jones, W., Improving Mechanical Properties of Crystalline Solids by Cocrystal Formation: New Compressible Forms of Paracetamol. *Adv Mater* **2009,** 21, (38-39), 3905-3909.

(74) Sun, C. C.; Hou, H., Improving mechanical properties of caffeine and methyl gallate crystals by cocrystallization. *Cryst Growth Des* **2008,** 8, (5), 1575-1579.

(75) Cheney, M. L.; McManus, G. J.; Perman, J. A.; Wang, Z. Q.; Zaworotko, M. J., The role of cocrystals in solid-state synthesis: Cocrystal-controlled solid-state synthesis of imides. *Cryst Growth Des* **2007,** 7, (4), 616-617.

(76) Good, D. J.; Rodríguez-Hornedo, N., Solubility Advantage of Pharmaceutical Cocrystals. *Cryst Growth Des* **2009,** 9, (5), 2252-2264.

(77) Stanton, M.; Bak, A., Physicochemical Properties of Pharmaceutical Co-crystals: A Case Study of Ten AMG 517 Co-Crystals. *Cryst Growth Des* **2008,** 8, 3856-3862.

(78) Aakeroy, C. B.; Forbes, S.; Desper, J., Using Cocrystals To Systematically Modulate Aqueous Solubility and Melting Behavior of an Anticancer Drug. *J Am Chem Soc* **2009,** 131, (47), 17048-17049.

(79) Higuchi, T.; Bolton, S., The Solubility and Complexing Properties of Oxytetracycline and Tetracycline III. *Journal of the American Pharmaceutical Association* **1959,** 48, 557-564.

(80) Higuchi, T.; Connors, K. A., Phase-Solubility Techniques. In *Advances in Analytical Chemistry and Instrumentation*, Nurnberg, H. W., Ed. Wiley-Interscience: New York, 1965; pp 117-212.

(81) Higuchi, T.; Dayal, S.; Pitman, I. H., Effects of Solute-Solvent Complexation Reactions on Dissolution Kinetics: Testing of a Model by Using a Concentation Jump Technique. *Journal of Pharmaceutical Sciences* **1972,** 61, 695-700.

(82) Higuchi, T.; Kristiansen, H., Binding Specificity between Small Organic Solutes in Aqueous Solution: Classification of Some Solutes into Two Groups According to Binding Tendencies. *Journal of Pharmaceutical Sciences* **1970,** 59, 1601-1680.

(83) Higuchi, T.; Pitman, I. H., Caffeine Complexes with Low Water Solubility: Synthesis and Dissolution Rates of 1:1 and 1:2 Caffeine-Gentisic Acid Complexes. *Journal of Pharmaceutical Sciences* **1973,** 62, 55-58.

(84) Higuchi, T.; Zuck, D. A., Solubilizing Action of Caffeine on Benzoic Acid. *Journal of the American Pharmaceutical Association* **1952,** 41, 10-13.

(85) Higuchi, T.; Zuck, D. A., Investigation of Some Complexes Formed in Solution by Caffeine. II. Benzoic Acid and Benzoate Ion. *Journal of the American Pharmaceutical Association* **1953,** 42, 132-138.

(86) Higuchi, T.; Zuck, D. A., Investigation of Some Complexes Formed in Solution. III. Interactions Between Caffeine and Aspirin, p-Hydroxybenzoic Acid, m-Hydroxybenzoic Acid, Salicylic Acid, Salicylate Ion, and Butyl Paraben. *Journal of the American Pharmaceutical Association* **1953,** 42, 138-145.

(87) Bethune, S. J.; Huang, N.; Jayasankar, A.; Rodríguez-Hornedo, N., Understanding and Predicting the Effect of Cocrystal Components and pH on Cocrystal Solubility. *Cryst Growth Des* **2009,** 9, (9), 3976-3988.

(88) Reddy, L. S.; Bethune, S. J.; Kampf, J. W.; Rodríguez-Hornedo, N., Cocrystals and Salts of Gabapentin: pH dependent cocrystal stability and solubility. *Cryst Growth Des* **2009,** 9, 378-385.

(89) Cooke, C. L.; Davey, R. J., On the solubility of saccharinate salts and cocrystals. *Cryst Growth Des* **2008,** 8, 3483-3485.

(90) Black, S.; Collier, E.; Davey, R. J.; Roberts, R. J., Structure, solubility, screening, and synthesis of molecular salts. *Journal of Pharmaceutical Sciences* **2007,** 96, 1053-1068.

(91) Serajuddin, A. T. M., Salt formation to improve drug solubility. *Advanced Drug Delivery Reviews* **2007,** 59, 603-616.

(92) Anderson, B. D.; Conrad, R. A., Predictive Relationships in the Water Solubility of Salts of a Nonsteroidal Anti-inflammatory Drug. *Journal of Pharmaceutical Sciences* **1985,** 74, 815-820.

(93) Yalkowsky, S. H.; Banerjee, S., *Aqueous solubility : methods of estimation for organic compounds*. ed.; Marcel Dekker: New York, 1992; p vi, 264 p.

(94) Tong, W.-Q. T.; Whitesell, G., In Situ Salt Screening-A Useful Technique for Discovery Support and Preformulation Studies. *Pharmaceutical Development and Technology* **1998,** 3, (2), 215-223.

(95) Childs, S. L.; Chyall, L. J.; Dunlap, J. T.; Smolenskaya, V. N.; Stahly, B. C.; Stahly, G. P., Crystal Engineering Approach to Forming Cocrystals of Amine Hydrochlorides with Organic Acids. Molecular Complexes of Fluoxetine Hydrochloride with Benzoic, Succinic, and Fumaric Acids. *J Am Chem Soc* **2004,** 126, 13335-13342.

(96) Meyerhoffer, W., Stereochemische Notizen. Die Pasteur'sche Splatung-methode mittels activer Verbindungen. *Ber. D. chem. Ges.* **1904**, (37), 2604-2610.

(97) Jacques, J.; Collet, A.; Wilen, S. H., *Enantiomers, racemates, and resolutions*. ed.; Wiley: New York, 1981; p xv, 447.

CHAPTER 2

THE STOICHIOMETRIC SOLUBILITY OF COCRYSTALS FROM SOLUTION EUTECTIC CONCENTRATIONS OF COCRYSTAL COMPONENTS

An important goal of solid-state pharmaceutical development is to increase drug solubility while maintaining a stable form. This objective is critical because solubility and permeability are the major factors used to describe oral absorption according to the biopharmaceutics classification system (BCS). Oral absorption of BCS class II drugs is solubility limited. This class of drugs is currently estimated to account for about thirty percent of both commercial and developmental drugs.[1, 2] Class I and III BCS drugs have high solubility and oral absorption primarily limited by dissolution rate and permeability, respectively. Increased solubility can significantly improve the oral absorption of class II drugs and would have lesser impact for the already soluble class I and III drugs.[3] Cocrystals have emerged as a promising means to modify solubility, dissolution, and other physicochemical properties of drug substances.[4-8] Pharmaceutical cocrystals provide an alternative to chemical modification of the drug substance as well as established salt, amorphous, solvate, and polymorphic drug forms that all have limitations in their utility. Cocrystals can be made for non-ionizable drugs, which are restricted from

salt formation. Also, for ionizable drugs the number of suitable cocrystal coformers can exceed the number of suitable counterions. One example is the ionizable drug piroxicam that has over fifty reported cocrystal coformers.[9] With unique properties for each drug form, there is great potential to form highly soluble and stable pharmaceutical cocrystals.

The purpose of this work is to establish how cocrystal solubility and stability are related to the properties of the pure components. To determine these relationships, methods are developed to calculate the true equilibrium solubility of cocrystals, which are often not the most stable solid phase in solution. Indeed some of the most relevant pharmaceutical cocrystals are more soluble than the pure drug form and therefore prone to transformation when exposed to solvent. This paper addresses the need for a readily measurable equilibrium between cocrystal and solution that can be used to calculate the often inaccessible equilibrium cocrystal solubility in pure solvent. The majority of studies relating to cocrystal solubility have focused on kinetic measurements of dissolution. Kinetic dissolution results are influenced by phase transformations, surface area, and particle size distribution of the drug as well as fluid dynamics and experimental apparatus.[10-13] These factors can be difficult to quantify and reproduce. Kinetic and equilibrium solubility measurements provide alternative and complementary characterization of drugs useful for addressing oral absorption limitations highlighted in the BCS. This paper focuses on methods for equilibrium measurements of cocrystal solubility that are experimentally accessible and reproducible.

Earlier reports from our laboratory have shown that cocrystal solubility is dependent on the concentration of coformer in solution. The dissociation of cocrystal in solution is described by the solubility product (K_{sp}) which is defined as a product of drug and coformer solution concentrations.[14] This is analogous to the K_{sp} of salt forms defined by the product of ionized drug and counterion concentrations.[13, 15] K_{sp} is a constant that reflects the strength of cocrystal solid-state interactions of drug and coformer relative to interactions with the solvent. The cocrystal solubility product behavior indicates that high coformer concentrations are associated with low solution drug levels. In a similar manner salt forms of drugs exhibit a common-ion effect where solubility decreases as the counterion concentration increases.[13, 16-18] Cocrystal solubility is also a function of the solubility product such that high K_{sp} values equate to high cocrystal solubility. Exceptions to this solubility product behavior can occur when cocrystal does not dissociate to its components in solution, there is high solution complexation, or the drug is highly solubilized by coformer.[14, 19, 20]

The cocrystal eutectic point is a key parameter that establishes the regions of thermodynamic stability of cocrystal relative to its components.[14, 21-24] This is an isothermal invariant point where two solid phases coexist in equilibrium with solution. The pharmaceutically relevant eutectic point in this work involves the equilibrium of drug and cocrystal solid phases because drug is often the least water soluble component (e.g. class II BCS drugs). It was previously shown that coformer in excess of the molar

ratio in the cocrystal is needed to reduce the cocrystal solubility to equal that of the drug.[14] Also it was predicted that cocrystals with high K_{sp} values require high coformer concentrations to achieve equivalent drug and cocrystal solubilities.[14] These concepts are developed in the current chapter to provide methods for calculating cocrystal solubility in pure solvent and understanding relationships between eutectic concentrations, cocrystal and component solubilities.

Carbamazepine (CBZ) cocrystals serve as the model system for this research. Carbamazepine is a widely used anti-epileptic drug that has low aqueous solubility and requires high blood levels for therapeutic efficacy. The low bioavailability of carbamazepine is due to low solubility and auto-induced metabolism.[5, 25] Carbamazepine has four known polymorphs and a dihydrate form.[26, 27] Over forty cocrystals of carbamazepine have been identified to date.[23, 28] One recent publication synthesized more than twenty-five carbamazepine cocrystals by screening carboxylic acid coformers.[23] Cocrystals of carbamazepine typically form through hydrogen bonding of the primary amide group with a coformer. One example of this bonding is shown in figure 1.1 for carbamazepine-succinic acid cocrystal. Pharmacokinetic studies of carbamazepine cocrystallized with saccharin have shown blood level increases due to dissolution improvement over the marketed pure drug (form III - monoclinic).[5] The carbamazepine cocrystals in this study have several coformers in common with reported cocrystals of theophylline and caffeine. Both these drugs are used to compare

physicochemical properties of carbamazepine cocrystals. Carbamazepine is a class II BCS drug while theophylline and caffeine are both class III.[2]

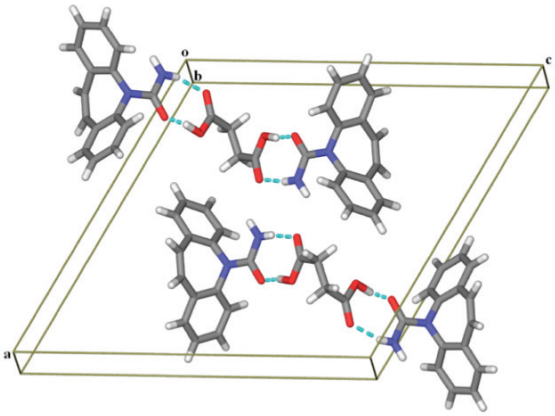

Figure 2.1: Diagram of carbamazepine-succinic acid cocrystal structure with hydrogen bonds indicated by dashed lines. Each carboxylic acid of the succinic acid forms two hydrogen bonds with the carbamazepine amide.[28]

This chapter has three principal objectives. Objective (1) is to enable the measurement of equilibrium cocrystal solubility from a single measurement of solution in equilibrium with solid drug and cocrystal. This includes cocrystals that are either stable or metastable when exposed to pure solvent. Objective (2) is to determine how the physicochemical properties of the reactants are related to cocrystal solubility and stability. Included in this is understanding how diverse cocrystal solubility can be relative to alternative drug forms (e.g. salt or amorphous). Objective (3) is to determine if crystal lattice properties such as melting temperature and enthalpy are sufficient indicators of cocrystal solubility.

2.1. THEORETICAL

2.1.1. Cocrystal solubility (S_{CC}) and solubility product (K_{sp})

For cocrystal $A_\alpha B_\beta$ where A is drug and B is coformer, solubility is described by the chemical equilibrium of solid cocrystal with solution and the corresponding equilibrium constant given by:

$$A_\alpha B_{\beta(s)} \overset{K}{\rightleftharpoons} \alpha A_{(soln)} + \beta B_{(soln)}$$

$$K = \frac{a^{\alpha}_{A(soln)} a^{\beta}_{B(soln)}}{a_{A_\alpha B_\beta (s)}} \qquad 2.1$$

Defining solid cocrystal activity as unity ($a_{A_\alpha B_\alpha (s)} = 1$) and assuming the activity coefficients (γ) of A and B equal unity for low solute levels Equation 2.1 reduces to:

$$K_{sp} = [A]^{\alpha}[B]^{\beta} \qquad 2.2$$

where K_{sp} is the solubility product of the cocrystal. Considering the equilibrium reaction above, the mass balance for $[A] = \alpha S_{A_\alpha B_\beta}$ and $[B] = \beta S_{A_\alpha B_\beta}$ can be substituted into Equation 2.2 to provide the cocrystal solubility:

$$S_{A_\alpha B_\beta} = \sqrt[\alpha+\beta]{K_{sp} \Big/ \alpha^{\alpha}\beta^{\beta}} \qquad 2.3$$

Cocrystal solubility always refers to intrinsic solubility in pure solvent, unless otherwise noted, as defined by Equation 2.3. This derivation of intrinsic cocrystal solubility is based on chemical equilibria for all solvents in which the drug and coformer substances are non-ionizing. Extensive considerations of ionization have been recently published

and indicate cocrystal K_{sp} is based on the concentrations of non-ionized drug and coformer; however, the expression of cocrystal solubility includes appropriate pH and pK_a factors for ionizing substances.[29-33] One case is the cocrystal of a neutral drug (*e.g.* carbamazepine) and an acidic coformer for which solubility is given by:

$$S_{A_\alpha B_\beta} = \sqrt[\alpha+\beta]{\frac{K_{sp}}{(\alpha^\alpha \beta^\beta)}\left(1+\frac{K_a}{[H^+]}\right)} \qquad 2.4$$

where pH and coformer pK_a are reflected in the hydrogen ion concentration and the acid dissociation constant.

2.1.2. Cocrystal solubility (S_{CC}) and the phase solubility diagram (PSD)

Phase solubility diagrams (PSDs) and triangular phase diagrams are used to represent the solubility and stability of cocrystals. The PSD in Figure 2.2 represents two different cocrystals, which are either stable (case 1: low solubility and K_{sp}) or metastable (case 2: high solubility and K_{sp}) with respect to the pure drug form in a given solvent. These curves represent cocrystal solubility product behavior with the drug concentration as a function of coformer given by $[drug]^\alpha = K_{sp}[coformer]^\beta$ from Equation 2.2. The drug solubility (horizontal line) is assumed to be much lower than the coformer solubility, which is not shown. A dashed line represents stoichiometric solution concentrations or stoichiometric dissolution of cocrystal in pure solvent and its intersection with the cocrystal solubility curves (marked by circles) indicates the

maximum drug concentration associated with the cocrystal solubilities. Unless otherwise specified the term cocrystal solubility refers to stoichiometric solubility in pure solvent at conditions where the components are non-ionized. For a metastable cocrystal (case 2) the drug concentration associated with the cocrystal solubility is greater than the solubility of the stable drug form (horizontal line). The solubility of a metastable cocrystal is not typically a measurable equilibrium and these cocrystals are referred to as incongruently saturating. As a metastable cocrystal dissolves the drug released into solution can crystallize due to supersaturation. This supersaturation is a necessary, but not sufficient condition for crystallization. In certain instances slow nucleation or other kinetic factors might delay crystallization of the favored thermodynamic form and enable measurement of the true equilibrium solubility. In the other case, a congruently saturating cocrystal (case 1) has a lower drug concentration than the pure drug form at their respective solubility values. Therefore, the solubility of congruently saturating cocrystals can be readily measured from solid cocrystal dissolved and equilibrated with solution.

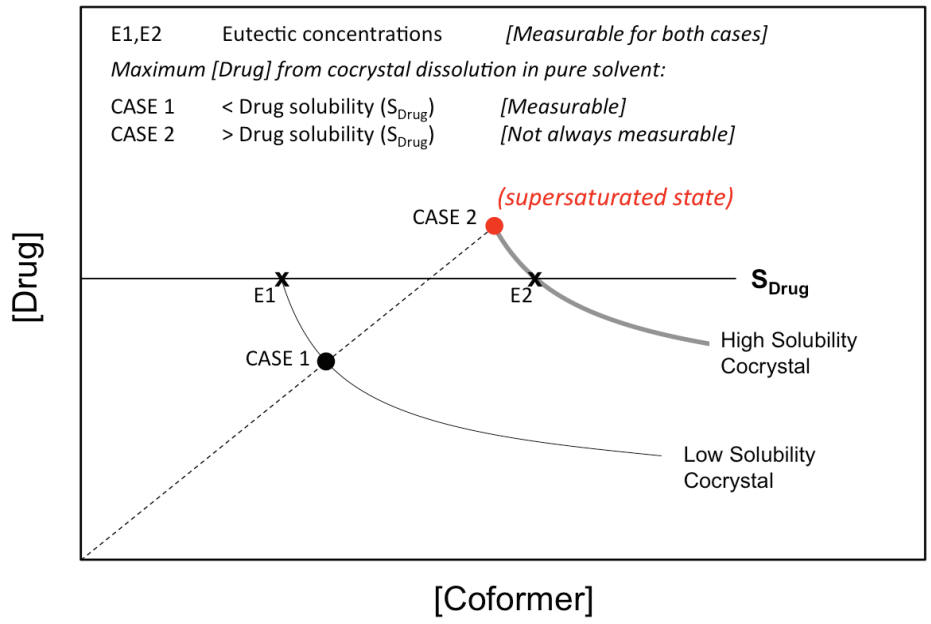

Figure 2.2: Schematic phase solubility diagram of two different cocrystals based on the K_{sp} of a stable (case 1) or metastable (case 2) cocrystal. Drug solubility is indicated and is much lower than the solubility of the coformer, which is not shown. X marks represent the eutectic points (*i.e.* invariant point) used to calculate equilibrium solubility. Circles represent the solubility of cocrystal in pure solvent. Dashed line illustrates stoichiometric concentrations of cocrystal components which dissolution could follow. This line represents a drug to coformer ratio equal to the cocrystal stoichiometric ratio of the components.

For both congruently and incongruently saturating cocrystals an isobarothermal invariant point (*i.e.* eutectic point), indicated by X marks in Figure 2.2, is the point where both solid drug and cocrystal are in equilibrium with a solution containing drug and coformer. Together the drug and coformer solution concentrations at the invariant point are referred to as the eutectic concentrations.[14, 19, 23, 34-37] Eutectic concentrations in this paper define the solution concentrations ($[drug]_{eu}$ and $[coformer]_{eu}$) that separate regions where either the solid cocrystal or drug are thermodynamically stable. Other invariant points and eutectic concentrations exist to describe the equilibria between solid cocrystal

and coformer, cocrystals of different stoichiometry, or cocrystal solvates. Systems where the coformer is less soluble than drug could utilize the eutectic associated with solid cocrystal and coformer to readily calculate cocrystal solubility.[38] For CBZ and the high solubility coformers in this study the equilibrium of solid cocrystal and drug is most relevant for calculating solubility of the cocrystal form in pure solvent.

Gibbs' condensed phase rule defines a system with three components (solvent, drug, and coformer) and three phases (drug, cocrystal, and solution) as having only one degree of freedom. At constant temperature the phase rule indicates zero degrees of freedom (invariant point) where the solution composition is fixed (eutectic concentration). At the eutectic concentration the free energy of solid cocrystal and drug are equal (*i.e.* $\Delta G = 0$). Below or above the eutectic point either the drug or the cocrystal is less soluble, the free energy difference is nonzero, and only one solid phase is stable. A solid phase of cocrystal is stable beyond the eutectic while pure drug is stable below this concentration.

Any cocrystal eutectic concentration wherein $[\text{drug}]_{eu}$ equals or exceeds $[\text{coformer}]_{eu}$ by a factor equivalent to the cocrystal's stoichiometric coefficient ratio (α/β) is known to be congruently saturating provided the coformer is more soluble, while all others are incongruently saturating. If we assume Figure 2.2 represents a 1:1 cocrystal, where drug is the least soluble component in pure solvent, the eutectic concentration for the low solubility cocrystal is above the dashed line representing stoichiometric

concentrations. Therefore, $[drug]_{eu}>[coformer]_{eu}$ and the cocrystal is congruently saturating.

The eutectic concentration is a readily measurable equilibrium state that can be used to determine cocrystal solubility. Furthermore, for incongruently saturating cocrystals the eutectic is the nearest accessible solid-solution equilibrium to the solubility and a good surrogate measurement from which to calculate cocrystal solubility. Only kinetic measurements can provide alternative quantitative solubilities to those based on the solubility product. While these kinetic measurements are useful for a variety of pharmaceutical analyses there is a need for direct information regarding the magnitude of thermodynamic cocrystal solubility. For cocrystal-solvent systems where solubility, dissolution behavior, or phase stability are unknown, determining the eutectic concentrations provides the cocrystal solubility and solution stability. Additionally, eutectic concentrations can be measured with small amounts of drug since only slight excess of the solubility is needed to generate the requisite solid phases in amounts detectable by a variety of analytical methods.

The solubility product expresses all possible solution concentrations of drug and coformer in equilibrium with solid cocrystal and is directly related to cocrystal solubility by Equation 2.3. Inserting the cocrystal eutectic concentrations ($[A]_{eu}$ and $[B]_{eu}$) into Equation 2.2 allows Equation 2.3 to be rewritten as:

$$S_{A_\alpha B_\beta} = \sqrt[\alpha+\beta]{[A]_{eu}^{\alpha}[B]_{eu}^{\beta} \Big/ \alpha^{\alpha}\beta^{\beta}} \qquad 2.5$$

Equation 2.5 can be used to calculate cocrystal solubility from measurement of the eutectic concentration. Drug and coformer eutectic concentrations describe both the solubility and thermodynamic stability of the cocrystal in a given solvent, thus the eutectic concentrations are a logical first measurement for evaluating and comparing cocrystals. For the case where drug solubility (S_A) is unchanged with coformer concentration in a particular solvent system, as shown in Figure 2.2, Equation 2.5 can further simplify by the substitution of $[A]_{eu}$ with S_A to give:

$$S_{A_\alpha B_\beta} = \sqrt[\alpha+\beta]{S_A^\alpha [B]_{eu}^\beta / \alpha^\alpha \beta^\beta} \qquad 2.6$$

The estimation of cocrystal solubility based on the coformer eutectic concentration ($[B]_{eu}$) and drug solubility is possible from Equation 2.6. Equation 2.5 uses the full measure of eutectic concentrations (both $[A]_{eu}$ and $[B]_{eu}$) to calculate cocrystal solubility; however, the constant drug solubility assumption of Equation 2.6 is valid for many solute-solvent systems and can simplify the requisite experimental methodology.

2.1.3. Cocrystal solubility and chemical potential at the eutectic concentration

Cocrystal solubility is a function of chemical potential (μ). The chemical potential expression for the equilibrium of cocrystal with solution is:

$$A_\alpha B_{\beta(s)} \rightleftharpoons \alpha A_{(soln)} + \beta B_{(soln)}$$
$$\mu_{A_\alpha B_\beta}^{solid} = \alpha(\mu_A^{soln}) + \beta(\mu_B^{soln})$$

At the eutectic concentration the solution is saturated with drug (A). The chemical potential of solid drug and drug in solution are equal because they are at equilibrium.

$$\mu_A^{soln} = \mu_A^{solid}$$

When considering only one drug substance μ_A^{solid} remains constant and substituting $\mu_A^{solid} = C = \mu_A^{soln}$ gives:

$$\mu_{A_\alpha B_\beta}^{solid} = \beta(\mu_B^{soln}) + C \qquad 2.7$$

Therefore, the cocrystal chemical potential is proportional to that of the coformer solute. From Equation 2.7 it can be stated that cocrystal solubility is proportional to coformer solubility.

2.1.4. Thermal analysis and predictions of cocrystal solubility (S_{CC}).

Melting temperatures and enthalpies of pharmaceutical crystals have found prevalent utility as indicators of ideal solubility. These are readily measurable properties associated with the crystal lattice energy that must be overcome for dissolution to occur. Among structurally similar pharmaceutical crystalline drug substances, those with high melt temperatures are generally recognized to possess lower solubility.[39, 40] Equation 2.8 is a fundamental and common thermodynamic model for the relation between solubility and melt properties.[40] For an ideal solution the solute solubility, *x* (mole fraction), is a function of the heat of fusion, melt temperature, and solution temperature.

$$\ln x_{solute}^{ideal} = \frac{-\Delta H_m}{R}\frac{(T_m - T)}{(T_m T)} \qquad 2.8$$

where $\Delta H_m \cong \Delta H_s^{ideal}$

The two main assumptions in the derivation of this ideal solubility expression are that enthalpy of fusion is temperature independent (*i.e.* heat capacity is zero) and is approximately equal to the ideal enthalpy of solution. More involved expressions have been derived to address these assumptions by including additional thermodynamic parameters such as solute heat capacity. The Equation 2.8 approximation of ideal solubility, often regarded as an upper solubility limit, provides a good comparison for experimental cocrystal solubilities.[39]

2.2. MATERIALS AND METHODS

2.2.1. Materials

Anhydrous monoclinic form III carbamazepine (CBZ(III)) as well as anhydrous theophylline (THP) and caffeine (CAF) were obtained from Sigma-Aldrich (99+% purity) and were used as received. Carbamazepine dihydrate (CBZ(D)) was prepared by stirring CBZ(III) in water for at least twenty-four hours. Hydrates of theophylline and caffeine were prepared in the same manner. The cocrystal coformers nicotinamide (NCT), malonic acid (MLN), glutaric acid (GTA), saccharin (SAC), anhydrous oxalic acid (OXA), succinic acid (SUC), and salicylic acid (SLC) were obtained from Sigma-Aldrich (99+% purity) and used as received. All crystalline drugs and coformers were

characterized by X-ray powder diffraction (XRPD) and Raman spectroscopy before carrying out experiments. No impurities in the form of additional peaks were resolved during HPLC analysis of solutions containing the drugs or coformers in this study. Ethanol (EtOH), isopropyl alcohol (IPA), and ethyl acetate (EtOAc) were obtained from Fisher Scientific and dried using molecular sieves prior to use. All the cocrystals used for solubility studies were precipitated from coformer solutions by adding solid drug according to the reaction crystallization method (RCM).[21, 23] Cocrystals of CBZ-NCT and CBZ-SAC throughout the paper refer to the form I polymorphs.[41] CBZ-MLN is the form B polymorph which is a hydrated crystal form.[23]

2.2.2. Determination of eutectic concentrations ($[A]_{eu}$ and $[B]_{eu}$)

The measurements of cocrystal eutectic concentrations were preformed by precipitating cocrystal as a result of stirring excess solid drug in a coformer solution wherein cocrystal synthesis occurs through RCM.[21, 23] Eutectic concentrations were also obtained by dissolution of cocrystal in saturated drug solutions containing excess solid drug. Each cocrystal eutectic concentration was determined from both supersaturated cocrystal conditions by RCM and from undersaturation by cocrystal dissolution. Samples were confirmed to have two solid phases (drug and cocrystal) at equilibrium for at least twenty-four hours before the solution was isolated from the solids and analyzed by HPLC. A flowchart of the processes used to determine cocrystal

eutectic concentrations is given in Figure 2.3(a). An aliquot of the solid phase was isolated from solution for x-ray analysis then solid reactant(s) were added as required to reach mixed solid phase equilibrium. This process was repeated in twenty-four hour iterations until a stable mixed solid phase was achieved. Samples were held between 23-25^{o}C for all eutectic concentration measurements.

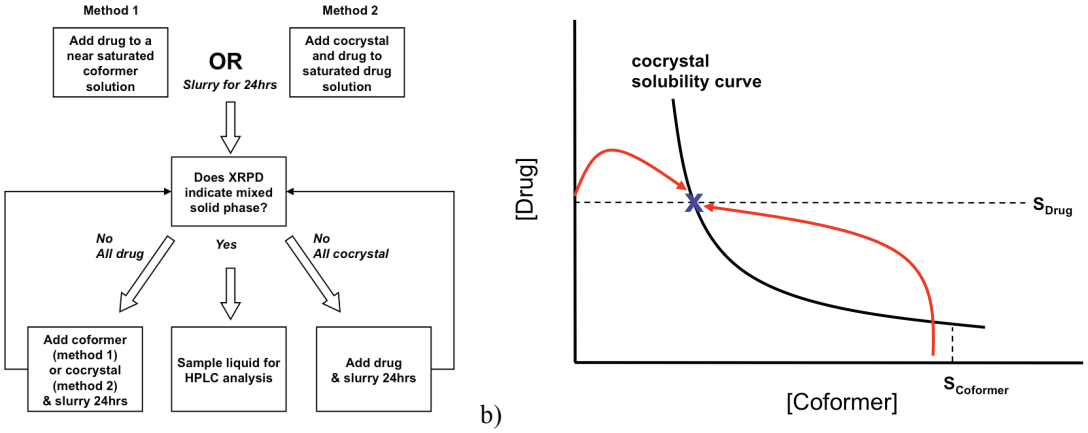

Figure 2.3: a) Flowchart of method used to establish the invariant point and determine equilibrium solution eutectic concentrations of cocrystal components. b) Schematic PSD illustrating two pathways to reach the eutectic marked with an X. The solubility curve is generated from drug and coformer concentrations that equal the cocrystal solubility product.

Figure 2.3(b) is a PSD illustrating theoretical pathways for the two methods used to establish cocrystal eutectic concentrations. The method utilizing RCM starts to the right of the eutectic (graphically) with a near saturated coformer solution to which excess drug is added. As the drug dissolves in coformer solution the cocrystal becomes supersaturated (i.e. solution reactant concentrations increase above the cocrystal solubility curve) and crystallizes from solution. Precipitation of cocrystal continues until

coformer becomes the limiting reagent and the excess solid drug remains in equilibrium with the cocrystal formed. In the cocrystal dissolution method a pre-saturated drug solution, which lies to the left of the eutectic (graphically), is combined with solid cocrystal and drug. When starting with saturated drug solution the driving force to reach equilibrium is cocrystal dissolution and the concurrent increase of coformer solute. As cocrystal dissolves the drug released into solution is likely to crystallize in the pre-saturated drug solution. Cocrystal dissolution may not lead to drug crystallization in instances where the coformer solubilizes the drug. In these instances, when drug solubilization by coformer occurs, the excess solid drug initially added with the cocrystal maintains drug saturation. Together these methods confirm the eutectic is reached by converging to the same equilibrium from two different initial states. Eutectic concentrations can be expressed as the range established from the two methods. Steps for both methods to reach the eutectic are:

Cocrystal Precipitation Method:

Step 1 - Prepare ligand solution

$$B_{(s)} \xrightarrow{solvent} B_{(soln)}$$ (slightly undersaturated)

Step 2 - Add excess drug

$$A_{(s)xs} \overset{B_{(soln)}}{\rightleftharpoons} A_{(soln)} + A_{\alpha}B_{\beta(s)}$$

Cocrystal Dissolution Method:

Step 1 - Presaturate solution with drug

$$A_{(s)xs} \overset{solvent}{\rightleftharpoons} A_{(soln)}$$ (saturated)

Step 2 - Add excess cocrystal

$$A_{\alpha}B_{\beta(s)xs} \overset{A_{(soln)}}{\rightleftharpoons} B_{(soln)} + A_{(s)}$$

2.2.3. High performance liquid chromatography (HPLC)

Solution concentrations of drug and coformer were analyzed by Waters HPLC (Milford, MA) equipped with a UV/Vis spectrometer detector. A C18 Atlantis column (5µm, 4.6 x 250mm; Waters, Milford, MA) at ambient temperature was used to separate the drug and the coformer. A gradient method with a water, methanol, and trifluoroacetic acid mobile phase was used with a flow rate of 1mL/min. Sample injection volume was 20µL. Absorbance of the drug and coformer analytes was monitored between 210-300nm. Empower software from Waters was used to collect and process the data. All concentrations are reported in molality (moles solute/kilogram solvent).

2.2.4. X-ray powder diffraction (XRPD)

XRPD was used to identify crystalline phases after slurrying samples to determine cocrystal eutectic concentrations and confirm the proper two solid phases (drug and cocrystal) were in equilibrium with the solution. XRPD patterns of solid phases were recorded with a Rigaku MiniFlex X-ray diffractometer (Danvers, MA) using Cu Kα radiation (λ = 1.5418 Å), a tube voltage of 30 kV, and a tube current of 15 mA. The intensities were measured at 2θ values from 2° to 30° with a continuous scan rate of 2.5°/min. Samples, prior to and after slurry reactions, were analyzed by XRPD. Results were compared to diffraction patterns reported in literature or calculated from crystal structures published in the Cambridge Structural Database. THP-NCT is the only cocrystal in this study whose XRPD pattern has not been published to our knowledge. This diffraction pattern is provided in Appendix 2.6.

2.2.5. Thermal Analysis

Crystalline samples of 3-6 mg were analyzed by differential scanning calorimetry (DSC) using a TA instrument (Newark, DE) 2910 MDSC system equipped with a refrigerated cooling unit. DSC experiments were performed by heating the samples at a rate of 10^{o}K per minute under a dry nitrogen atmosphere. Temperature and enthalpy calibration of the instruments was achieved using a high purity indium standard.

Hermetic aluminum sample pans were used for all measurements. The mean result of three or more samples are reported for each substance.

Cocrystal samples for DSC analysis were comprised of several large crystals grown by slow partial evaporation of solutions containing the reactants. These crystals were isolated from solution, washed, and characterized by Raman microscopy before being combined to yield an adequate mass for DSC analysis.

2.3. RESULTS AND DISCUSSION

2.3.1. Cocrystal solubility from eutectic concentrations

Table 2.1 lists the eutectic concentrations ($[drug]_{eu}$ and $[coformer]_{eu}$) for a series of cocrystals measured at the invariant point where two solid phases (drug and cocrystal) are in equilibrium with aqueous or organic solution. All cocrystal eutectics were confirmed by XRPD analysis of the solid phase, isolated from equilibrium with solution, as exemplified in Figure 2.4 for CBZ-SUC. In Figure 2.4, each of the isolated solid phases contains the equilibrium mixture of CBZ-SUC cocrystal and CBZ(form III in organic solvents or dihydrate in water) indicating these solids are both stable in solution.

Cocrystal K_{sp} and intrinsic solubility values, that represent non-ionized drug and coformer in solution, were calculated from eutectic concentrations according to Equations 2.2 and 2.5, respectively. For aqueous samples the pH was first used to calculate the non-ionized concentration of drug and coformer at the eutectic. Cocrystal solubilities were multiplied by the stoichiometric coefficient to provide the associated drug concentration and normalized with the relevant stable crystalline drug solubility to provide solubility ratios ($[drug]_{Scc}/S_{drug}$). For 1:1 cocrystals this ratio is the same as the cocrystal solubility divided by the drug solubility.

Solubility ratios emphasize the magnitude of change in solubility achieved by various cocrystals and facilitate comparisons between different solvents. The CBZ cocrystals studied have a range of aqueous solubility ratios from 2 to 152. In organic

solvents, where coformer solubilities are closer to the solubility of CBZ, cocrystal solubility ratios have a lower range between 0.1 and 4.4. The aqueous intrinsic solubility of CBZ-SAC is $1.2x10^{-3}$m and the solubility of CBZ form III is $1.6\ x10^{-3}$m. Because saccharin is acidic (pKa=1.6 at 25°C) the CBZ-SAC aqueous solubility from Equation 2.4 increases greatly in the small intestine (*e.g.* more than 150 times at pH=6), but CBZ form III does not. This CBZ-SAC aqueous solubility is consistent with previous *in vivo* animal studies by Hickey et al. that show the cocrystal has higher CBZ blood levels relative to the marketed CBZ form III that persist several hours after dosing, although high variability was observed for the pharmacokinetic parameters.[5, 42] Dissolution studies by Nehm et al. also have shown higher dissolution rate for CBZ-SAC relative to CBZ form III in pH=7 solutions.[30] Table 2.1 lists coformer solubilities and the drug solubilities used to calculate solubility ratios in various solvents.

Table 2.1: Cocrystal eutectic concentrations ($[drug]_{eu}$ and $[coformer]_{eu}$), component solubilities, and calculated cocrystal K_{sp} values, solubilities and solubility ratios. Table is sorted by solvent and descending $[coformer]_{eu}$. At eutectic cocrystal and hydrated or anhydrous drug exist in equilibrium with solution.

	A: B			*C*	*D*		*E*	*F*	*G*	*H*	*I*	*J*
Cocrystal (drug-coformer)	**Cocrystal Stoichiometry** (drug:coformer)	**Solvent**	**pH**	**$[coformer]_{eu}$ (m)** Mean ± Range/2	**$[drug]_{eu}$ (m)** Mean ± Range/2	**$S_{coformer}$ (m)**	**S_{drug} (m)**[a]	**coformer ionization** % non-ionized[b]	pKa	**K_{sp}**[c]	**Cocrystal Solubility (m)**[d]	**Solubility Ratio** $[drug]_{S_{cc}}/S_{drug}$
CBZ-MLN[e]	2: 1[f]	Water	1.4	$1.5x10^{0}$ ±$2x10^{-2}$	$7.5x10^{-4}$ ±$5x10^{-6}$	$1.5X10^{+1}$	$4.6x10^{-4}$	96	2.8	$8.1x10^{-7}$	$5.9x10^{-3}$	26
CBZ-GTA	1: 1	Water	2.0	$8.9x10^{-1}$ ±$4x10^{-2}$	$3.3x10^{-3}$ ±$3x10^{-4}$	$1.0x10^{+1}$	$4.6x10^{-4}$	100	4.4	$2.9x10^{-3}$	$5.4x10^{-2}$	117
CBZ-NCT	1: 1	Water	6.0	$8.5x10^{-1}$ ±$4x10^{-2}$	$5.8x10^{-3}$ ±$5x10^{-4}$	$7.5x10^{0}$	$4.6x10^{-4}$	100	3.5	$4.9x10^{-3}$	$7.0x10^{-2}$	152
THP-NCT	1: 1	Water	5.8	$8.1x10^{-1}$ ±$3x10^{-2}$	$2.5x10^{-1}$ ±$3x10^{-2}$	$7.5x10^{0}$	$3.1x10^{-2}$	100	3.5	$2.0x10^{-1}$	$4.5x10^{-1}$	15
CBZ-OXA	2: 1[f]	Water	1.3	$2.8x10^{-2}$ ±$2x10^{-3}$	$8.0x10^{-4}$ ±$5x10^{-5}$	$1.3x10^{0}$	$4.6x10^{-4}$	50	1.3	$9.0x10^{-9}$	$1.3x10^{-3}$	5.7
CBZ-SUC	2: 1	Water	3.0	$1.8x10^{-2}$ ±$3x10^{-4}$	$6.6x10^{-4}$ ±$2x10^{-4}$	$5.4x10^{-1}$	$4.6x10^{-4}$	94	4.2	$7.4x10^{-9}$	$1.2x10^{-3}$	5.2
CBZ-SAC	1: 1	Water	2.1	$8.6x10^{-3}$ ±$9x10^{-5}$	$6.8x10^{-4}$ ±$4x10^{-6}$	$1.8x10^{-2}$	$4.6x10^{-4}$	24	1.6	$1.4x10^{-6}$	$1.2x10^{-3}$	2.6
CAF-SLC	1: 1	Water	2.6	$8.4x10^{-3}$ ±$1x10^{-3}$	$1.4x10^{-1}$ ±$5x10^{-4}$	$1.4x10^{-2}$	$1.1x10^{-1}$	72	3.0	$8.5x10^{-4}$	$2.9x10^{-2}$	0.3
THP-SLC	1: 1	Water	2.6	$5.3x10^{-3}$ ±$8x10^{-4}$	$4.3x10^{-2}$ ±$3x10^{-3}$	$1.4x10^{-2}$	$3.1x10^{-2}$	72	3.0	$1.6x10^{-4}$	$1.3x10^{-2}$	0.4
CBZ-SLC	1: 1	Water	2.9	$2.3x10^{-3}$ ±$1x10^{-4}$	$6.4x10^{-4}$ ±$1x10^{-5}$	$1.4x10^{-2}$	$4.6x10^{-4}$	56	3.0	$8.2x10^{-7}$	$9.1x10^{-4}$	2.0
CBZ-GTA	1: 1	IPA	-	$5.4x10^{-1}$ ±$2x10^{-2}$	$9.1x10^{-2}$ ±$3x10^{-3}$	$3.6x10^{0}$	$5.0x10^{-2}$	-	-	$4.9x10^{-2}$	$2.2x10^{-1}$	4.4
THP-NCT	1: 1	IPA	-	$1.1x10^{-1}$ ±$2x10^{-2}$	$2.1x10^{-2}$ ±$5x10^{-3}$	$6.3x10^{-1}$	$3.0x10^{-3}$	-	-	$2.3x10^{-3}$	$4.8x10^{-2}$	16
CBZ-NCT	1: 1	IPA	-	$6.0x10^{-2}$ ±$4x10^{-3}$	$6.1x10^{-2}$ ±$2x10^{-3}$	$6.3x10^{-1}$	$5.0x10^{-2}$	-	-	$3.7x10^{-3}$	$6.1x10^{-2}$	1.2
CBZ-SAC	1: 1	IPA	-	$9.0x10^{-3}$ ±$1x10^{-3}$	$4.3x10^{-2}$ ±$6x10^{-3}$	$1.6x10^{-1}$	$5.0x10^{-2}$	-	-	$3.9x10^{-4}$	$2.0x10^{-2}$	0.4
CBZ-SUC	2: 1	IPA	-	$1.3x10^{-3}$ ±$6x10^{-4}$	$4.6x10^{-2}$ ±$4x10^{-3}$	$5.5x10^{-1}$	$5.0x10^{-2}$	-	-	$2.8x10^{-6}$	$8.8x10^{-3}$	0.4
CBZ-GTA	1: 1	EtOH	-	$5.3x10^{-1}$ ±$1x10^{-2}$	$1.8x10^{-1}$ ±$4x10^{-3}$	$2.8x10^{0}$	$1.4x10^{-1}$	-	-	$9.4x10^{-2}$	$3.1x10^{-1}$	2.2
THP-NCT	1: 1	EtOH	-	$2.0x10^{-1}$ ±$2x10^{-2}$	$2.9x10^{-2}$ ±$4x10^{-3}$	$1.1x10^{0}$	$1.8x10^{-2}$	-	-	$5.8x10^{-3}$	$7.6x10^{-2}$	4.2
CBZ-NCT	1: 1	EtOH	-	$1.5x10^{-1}$ ±$9x10^{-3}$	$1.4x10^{-1}$ ±$1x10^{-2}$	$1.1x10^{0}$	$1.4x10^{-1}$	-	-	$2.2x10^{-2}$	$1.5x10^{-1}$	1.1
CBZ-SAC	1: 1	EtOH	-	$3.5x10^{-2}$ ±$3x10^{-3}$	$1.2x10^{-1}$ ±$2x10^{-2}$	$2.4x10^{-1}$	$1.4x10^{-1}$	-	-	$4.2x10^{-3}$	$6.5x10^{-2}$	0.5
CBZ-SUC	2: 1	EtOH	-	$1.8x10^{-2}$ ±$3x10^{-3}$	$1.4x10^{-1}$ ±$2x10^{-2}$	$8.1x10^{-1}$	$1.4x10^{-1}$	-	-	$3.5x10^{-4}$	$4.5x10^{-2}$	0.6
CBZ-GTA	1: 1	EtOAc	-	$9.0x10^{-2}$ ±$1x10^{-2}$	$9.9x10^{-2}$ ±$4x10^{-3}$	$1.0x10^{0}$	$4.9x10^{-2}$	-	-	$8.9x10^{-3}$	$9.4x10^{-2}$	1.9
CBZ-SAC	1: 1	EtOAc	-	$4.7x10^{-2}$ ±$4x10^{-3}$	$5.4x10^{-2}$ ±$2x10^{-3}$	$1.8x10^{-1}$	$4.9x10^{-2}$	-	-	$2.5x10^{-3}$	$5.0x10^{-2}$	1.0
THP-NCT	1: 1	EtOAc	-	$2.0x10^{-2}$ ±$1x10^{-3}$	$9.7x10^{-3}$ ±$4x10^{-4}$	$1.1x10^{-1}$	$6.2x10^{-3}$	-	-	$2.0x10^{-4}$	$1.4x10^{-2}$	2.3
CBZ-NCT	1: 1	EtOAc	-	$1.3x10^{-2}$ ±$2x10^{-3}$	$5.0x10^{-2}$ ±$3x10^{-3}$	$1.1x10^{-1}$	$4.9x10^{-2}$	-	-	$6.7x10^{-4}$	$2.6x10^{-2}$	0.5
CBZ-SUC	2: 1	EtOAc	-	$8.5x10^{-4}$ ±$2x10^{-4}$	$4.3x10^{-2}$ ±$5x10^{-3}$	$4.6x10^{-2}$	$4.9x10^{-2}$	-	-	$3.1x10^{-8}$	$2.0x10^{-3}$	0.1

[a]solubility of hydrated forms are indicated for aqueous samples [b]calculated for the measured pH using referenced pKa values[43] [c]K_{sp} units are m^2 and m^3 for 1:1 and 2:1 cocrystals, respectively [d]calculated using Equation 2.5 [e]form B (hydrated cocrystal)[23] [f]disordered crystal structure that does not provide definitive stoichiometry.[28] Indicated values reflect HPLC measurement of dissolved cocrystals. Calculations: $H = (C \times (F/100))^{B} (D)^{A}$ $I = \sqrt[A+B]{H/(A^{A}B^{B})}$ $J = (A \times I)/E$

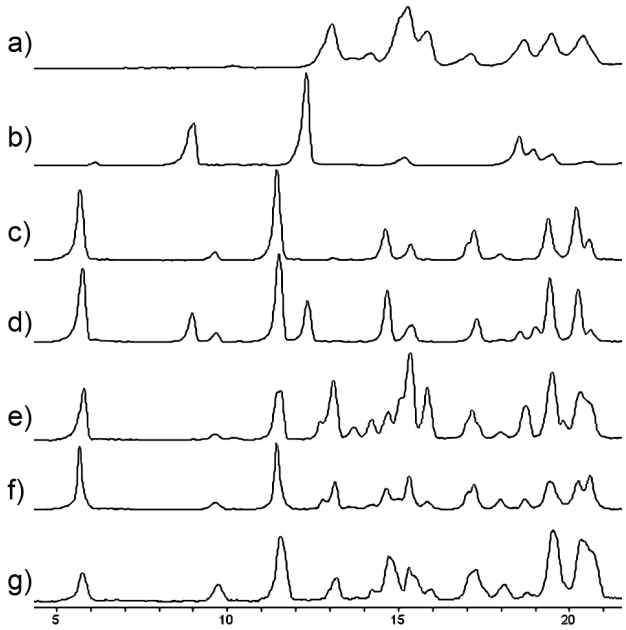

Figure 2.4: XRPD patterns of reference materials and solid phases isolated from suspensions at the eutectic concentration: a) CBZ(III), b) CBZ(D), and c) CBZ-SUC followed by solid phases isolated from d) water, e) ethanol, f) ethyl acetate, and g) 2-propanol.

The solubility ratios of the cocrystals in Table 2.1 exceed ranges previously reported for salt, polymorph, and amorphous forms of drug substances. Pudipeddi et al. have surveyed polymorph solubility ratios for fifty-five drug substances, some with multiple forms, to provide eighty-one solubility ratios and all the values fell below five with only one exception.[44] The highest polymorph solubility ratio was 23.1 (Premafloxacin I/III) followed by 4.7 (Acemetacin III/I). The solubility ratio of CBZ III/I polymorphs in IPA was almost 1.4. In comparison, the CBZ-GTA cocrystal ratio in IPA is more than four times the solubility of CBZ III. Hancock and Parks published

amorphous drug solubility ratios (amorphous/crystalline) of seven compounds in a variety of aqueous and organic solvent systems.[45] The maximum measured solubility enhancement of amorphous drug or excipients was twenty-four times (glucose in methanol 20^{o}C) the crystalline form. Two other pharmaceutical compounds (glibenclamide and polythiazide) had solubility ratios greater than five. While the cocrystals in this study show a greater range of equilibrium solubility ratios than many of these surveyed, amorphous, polymorph, or salt forms the benefits in terms of dissolution rates are not known. The rate in which any of these more soluble solid forms transform in solution could be a determining factor in their utility.

2.3.2. Cocrystal solubility, eutectic concentration, and coformer solubility relationship

Examination of results in Table 2.1 reveals regular patterns in the effects of solubility of components on eutectic concentrations and cocrystal solubilities. Within the series of carbamazepine cocrystals it is observed that experimentally measured $[\text{coformer}]_{eu}$ increases with coformer solubility and that $[\text{coformer}]_{eu}$ can be orders of magnitude above $[\text{drug}]_{eu}$. Based on K_{sp} behavior, $[\text{coformer}]_{eu}$ in excess of $[\text{drug}]_{eu}$ is associated with cocrystal solubility greater than drug solubility. The relationship between cocrystal $[\text{coformer}]_{eu}$ and coformer solubility is evident for carbamazepine cocrystals in water (Figure 2.5a). This relationship is maintained for other cocrystals and other

solvents in Figure 2.5b. Higher $[\text{coformer}]_{eu}$ values are associated with higher K_{sp} as predicted by Equation 2.5 and previous models.[14]

Cocrystal solubility ratios or drug concentrations associated with cocrystal solubility are directly proportional to coformer solubility, as expected from the derived chemical potential expression (Equation 2.7). This is shown in Figure 2.5b where both cocrystal and coformer solubilities are normalized by drug solubility and a clear trend is observed in all solvents studied. For cocrystals of the same drug and different coformers the pattern is maintained, i.e. high cocrystal solubility ratios for high ratios of coformer to drug solubilities. For this small series of 1:1 cocrystals it appears that a coformer solubility about ten times the drug solubility is needed for cocrystal solubilities to be greater than drug solubility. 2:1 cocrystals demonstrate the same correlation (data not graphed) however the slope is slightly lower as anticipated from Equation 2.5. For each cocrystal, the ratio of coformer and drug concentrations at the eutectic concentration is also proportional with the coformer to drug solubility ratio.

Cocrystal solubility behavior was further examined in each solvent as shown in Figure 2.6. Cocrystal solubility ratio as a function of coformer solubility for each solvent confirms that high coformer solubility equates to high cocrystal solubility. A notable exception is CBZ-NCT (positive deviation) in water where high CBZ aqueous solubility enhancement occurs in the presence of $NCT_{(aq)}$. In ethyl acetate (least polar solvent - Figure 2.6c) the solubility order for three of the four coformers differ from the other

solvents. Yet, cocrystal solubility remains a function of coformer solubility. Similarly a proportional relationship has been suggested between the aqueous solubility of pharmaceutical salts and the hydrophilicity of their organic counterions. Counterions of erythromycin with extended alkyl chains (*i.e.* more hydrophobic) decreased the aqueous salt solubility.[46] Similar results have been shown for counterion studies of lincomycin salts.[47] Studies of other drugs are consistent with this trend and have shown counterions with more hydroxyl groups (i.e. more hydrophilic) can provide higher salt solubility.[48, 49] Alternatively analysis of several flurbiprofen salts have not found a link between solubility and counterion hydrophilicity, but suggest crystal lattice interactions could become stronger in some instances where counterions are more polar.[50] Whether lattice energies and/or component solubilities predict cocrystal or salt solubilities depends on the interplay between solid-state and solute-solvent interactions.

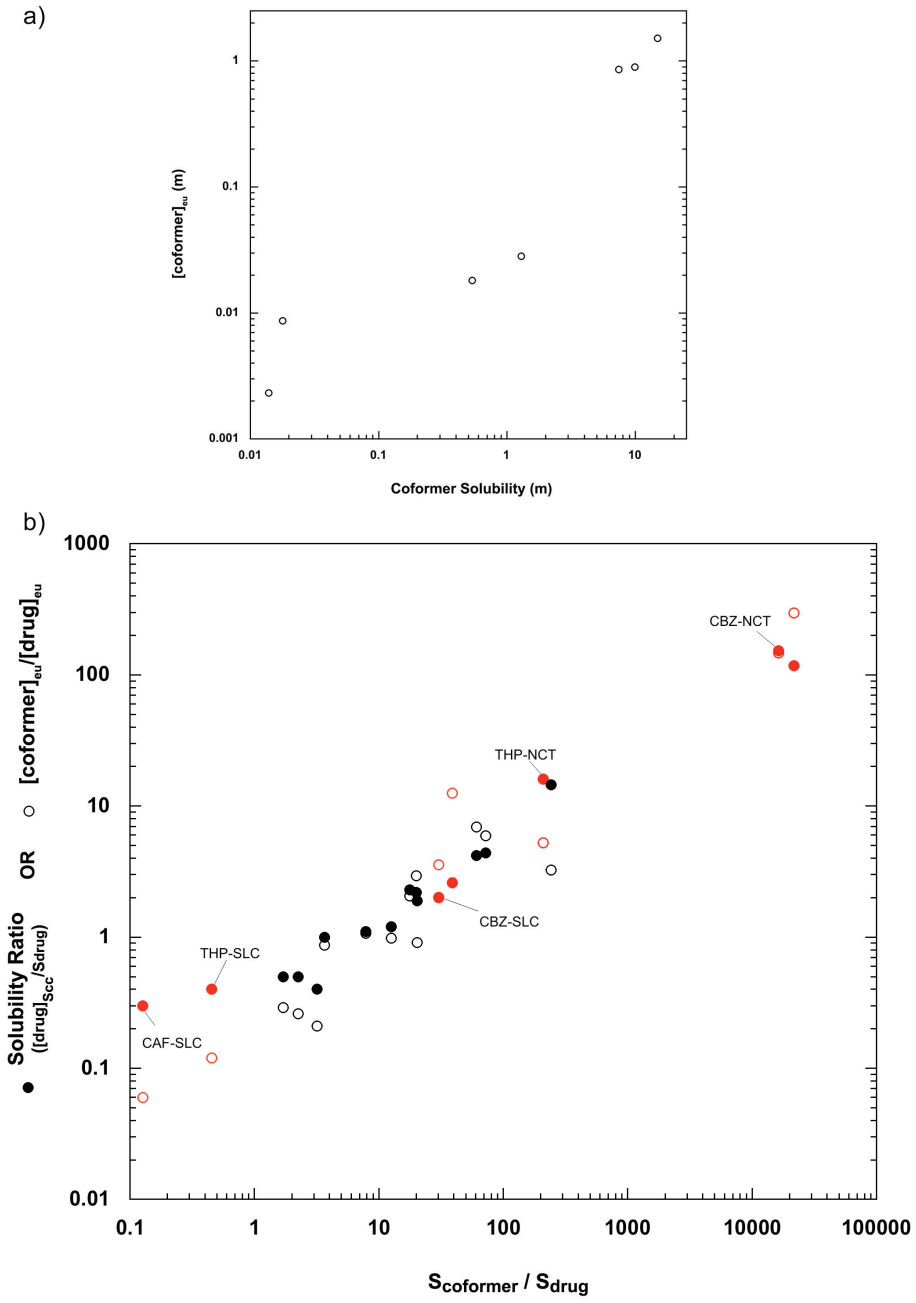

Figure 2.5: a) The relationship between $[coformer]_{eu}$ and coformer solubility for CBZ cocrystals in water. Log axes are shown to aid visualization of the individual points due to the large range of values. The linear regression for the untransformed data in Table 2.1 is r^2=0.986. b) The ratio of coformer to drug solubility plotted against the cocrystal solubility ratio (filled circles) and the ratio of coformer to drug eutectic concentrations (open circles). All aqueous samples are shown in red. Several cocrystals with the same coformers are labeled. $[coformer]_{eu}$ in a) and b) refers to the non-ionized [coformer] at the eutectic based on pH values listed in Table 2.1.

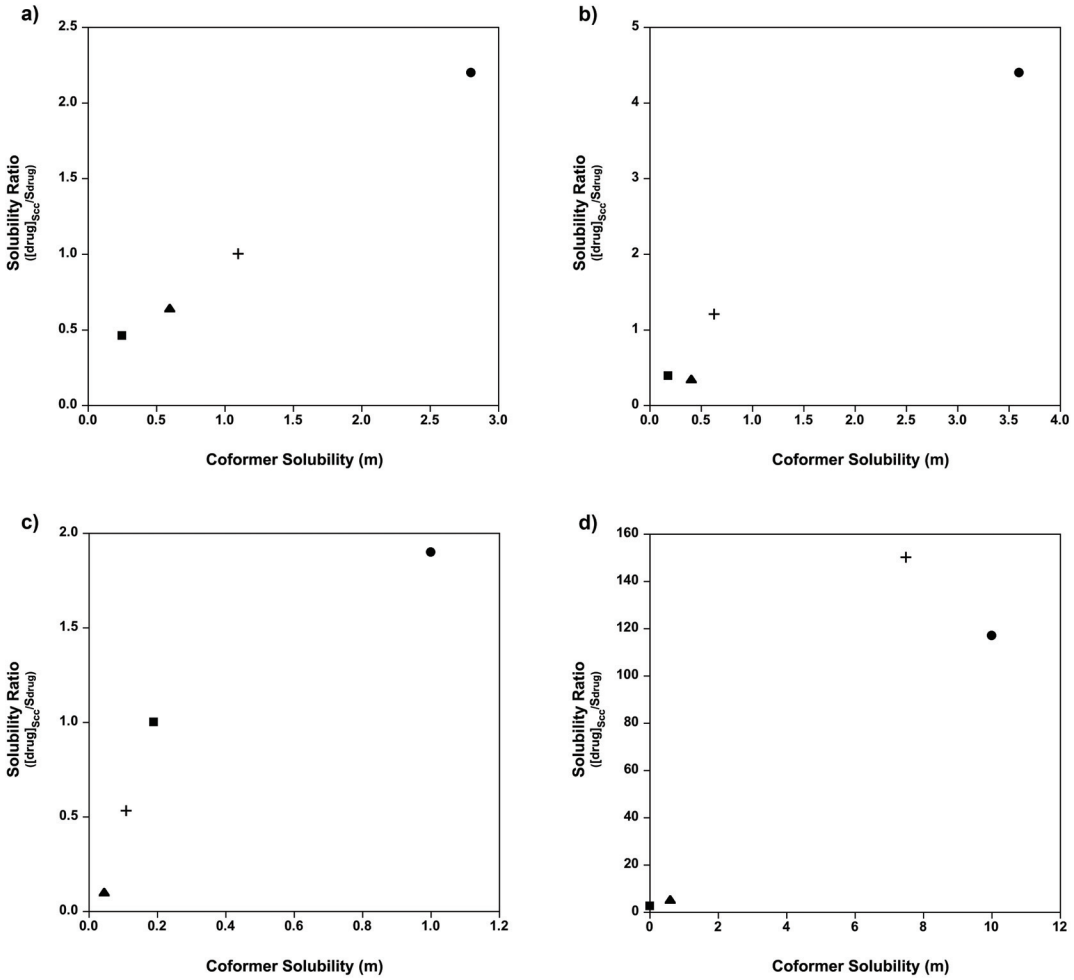

Figure 2.6: Solubility ratio of CBZ cocrystal to CBZ(D) as a function of the constituent coformer solubility (molal). The graphs represent: (a) ethanol, (b) 2-propanol, (c) ethyl acetate, (d) water. The points in each graph represent the cocrystal CBZ-coformer by the corresponding coformer component (●:GTA, +:NCT, ▲:SUC, ■:SAC).

2.3.3. Cocrystal coformers that increase drug solubility

Some coformers are capable of solubilizing the drug substance with which they form cocrystals. The direct measurement of drug concentration is critical for accurately expressing the eutectic and calculating cocrystal solubility. One example is the CBZ-

NCT cocrystal where CBZ is highly solubilized by $NCT_{(aq)}$ (Figure 2.6d and Table 2.1). The $[CBZ]_{eu}$ is more than tenfold the solubility of CBZ(D). Other coformers have minimal effect on drug solubility, with $[CBZ]_{eu}$ slightly above CBZ solubility in pure solvent, but this effect is prominent for CBZ-NCT in water. The CBZ solubilization by $NCT_{(aq)}$, indicated by $[CBZ]_{eu}>S_{CBZ(D)}$, leads to higher cocrystal solubility than expected by considering NCT aqueous solubility alone.

A series of CBZ cocrystal solubilities in aqueous media were calculated by two approaches to highlight the importance of considering $[CBZ]_{eu}$. The first approach is using Equation 2.3 where $K_{sp} = [CBZ]_{eu}^{\alpha}[B]_{eu}^{\beta}$ and the second assumes $[CBZ]_{eu} = S_{CBZ(D)}$ so that $K_{sp} = S_{CBZ}^{\alpha}[B]_{eu}^{\beta}$. Figure 2.7 plots aqueous CBZ cocrystal solubility ratios as a function of coformer solubility. A direct trend between coformer and cocrystal solubility ratio is evident in Figure 2.7 when it is assumed that $[CBZ]_{eu} = S_{CBZ(D)}$ (open squares). A notable exception is the cocrystal hydrate CBZ-MLN (negative deviation) identified to have a more soluble 2:1 anhydrous form (data not shown). Several cocrystals exhibit large increases in solubility when calculated using measured $[CBZ]_{eu}$. This is evident for cocrystals of the three most soluble coformers (NCT, GTA, and MLN). For this group of highly soluble coformers the ability to solubilize CBZ is distinctly different. $[CBZ]_{eu}$ values range from 2 to 13 times $S_{CBZ(D)}$, and this makes measuring $[CBZ]_{eu}$ critical to evaluating cocrystal solubility. For these cocrystals $[coformer]_{eu}$ values (Table 2.1) follow the order of coformer solubility (MLN>GTA>NCT), but the $[CBZ]_{eu}$, indicative of drug solubilization by coformer, has an inverse order (NCT>GTA>MLN). NCT has been previously shown to solubilize hydrophobic drug substances.[51] For the low

solubility CBZ coformers (OXA, SUC, SAC), little or no difference is exhibited between cocrystal solubility calculated from Equation 2.5 and 2.6.

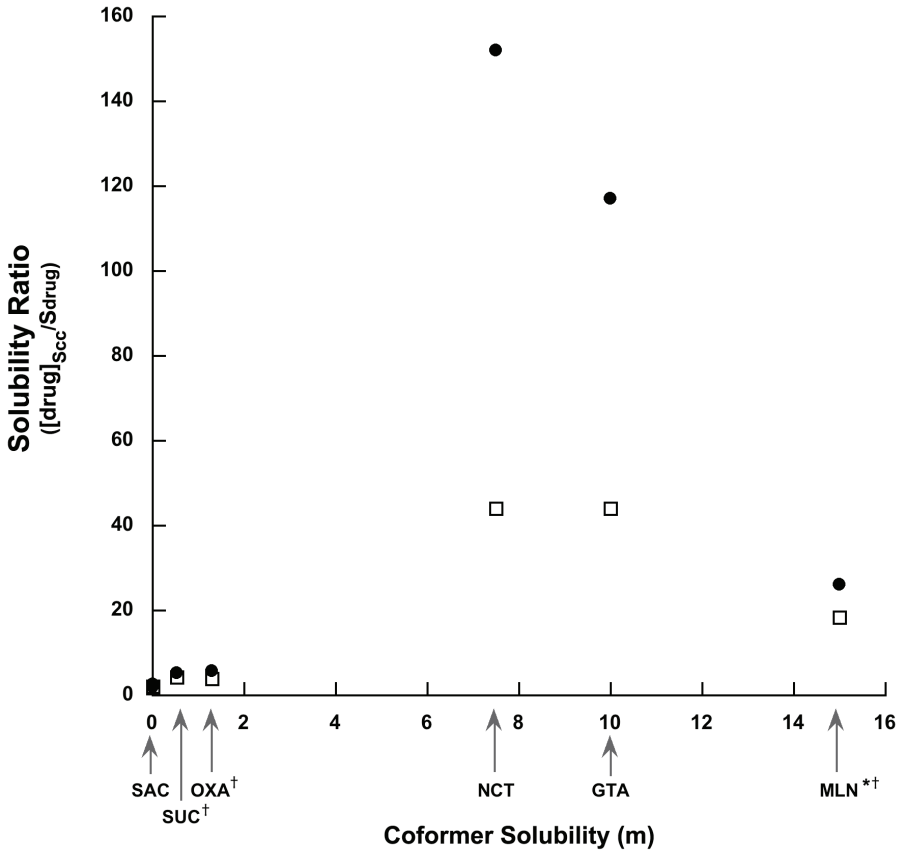

Figure 2.7: Aqueous solubility ratio of CBZ cocrystals to CBZ(D) (*i.e.* $[drug]_{Scc}/S_{drug}$) plotted against coformer solubility. Data labels indicate the coformer component of the cocrystal. Cocrystal solubility calculated from Equation 2.5 (●: $[drug]_{eu}$ measured) or from Equation 2.6 (□: $[drug]_{eu}$ approximated by drug solubility (S_{drug}) in pure solvent). *hydrated cocrystal †2:1 cocrystal stoichiometry

2.3.4. Cocrystal stoichiometry and solubility

Carbamazepine cocrystals of succinic, oxalic, and malonic acid are the only 2:1 (drug:coformer) cocrystals in Table 2.1 and they exhibit a negative deviation from the

trend between cocrystal and coformer solubility. Since these coformers (more soluble than CBZ) account for a lesser mole fraction of the cocrystal they have reduced capacity to impart high solubility to the cocrystal. From Equation 2.3 it is expected that cocrystals with high mole fractions of the least soluble component will have less solubility enhancement over pure drug. The solubility value of a 2:1 cocrystal does not equal the equilibrium drug concentration as in the case of a 1:1 cocrystal. Cocrystal stoichiometry defines the relationship between solubility and the equilibrium drug concentration achieved.

2.3.5. Cocrystal and drug solubility

The solubility of cocrystal and drug exhibited a direct proportionality, as did the solubility of cocrystal and coformer. Figure 2.8a shows aqueous solubility of CBZ, theophylline (THP), and caffeine (CAF) cocrystals with salicylic acid (SLC) as a function of the drug solubility. These results indicate the cocrystal solubility trend follows drug solubility (CAF>THP>CBZ) for salicylic acid cocrystals. It is worth noting that SLC is less water soluble than CAF and THP, but more soluble than CBZ. Cocrystal solubility is higher than drug hydrate solubility for CBZ-SLC and higher than SLC solubility for CAF-SLC, thus these cocrystals are incongruently saturating. THP-SLC is congruently saturating with both components more soluble than cocrystal.

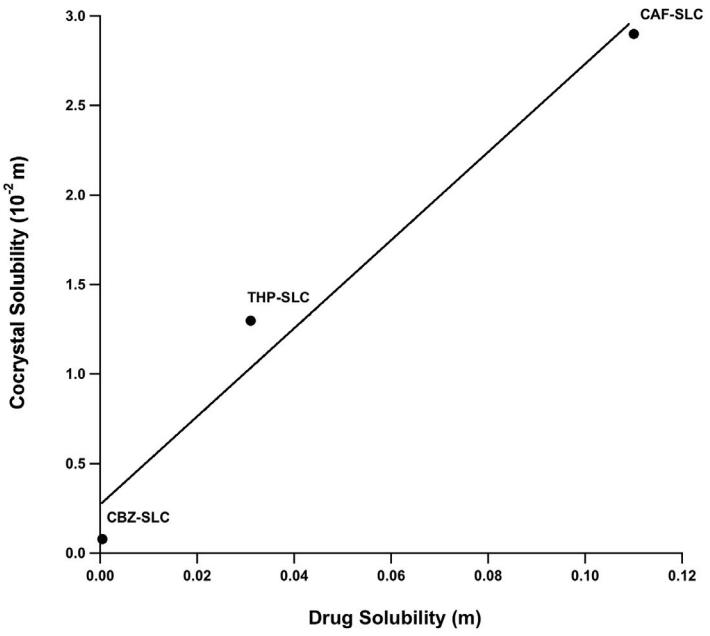

a)

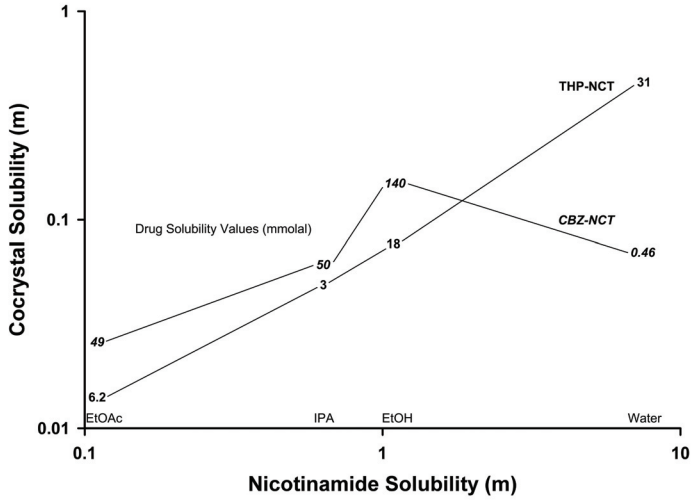

b)

Figure 2.8: a) Aqueous solubility of salicylic acid cocrystals (with CBZ, THP, or CAF) plotted against the solubility of the hydrated drug. b) Solubility of NCT cocrystals of CBZ and THP in water, EtOH, EtOAc, and IPA plotted against the respective NCT solubility. The numerical data points represent dug solubility from Table 2.1 in mmolal.

Nicotinamide cocrystals of CBZ and THP listed in Table 2.1 are plotted in Figure 2.8b to further illustrate the relationship between cocrystal and drug solubility. Each numerical data point represents the drug solubility and in each solvent the more soluble drug has the higher cocrystal solubility. THP aqueous solubility is greater than CBZ and THP-NCT has the higher aqueous solubility (far right points). For all organic solvents CBZ is more soluble than THP and accordingly the CBZ-NCT cocrystals are more soluble. Figure 2.8b additionally demonstrates the effect of coformer solubility on cocrystal solubility. All cocrystal solubilities increase with NCT except for CBZ-NCT in water (negative deviation). It is clear the CBZ solubility decrease in water overshadows a smaller relative NCT solubility increase. Together these NCT cocrystals of CBZ and THP indicate the combined effect drug and coformer solubility have on cocrystal solubility. Cocrystal solubility is proportional to the solubility of both drug and coformer components.

2.3.6. Accuracy of solubility product measurements

The CBZ-NCT cocrystal K_{sp} values based on a single measurement of the eutectic in this paper are very similar to those previously determined by measuring cocrystal solubility for a variety of coformer concentrations.[14] K_{sp} values (Table 2.1) for CBZ-NCT in EtOH, IPA, and EtOAc are within the experimental error of those previously

reported. Although these deviations are minimal, other systems could exhibit less accuracy.

One factor that may contribute to error is the proximity of the eutectic concentrations to the concentrations of drug and coformer at the equilibrium cocrystal solubility in pure solvent. There is close eutectic proximity if the ratio of $[drug]_{eu}$ to $[coformer]_{eu}$ is near the stoichiometric ratio of components in the cocrystal. When the equilibrium solubility is far away from the measurable eutectic concentration it is necessary to make large extrapolations based on ideal K_{sp} behavior. In this case the solute activities may no longer be replaced by concentrations. Additionally, solution complexation of cocrystal components can be concentration dependent. Solubility products based on eutectic concentrations do not account for this solution complexation or solubilization. Eutectic concentrations only reflect the level of solubilization for that particular solution composition. Therefore, solubility calculations from the eutectic concentrations may not provide a good estimate of the level of complexation or solubilization and, as a result, the true solubility. Accuracy could decrease for coformers that exhibit high drug solubilization, as reflected by $S_{drug} << [drug]_{eu}$, and eutectic concentrations are far from stoichiometric solubility. For these instances it would be prudent to measure complexation constants or activity coefficients to assure accuracy of K_{sp} and solubility calculations.

When designing screening methods for cocrystal solubility it is possible to evaluate K_{sp} by measuring the drug and coformer concentrations at any point where the solution is in equilibrium with solid cocrystal. However, by measuring the eutectic concentrations it is also possible to establish the range of cocrystal thermodynamic stability in solution. In either case, the prior discussion of eutectic proximity, complexation, and activity apply to the calculations of cocrystal solubility. Most pharmaceutically relevant cocrystals have solubility higher than the drug and are incongruently saturating. This means measurements based on eutectic concentrations will have the closest proximity and the most accuracy for a single point measurement used to calculate K_{sp}. Solubility product calculations based on eutectic points have been used successfully to identify the phase stability and solution chemistry of enatiomers.[36]

2.3.7. Ideal solubilities from thermal properties

Cocrystal melting temperature and enthalpy were obtained from analysis of DSC data shown in Figure 2.9. These cocrystals show unique fusion properties relative to their constituent reactants. Two cocrystals (CBZ-SAC and CBZ-OXA) have lower melt temperatures than their pure components. CBZ-SAC and CBZ-OXA melt temperatures are 177.5^{o}C and 164.7^{o}C respectively, and for pure components SAC T_m=229.7^{o}C, OXA T_m=191.2^{o}C, and CBZ T_m=191.1^{o}C. The other five cocrystal melt temperatures are very close to or between those of their reactants. To determine the ideal solubility of

cocrystals from Equation 2.8 the melting enthalpy was first normalized by the cocrystal stoichiometry. The cocrystal enthalpy of melting listed in Table 2.2 is the measured value divided by the number of moles of reactant per mole of cocrystal (i.e. 2 for 1:1 cocrystals and 3 for 2:1 cocrystals). This method is analogous to ideal solubility values of drug salt forms wherein the melting enthalpy is normalized per mole of constituent ions.[52]

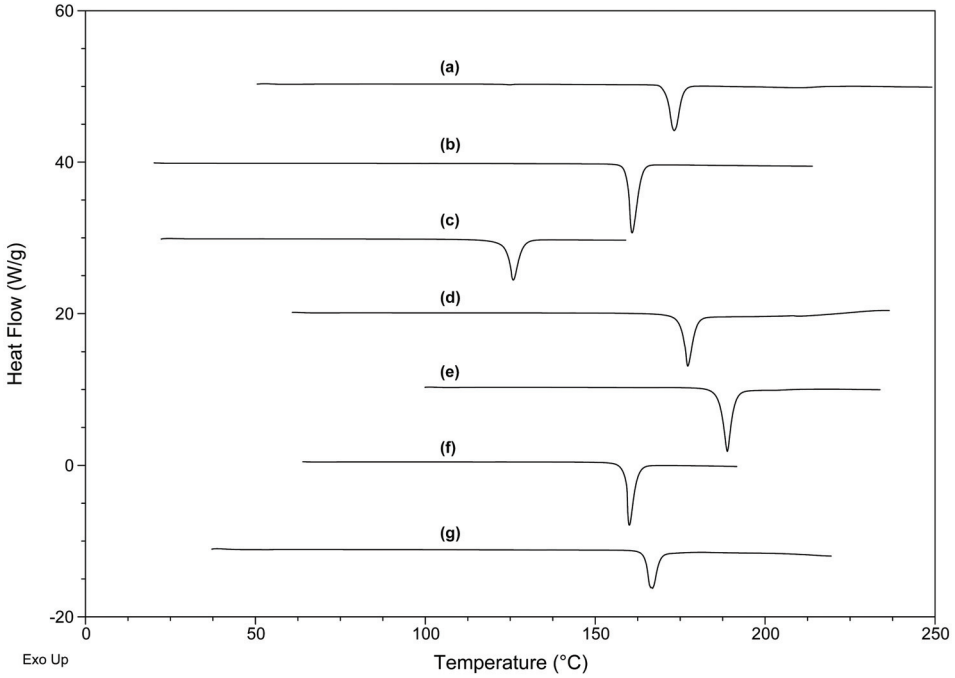

Figure 2.9: DSC for cocrystals of: (a)THP-NCT, (b)CBZ-NCT (c)CBZ-GTA, (d)CBZ-SAC, (e)CBZ-SUC, (f)CBZ-SLC, and (g)CBZ-OXA.

Table 2.2: Melt temperature and enthalpy used in calculation of ideal solubility and comparisons with experimental solubility values.

Reactants	aqueous solubility (m)[a]	ideal solubility (m)[b]	T_m (°C)	ΔH_m (kJ/mol)[c]	aqueous solubility ratio (exp/ideal)	ideal cocrystal solubility ratio (cocrystal/drug)
Glutaric acid (GTA)	1.0×10^{1}	13.5	97.7	20.7	7.4×10^{-1}	-
Nicotinamide (NCT)	7.5×10^{0}	4.9	130.6	23.8	1.5×10^{0}	-
Succinic acid (SUC)	5.4×10^{-1}	0.6	188.1	32.4	9.0×10^{-1}	-
Theophylline (THP)	5.8×10^{-2}	1.8	273.6	29.0	3.2×10^{-2}	-
Salicylic acid (SLC)	1.8×10^{-2}	1.9	160.9	27.1	9.5×10^{-3}	-
Saccharin (SAC)	1.1×10^{-2}	0.3	229.7	32.1	3.7×10^{-2}	-
Carbamazepine (CBZ)	1.6×10^{-3}	1.4	192.1	25.6	1.1×10^{-3}	-
Cocrystals						
THP-NCT	4.5×10^{-1}	8.9	175.0	14.6	5.1×10^{-2}	5.1
CBZ-NCT	7.0×10^{-2}	1.8	160.8	27.6	3.9×10^{-2}	1.3
CBZ-GTA	5.4×10^{-2}	5.7	125.9	23.2	9.5×10^{-3}	4.1
CBZ-SAC	1.2×10^{-3}	1.3	177.5	27.5	9.2×10^{-4}	1.0
CBZ-SUC	1.2×10^{-3}	0.5	188.9	20.0	2.4×10^{-3}	0.4
CBZ-SLC	9.1×10^{-4}	2.6	160.1	24.6	3.5×10^{-4}	1.9
CBZ-OXA	1.3×10^{-3}	4.6	164.7	20.0	2.8×10^{-4}	3.3

[(a)]Measured solubility for reactants and cocrystals (from Table 2.1) and [(b)]ideal solubility calculated from Equation 2.8 using melt temperature and heat of fusion. Mole fractions were converted to molality units in water. [(c)]The enthalpy of melting for cocrystals is normalized by moles of component molecules (drug + coformer) per mole of cocrystal. All aqueous solubility, thermal data, and ratios listed are for anhydrous crystal forms.

The association between coformer and cocrystal melt temperature is scattered for the CBZ cocrystals in Table 2.2. These five cocrystals show the same relation as an expanded group of eighteen CBZ cocrystals (single endotherm non-hydrate forms) recently reported.[23] The linear regression for coformer and cocrystal melting in the two studies (r^2=0.67-0.72) reflects a limited qualitative relationship. This regression value is in agreement with previous correlations of coformer and cocrystal melt temperatures for different drug substances.[53, 54] Since cocrystal lattice energy and melt temperature are

based in part on the lattice arrangement and intermolecular interactions it is reasonable that coformer and cocrystal melt temperatures do not exhibit a strict correlation.

Experimental reactant and cocrystal aqueous solubilities also show a qualitative trend with melting temperature in Figure 2.10a and 10b, respectively. The organic solvents appear to have a better correlation than the aqueous solubility values. This observation seems reasonable given the potential of drug or coformer polar functional moieties for specific interactions with water and therefore deviations from ideal solubility behavior. The solubility of cocrystals in ethanol and isopropanol (from Table 2.1) are quite linear (linear regression: r^2>0.95) as a function of melt temperatures listed in Table 2.2. This correlation is apparent in Figure 2.10b where melt temperature and cocrystal solubility (log axis) are plotted for the four solvents. However, from this limited data set it would be speculative to consider the correlation of melt temperature and solubility superior for either cocrystals or reactants. The relation of cocrystal solubilities and melt temperatures (Table 2.2 and Figure 2.10b) is stronger than reported for aqueous kinetic solubility and melt temperature for cocrystals comprised of similar acidic coformers.[54] This data seems comparable to studies of salt forms that indicate qualitative trends between solubility and melt temperature.[40, 50, 52, 55, 56] Previous reports of ephedrine salts have shown qualitative relations between log solubility and melt temperature with approximately similar levels of scatter seen in this cocrystal study.[52]

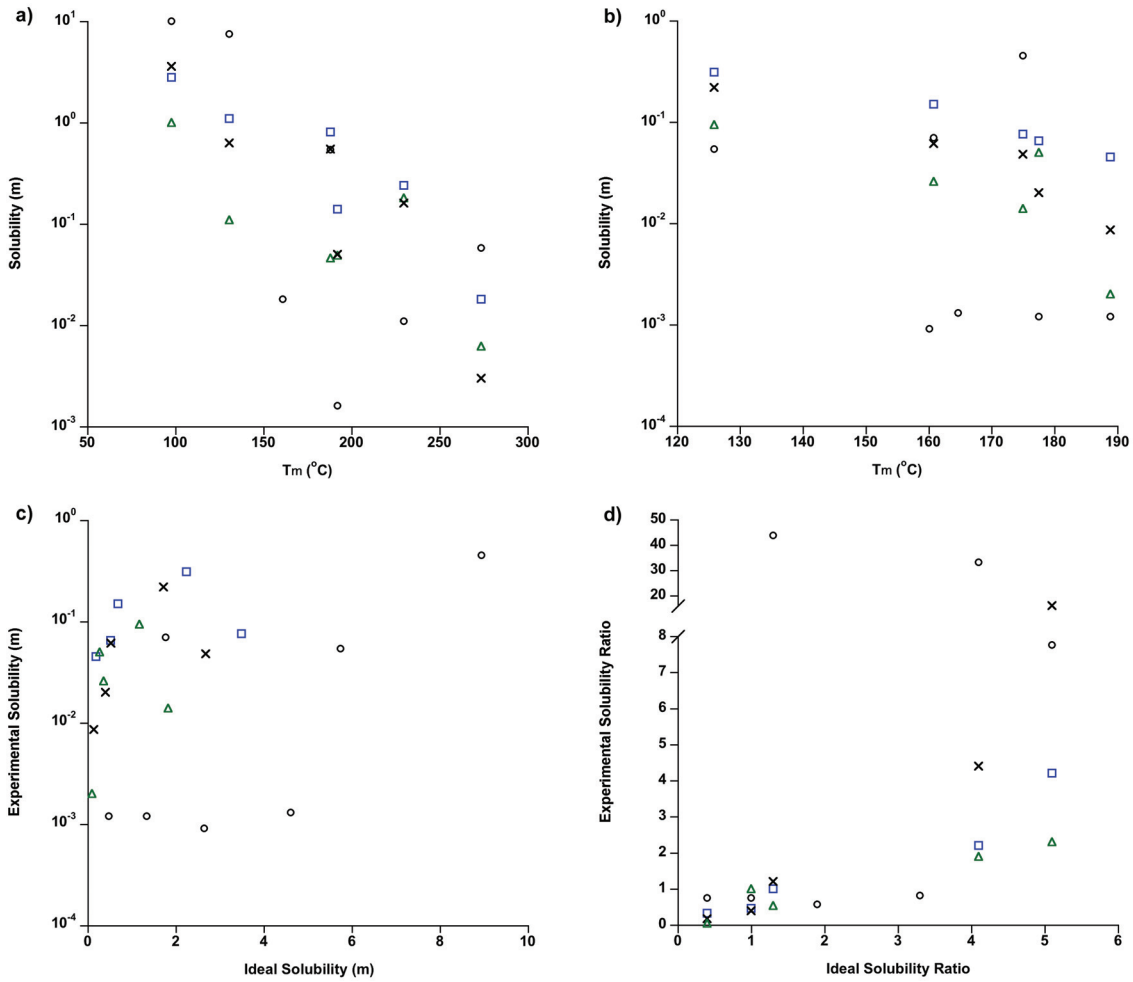

Figure 2.10: Equilibrium cocrystal and reactant solubilities or solubility ratios in water(○), EtOH(□), IPA(X), and EtOAc(△). Solubility as a function of melt temperature for (a) reactants and (b) cocrystals. (c) Experimental cocrystal solubility versus ideal solubility. (d) Experimental against ideal cocrystal solubility ratio (cocrystal/CBZ form III).

Experimental cocrystal solubilities are not well correlated with ideal values derived from the melting enthalpy and temperature of the crystals (Figure 2.10c). The ratios of experimental aqueous solubility to ideal solubility are listed in Table 2.2 to emphasize these deviations. Both aqueous and organic solvents included in Figure 2.10c

seem to suggest that crystal fusion properties alone are not sufficient for predicting cocrystal solubility. The solution chemistry of cocrystals appears to be critical for describing solubility behavior. The reactants in Table 2.2 have a better correlation between experimental and ideal (linear regression: r^2=0.87-0.92) solubilities. Still several instances of large deviations suggest ideal solubilities are not adequate indicators of drug and coformer solubility from solution measurements. The results further illustrate melting properties associated with the breaking of the crystal lattice are not sufficiently predictive of cocrystal solubility relations that involve solvent interactions.

Ratios of the ideal cocrystal and ideal drug solubilities listed in Table 2.2 were of a similar order of magnitude to the solution measurements in Table 2.1. The measured solubility ratios of CBZ cocrystal/CBZ(III) are plotted in Figure 2.10d against the ideal solubility ratio. These ideal ratios have significant discrepancies with aqueous experimental ratios for CBZ-NCT and CBZ-GTA cocrystals where the coformer is known to solubilize the drug substance. Correlations for organic solvents are significantly better than aqueous samples. The thermodynamic ideal solubilities seem to more adequately quantify the relative change between cocrystal and drug (Figure 2.10d) than absolute solubility values (Figure 2.10c).

Solubility predictions have been reported for many polymorph, amorphous, and salt forms. These predictions are often based on the free energy difference between the two solid forms. This difference is typically estimated from fusion data combined in

some cases with heat capacity values. This type of solubility prediction for amorphous drugs mostly overestimates the measured solubilities and is complicated by transformations to less soluble drug forms. The majority of measured amorphous solubility ratios fell well below the predicted ranges that span about one order of magnitude (*e.g.* 48-455 for polythiazide). In the case of amorphous glibenclamide the measured solubility ratio was 14 and the predicted ratio was 112-1,652 times the crystalline solubility.[45] Polymorphs have shown much closer agreement between predicted and actual solubility ratios than these amorphous forms. This is possibly due to minimal free energy differences between polymorphs, as opposed to large differences for crystalline and amorphous forms. Polymorph studies of ten drug substances by Pudipeddi and Serajuddin provided calculated solubility ratios in good agreement with experimental ratios.[44] From our limited set, it appears ideal cocrystal solubility ratio predictions (Table 2.2 far right column) show better agreement with solution based solubility ratios (Table 2.1) than is the case for amorphous systems. Cocrystals in this study also have a weaker correlation than previously cited polymorph studies. The potential for deviations could be high for cocrystals because they can exhibit solution complexation or solubilization of drug by other crystal components. Neither of these is applicable to polymorphs.

2.4. CONCLUSIONS

This work developed methods to predict cocrystal solubilities in pure solvent from measurement of eutectic concentrations. These predictions are based on solubility product equations that include measured solution concentrations at the eutectic, where solid cocrystal and drug are in equilibrium with solution. Results show that: (1) cocrystal solubility increases with the solubility of the cocrystal components, (2) coformer eutectic concentrations increase with cocrystal and coformer solubilities for cocrystals of the same drug, and (3) coformer solubility about tenfold higher than drug leads to cocrystal being more soluble than drug. While it is generally expected that solubility and melting point are correlated, the small series of cocrystals studied show that solvent-solute interactions dominate over lattice energies, particularly in water.

Eutectic concentrations are essential indicators of cocrystal stability and solubility and provide useful insights for cocrystal selection. Furthermore, pharmaceutical processes that involve solutions can be designed with an understanding of solubility and stability provided by eutectic concentrations. Solution processes such as cocrystal screening, synthesis, manufacture, formulation, and dosing of cocrystal drug products are influenced by eutectic concentrations. The analysis of solution chemistry and phase behavior presented enables the calculation of true equilibrium solubility and stability through a single measurement of solution concentrations at The eutectic under equilibrium conditions.

2.5. REFERENCES

(1) Lipinski, C. A., Solubility in water and DMSO: issues and potential solutions. In *Pharmaceutical Profiling in Drug Discovery for Lead Selection*, Borchardt, R. T.; Kerns, E. H.; Lipinski, C. A.; Thakker, D. R.; Wang, B., Eds. AAPS Press: Arlington, Virginia, 2004; pp 93–125.

(2) Takagi, T.; Ramachandran, C.; Bermejo, M.; Yamashita, S.; Yu, L. X.; Amidon, G. L., A Provisional Biopharmaceutical Classification of the Top 200 Oral Drug Products in the United States, Great Britain, Spain, and Japan. *Mol Pharm* **2006,** 3, (6), 631-643.

(3) Amidon, G. L.; Lennernas, H.; Shah, V. P.; Crison, J. R., A theoretical basis for a biopharmaceutic drug classification: the correlation of in vitro drug product dissolution and in vivo bioavailability. *Pharm Res* **1995,** 12, (3), 413-20.

(4) Bak, A.; Gore, A.; Yanez, E.; Stanton, M.; Tufekcic, S.; Syed, R.; Akrami, A.; Rose, M.; Surapaneni, S.; Bostick, T.; King, A.; Neervannan, S.; Ostovic, D.; Koparkar, A., The co-crystal approach to improve the exposure of a water-insoluble compound: AMG 517 sorbic acid co-crystal characterization and pharmacokinetics. *J Pharm Sci* **2008,** 97, (9), 3942-56.

(5) Hickey, M. B.; Peterson, M. L.; Scoppettuolo, L. A.; Morrisette, S. L.; Vetter, A.; Guzman, H.; Remenar, J. F.; Zhang, Z.; Tawa, M. D.; Haley, S.; Zaworotko, M. J.; Almarsson, O., Performance comparison of a co-crystal of carbamazepine with marketed product. *Eur J Pharm Biopharm* **2007,** 67, (1), 112-9.

(6) McNamara, D. P.; Childs, S. L.; Giordano, J.; Iarriccio, A.; Cassidy, J.; Shet, M. S.; Mannion, R.; O'Donnell, E.; Park, A., Use of a glutaric acid cocrystal to improve oral bioavailability of a low solubility API. *Pharm Res* **2006,** 23, (8), 1888-97.

(7) Remenar, J. F.; Morissette, S. L.; Peterson, M. L.; Moulton, B.; MacPhee, J. M.; Guzman, H. R.; Almarsson, O., Crystal engineering of novel cocrystals of a triazole drug with 1,4-dicarboxylic acids. *J Am Chem Soc* **2003,** 125, (28), 8456-7.

(8) Remenar, J. F.; Peterson, M. L.; Stephens, P. W.; Zhang, Z.; Zimenkov, Y.; Hickey, M. B., Celecoxib:nicotinamide dissociation: using excipients to capture the cocrystal's potential. *Mol Pharm* **2007,** 4, (3), 386-400.

(9) Childs, S. L.; Hardcastle, K. I., Cocrystals of Piroxicam with Carboxylic Acids. *Cryst. Growth Des.* **2007,** 7, (7), 1291-1304.

(10) Higuchi, W. I.; Parker, A. P.; Hamlin, W. E., Dissolution Kinetics of a Weak Acid, 1,1-Hexamethylene P-Tolylsulfonylsemicarbazide, and Its Sodium Salt. *J Pharm Sci* **1965,** 54, 8-11.

(11) Serajuddin, A. T.; Jarowski, C. I., Effect of diffusion layer pH and solubility on the dissolution rate of pharmaceutical acids and their sodium salts. II: Salicylic acid, theophylline, and benzoic acid. *J Pharm Sci* **1985,** 74, (2), 148-54.

(12) Serajuddin, A. T.; Jarowski, C. I., Effect of diffusion layer pH and solubility on the dissolution rate of pharmaceutical bases and their hydrochloride salts. I: Phenazopyridine. *J Pharm Sci* **1985,** 74, (2), 142-7.

(13) Stahl, P. H.; Wermuth, C. G.; International Union of Pure and Applied Chemistry., *Handbook of pharmaceutical salts : properties, selection, and use*. ed.; VHCA ; Wiley-VCH: Weinheim ; New York, 2002; p xiv, 374 p.

(14) Nehm, S. J.; Rodriguez-Spong, B.; Rodriguez-Hornedo, N., Phase solubility diagrams of cocrystals are explained by solubility product and solution complexation. *Cryst. Growth Des.* **2006,** 6, (2), 592-600.

(15) Bhattachar, S. N.; Deschenes, L. A.; Wesley, J. A., Solubility: it's not just for physical chemists. *Drug Discov Today* **2006,** 11, (21-22), 1012-8.

(16) Corrigan, O. I., Salt Forms: Pharmaceutical Aspects. In *Encyclopedia of pharmaceutical technology*, 2nd ed.; Swarbrick, J.; Boylan, J. C., Eds. Marcel Dekker: New York, 2002; p v.

(17) Miyazaki, S.; Nakano, M.; Arita, T., A comparison of solubility characteristics of free bases and hydrochloride salts of tetracycline antibiotics in hydrochloric acid solutions. *Chem Pharm Bull (Tokyo)* **1975,** 23, (6), 1197-204.

(18) Miyazaki, S.; Oshiba, M.; Nadai, T., Precaution on use of hydrochloride salts in pharmaceutical formulation. *J Pharm Sci* **1981,** 70, (6), 594-6.

(19) Jayasankar, A.; Reddy, L. S.; Bethune, S. J.; Rodríguez-Hornedo, N., The role of cocrystal and solution chemistry on the formation and stability of cocrystals with different stoichiometry. *Cryst. Growth Des.* **2008,** Accepted.

(20) Nicoli, S.; Bilzi, S.; Santi, P.; Caira, M. R.; Li, J.; Bettini, R., Ethyl-paraben and nicotinamide mixtures: Apparent solubility, thermal behavior and X-ray structure of the 1:1 co-crystal. *J Pharm Sci* **2008**.

(21) Rodríguez-Hornedo, N.; Nehm, S. J.; Seefeldt, K. F.; Pagan-Torres, Y.; Falkiewicz, C. J., Reaction crystallization of pharmaceutical molecular complexes. *Mol Pharm* **2006,** 3, (3), 362-7.

(22) Klussmann, M.; White, A. J. P.; Armstrong, A.; Blackmond, D. G., Rationalization and Prediction of Solution Enantiomeric Excess in Ternary Phase Systems. *Angewandte Chemie International Edition* **2006,** 45, (47), 7985-7989.

(23) Childs, S. L.; Rodríguez-Hornedo, N.; Reddy, L. S.; Jayasankar, A.; Maheshwari, C.; McCausland, L.; Shipplett, R.; Stahly, B. C., Screening strategies based on solubility and solution composition generate pharmaceutically acceptable cocrystals of carbamazepine. *Cryst Eng Comm* **2008,** 10, (7), 856-864.

(24) Chiarella, R. A.; Davey, R. J.; Peterson, M. L., Making Co-Crystals The Utility of Ternary Phase Diagrams. *Cryst. Growth Des.* **2007,** 7, (7), 1223-1226.

(25) Kobayashi, Y.; Ito, S.; Itai, S.; Yamamoto, K., Physicochemical properties and bioavailability of carbamazepine polymorphs and dihydrate. *Int J Pharm* **2000,** 193, (2), 137-46.

(26) Lang, M.; Kampf, J. W.; Matzger, A. J., Form IV of carbamazepine. *J Pharm Sci* **2002,** 91, (4), 1186-90.

(27) Rodríguez-Spong, B.; Price, C. P.; Jayasankar, A.; Matzger, A. J.; Rodríguez-Hornedo, N., General principles of pharmaceutical solid polymorphism: a supramolecular perspective. *Adv Drug Deliv Rev* **2004,** 56, (3), 241-74.

(28) Childs, S. L.; Wood, P. A.; Rodríguez-Hornedo, N.; Reddy, L. S.; Bates, S.; Hardcastle, K. I., Analysis of fifty structures containing carbamazepine using the Materials Module of Mercury CSD. *Cryst. Growth Des.* **2008**.

(29) Bethune, S.; Maheshwari, C.; Jayasankar, A.; Huang, N.; Rodríguez-Hornedo, N., Designing Cocrystals with Desired pH-dependent Solubility. In *Manuscript in preparation*, ed.; 2008.

(30) Bethune, S. J. Thermodynamic and kinetic parameters that explain solubility and crystallization of pharmaceutical cocrystals. PhD., University of Michigan, Ann Arbor, 2008.

(31) Nehm, S. J.; Jayasankar, A.; Rodríguez-Hornedo, N. In *Cocrystals Impart pH Dependent Solubility to Non-ionizable APIs*, The AAPS Journal, 2006; Abstract W5205: 2006.

(32) Rodríguez-Hornedo, N.; Nehm, S. J.; Jayasankar, A., Cocrystals: Design, Properties and Formation Mechanisms. In *Encyclopedia of Pharmaceutical Technology*, Third ed.; 2006; pp 615 - 635.

(33) Cooke, C. L.; Davey, R. J., On the Solubility of Saccharinate Salts and Cocrystals. *Cryst. Growth Des.* **2008,** 8, (10), 3483-3485.

(34) We adopt the term eutectic to for ternary systems of two solid forms and one solvent in equilibrium consistent with references 35-36. This is not to be confused with origional use of eutiectic for describing binary phase behavior. The eutectic point for these ternary systems are alternartively refered to as an "iosbarothermal or isothermal invariant point" (see reference 37).

(35) Jacques, J.; Wilen, S. H., *Enantiomers, Racemates, and Resolution*. ed.; Krieger Publishing Company: Florida, 1991.

(36) Martin Klussmann, A. J. P. W., Alan Armstrong, Donna G. Blackmond, Rationalization and Prediction of Solution Enantiomeric Excess in Ternary Phase Systems. *Angewandte Chemie International Edition* **2006,** 45, (47), 7985-7989.

(37) Glasstone, S., *Textbook of Physical Chemistry*. 2nd ed.; MacMillan: London, 1948.

(38) Reddy, L. S.; Bethune, S. J.; Kampf, J. W.; Rodríguez-Hornedo, N., Cocrystals and Salts of Gabapentin: pH Dependent Cocrystal Stability and Solubility. *Cryst. Growth Des.* **2009,** 1, (1), 378-385.

(39) Grant, D. J. W.; Higuchi, T., *Solubility behavior of organic compounds*. ed.; Wiley: New York, 1990; p liii, 600 p.

(40) Yalkowsky, S. H., *Solubility and solubilization in aqueous media*. p.61-77 ed.; American Chemical Society ;Oxford University Press: Washington, D.C. New York, 1999; p xvi, 464 p.

(41) Porter III, W. W.; Elie, S. C.; Matzger, A. J., Polymorphism in Carbamazepine Cocrystals. *Cryst. Growth Des.* **2008,** 8, (1), 14-16.

(42) Shan, N.; Zaworotko, M. J., The role of cocrystals in pharmaceutical science. *Drug Discov Today* **2008,** 13, (9-10), 440-6.

(43) Das, S. N.; Ives, D. J. G., Hydrogen Bonding in Acid Malonate Ion. *Proceedings of the Chemical Society of London* **1961**, (OCT), 373-374.

(44) Pudipeddi, M.; Serajuddin, A. T., Trends in solubility of polymorphs. *J Pharm Sci* **2005,** 94, (5), 929-39.

(45) Hancock, B. C.; Parks, M., What is the true solubility advantage for amorphous pharmaceuticals? *Pharm Res* **2000,** 17, (4), 397-404.

(46) Jones, P. H.; Rowley, E.; Weiss, A. L.; Bishop, D. L.; Chun, A. H., Insoluble erythromycin salts. *J Pharm Sci* **1969,** 58, (3), 337-9.

(47) Magerlein, B. J., N-alkylsulfamate salts of lincomycin. *J Pharm Sci* **1965,** 54, (7), 1065-7.

(48) Agharkar, S.; Lindenbaum, S.; Higuchi, T., Enhancement of solubility of drug salts by hydrophilic counterions: properties of organic salts of an antimalarial drug. *J Pharm Sci* **1976,** 65, (5), 747-749.

(49) Wells, J. I., *Pharmaceutical preformulation : the physicochemical properties of drug substances*. ed.; E. Horwood; Halsted Press: Chichester New York, 1988; p 227 p.

(50) Anderson, B. D.; Conradi, R. A., Predictive relationships in the water solubility of salts of a nonsteroidal anti-inflammatory drug. *J Pharm Sci* **1985,** 74, (8), 815-820.

(51) Sanghvi, R.; Evans, D.; Yalkowsky, S. H., Stacking complexation by nicotinamide: a useful way of enhancing drug solubility. *Int J Pharm* **2007,** 336, (1), 35-41.

(52) Black, S. N.; Collier, E. A.; Davey, R. J.; Roberts, R. J., Structure, solubility, screening, and synthesis of molecular salts. *J Pharm Sci* **2007,** 96, (5), 1053-1068.

(53) Aakeroy, C. B.; Desper, J.; Scott, B. M., Balancing supramolecular reagents for reliable formation of co-crystals. *Chem Commun (Camb)* **2006**, (13), 1445-7.

(54) Stanton, M. K.; Bak, A., Physicochemical Properties of Pharmaceutical Co-Crystals: A Case Study of Ten AMG 517 Co-Crystals. *Cryst. Growth Des.* **2008**.

(55) Rubino, J. T., Solubilities and solid state properties of the sodium salts of drugs. *J Pharm Sci* **1989,** 78, (6), 485-489.

(56) Thomas, E.; Rubino, J., Solubility, melting point and salting-out relationships in a group of secondary amine hydrochloride salts. *Int. J. Pharm.* **1996,** 130, (2), 179-185.

2.6. APPENDIX

X-ray powder diffraction pattern of the THP-NCT cocrystal.

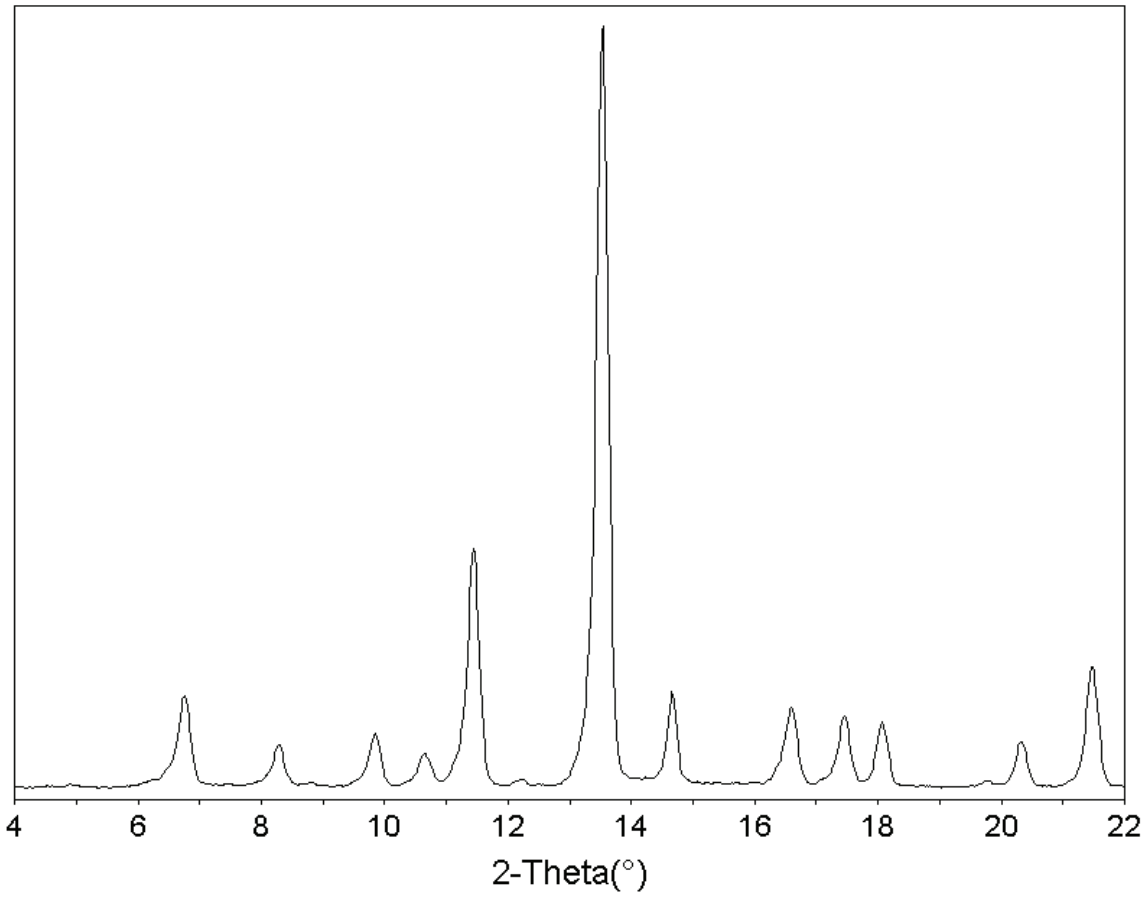

CHAPTER 3

COCRYSTAL EUTECTIC CONSTANTS AND PREDICTION OF SOLUBILITY BEHAVIOR

Cocrystals are an emerging class of engineered solid forms and understanding their solution phase behavior and solubility is essential to their screening, synthesis, characterization, manufacture and utility.[1-3] Pharmaceutical cocrystals are important for improving the physicochemical and biopharmaceutical properties of drugs without changing their chemical structure. For the first time we are showing that the eutectic solution composition of cocrystal components (drug and coformer) is defined by the solubility of cocrystal and drug in pure solvent. The cocrystal to drug solubility ratio (α) is shown to determine the excess eutectic coformer concentration and the eutectic constant (K_{eu}), which is the ratio of solution concentrations of cocrystal components at the eutectic. The solution eutectic composition and cocrystal solubility ratio are a function of component ionization, complexation, solvent, and stoichiometry. These fundamental relationships can be applied to predict the solubility and thermodynamic stability of new cocrystals.

The importance of eutectic constants has been demonstrated for the enantiomeric purification and stability of racemic compounds.[4-6] However, the relationships

established for racemates are not directly applicable to cocrystals where the components differ greatly in structural and chemical properties. The equilibrium equations that specify eutectic points also differ between cocrystals and racemates. We additionally seek to describe complexation and ionization effects on cocrystal eutectic and solubility behavior and include the relevant chemical equilibria.

3.1. THEORETICAL

3.1.1. Cocrystal eutectic constants and solution equilibrium

Three equations and equilibrium constants are considered to predict the cocrystal solubility, eutectic composition, and solution complexation from the eutectic of solid drug A and cocrystal A_yB_z where B is coformer:

I. $A_{solid} \rightleftharpoons A_{soln}$ $\qquad S_{drug} = a_{drug}$

II. $A_yB_z{}_{solid} \rightleftharpoons yA_{soln} + zB_{soln}$ $\qquad K_{sp} = a_{drug}^{y} a_{coformer}^{z}$

III. $A_{soln} + B_{soln} \rightleftharpoons AB_{soln}$ $\qquad K_{11} = \dfrac{a_{complex}}{a_{drug} a_{coformer}}$

where S_{drug}, K_{sp}, and K_{11} are the drug solubility in pure solvent, cocrystal solubility product and complexation constant, respectively. Apparent K_{11} values have been shown as adequate quantitative descriptors of complexation for 2:1 and 1:1 cocrystals considered in this chapter.[7] Activity coefficients are relatively constant for the dilute solutions and concentration ranges considered in this work. Thermodynamic and apparent equilibrium constants for these expressions are proportional such that any non-ideal mixing of solution species does not necessitate a detailed analysis of activity coefficients as a function of composition. Combining the K_{11}, K_{sp} and S_{drug} gives the concentration of complex at the eutectic as:

$$[AB]_{soln} = K_{11}\left(K_{sp} S_{drug}^{(z-y)}\right)^{1/z}$$

For poorly water soluble drugs and more soluble coformers we consider the eutectic (E_1) for solid drug and cocrystal in equilibrium with solution. This eutectic is most relevant for describing cocrystal solubility, stability, and equilibrium behavior relative to the drug. The eutectic constant (K_{eu}) is the concentration ratio of total coformer to total drug that satisfies the equilibrium equations I-III.

$$K_{eu} = \frac{[B]_{eu}}{[A]_{eu}} = \frac{[B]+[AB]}{[A]+[AB]} = \left[\frac{(K_{sp} \Big/ S_{drug}^{y})^{1/z} + K_{11}\left(K_{sp} S_{drug}^{(z-y)}\right)^{1/z}}{S_{drug} + K_{11}\left(K_{sp} S_{drug}^{(z-y)}\right)^{1/z}} \right] \qquad 3.1$$

Cocrystal K_{sp} and drug solubility represent the eutectic concentrations of free components and are combined with the prior expression for the concentration of the eutectic complex based on K_{11}. Considerations of ionization for either component can be added to this equation. For the case of a monoprotic acidic coformer and basic drug Equation 3.1 is rewritten as:

$$\begin{aligned} K_{eu} &= \frac{[B]_{eu}}{[A]_{eu}} = \frac{[B]_{\text{unionized}} + [B]_{\text{ionized}} + [AB]}{[A]_{\text{unionized}} + [A]_{\text{ionized}} + [AB]} \\ &= \left[\frac{(K_{sp} \Big/ S_{drug}^{y})^{1/z}\left(1 + \frac{Ka_{coformer}}{[H^+]}\right) + K_{11}\left(K_{sp} S_{drug}^{(z-y)}\right)^{1/z}}{S_{drug}\left(1 + \frac{[H^+]}{Ka_{drug}}\right) + K_{11}\left(K_{sp} S_{drug}^{(z-y)}\right)^{1/z}} \right] \end{aligned} \qquad 3.2$$

where $[H^+]$ is the hydrogen ion concentration and (K_a) is the dissociation constant for the acidic coformer or the conjugate acid of the basic drug. In this case high pH decreases the solubility of basic drug and increases K_{eu}, resulting in an increase of cocrystal solubility relative to the drug. For cases of other acidic or basic components, the reader is

referred to recent publications on cocrystal ionization.[8-10] Considering the general case of components with multiple K_a's the K_{eu} as a function of pH is:

$$K_{eu} = \frac{\left(\frac{K_{sp}}{S_{drug}^{y}}\right)^{1/z}\left(1+\sum_{f=1}^{g}\frac{\prod_{h=1}^{f}Ka_h^{acidic}}{[H^+]^f}+\sum_{i=1}^{j}\frac{[H^+]^i}{\prod_{k=1}^{i}Ka_k^{basic}}\right)_{coformer} + K_{11}\left(K_{sp}S_{drug}^{(z-y)}\right)^{1/z}}{S_{drug}\left(1+\sum_{l=1}^{m}\frac{\prod_{n=1}^{l}Ka_n^{acidic}}{[H^+]^l}+\sum_{p=1}^{q}\frac{[H^+]^p}{\prod_{r=1}^{p}Ka_r^{basic}}\right)_{drug} + K_{11}\left(K_{sp}S_{drug}^{(z-y)}\right)^{1/z}} \quad 3.3$$

where g and m are the total number of acidic groups for each component and j and q are the corresponding total number of basic groups. In this case, the eutectic constant is a function of the cocrystal solubility product, drug solubility, and ionization. This equation simplifies to Equation 3.1 when none of the cocrystal components are ionizable (*g=m=j=q=0)*. For the case of negligible solution complexation Equation 3.3 simplifies to:

$$K_{eu} = \left(\frac{K_{sp}\delta_{coformer}^{z}}{S_{drug}^{(y+z)}\delta_{drug}^{z}}\right)^{\frac{1}{z}} \quad 3.4$$

where the ionization terms in Equation 3.3 for drug and coformer equal δ_{drug} and $\delta_{coformer}$, respectively:

$$\delta_{drug} = \left(1 + \sum_{l=1}^{m} \frac{\prod_{n=1}^{l} Ka_n^{acidic}}{[H^+]^l} + \sum_{p=1}^{q} \frac{[H^+]^p}{\prod_{r=1}^{p} Ka_r^{basic}} \right)_{drug}$$

and $$\delta_{coformer} = \left(1 + \sum_{f=1}^{g} \frac{\prod_{h=1}^{f} Ka_h^{acidic}}{[H^+]^f} + \sum_{i=1}^{j} \frac{[H^+]^i}{\prod_{k=1}^{i} Ka_k^{basic}} \right)_{coformer}$$

K_{eu} can also be expressed as a function of the cocrystal to drug solubility ratio (α) in pure solvent using the previously described equation for cocrystal solubility[11]:

$$K_{eu} = z y^{y/z} \alpha^{\frac{y+z}{z}} \qquad 3.5$$

where $\alpha = S_{cocrystal} \Big/ (S_{drug}\, \delta_{drug})$ and $S_{cocrystal} = \sqrt[y+z]{K_{sp} \delta_{coformer}^{z} \delta_{drug}^{y} / \left(y^y z^z \right)}$

For a drug with known solubility, Equation 3.5 allows prediction of cocrystal solubility from the eutectic constant or vice versa. For a 1:1 cocrystal (*i.e.* y=z=1) K_{eu} from Equation 3.5 becomes the square of the solubility ratio of cocrystal to drug in pure solvent:

$$K_{eu} = \frac{[B]_{eu}}{[A]_{eu}} = \alpha^2$$

Therefore, a cocrystal with five times higher solubility has a twenty five times greater K_{eu}. Furthermore, a K_{eu} greater than one indicates the 1:1 cocrystal is more soluble than the drug, whereas cocrystals less soluble than the drug have K_{eu} values below one. The

predicted relationship according to Equation 3.5 is presented in Figure 3.1. The derived equations apply to any ionization or temperature condition as long as the appropriate equilibria constants and solubilites are taken into consideration. Description of the temperature dependence of K_{eu} is presented in Chapter 4.

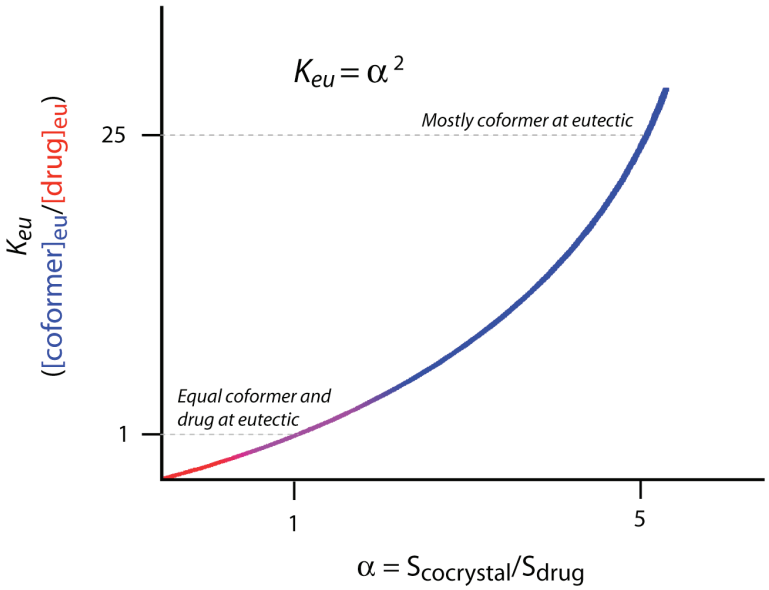

Figure 3.1: Plot of K_{eu} against α from Equation 3.5 for a 1:1 cocrystal. The color change of the line from red to blue is representative of the eutectic concentrations changing from mostly drug (low K_{eu}) to mostly coformer (high K_{eu}).

It can also be shown for 1:1 cocrystals that the percent excess coformer at the eutectic (xs_B) is purely a function of the solubility ratio. The eutectic ratio of coformer to drug minus one divided by the eutectic ratio plus one gives the fraction of excess coformer relative to the total solute (drug and coformer) at the eutectic. Here we substitute K_{eu} for α as defined in Equation 3.5 for a 1:1 cocrystal:

$$xs_b = \frac{\frac{[B]_{eu}}{[A]_{eu}} - 1}{\frac{[B]_{eu}}{[A]_{eu}} + 1} = \frac{[B]_{eu} - [A]_{eu}}{[B]_{eu} + [A]_{eu}} =$$

$$\frac{K_{eu} - 1}{K_{eu} + 1} = \frac{\alpha^2 - 1}{\alpha^2 + 1}$$

Therefore:

$$xs_B = \frac{\left(\alpha^2 - 1\right)}{\left(\alpha^2 + 1\right)} \times 100 = \frac{\left([coformer]_{eu} - [drug]_{eu}\right)}{\left([coformer]_{eu} + [drug]_{eu}\right)} \times 100 \qquad 3.6$$

A 1:1 cocrystal with $xs_B>0$ requires a solution excess of coformer to form cocrystal. Conversely, cocrystal is thermodynamically stable relative to drug in pure solvent for cases with equal or excess $[drug]_{eu}$ ($xs_B \leq 0$). Additional eutectic considerations are recommended for systems that require excess drug in solution to form cocrystal or when coformer is less soluble than drug (following section).

3.1.2. K_{eu} values and triangular phase diagrams for cocrystals with multiple solution eutectic points

The relationships presented for the eutectic constants in the previous section apply to the eutectic involving solid drug and cocrystal in equilibrium with solution (E_1). A second eutectic (E_2) can be considered for solid coformer and cocrystal in equilibrium with solution. Either eutectic can be used to calculate cocrystal solubility behavior. Determining E_2 can be useful in instances where coformer is less soluble than drug and

therefore excess drug is require to form cocrystal. The three equations and equilibrium constants for E_2 with solid coformer B and cocrystal A_yB_z where A is drug are:

IV. $B_{solid} \rightleftharpoons B_{soln}$ $\qquad S_{coformer} = a_{coformer}$

V. $A_yB_z{}_{solid} \rightleftharpoons yA_{soln} + zB_{soln}$ $\qquad K_{sp} = a_{drug}^{y} a_{coformer}^{z}$

VI. $A_{soln} + B_{soln} \rightleftharpoons AB_{soln}$ $\qquad K_{11} = \dfrac{a_{complex}}{a_{drug} a_{coformer}}$

The same methods presented for E_1 were followed for E_2 to solve the eutectic constant (K_{eu2}) that is the concentration ratio of total coformer to total drug satisfying the equilibrium equations IV-VI.

$$K_{eu2} = \frac{[B]_{total}}{[A]_{total}} = \frac{[B]+[AB]}{[A]+[AB]} = \left[\frac{S_{coformer}\delta_{coformer} + K_{11}\left(K_{sp}S_{coformer}^{(y-z)}\right)^{1/y}}{(K_{sp}/S_{coformer}^{z})^{1/y}\delta_{drug} + K_{11}\left(K_{sp}S_{coformer}^{(y-z)}\right)^{1/y}} \right]$$

For systems that do not exhibit complexation this equation can be reduced to:

$$K_{eu2} = \frac{[B]_{total}}{[A]_{total}} = \left(\frac{S_{coformer}^{y+z}\delta_{coformer}^{y}}{K_{sp}\delta_{drug}^{y}} \right)^{\frac{1}{y}}$$

This equation is analogous to Equation 3.4 for E_1, however the component solubility and cocrystal K_{sp} are inverted. To express the K_{eu2} in terms of the cocrystal to component solubility values we take the reciprocal so that $1/K_{eu2}$ is:

$$K_{eu2}^{-1} = \frac{[A]_{total}}{[B]_{total}} = \left(\frac{K_{sp}\delta_{drug}^{y}}{S_{coformer}^{y+z}\delta_{coformer}^{y}} \right)^{\frac{1}{y}}$$

Inserting the cocrystal solubility to coformer solubility ratio (β) in pure solvent using the previously described equation for cocrystal solubility gives:

$$K_{eu2}^{-1} = yz^{z/y}\beta^{\frac{y+z}{y}}$$

where $\beta = S_{cocrystal} / (S_{coformer}\delta_{coformer})$ and $S_{cocrystal} = \sqrt[y+z]{K_{sp}\delta_{coformer}^{z}\delta_{drug}^{y} / (y^{y}z^{z})}$

This is comparable to Equation 3.5 for E_1 in that the eutectic concentrations are a function of cocrystal and component solubilities. Simplifying for the case of a 1:1 cocrystal gives:

$$K_{eu2}^{-1} = \beta^{2}$$

The E_1 eutectic involving solid drug and cocrystal is shown in the Figure 3.2 triangular phase diagram (TPD). The eutectic of solid coformer and cocrystal in equilibrium with solution is indicated by E_2. Here we demonstrate the K_{eu} expressions for both E_1 and E_2 as described by the TPD. For E_1 and E_2 the ratio of coformer to drug in solution is determined by extending a line from pure solvent through the eutectic to the base of the diagram to determine the points x_1 and x_2, respectively. The eutectic ratio (K_{eu1}) of coformer to drug at E_1 is then x_1 divided by ($1-x_1$). The same relation holds for E_2 and x_2. It is apparent from the TPD that saturated solutions with compositions between E_1 and E_2 are thermodynamically stable conditions with respect to cocrystal. All other saturated solutions for which compositions fall outside these two eutectic constants will correspond to regions where either pure drug or coformer is stable. For the case of a

1:1 cocrystal this would mean it is stable when suspended in pure solvent (i.e. congruently saturating) if $E_1<1< E_2$. Figure 3.2 represents the case where $1<E_1< E_2$, which means for a 1:1 cocrystal that it is unstable when suspended in pure solvent (i.e. incongruently saturating).

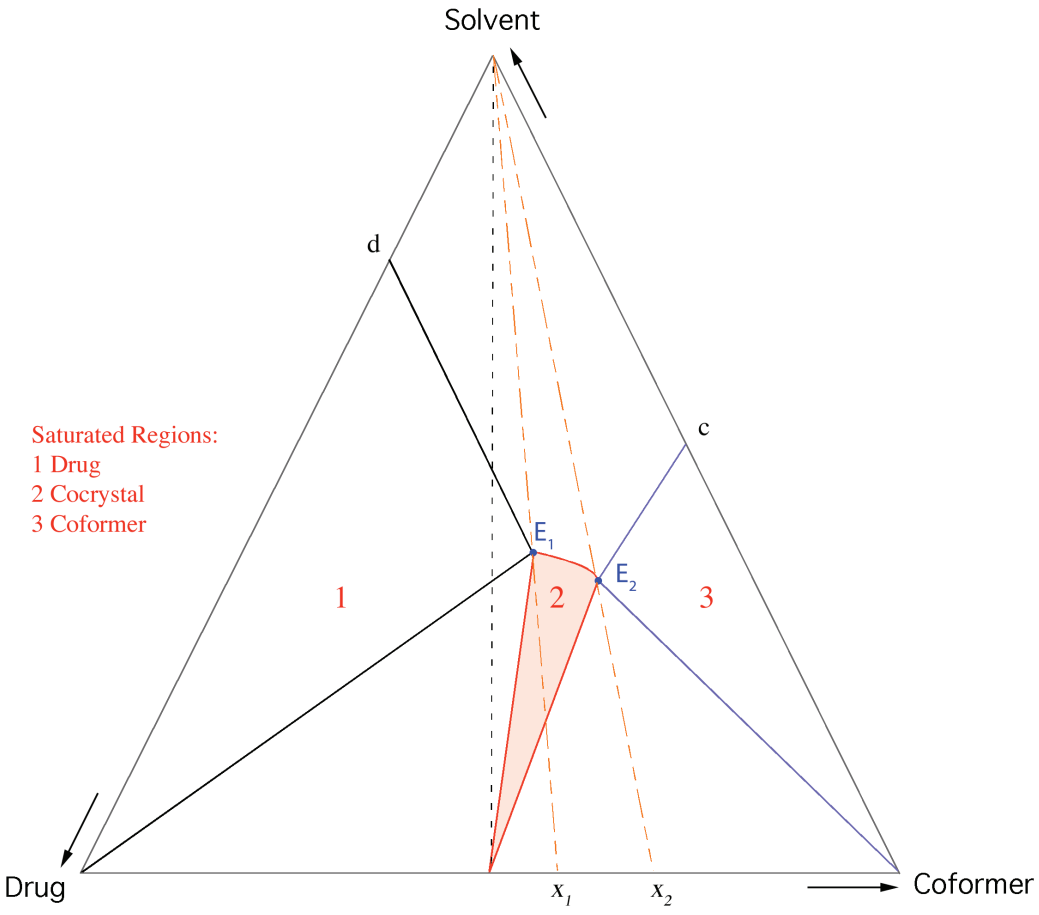

$$K_{eu1} = \frac{x_1}{1 - x_1} \qquad K_{eu2} = \frac{x_2}{1 - x_2}$$

Figure 3.2: Phase diagram of cocrystal (incongruently saturating) indicating the three regions saturated with respect to (1) drug, (2) cocrystal, or (3) coformer. The two eutectics are represented by E_1 and E_2 with lines extending from the solvent apex to the base to indicate the eutectic solution compositions x_1 and x_2. Drug and coformer solubilities in pure solvent are represented by d and c, respectively.

Because E_1 and E_2 involve different solid cocrystal components the K_{eu} values have an inverse relationship to the cocrystal solubility as described above. K_{eu1} for E_1 of a 1:1 cocrystal is the square of the ratio (α) of cocrystal solubility to drug solubility in pure solvent:

$$K_{eu1} = \left(\frac{S_{cocrystal}}{S_{drug}} \right)^2 = \alpha^2$$

Similarly for E_2 the square of the cocrystal to coformer solubility ratio (β) in pure solvent equals $1/K_{eu2}$:

$$K_{eu2}^{-1} = \left(\frac{S_{cocrystal}}{S_{coformer}} \right)^2 = \beta^2$$

For 1:1 cocrystals these two eutectic constants define the relationship between cocrystal and component solubilities. These equations apply to 1:1 cocrystals regardless of the relative solubilities of the two components in pure solvent. K_{eu} values from these equilibrium expressions and corresponding equations can be used to describe cocrystals comprised of a drug that is either equally, more, or less soluble than the coformer.

It follows from the analysis of E_1 and E_2 that similar equations can be derived for cocrystals with multiple stoichiometeries, which exhibit additional eutectics corresponding to two solid cocrystals with different ratios of the same components in equilibrium with solution. In these cases the eutectic concentrations of the coformer and drug will depend on the K_{sp} values and solubilities of the two cocrystal forms as well as the solution ionization and/or complexation. Equations for other solid phases in equilibrium with solution at the different eutectics involving cocrystal are presented in Table 3.1. These equations can be used to determine the cocrystal solubility ratio relative the other solid phase from measurement of the appropriate K_{eu} value. Alternatively,

known K_{sp} or $S_{cocrystal}$ values can be used together with know component solubilities to predict the K_{eu} value and therefore the excess amount of a component required in solution to stabilize a cocrystal suspension.

Table 3.1: Relationships of eutectic compositions and cocrystal/component solubilities based on ideal behavior for systems with negligible solution complexation.

Solid phases at eutectic	$K_{eu}\ f(K_{sp})$	$K_{eu}\ f(S_{cocrystal})$
1:1 + 2:1 cocrystals	$\frac{a_B}{a_A} = \frac{K_{sp(1:1)}^3}{K_{sp(2:1)}^2}$	$\frac{S_{(1:1)cocrystal}}{S_{(2:1)cocrystal}} = K_{eu}^{1/6}$
1:1 cocrystal + drug	$\frac{a_B}{a_A} = \frac{K_{sp}}{S_A^2}$	$\frac{S_{cocrystal}}{S_A} = K_{eu}^{1/2}$
1:1 cocrystal + coformer	$\frac{a_B}{a_A} = \frac{S_B^2}{K_{sp}}$	$\frac{S_{cocrystal}}{S_B} = K_{eu}^{-1/2}$
2:1 cocrystal + drug	$\frac{a_B}{a_A} = \frac{K_{sp}}{S_A^3}$	$\frac{S_{cocrystal}}{S_A} = K_{eu}^{1/3}$

3.2. MATERIALS AND METHODS

3.2.1. Calculation of solubility product from phase solubility diagrams

Several examples taken from the literature exhibit phase solubility behavior often referred to as B_s type behavior illustrated in Figure 3.3.[12] To extract the relevant eutectic and solubility product values under equilibrium conditions, solution concentrations at equilibrium with the various solid phases were calculated from the original plots that reported *initial* total concentration of B and measured concentration of A at *equilibrium*.

A similar analysis was presented by Zughul and Badwan.[13] As shown in Figure 3.3 the plateau (region II) of these phase diagrams is removed when plotting the equilibrium concentrations of A and B. The mass balance of this plateau equates to the amount of complex precipitated from solution in proportion to the mass of solid component A initially added to the sample vial. For our analysis all points in the descending portion (region III) are shifted toward the left most point of the plateau by a magnitude equal to the plateau length. This treatment excises the portion related to the formation and precipitation of complex due to the excess component A present based on the experimental methods. What remains is a representation of the equilibrium phase solubility diagram (PSD - Figure 3.3b) where the x-axis is solution concentration of component B. This axis previously (Figure 3.3a) indicated the amount of ligand added per volume of solvent, which was not the equilibrium concentration of ligand in solution. The new equilibrium PSD resembles those previously published from our laboratory where one point, the eutectic, separates two regions (1) an ascending portion where drug is the stable solid phase and solution complexation produces increasing drug concentrations and (2) the descending portion corresponding to K_{sp} behavior where cocrystal is thermodynamically stable.

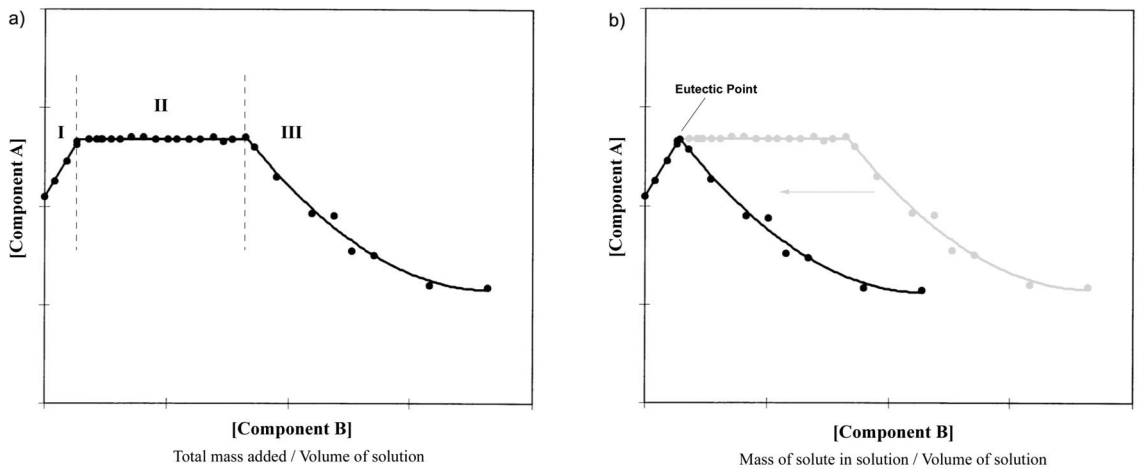

Figure 3.3: a) Typical literature B_s type phase solubility diagram indicating region I (complexation), II (conversion and precipitation of excess component A), and III (solubility of precipitated complex is decreased with increasing B in solution). b) Conversion of B_s type PSD into equilibrium PSD where the region three is shifted to the leftmost end of the region II plateau. Grey segments indicate original portions of the B_s PSD that were shifted or removed. Schematic based on Higuchi and Connors data for the concentration of 1,2-dimethylbenzoylurea (A) versus catechol (B) in CCl_4 at 25°C.[7]

The experimental K_{eu} values extracted are the ratio of concentrations for the left most point of the PSD plateau. This point is also labeled as the eutectic in Figure3.3b. K_{11} complexation constants (i.e. stability constants: K_c) were use directly as reported in the referenced articles, where they were calculated from region I of the phase diagrams. The reported K_{11} values for complexes from the literature were between 1 and 51 m^{-1}. The stoichiometries of the complexes were also used as reported in the referenced literature. K_{sp} values of systems that precipitate as 2:1 complexes were determined by non-linear regression of the descending portion of the equilibrium PSDs according to previously published equations:[14]

$$[A]_{total} = \sqrt{\frac{K_{sp}}{C_1}} + K_{11}\sqrt{C_1 K_{sp}} \qquad 3.7$$

where $C_1 = (2[B]_{total} + K_{11}^2 K_{sp} - 2K_{11}\sqrt{K_{sp}[B]_{total}}) / 2$

$$[A]_{total} = \sqrt{\frac{K_{sp}}{C_2}} + K_{11}\sqrt{C_2 K_{sp}} \qquad 3.8$$

where $C_2 = (2[B]_{total} + K_{11}^2 K_{sp} + 2K_{11}\sqrt{K_{sp}[B]_{total}}) / 2$

Both these equations were used to fit experimental data and the equation with the best statistical fit was used for determination of K_{sp} and K_{11} values. Solution of these equations was preformed using SigmaPlot statistical/graphing software. These two equations were solved with the dynamic fit function based on a minimum of five hundred iterations and values were used from the equation that provided the lowest standard error. A sample fit for benzodiazine-phenol (2:1) phase diagram determined at controlled pH is shown in Figure 3.4. The K_{sp} of 1:1 complexes were determined from the linear slope by plotting substrate concentration against the inverse of the ligand concentration as described previously by the equation:[15]

$$[A]_{total} = \frac{K_{sp}}{[B]_{total} - K_{11}K_{sp}} + K_{11}K_{sp}$$
$$\text{for} \quad K_{11}K_{sp} << [B]_{total} \qquad 3.9$$
$$[A]_{total} = \frac{K_{sp}}{[B]_{total}} + K_{11}K_{sp}$$

All predicted K_{eu} and α values were calculated using K_{sp} and K_{11} values determined by these methods from experimental phase diagrams unless otherwise noted. For those samples that phase solubility diagrams were not determined the predicted K_{eu} and α values are from the eutectic concentrations where $K_{sp} = S_{drug}^{y}[B]_{eu}^{z}$ as indicated in Chapter 2. K_{11} values for these samples were either determine from the difference between $[drug]_{eu}$ and S_{drug} or from measurement of the drug concentration as a function of coformer in dilute coformer solutions. Samples for which these alternative methods were used based on eutectic concentrations are noted in Table 3.2 and Appendix 3.6.

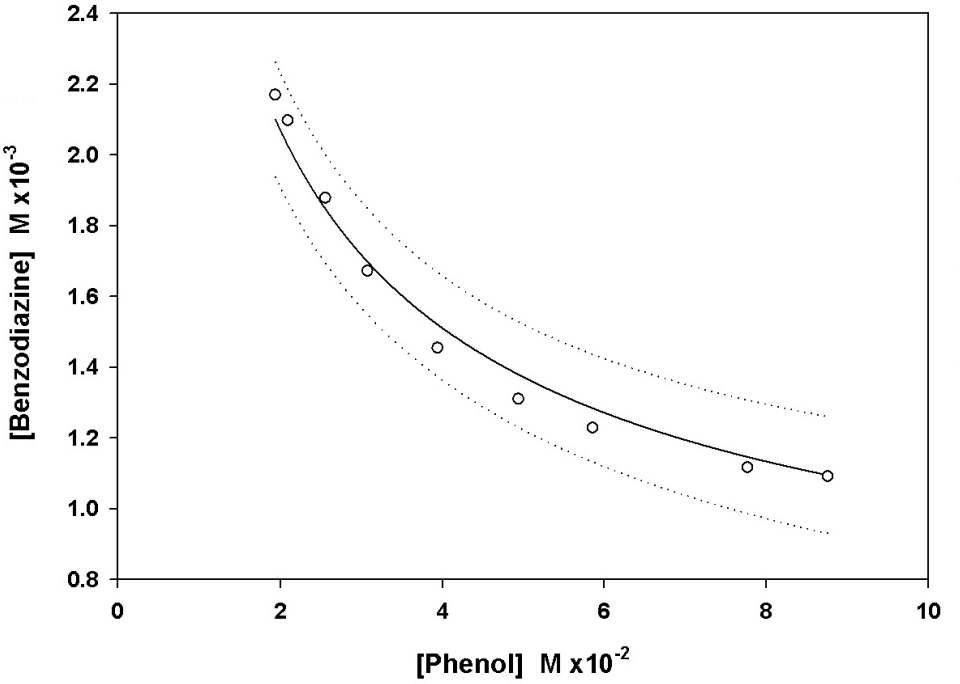

Figure 3.4: K_{sp} determined by nonlinear fit of the PSD for 2,3-diketo-1,2,3,4-tetrahydroquinoxaline and phenol. The solid line represents the best fit from Equations 3.7 and 3.8 corresponding to $K_{sp} = 8.08\text{x}10^{-8}\text{M}^3(\pm 4.29\text{x}10^{-9}$ SE) and $K_{11} = 1.6\text{M}^{-1}$. Dotted lines represent the 95th percent confidence interval based on the standard error. Data taken from reference [16].

3.2.2. High performance liquid chromatography (HPLC)

Solution concentrations of drug and ligand were analyzed by Waters HPLC (Milford, MA) equipped with a UV/Vis spectrometer detector. A C18 Atlantis column (5μm, 4.6 x 250mm; Waters, Milford, MA) at ambient temperature was used to separate the drug and the ligand. A gradient method with a water, methanol, and trifluoroacetic acid mobile phase was used with a flow rate of 1mL/min. Sample injection volume was 20μL. Absorbance of the drug and ligand analytes was monitored between 210-300nm. Empower software from Waters was used to collect and process the data. All concentrations are reported in molality (moles solute/kilogram solvent).

3.2.3. X-ray powder diffraction (XRPD)

XRPD was used to identify crystalline phases after slurrying samples to determine cocrystal eutectic concentrations and confirm the proper two solid phases (drug and cocrystal) were in equilibrium with the solution. XRPD patterns of solid phases were obtained with a Rigaku MiniFlex X-ray diffractometer (Danvers, MA) using Cu Kα radiation (λ = 1.5418 Å), a tube voltage of 30 kV, and a tube current of 15 mA. The intensities were measured at 2θ values from 2° to 30° with a continuous scan rate of 2.5°/min. Samples, prior to and after slurry reactions, were analyzed by XRPD. Results

were compared to diffraction patterns reported in literature or calculated from crystal structures published in the Cambridge Structural Database.

3.2.4. Materials

Anhydrous monoclinic form III carbamazepine (CBZ(III)) was purchased from Sigma-Aldrich (99+% purity) and were used as received. Carbamazepine dihydrate (CBZ(D)) was prepared by stirring CBZ(III) in water for at least twenty-four hours. The cocrystal ligands nicotinamide (NCT), glutaric acid (GTA), saccharin (SAC), anhydrous oxalic acid (OXA), succinic acid (SUC), and salicylic acid (SLC) were purchased from Sigma-Aldrich (99+% purity) and used as received. All crystalline drugs and ligands were characterized by X-ray powder diffraction (XRPD) and Raman spectroscopy before carrying out experiments. No impurities in the form of additional peaks were resolved during HPLC analysis of solutions containing the drugs or ligands in this study. Ethanol (EtOH), isopropyl alcohol (IPA), and ethyl acetate (EtOAc) were obtained from Fisher Scientific and dried using molecular sieves prior to use. All the cocrystals used for solubility studies were precipitated from ligand solutions by adding solid drug according to the reaction crystallization method (RCM).[17, 18] Cocrystals of CBZ-NCT and CBZ-SAC throughout the chapter refer to the form I polymorphs.[19]

3.3. RESULTS AND DISCUSSION

3.3.1. Solution properties of cocrystals and cocrystal components

More than forty cocrystal and solvent combinations were analyzed to examine the general applicability of the derived relationships. These cocrystals represent a diverse range of solution chemistry with various levels of solution complexation and ionization, as well as different crystal stoichiometries and supramolecular interactions. Cocrystals were predominantly studied in aqueous solutions by previously reported methods.[11] Several organic solvents were used as non-ionizing alternatives or to alter component solubilities. Tables 3.2 and 3.3 show the cocrystals analyzed, their components, and the range of several critical parameters associated with their solubility and thermodynamic stability. K_{sp} values were calculated from the descending portion of phase solubility diagrams according to published methods, unless otherwise noted.[14, 15, 20] Complexation constants were also calculated or used as reported in the literature. Sample calculations are provided in Appendix 3.6.

Table 3.2: Cocrystals analyzed for solubility behavior and eutectic constants.

Group	Component(s) A	Component(s) B	Stoichiometry	Solvent (pH)	Temperature (^{O}C)	Reference
I	(1) 4-hydroxybenzoic acid; (2) phenobarbital	caffeine	1:1	a (<1)	15	21, 22
I	(3) 2-hydroxybenzoic acid; (4) 3-hydroxybenzoic acid; (5) 4-aminobenzoic acid	caffeine	1:1	a (<1)	30	22-24
I	acetaminophen	(6) caffeine; (7) theophylline	1:1	a (<1)	25	25
II	1,4-diketo-2,3-dimethyl-1,2,3,4-tetrahydrophthalazine	(1) hydroquinone	2:1	a (<1)	30	16
II	1,4-dimethyl-1,2,3,4-tetrahydroquinoxaline	(2) catechol; (3) phenol; (4) resorcinol	2:1	a (<1)	30	16
II	1-methyl-2,3-diketo-1,2,3,4-tetrahydroquinoxaline	(5) resorcinol	2:1	a (<1)	30	16
II	1-methyl-2-keto-3-methoxy-1,2-dihydroquinoxaline	(6) hydroquinone; (7) phenol	2:1	a (<1)	30	16
II	2,3-diketo-1,2,3,4-tetrahydroquinoxaline	(8) catechol; (9) phenol; (10) resorcinol	2:1	a (<1)	30	16
III	(1) 2-hydroxybenzoic acid; (2) 4-hydroxybenzoic acid; (3) 2,4-dihydroxybenzoic acid; (4) 3,4-dihydroxybenzoic acid	sarcosine anhydride	2:1	a (<1)	25	26
III	(5) 1,5-napthalenediol	sarcosine anhydride	1:1	a (<1)	25	26
IV	carbamazepine	(1) saccharin; (2) salicylic acid	1:1	a(1-5),b,c,d	25	[b]
IV	carbamazepine	(3) 4-aminobenzoic acid	2:1	b	25	[b]
IV	carbamazepine	(4)[a] succinic acid; (5)[a] oxalic acid	2:1	a(3,1.3)	25	[b]
IV	carbamazepine	(6)[a] glutaric acid; (7)[a] nicotinamide	1:1	a(2,6),b,c,d	25	[b]
V	sulfamethazine	benzoic acid	1:1	a(4.3)	25	[b]

Samples are referred to by group, number, and solvent such as: IV(3)b. The eutectics studied involve solid phases of component A and cocrystal in equilibrium with solution. The samples are grouped based on source and common components, properties, or experimental conditions. Solvents: a) water, b) ethanol, c) 2-propanol, d) ethyl acetate. [a] Denotes samples where the eutectic concentrations were used to calculate both K_{eu} and K_{sp}. [b] Data from current work in addition to results from references[9, 11, 14, 15, 27].

Table 3.3: Range of cocrystal and component parameters.

	Minimum	Maximum
K_{eu}	0.1	270
K_{sp}	8.1×10^{-8} m^3	7.3×10^{-2} m^2
K_{11}	0 m^{-1}	51 m^{-1}
Component solubility	5×10^{-4} m	10 m

All cocrystals in Table 3.2 demonstrated solubility product behavior and measured or reported phase solubility diagrams were used to calculate K_{sp} values for the majority of these samples. The data used for Group I-V samples to calculate K_{sp} values is shown in Figure 3.5. Solid lines indicate the predicted solubility behavior for each cocrystal based on K_{11} values and the calculated K_{sp} from Equations 3.7-3.9. The calculated K_{eu}, K_{sp} and K_{11} values for these cocrystals are listed in Appendix II along with the observed K_{eu} values and plots of the data for each cocrystal studied. The observed eutectic concentrations for group IV cocrystals were determined in Chapter 2 and the corresponding K_{eu} values are listed in Appendix 3.6. For all other cocrystals the point corresponding to the maximum drug concentration from the phase solubility diagrams (Figure 3.5 or Appendix 3.6) were used as the observed eutectic concentrations for determining the observed K_{eu} values.

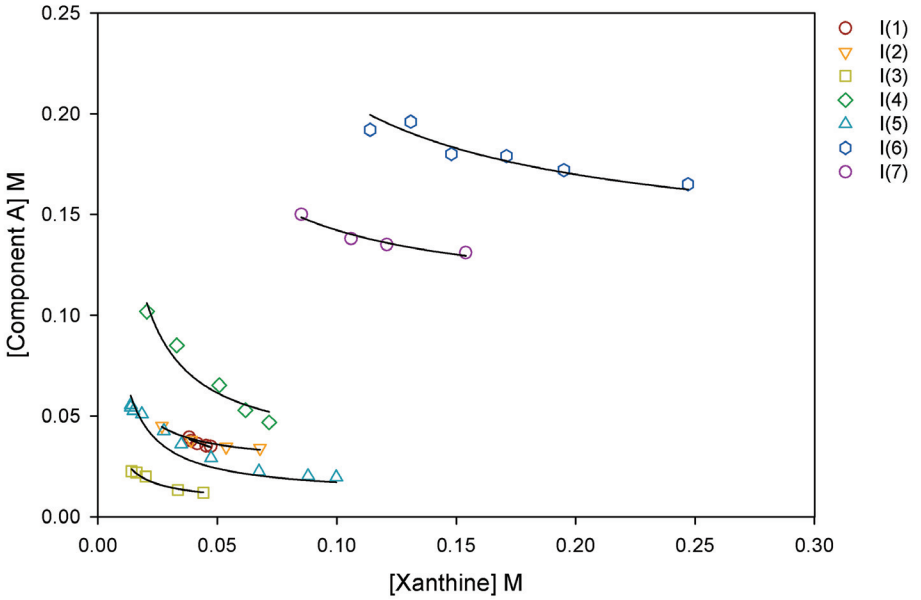

(a)

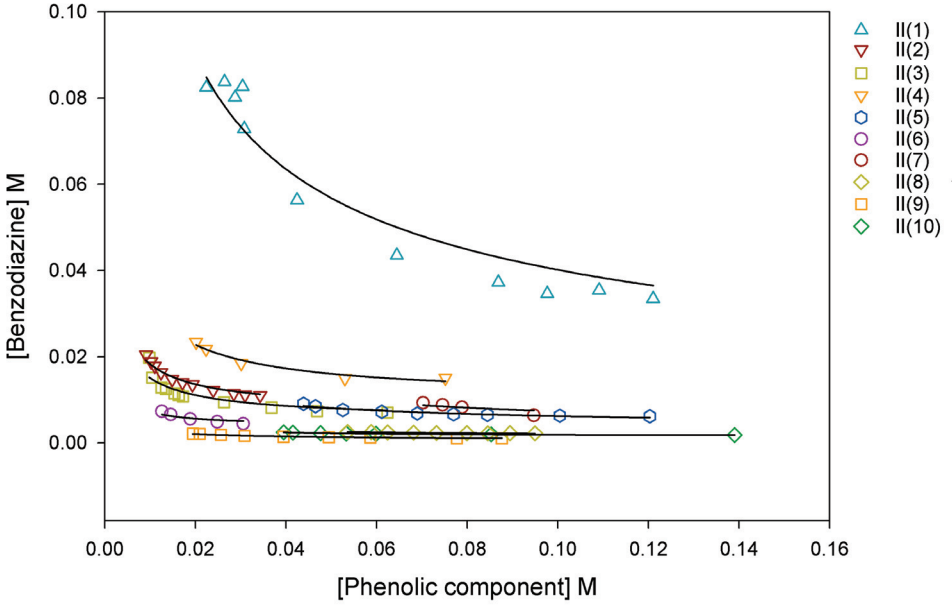

(b)

Figure 3.5: Phase solubility diagrams for the cocrystals listed in Table 3.2. The solid lines represent the predicted solubility behavior based on the calculated K_{sp} and K_{11} values listed in Appendix 3.6. Group I and II samples from Table 3.2 are shown in plots (a) and (b), respectively. Data points were taken from references in Table 3.2.

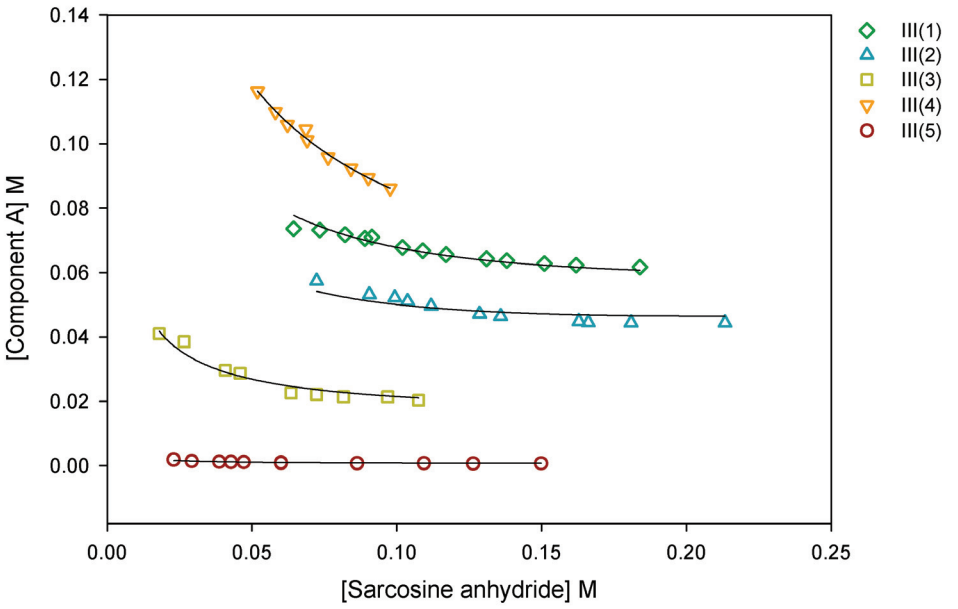

(c)

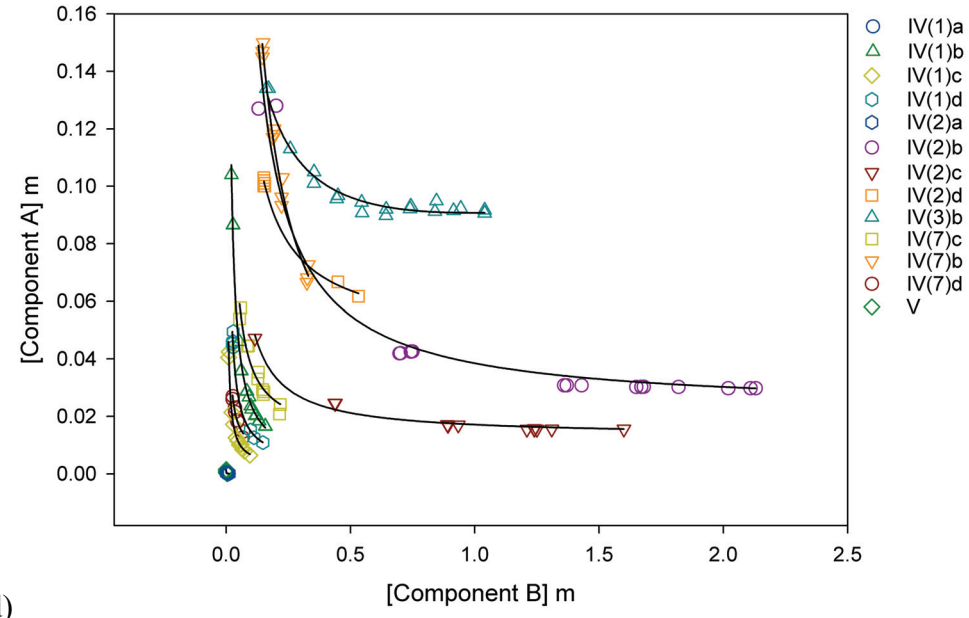

(d)

Figure 3.5: Phase solubility diagrams for the cocrystals listed in Table 3.2. The solid lines represent the predicted solubility behavior based on the calculated K_{sp} and K_{11} values listed in Appendix 3.6. Group III samples from Table 3.2 are shown in plot (c) and IV-V samples are in plot (d). Data points were taken from references in Table 3.2.

The K_{sp} values of several cocrystals from Table 3.2 were not calculated from phase solubility diagrams but instead were determined from the eutectic concentrations where $K_{sp} = S_{drug}^{y}[B]_{eu}^{z}$ as indicated in Chapter 2. For K_{sp} values determined from the eutectic concentrations the corresponding K_{11} values were also determined if the $[drug]_{eu}$ was greater than the S_{drug}. Results of the complexation analysis for carbamazepine cocrystals of nicotinamide and glutaric acid in water are shown in the Appendix 3.6. Both of these carbamazepine cocrystals exhibit high solubilization of carbamazepine in water. K_{11} values were calculated as described by Higuchi and coworkers. For carbamazepine in water the K_{11} values were determined to be 7.6 and 3.4 m^{-1} for nicotinamide and glutaric acid coformers, respectively.

3.3.2. Validation of solution models and calculated eutectic constants

Eutectic constants calculated from Equations 3.3 using measured or reported K_{sp}, K_{11}, and S_{drug} values are plotted against the observed K_{eu} in Figure 3.6. It is clear the derived relationship holds whereby the eutectic constant is a function of the cocrystal solubility across a broad set of cocrystal components, solvents, and pH values. For a set of cocrystals of one drug the most soluble cocrystals have large K_{eu} values for the eutectic with cocrystal drug and solution. High K_{eu} can also correspond to cocrystals of highly soluble coformers with low relative drug solubility, as was the case of carbamazepine, theophylline, and caffeine cocrystals in Chapter 2. Therefore, highly soluble cocrystals

require a large excess of coformer in solution to establish the eutectic condition where cocrystal is thermodynamically stable and to prevent conversion to pure component. For the eutectic concerning drug and cocrystal it is the transformation from cocrystal to drug that is prevented by excess coformer. Depending on the cocrystal and eutectic of interest the transformation can be between any number of cocrystal or component solvates, hydrates, polymorphs, or different cocrystal stoichiometries.

K_{eu} values for many of the carbamazepine cocrystals in organic solvents were found to be around one or less. In these organic solvents carbamazepine has similar or higher solubility than most of the more hydrophilic coformers studied. The opposite was true for aqueous carbamazepine samples and their eutectic constants. This indicates that 1:1 cocrystals of poorly water soluble drugs with hydrophilic coformers can be readily synthesized or stabilized in organic solvents when $K_{eu} \leq 1$. In these solvents cocrystal solubility is equal or less than drug in pure solvent (i.e. $\alpha \leq 1$). In this way, K_{eu} can be used to identify conditions for solution processes involving a stable cocrystal phase. Considerations of coformer solubility and other eutectics (e.g. solution in equilibrium with solid cocrystal and coformer) should be made to ensure the desired stable solid phase(s).

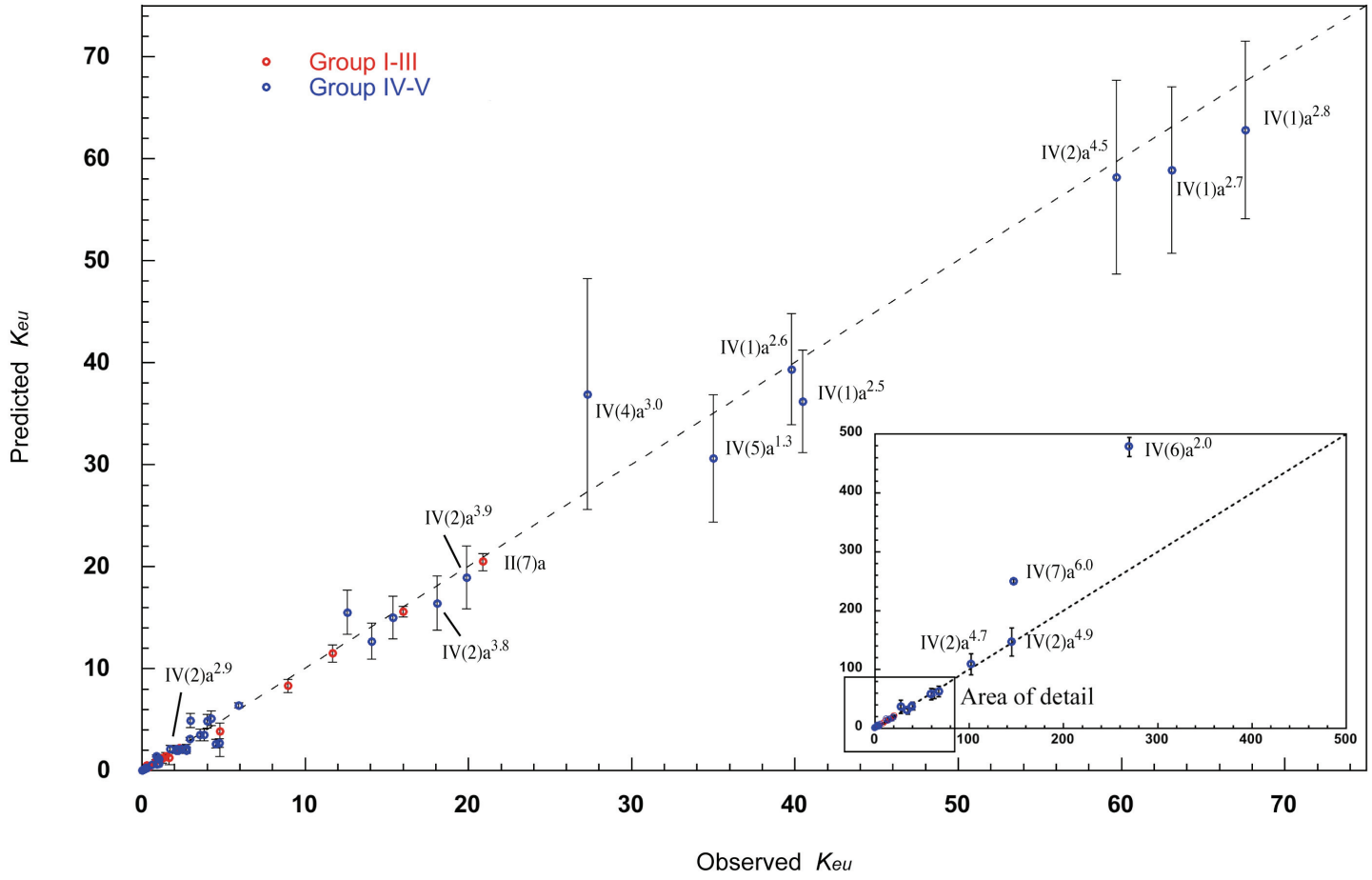

Figure 3.6: Predicted K_{eu} from Equation 3.3 using K_{sp}, K_{11}, and S_{drug} values against observed K_{eu} for cocrystals in Table 3.2. Dashed line indicates equality of predicted and observed K_{eu}. Error bars represent the 95th percentile confidence interval based on the K_{sp} standard error obtained from fit of phase solubility diagrams according to references.[14, 15, 20] Labeled points correspond to Table 3.2 notation with pH values in superscript.

To describe the deviation of predicted K_{eu} values from observed (Figure 3.6 dashed line) a linear regression and standard error were calculated. Statistics for each group of cocrystals (Table 3.3) indicate the derived K_{eu} expression predicts the observed values accounting for changes in i) cocrystal components, ii) ionization, iii) complexation, and iv) solvent for this distribution of cocrystals. The results emphasize that K_{eu} is a critical parameter for describing the cocrystal solubility and solution chemistry and K_{eu} is experimentally accessible for high solubility cocrystals that convert to pure component(s) in solution. The K_{eu} predictions show a slightly lower correlation when K_{sp} was estimated from the eutectic coformer concentration and the drug solubility in pure solvent (i.e. $K_{sp} = S_{drug}^{y}[B]_{eu}^{z}$). For these estimations, the drug solubility is used to represent the free drug concentration and any solute complexation at the eutectic is assumed as negligible relative to the coformer concentration. S_{drug} represents the solubility of drug in the absence of coformer.

Large deviations for carbamazepine cocrystals of glutaric acid and nicotinamide in water are a result of inadequate prediction of K_{eu} (Figure 3.6). This may be a consequence of large extrapolations between measured and predicted conditions, such as high eutectic coformer concentrations or the large change in solution composition. Assumptions of the model are not applicable to concentrated solutions and in such cases must be extended to include activities, higher complexes and hydrotropic behavior. Nicotinamide has been extensively studied for its hydrotropic behavior, aqueous self-

association/complexation, and stacking arrangements in solution. The solubilization of many hydrophobic drug substances have been demonstrated in aqueous nicotinamide solutions.[28-36] Sanghvi *et al.* reported the range of solubilization for 11 hydrophobic drugs was from 1.3 to ~4000 times in 1.6 molal nicotinamide solutions. Corresponding K_{11} values were between 0.02 and 172 M^{-1}.[35] An inflection was found around 10wt% (0.82 molal) nicotinamide above which drug solubilization, water conductivity, and surface tension rose more rapidly with increased nicotinamide corresponding to higher order complexation between nicotinamide and the drug substances studied. The combined results of several studies of nicotinamide hydrotropic behavior agree with the level of solubilization we report for carbamazepine (K_{11}=7.3m^{-1}).[32, 35, 36] Our observed nicotinamide eutectic concentration (Chapter 2) is 0.86 molal, which is just above the inflection observed for these studies of hydrotropic nicotinamide behavior. Carbamazepine-nicotinamide has characteristic K_{sp} behavior (i.e. cocrystal solubility is less than drug at high nicotinamide concentrations), however the PSD (Appendix 3.6) indicates a linear increase for carbamazepine and cocrystal solubility as a function of the nicotinamide concentration. This behavior is consistent with hydrotropic nicotinamide solubilization reported for other drugs. The causes of carbamazepine solubilization by nicotinamide and glutaric acid are the subject of ongoing research.

A list of possible solution characteristics that could lead to deviation of predicted and observed K_{eu} values are provided in Table 3.5. These factors represent several possible situations and are not an exhaustive list. A complete listing would indicate all

parameters that are assumed in the derivation of K_{eu} or were not expressed in equilibrium equations I-III. In some cases, systems that exhibit weak complex formation (low complexation constants) at high coformer concentrations can change the solvent composition significantly such that it behaves as a solvent component.[12] This behavior can lead to activity coefficients that deviate from unity or are not constant over the range of concentrations studied. Additional equilibrium for considering the self-association of a known hydrotropic component (*B*) include:

$$B_{soln} + B_{soln} \rightleftharpoons nB_{soln}$$

$$A_{soln} + nB_{soln} \rightleftharpoons AB_{n\ soln}$$

Here component *B* self associates in solution which would increase K_{eu} values, however a second equilibrium could occur where self associated coformer complexes with drug substance. When multiple complexation interactions occur it becomes more difficult to predict the expected variance in eutectic concentrations. Determining the mechanism(s) of self-association and corresponding equilibrium constants is beyond the scope of this work. However, based on observed solubilization behavior nicotinamide and glutaric acid represent coformers that can increase drug solubility through physicochemical changes due to cocrystal formation as well as independent drug solubilization based on their self-association or solute-solvent interactions. These types of coformers offer advantages because beyond having strong solid-state interactions that facilitate stable

cocrystal formation they also have strong solution interactions, which cause drug solubilization.

Table 3.4: Statistical analysis of observed and calculated K_{eu} with respect to linear behavior (dashed line) shown in Figure 3.6.

Cocrystals	r^2	standard error [a]
Group I-III	0.997	0.38
Group IV [b]	0.993	2.50
organic solvents only	0.976	0.24
aqueous samples only	0.992	3.13
variable pH samples	0.995	2.44
K_{sp} and K_{11} from phase diagrams	0.996	2.19
K_{sp} from single eutectic	0.926	3.34

[a] The square root of the average squared deviation from the regression line. [b] Excludes aqueous glutaric acid and nicotinamide cocrystals.

Table 3.5: Solubility behaviors that can cause deviation of predicted K_{eu} values from ideal behavior as represented in Figure 3.6.

Positive (higher predicted K_{eu})	Negative (lower predicted K_{eu})
Solute-solute complexation (drug) $A_{soln} + A_{soln} \rightleftharpoons nA_{soln}$	Solute-solute complexation (coformer) $B_{soln} + B_{soln} \rightleftharpoons nB_{soln}$
Higher order drug complexation (i.e. 2:1 drug:coformer) $nA_{soln} + B_{soln} \rightleftharpoons A_nB_{soln}$	Higher order coformer complexation (i.e. 1:2 drug:coformer) $A_{soln} + nB_{soln} \rightleftharpoons AB_{n\ soln}$
Nonideal coformer solution behavior: $\gamma_{coformer}>1$ as $x_{coformer}\rightarrow 1$ $(a/x)_{coformer} = \gamma_{coformer} > 1$	Nonideal coformer solution behavior: $\gamma_{coformer}<1$ as $x_{coformer}\rightarrow 1$ $(a/x)_{coformer} = \gamma_{coformer} < 1$
Nonideal drug solution behavior: $\gamma_{drug} <1$ as $x_{coformer}\rightarrow 1$ $(a/x)_{drug} = \gamma_{drug} < 1$	Nonideal drug solution behavior: $\gamma_{drug}>1$ as $x_{coformer}\rightarrow 1$ $(a/x)_{drug} = \gamma_{drug} > 1$
Coformers that disrupt of solvent-solvent interactions and cause drug solubilization (e.g. hydrotropic coformers)	Drugs that disrupt of solvent-solvent interactions and cause coformer solubilization (e.g. hydrotropic drugs)

Carbamazepine-saccharin and carbamazepine-salicylic acid cocrystals exemplify the relationship presented between excess coformer and the solubility ratio in equation 3.5 because both have 1:1 stoichiometry and low solution complexation in the solvents studied. For cocrystals with ionizing components it has been reported that aqueous solubility and stability are a function of pH.[8, 9, 27, 37] Since carbamazepine is non-ionizing α increases with higher pH values for these cocrystals with acidic ligands. Figure 3.7a and the data listed in Table 3.6 show the excess coformer increases with increasing pH values. The various solubility ratios for different solvents can also change the excess coformer at the eutectic point. The lower solubility of saccharin relative to carbamazepine in some organic solvents corresponds to excess eutectic carbamazepine concentrations (i.e. negative excess of saccharin). In these cases α is less than one and saturating a solution with cocrystal will not cause conversion to drug.

The direct relation of K_{eu} and α is shown for carbamazepine cocrystals in Figure 3.7b. To emphasize the relationship (Equation 3.5) between the eutectic concentrations and the solubility of the crystalline forms in pure solvent the data is presented as the observed eutectic ratio of cocrystal components in solution (K_{eu}, y-axis) against the solubility ratio of cocrystal and drug (α, x-axis). Cocrystal solubilities increase relative to drug solubility in pure solvent as the $[coformer]_{eu}$ also increases relative to $[drug]_{eu}$.

Additionally, it is apparent from Figure 3.7b that comparing cocrystals of the same drug, those with low K_{eu} values will have large solubility differences (low slope

region in Figure 3.7b). However, solubility differences between two cocrystals with large K_{eu} values will be relatively small (high slope region in Figure 3.7b). When engineering or selecting cocrystals of the same drug for a given solvent system it is important to highlight the diminishing return in solubility for improving over already high K_{eu} values. This is even more pronounced for cocrystals with 2:1 or higher stoichiometric ratios where K_{eu} is a function of the solubility ratio raised to a higher power (Equation 3.5).

Table 3.6: Observed K_{eu} values and calculated α values for carbamazepine cocrystals with acidic ligands in water as a function of pH.

Coformer	K_{sp} (m^2)	*pH*	α calculated[a]	K_{eu} observed[b]	*%xs* eutectic coformer[b]
Saccharin	9.3×10^{-7}	2.80	7.62	67.6	97.1
		2.77	7.38	63.1	96.9
		2.58	6.03	39.8	95.1
		2.54	5.79	40.5	95.2
		2.08	3.72	15.4	87.8
		1.98	3.42	14.1	86.7
		1.17	2.17	4.3	62.0
		1.10	2.33	3.0	85.1
		1.07	2.11	4.0	60.0
Salicylic acid	4.9×10^{-7}	4.87	12.10	145.0	98.6
		4.74	10.40	102.0	98.1
		4.46	7.63	59.7	96.7
		1.96	1.46	2.2	36.6

[a] From listed Ksp value and pH using Equation 3.5. [b] From measurement of solution eutectic concentrations.

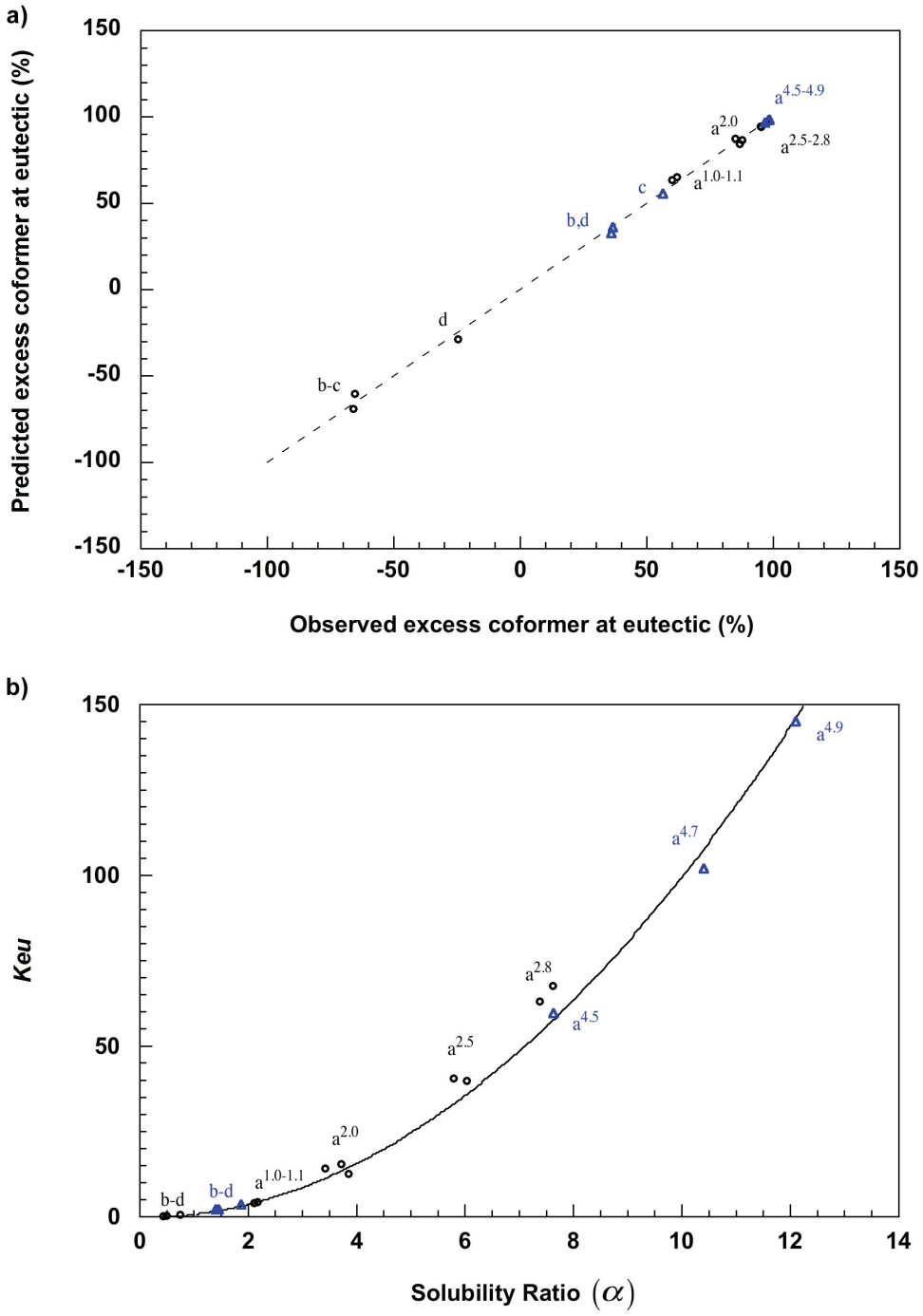

Figure 3.7: a) Predicted eutectic coformer excess (Equation 3.5) against observed excess. b) Observed K_{eu} plotted against the cocrystal to drug solubility ratio. Curve corresponds to $K_{eu} = \alpha^2$. The points in a) and b) correspond to carbamazepine cocrystals of salicylic acid (triangles-blue) and saccharin (circles-black) at various pHs or in different solvents. Solvents indicated in Table 3.2 (superscript is pH).

Figure 3.8 presents a flowchart to guide analysis of cocrystal solubility and stability. This scheme indicates steps for analyzing cocrystal solution phase including the case of ionizing components. The corresponding equations are based on the presented eutectic relationships solved in terms of cocrystal K_{sp} and solubility as well as K_{eu} and α.

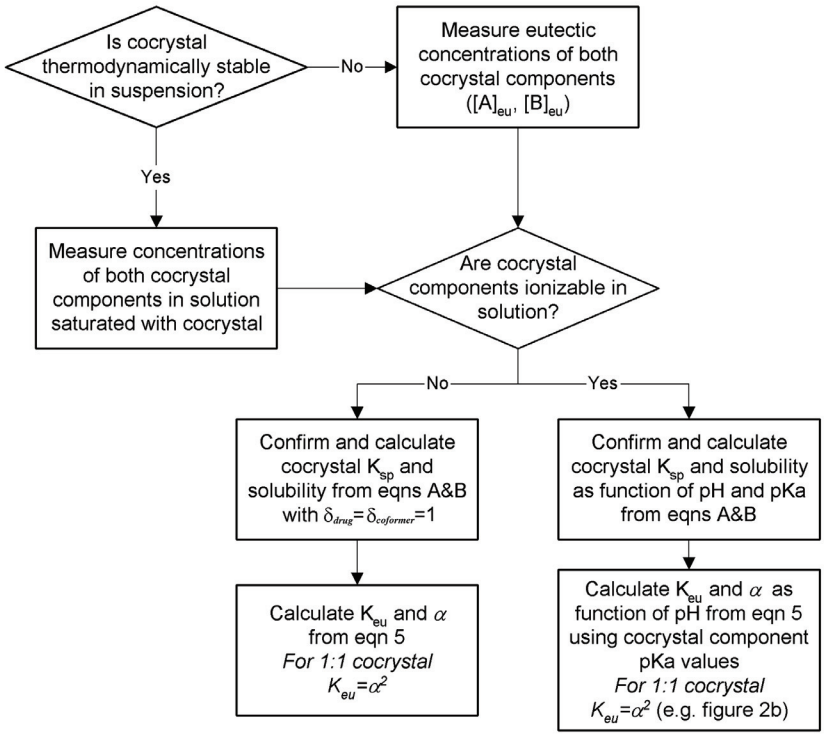

A. $$K_{sp} = \left([A]_{total} + [A]_{total}(1-\delta_{drug})\right)^{y} \left([B]_{total} + [B]_{total}(1-\delta_{coformer})\right)^{z}$$

B. $$S_{cocrystal} = \sqrt[y+z]{K_{sp}\delta_{coformer}^{z}\delta_{drug}^{y} / y^{y}z^{z}} = \left(z^{-1}y^{-y/z}K_{eu}\right)^{z/(y+z)} S_{drug}\delta_{drug}$$

Figure 3.8: Scheme to determine cocrystal solution phase stability for systems with ideal solution behavior and no complexation.

3.4. CONCLUSIONS

We have demonstrated that the eutectic solution excess of a cocrystal component is controlled by the relative solubility of the cocrystal and the component in pure solvent. When the molecular structure and properties of the components differ it is the solubility of the cocrystal and its components (e.g. cocrystal and drug) that determine the solution eutectic concentrations. Differences in cocrystal stoichiometry as well as solubility of the components due to ionization and complexation are critical in determining K_{eu}. Therefore, cocrystal stability can be altered by solvent selection and pH.

In summary, eutectic constants are valuable to guide cocrystal selection, synthesis and formulation without the materials and time requirements of traditional methods. K_{eu} values explain cocrystal solubility and phase behavior as a function of i) solvent, ii) ionization, and iii) solution complexation. We have demonstrated the applicability of K_{eu} toward describing the cocrystal solubility ratio and solution chemistry for a set of more than forty cocrystal and solvent combinations. Equilibrium eutectic measurements can be used to predict cocrystal solubility in pure solvent.

3.5. REFERENCES

(1) Chadwick, K.; Davey, R.; Sadiq, G.; Cross, W.; Pritchard, R., The utility of a ternary phase diagram in the discovery of new co-crystal forms. *Crystengcomm* **2009,** 11, (3), 412-414.

(2) Childs, S. L.; Rodríguez-Hornedo, N.; Reddy, L. S.; Jayasankar, A.; Maheshwari, C.; McCausland, L.; Shipplett, R.; Stahly, B. C., Screening strategies based on solubility and solution composition generate pharmaceutically acceptable cocrystals of carbamazepine. *Crystengcomm* **2008,** 10, (7), 856-864.

(3) Shan, N.; Zaworotko, M. J., The role of cocrystals in pharmaceutical science. *Drug Discov Today* **2008,** 13, (9-10), 440-6.

(4) Jacques, J.; Collet, A.; Wilen, S. H., *Enantiomers, racemates, and resolutions*. ed.; Wiley: New York, 1981; p xv, 447 p.

(5) Klussmann, M.; White, A. J. R.; Armstrong, A.; Blackmond, D. G., Rationalization and prediction of solution enantiomeric excess in ternary phase systems. *Angewandte Chemie-International Edition* **2006,** 45, (47), 7985-7989.

(6) Wang, Y. L.; LoBrutto, R.; Wenslow, R. W.; Santos, I., Eutectic composition of a chiral mixture containing a racemic compound. *Organic Process Research & Development* **2005,** 9, (5), 670-676.

(7) Higuchi, T.; Connors, K. A., Phase-Solubility Techniques. In *Advances in analytical chemistry and instrumentation*, Reilley, C., Ed. Wiley-Interscience: New York, 1965; Vol. 4, pp 144-194.

(8) Reddy, L. S.; Bethune, S. J.; Kampf, J. W.; Rodríguez-Hornedo, N., Cocrystals and Salts of Gabapentin: pH Dependent Cocrystal Stability and Solubility. *Crystal Growth & Design* **2009,** 9, (1), 378-385.

(9) Bethune, S.; Huang, N.; Jayasankar, A.; Rodríguez-Hornedo, N., Designing Cocrystals with Desired pH-dependent Solubility. *Crystal Growth & Design* **2009,** Manuscript accepted.

(10) Cooke, C. L.; Davey, R. J., On the Solubility of Saccharinate Salts and Cocrystals. *Crystal Growth & Design* **2008,** 8, (10), 3483-3485.

(11) Good, D. J.; Rodríguez-Hornedo, N., Solubility Advantage of Pharmaceutical Cocrystals. *Crystal Growth & Design* **2009,** 9, (5), 2252-2264.

(12) Connors, K. A., *Binding constants : the measurement of molecular complex stability*. ed.; Wiley: New York, 1987; p xiv, 411 p.

(13) Zughul, M. B.; Badwan, A. a., SL2 Type Phase Solubility Diagrams, Complex Formation and Chemical Speciation of Soluble Species. *Journal of Inclusion Phenomena and Macrocyclic Chemistry* **1998,** 31, (3), 243-264.

(14) Jayasankar, A.; Reddy, L. S.; Bethune, S. J.; Rodríguez-Hornedo, N., Role of Cocrystal and Solution Chemistry on the Formation and Stability of Cocrystals with Different Stoichiometry. *Crystal Growth & Design* **2009,** 9, (2), 889-897.

(15) Nehm, S. J.; Rodriguez-Spong, B.; Rodríguez-Hornedo, N., Phase solubility diagrams of cocrystals are explained by solubility product and solution complexation. *Crystal Growth & Design* **2006,** 6, (2), 592-600.

(16) Higuchi, T.; Sciarrone, B. J.; Haddad, A. F., Formation of Molecular Complexes by Diketobenzodiazines and Their Methylated Derivatives with Phenol and

Dihydroxybenzenes in Aqueous Solutions. *Journal of Medicinal & Pharmaceutical Chemistry* **1961,** 3, (2), 195-&.

(17) Childs, S. L.; Rodríguez-Hornedo, N.; Reddy, L. S.; Jayasankar, A.; Maheshwari, C.; McCausland, L.; Shipplett, R.; Stahly, B. C., Screening strategies based on solubility and solution composition generate pharmaceutically acceptable cocrystals of carbamazepine. *Cryst Eng Comm* **2008,** 10, (7), 856-864.

(18) Rodríguez-Hornedo, N.; Nehm, S. J.; Seefeldt, K. F.; Pagan-Torres, Y.; Falkiewicz, C. J., Reaction crystallization of pharmaceutical molecular complexes. *Mol Pharm* **2006,** 3, (3), 362-7.

(19) Porter III, W. W.; Elie, S. C.; Matzger, A. J., Polymorphism in Carbamazepine Cocrystals. *Cryst. Growth Des.* **2008,** 8, (1), 14-16.

(20) Zughul, M. B.; Badwan, A. A., Rigorous analysis of S2L-type phase solubility diagrams to obtain individual formation and solubility product constants of both SL- and S2L-type complexes. *International Journal of Pharmaceutics* **1997,** 151, (1), 109-119.

(21) Higuchi, T.; Lach, J. L., Investigation of Some Complexes Formed in Solution by Caffeine 4. Interactions between Caffeine and Sulfathiazole, Sulfadiazine, Para-Aminobenzoic Acid, Benzocaine, Phenobarbital, and Barbital. *Journal of the American Pharmaceutical Association-Scientific Edition* **1954,** 43, (6), 349-354.

(22) Higuchi, T.; Zuck, D. A., Investigation of Some Complexes Formed in Solution by Caffeine 3. Interactions between Caffeine and Aspirin, Para-Hydroxybenzoic Acid, Meta-Hydroxybenzoic Acid, Salicylic Acid, Salicylate Ion, and Butyl Paraben. *Journal of the American Pharmaceutical Association-Scientific Edition* **1953,** 42, (3), 138-145.

(23) Higuchi, T.; Lach, J. L., Investigation of Complexes Formed in Solution by Caffeine 6. Comparison of Complexing Behaviors of Methylated Xanthines with Para-Aminobenzoic Acid, Salicylic Acid, Acetylsalicylic Acid, and Para-Hydroxybenzoic Acid. *Journal of the American Pharmaceutical Association-Scientific Edition* **1954,** 43, (9), 527-530.

(24) Higuchi, T.; Lach, J. L., Investigation of Some Complexes Formed in Solution by Caffeine 5. Interactions between Caffeine and Para-Aminobenzoic Acid, Meta-Hydroxybenzoic Acid, Picric Acid, Ortho-Phthalic Acid, Suberic Acid, and Valeric Acid. *Journal of the American Pharmaceutical Association-Scientific Edition* **1954,** 43, (9), 524-527.

(25) Chow, Y. P.; Repta, A. J., Complexation of Acetaminophen with Methyl Xanthines. *Journal of Pharmaceutical Sciences* **1972,** 61, (9), 1454-&.

(26) Poole, J. W.; Higuchi, T., Complexes Formed in Aqueous Solutions by Sarcosine Anhydride - Interactions with Organic Acids, Phenols, and Aromatic Alcohols. *Journal of the American Pharmaceutical Association* **1959,** 48, (10), 592-601.

(27) Bethune, S. J., Thermodynamic and kinetic parameters that explain crystallization and solubility of pharmaceutical cocrystals. Ph.D., University of Michigan, Ann Arbor, 2009.

(28) Coffman, R. E.; Kildsig, D. O., Effect of nicotinamide and urea on the solubility of riboflavin in various solvents. *Journal of Pharmaceutical Sciences* **1996,** 85, (9), 951-954.

(29) Coffman, R. E.; Kildsig, D. O., Hydrotropic solubilization - Mechanistic studies. *Pharmaceutical Research* **1996,** 13, (10), 1460-1463.

(30) da Silva, R. C.; Spitzer, M.; da Silva, L. H. M.; Loh, W., Investigations on the mechanism of aqueous solubility increase caused by some hydrotropes. *Thermochimica Acta* **1999,** 328, (1-2), 161-167.

(31) Jain, A. K., Solubilization of indomethacin using hydrotropes for aqueous injection. *European Journal of Pharmaceutics and Biopharmaceutics* **2008,** 68, (3), 701-714.

(32) Lim, L. Y.; Go, M. L., Caffeine and nicotinamide enhances the aqueous solubility of the antimalarial agent halofantrine. *European Journal of Pharmaceutical Sciences* **2000,** 10, (1), 17-28.

(33) Nicoli, S.; Bilzi, S.; Santi, P.; Caira, M. R.; Li, J.; Bettini, R., Ethyl-Paraben and Nicotinamide Mixtures: Apparent Solubility, Thermal Behavior and X-Ray Structure of the 1:1 Co-Crystal. *Journal of Pharmaceutical Sciences* **2008,** 97, (11), 4830-4839.

(34) Nicoli, S.; Zani, F.; Bilzi, S.; Bettini, R.; Santi, P., Association of nicotinamide with parabens: Effect on solubility, partition and transdermal permeation. *European Journal of Pharmaceutics and Biopharmaceutics* **2008,** 69, (2), 613-621.

(35) Sanghvi, R.; Evans, D.; Yalkowsky, S. H., Stacking complexation by nicotinamide: A useful way of enhancing drug solubility. *International Journal of Pharmaceutics* **2007,** 336, (1), 35-41.

(36) Suzuki, H.; Sunada, H., Mechanistic studies on hydrotropic solubilization of nifedipine in nicotinamide solution. *Chemical & Pharmaceutical Bulletin* **1998,** 46, (1), 125-130.

(37) Wenger, M.; Bernstein, J., Designing a Cocrystal of gamma-Amino Butyric Acid. *Angewandte Chemie International Edition* **2006,** 45, (47), 7966-7969.

3.6. APPENDIX

Table 3.7: Summary data for solution behavior of cocrystals listed in Table 3.2:

Group	#	Solvent	*Ksp*	K_{11} (m^-)	$\alpha^{[a]}$ Predicted	*Keu* Predicted	*Keu* Observed	S_A (m)
I	1	water	2.4×10^{-4} m^2 (5×10^{-4})	92	1.5	0.66 ±0.8	0.74	2.6×10^{-2}
	2	water	5.0×10^{-4} m^2 (5×10^{-5})	51	1.2	0.59 ±0.1	0.69	4.0×10^{-2}
	3	water	3.4×10^{-4} m^2 (6×10^{-5})	4.6	1.1	1.0 ±0.4	0.62	1.8×10^{-2}
	4	water	1.6×10^{-3} m^2 (2×10^{-4})	0.5	0.7	0.23 ±0.1	0.19	8.4×10^{-2}
	5	water	4.2×10^{-4} m^2 (4×10^{-4})	14.8	0.6	0.30 ±0.2	0.25	4.6×10^{-2}
	6	water	4.7×10^{-3} m^2 (6×10^{-4})	16.7	7.4	0.67 ±0.1	0.60	1.1×10^{-1}
	7	water	3.6×10^{-3} m^2 (6×10^{-4})	29	8.1	0.61 ±0.1	0.58	1.2×10^{-1}
II	1	water	1.6×10^{-4} m^3 (1×10^{-5})	18.4	1.2	0.72 ±0.1	0.32	6.7×10^{-2}
	2	water	3.0×10^{-6} m^3 (2×10^{-7})	8.3	0.5	0.48 ±0.1	0.44	1.9×10^{-2}
	3	water	1.9×10^{-6} m^3 (4×10^{-7})	5.9	0.4	0.30 ±0.2	0.47	1.9×10^{-2}
	4	water	4.9×10^{-6} m^3 (2×10^{-7})	14.2	0.8	0.76 ±0.4	0.86	1.9×10^{-2}
	5	water	1.4×10^{-6} m^3 (5×10^{-7})	8.6	1.3	3.8 ±1.6	4.8	6.7×10^{-3}
	6	water	3.2×10^{-7} m^3 (9×10^{-8})	1.5	0.7	1.3 ±0.6	1.7	6.3×10^{-3}
	7	water	1.4×10^{-6} m^3 (3×10^{-6})	7.3	1.7	7.7 ±7.7	7.5	5.2×10^{-3}
	8	water	2.5×10^{-7} m^3 (1×10^{-8})	3.8	2.0	20.5 ±0.9	20.9	2.2×10^{-3}
	9	water	8.1×10^{-8} m^3 (4×10^{-9})	1.6	1.3	8.3 ±0.7	8.6	2.1×10^{-3}
	10	water	1.6×10^{-7} m^3 (5×10^{-9})	4.2	1.8	15.6 ±0.5	16.0	2.1×10^{-3}

Table 3.7: continued

Group	#	Solvent	*Ksp*	K_{II} (m^-)	α[a] Predicted	*Keu* Predicted	*Keu* Observed	S_A (m)
III	1	water	2.0×10^{-4} m^3 (1×10^{-5})	4.3	0.9	0.96 ±0.1	0.88	5.9×10^{-2}
	2	water	1.1×10^{-4} m^3 (1×10^{-5})	5.4	1.0	1.2 ±0.2	1.3	4.4×10^{-2}
	3	water	2.4×10^{-5} m^3 (3×10^{-6})	3.4	0.5	0.47 ±0.1	0.45	3.8×10^{-2}
	4	water	2.2×10^{-4} m^3 (8×10^{-5})	9.6	0.7	0.45 ±0.1	0.45	8.9×10^{-2}
	5	water	3.1×10^{-5} m^2 (2×10^{-6})	23	4.5	11.5 ±0.9	11.7	1.4×10^{-3}
IV	1	water	9.3×10^{-7} m^2 (1×10^{-7})	-	1.9	3.7 ±1.4	3.7	5.0×10^{-4}
		ethanol	2.2×10^{-3} m^2 (3×10^{-5})	-	0.4	0.2 ±0.0	0.2	1.1×10^{-1}
		2-propanol	4.4×10^{-4} m^2 (1×10^{-5})	-	0.5	0.3 ±0.0	0.3	4.2×10^{-2}
		ethyl acetate	1.2×10^{-3} m^2 (9×10^{-5})	-	0.8	0.6 ±0.0	0.6	4.6×10^{-2}
	2	water	4.9×10^{-7} m^2 (4×10^{-8})	-	1.4	2.0 ±0.1	2.3	5.0×10^{-4}
		ethanol	2.7×10^{-2} m^2 (1×10^{-3})	-	1.3	1.6 ±0.1	1.5	1.3×10^{-1}
		2-propanol	8.3×10^{-3} m^2 (2×10^{-4})	-	1.8	3.2 ±0.1	2.5	5.0×10^{-2}
		ethyl acetate	4.1×10^{-3} m^2 (2×10^{-4})	5.7	1.5	1.1 ±0.0	1.5	6.0×10^{-2}
	3	ethanol	2.0×10^{-3} m^2 (5×10^{-5})	1.1	0.7	1.1 ±0.0	1.1	1.3×10^{-1}
	4	water	*3.6×10^{-9} m^3 (1×10^{-9})	-	2.1	37 ±11.3	27	4.6×10^{-4}
	5	water	*3.0×10^{-9} m^3 (6×10^{-10})	-	2.0	31 ±6.2	35	4.6×10^{-4}
	6	water	*4.8×10^{-4} m^2 (5×10^{-5})	3.4	44	410 ±16.5	270	5.4×10^{-4}
		ethanol	*7.3×10^{-2} m^2 (1×10^{-3})	*0.5	2.2	3.1 ±0.1	2.9	1.4×10^{-1}

Table 3.7: continued

Group	#	Solvent	*Ksp*	K_{11} (m^-)	α[a] Predicted	*Keu* Predicted	*Keu* Observed	S_A (m)
		2-propanol	*2.7 x10^{-2} m^2 (2 x10^{-3})	*1.5	4.1	6.4 ±0.3	5.9	5.0 x10^{-2}
		ethyl acetate	*4.4 x10^{-3} m^2 (1 x10^{-3})	*11.4	2.4	1.4 ±0.2	0.91	4.9 x10^{-2}
	7	water	*4.6 x10^{-4} m^2 (5 x10^{-5})	7.6	46	210 ±4.3	150	5.4 x10^{-4}
		ethanol	2.1 x10^{-2} m^2 (9 x10^{-4})	0.2	1.1	1.1 ±0.0	1.1	1.4 x10^{-1}
		2-propanol	2.5 x10^{-3} m^2 (2 x10^{-4})	5.0	1.3	1.0 ±0.1	1.0	5.0 x10^{-2}
		ethyl acetate	5.6 x10^{-4} m^2 (5 x10^{-5})	10.7	0.6	0.32 ±0.02	0.26	4.9 x10^{-2}
V		water	6.3 x10^{-7} m^2 (7 x10^{-8})	-	0.5	0.25 ±0.03	0.25	1.6 x10^{-3}

* Values calculated from eutectic concentrations as described in methods section
[a] Ratio calculated from listed drug solubility and the calculated cocrystal solubility based on K_{sp} and K_{11} values.

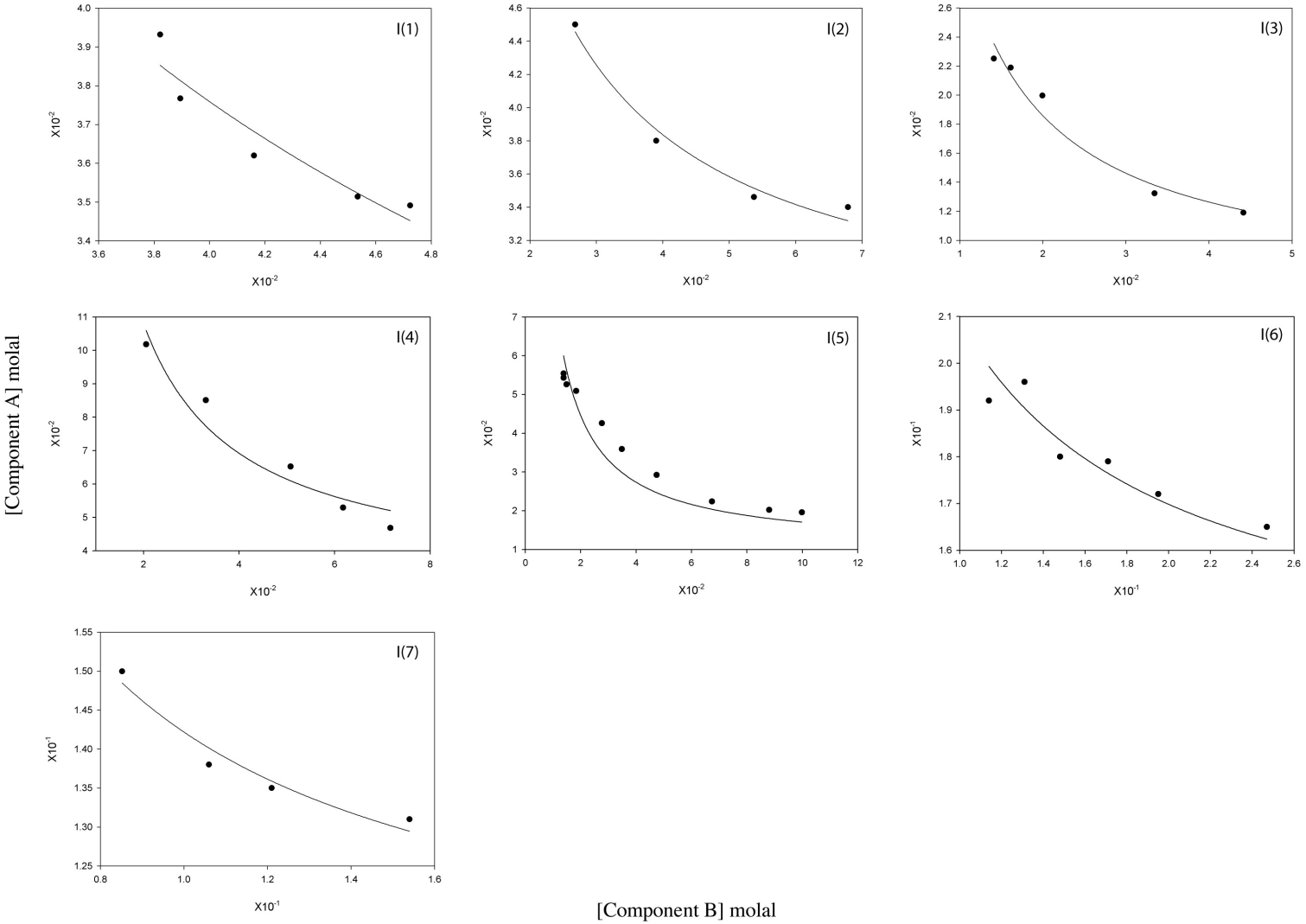

Figure 3.9: Solubility data for group I cocrystals listed in Table 3.2. Lines represent best fit according to Equation 3.7-3.9.[21-24]

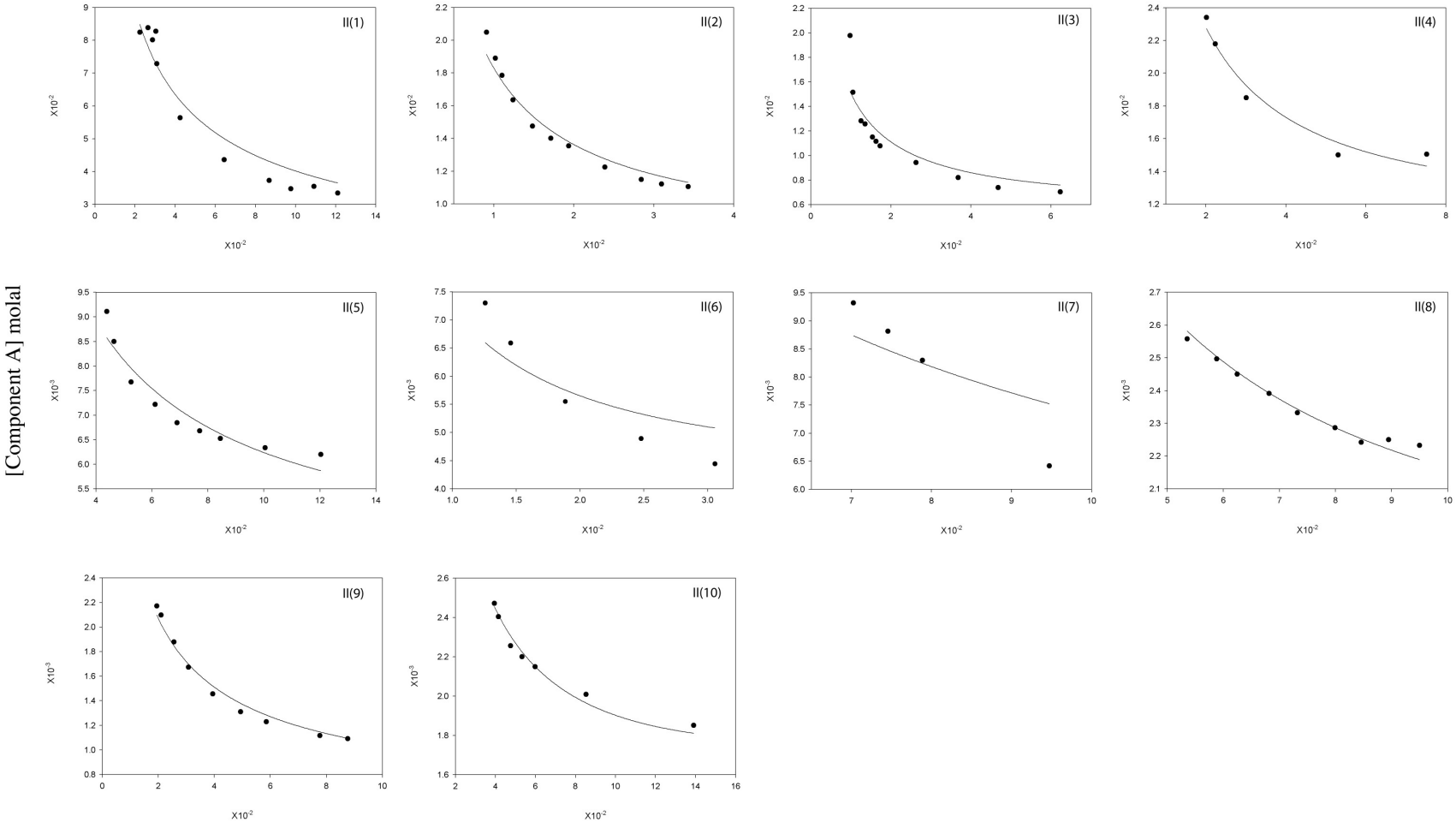

Figure 3.10: Solubility data for group II cocrystals listed in Table 3.2. Lines represent best fit according to Equations 3.7-3.9.[16]

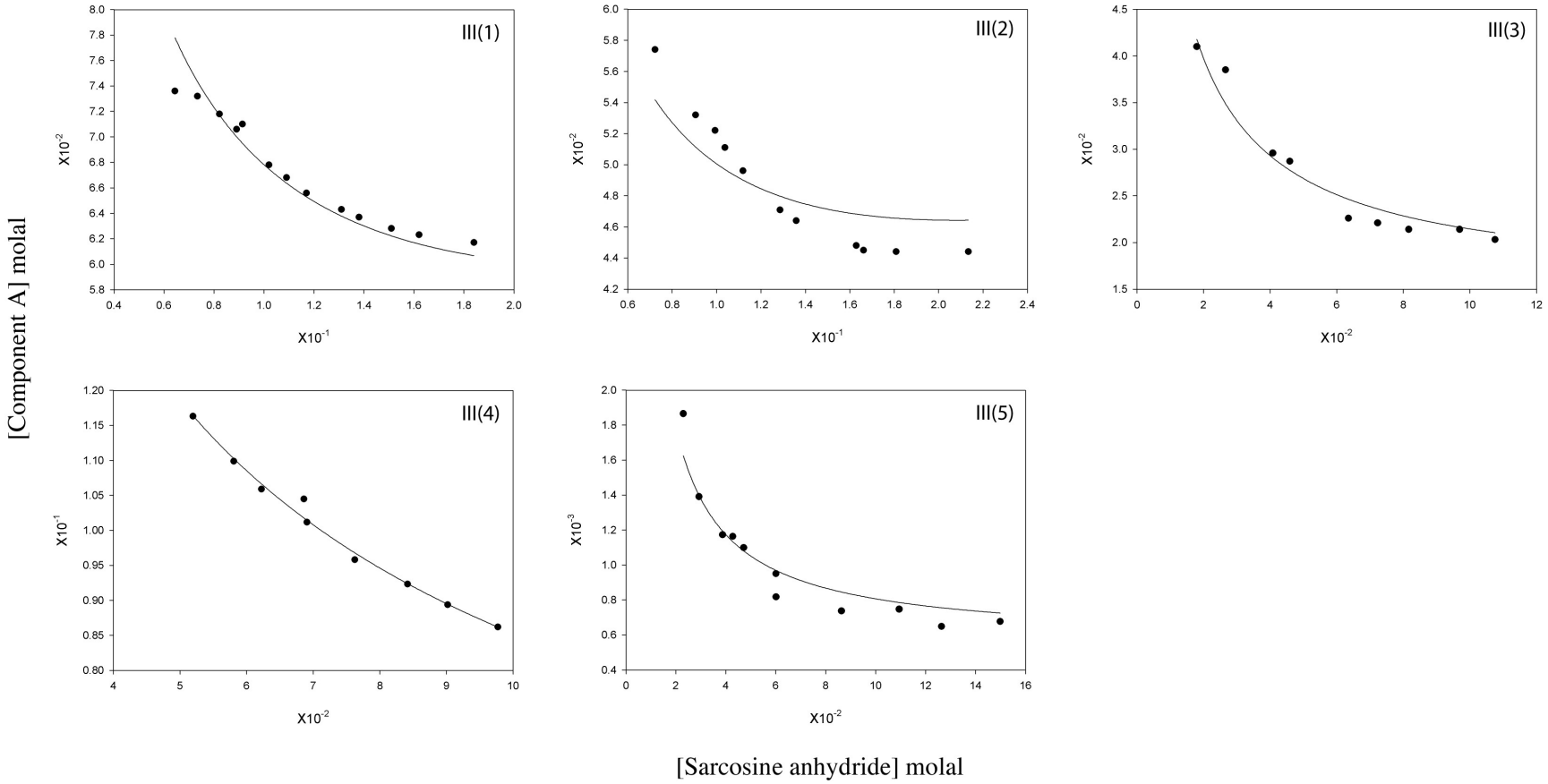

Figure 3.11: Solubility data for group III cocrystals listed in Table 3.2. Lines represent best fit according to Equations 3.7-3.9.[26]

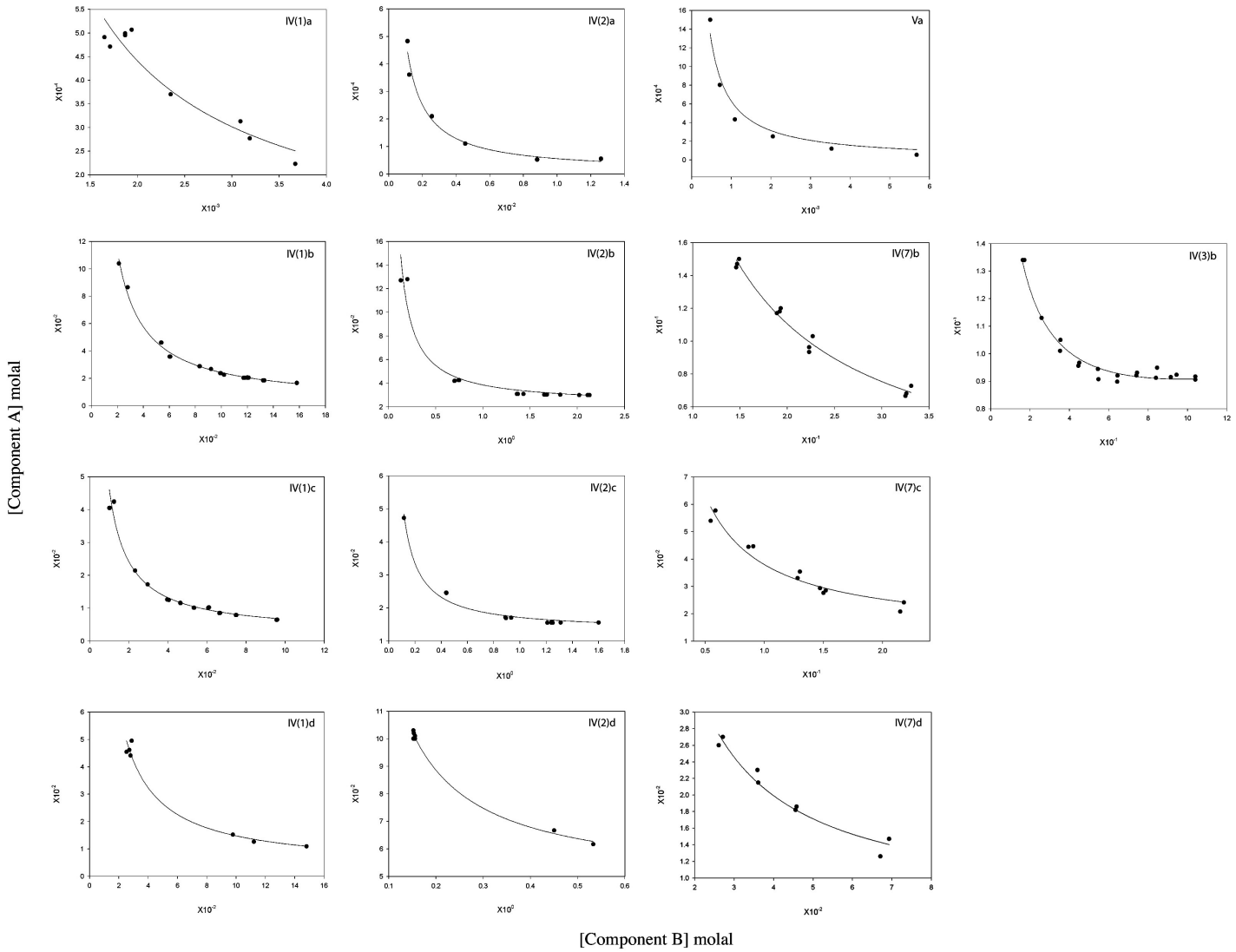

Figure 3.12: Solubility data for group IV-V cocrystals listed in Table 3.2. Lines represent best fit by Equations 3.7-3.9.[9, 11, 14, 15, 27]

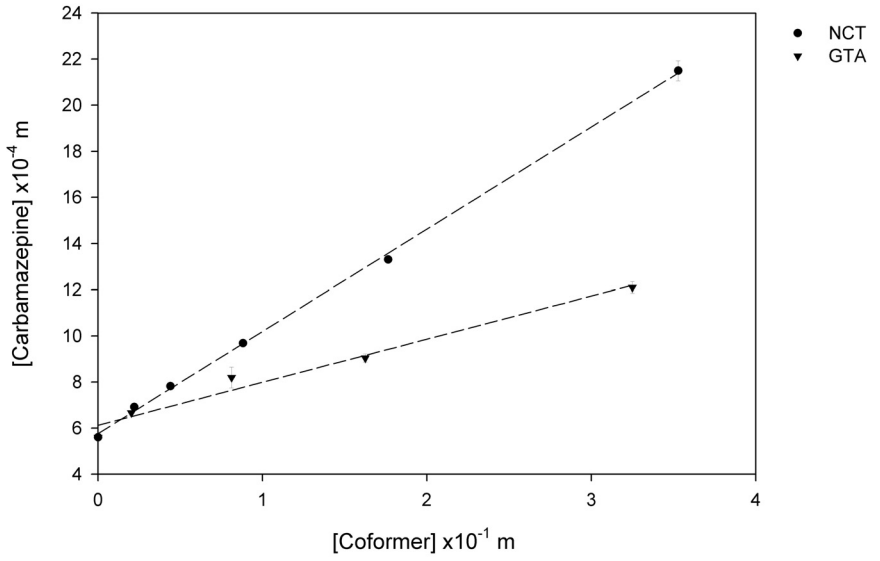

Figure 3.13: Aqueous solubility of carbamazepine as a function of nicotinamide (circles) and glutaric acid (triangles) at 25˚C. Dashed lines indicated the slopes used to calculate K_{11} values of 7.3 and 3.4 m^{-1} for nicotinamide and glutaric acid, respectively.

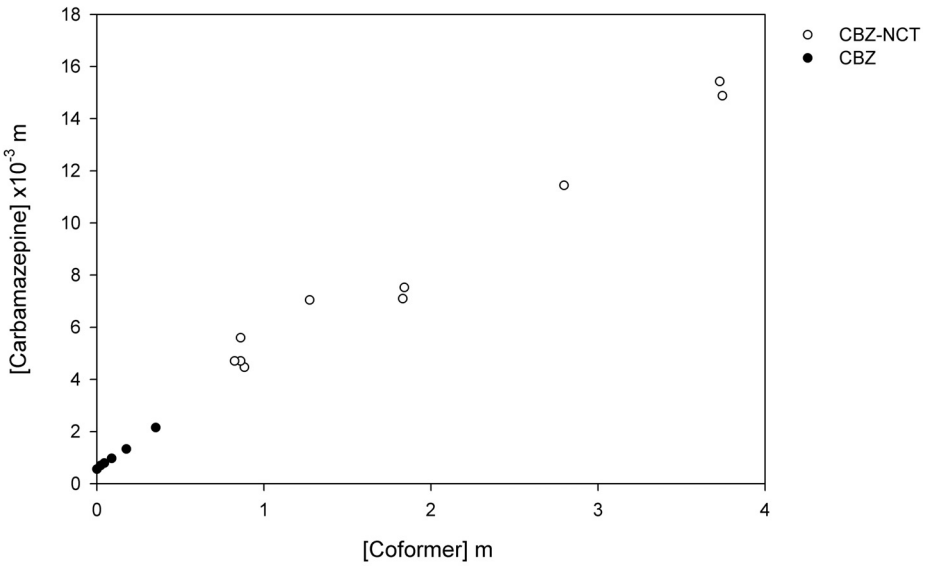

Figure 3.14: Aqueous solubility of carbamazepine as a function of nicotinamide at 25˚C. Points are shown at or above the eutectic concentration where the solution is the saturated with respect to cocrystal (open circles) and below the eutectic (filled circles) where carbamazepine is saturated.

Sample calculation of predicted and observed K_{eu}:

Predicted eutectic constants were calculated from cocrystal and component solubilities using the reported data for the 2,3-diketo-1,2,3,4-tetrahydroquinoxaline and phenol system presented in Figure 3.4 and Figure 3.10 plot IV(9). Solution complexation was evaluated in the primary literature and a K_{11} value of 1.6 M^{-1} reported. Equation 1 was used to predict the eutectic constant from the cocrystal and component solubilities as well as the solution complexation constant.

$$K_{eu} = \frac{[B]_{total}}{[A]_{total}} = \frac{[B]+[AB]}{[A]+[AB]} = \left[\frac{(K_{sp} / S_{drug}^{y})^{1/z} + K_{11}\left(K_{sp} S_{drug}^{(z-y)}\right)^{1/z}}{S_{drug} + K_{11}\left(K_{sp} S_{drug}^{(z-y)}\right)^{1/z}} \right]$$

The eutectic phases are solid cocrystal and benzodiazine in equilibrium with solution, therefore we substitute benzodiazine solubility (2.12×10^{-3} M) and cocrystal K_{sp} which gives:

$$K_{eu} = \left[\frac{(8.08\times10^{-8}\,M^3)/(2.12\times10^{-3}\ M)^2 + 1.6\,M^{-1}\left(8.08\times10^{-8}\,M^3 / 2.12\times10^{-3}\ M\right)}{2.12\times10^{-3}\ M + 1.6\,M^{-1}\left(8.08\times10^{-8}\,M^3 / 2.12\times10^{-3}\ M\right)} \right] = 8.3$$

From reported data the eutectic concentrations of benzodiazine and phenol are 2.2×10^{-3} M and 1.9×10^{-2} M, respectively. This corresponds to an experimental eutectic ratio of 8.6, compared to 8.3 predicted from the cocrystal and benzodiazine acid solubilities. This demonstrates the procedure for determining the eutectic constant from cocrystal and component solubilities. Conversely a known eutectic constant, which is a convenient equilibrium measurement, can be used to predict the cocrystal solubility.

CHAPTER 4

THERMODYNAMIC STABILITY OF COCRYSTALS AND THE TEMPERATURE DEPENDENCE OF EUTECTICS

Eutectic constant (K_{eu}) values are important for describing the thermodynamic phase stability of cocrystals in solutions. The measurement of K_{eu} provides information for predicting the solubility relation of cocrystal to its components in pure solvent as well as the conditions suitable for synthesis by crystallization processes from solutions. It is often necessary to understand the stability of cocrystals in solutions as a function of temperature to identify favorable conditions for storage or synthesis and to determine their stability at relevant biological conditions (37˚C). The development of models that describe the dependence of K_{eu} on thermodynamic properties of the cocrystal components is sought to enable the calculation of cocrystal stability in suspension as a function of temperature.

Pharmaceutical cocrystals that are developed for the improvement of drug solubility are typically comprised of components with differing solubilities. These components have different thermodynamic properties including melt temperature as well as enthalpy and entropy of fusion, solution, and mixing. Therefore, it is intuitive that the solubility of the pure cocrystal components each change to a different extent for an

equivalent temperature change. Furthermore, these temperature changes can lead to stability changes for a cocrystal in solution or suspension. A transition temperature can exist for a cocrystal that separates two temperature ranges in which either cocrystal or a component is the stable solid phase in equilibrium with a saturated solution of a given composition. The K_{eu} of a 1:1 cocrystal can be less than one for a given temperature range, where cocrystal is stable when suspended in pure solvent (i.e. congruently saturating), or greater than one and therefore cocrystal is unstable when suspended in pure solvent (i.e. incongruently saturating). In this chapter we seek to describe the effects of temperature on K_{eu} and predict the transition temperature for cocrystal stability in pure solvent.

4.1. THEORETICAL

4.1.1. Thermodynamic models for temperature dependence of S_{drug}, K_{sp}, and K_{eu}.

The equations presented in Chapter 3 for solid drug or cocrystal component (A) and solid cocrystal (AB) in equilibrium with a solution can be used to determine the temperature dependence of K_{eu}. These two equilibria have associated constants (K_{sp} and S_{drug}) whose temperature dependence can be described by considering the corresponding free energy. For a 1:1 cocrystal the equilibrium constant and free energy change is:

$$AB_{solid} \rightleftharpoons A_{soln} + B_{soln}$$

$$K_{sp} = \frac{a_A a_B}{a_{AB}}$$

$$\Delta G = -RT \ln K_{sp} = \Delta H - T\Delta S$$

where ΔG, ΔH, and ΔS are the change in cocrystal molar free energy, enthalpy, and entropy of solution, respectively. R is the universal gas constant. Taking the partial derivative with respect to temperature gives the classical thermodynamic relationship (van't Hoff equation):

$$\frac{\partial \ln K_{sp}}{\partial T} = \frac{\Delta H_s^{AB}}{RT^2} \quad \text{or} \quad \frac{\partial \ln K_{sp}}{\partial 1/T} = -\frac{\Delta H_s^{AB}}{R} \qquad 4.1$$

Similarly, we can write the expression for temperature dependence of drug solubility (S_A):

$$\frac{\partial \ln S_A}{\partial T} = \frac{\Delta H_s^{A}}{RT^2} \quad \text{or} \quad \frac{\partial \ln S_A}{\partial 1/T} = -\frac{\Delta H_s^{A}}{R} \qquad 4.2$$

Both these equations assume constant pressure and that the enthalpy of solution (ΔH_s) is independent of temperature (i.e. no change in heat capacity). It has previously been shown that heat capacity values have little influence for calculations involving most solids that melt below 600 K.[1] Furthermore, these relationships are applicable to dilute solutions where Raoult's law ($a_2=x_2$) or Henry's law holds ($a_2=Kx_2$) such that the solute activity equals its concentration or its concentrtion times a constant value.[2] Subtracting Equations 4.1 and 4.2 gives the K_{eu} temperature dependence for the eutectic of solid cocrystal and drug in equilibrium with solution as:

$$\frac{d\ln K_{eu}}{dT} = \frac{d\ln(\frac{K_{sp}}{S_A^2})}{dT} = \frac{\Delta H_s^{AB} - 2\Delta H_s^{A}}{RT^2} \qquad 4.3$$

where $K_{eu} = K_{sp}/S_A^2$ for the eutectic (E_1) equilibrium of solution, cocrystal, and drug. This relationship describes the temperature dependence of K_{eu} in terms of the enthalpy of solution of the drug and cocrystal. It is apparent from Equation 4.3 that K_{eu} will increase with temperature if the cocrystal molar enthalpy of solution is greater than twice that of the drug ($\Delta H_s^{AB} > 2\Delta H_s^{A}$). However, K_{eu} will decrease with temperature if the cocrystal enthalpy of solution is less than twice that of the drug. For this case, ($\Delta H_s^{AB} < 2\Delta H_s^{A}$) the cocrystal at high temperatures will be more stable (lower K_{eu} value) relative to drug when suspended in pure solvent. For graphical determination of the K_{eu} temperature dependence, we can rewrite Equation 4.3 with respect to 1/T:

$$\frac{R\, d\ln K_{eu}}{d1/T} = 2\Delta H_s^{A} - \Delta H_s^{AB} \qquad 4.4$$

To calculate the cocrystal K_{eu} at different temperatures Equation 4.4 is integrated from temperature T_1 to T_2 which gives:

$$\ln(K_{eu\,T2}/K_{eu\,T1}) = \frac{2\Delta H_s^{A} - \Delta H_s^{AB}}{R}\left(\frac{1}{T_2} - \frac{1}{T_1}\right)$$
$$K_{eu\,T2} = K_{eu\,T1} \bullet \exp\left[\frac{2\Delta H_s^{A} - \Delta H_s^{AB}}{R}\left(\frac{1}{T_2} - \frac{1}{T_1}\right)\right] \qquad 4.5$$

From this equation, the K_{eu} at T_2 can be calculated from the K_{eu} at T_1 if the heat of solution of drug and cocrystal are known. The enthalpy of solution values can be directly measured from solution calorimetry or calculated from solubility or K_{sp} measurements as

a function of temperature using the van't Hoff relationship. Plots of the natural logarithm of drug solubility or cocrystal K_{sp} against the inverse temperature based on the thermodynamic relations in Equations 4.1 and 4.2 give the slope = $-\Delta H_s/R$.

The thermodynamic relationships for K_{eu} (Equations 4.3-4.5) are specific to the eutectic (E1) between cocrystal, drug, and solution. The derivations for several other cocrystal eutectics, including those involving coformer or component B as a solid phase at the eutectic, are presented in Appendix 4.6. Eutectic equations for cocrystals of different stoichiometries and/or different cocrystal components at the eutectic are summarized in Table 4.1.

The temperature dependence of K_{eu} can also be derived from the fusion properties of the cocrystal and its components. This thermodynamic analysis has been shown for the eutectic behavior of a 1:1 cocrystal and is presented in Appendix 4.6.

Table 4.1: The eutectic constants in terms of cocrystal and component solubilities listed according to the solid phases at the eutectic. Temperature dependence of K_{eu} is also indicated in terms of cocrystal and component enthalpies of solution based on ideal solution behavior.

Solid phases at eutectic	K_{eu}	$\frac{R\, d\ln K_{eu}}{d1/T} =$
1:1 + 2:1 cocrystals	$\frac{a_B}{a_A} = \frac{K_{sp(1:1)}^3}{K_{sp(2:1)}^2}$	$2\Delta H_s^{AB(2:1)} - 3\Delta H_s^{AB(1:1)}$
1:1 cocrystal + drug	$\frac{a_B}{a_A} = \frac{K_{sp}}{S_A^2}$	$2\Delta H_s^A - \Delta H_s^{AB}$
1:1 cocrystal + coformer	$\frac{a_B}{a_A} = \frac{S_B^2}{K_{sp}}$	$\Delta H_s^{AB} - 2\Delta H_s^B$
2:1 cocrystal + drug	$\frac{a_B}{a_A} = \frac{K_{sp}}{S_A^3}$	$3\Delta H_s^A - \Delta H_s^{AB}$

4.2. MATERIALS AND METHODS

4.2.1. Solubility analysis of cocrystal and drug

Heat of solution values were calculated from solubility measurements of cocrystal or drug at four temperatures (4, 23, 37, and 47˚C). Cocrystal solubility products (K_{sp}) were determined from the eutectic concentrations of both components as described in Chapter 2. Each drug solubility and cocrystal eutectic measurement was carried out a minimum of three times. Solutions were saturated with cocrystal and/or drug by adding excess solid and stirring with magnetic bars at controlled temperature. Temperature was controlled using a water bath and jacketed beakers to ±0.5˚C, except for 4˚C samples that

were placed in a cold room at controlled temperature (±1˚C). For drug solubility measurements, the solid phase was isolated by centrifugation using tubes with 0.45µm filters and analyzed by XRPD to verify no transformations occurred. Equilibration of solid drug and cocrystal phases was reached within 2-5 days and aliquots of solution were drawn syringes (0.2µm cellulose of PTFE filter) for measurement of the component concentrations by HPLC.

Determination of cocrystal solubility by measuring one component concentration

For congruently saturating cocrystals alternative methods could be used to determine the cocrystal K_{sp} and K_{eu} using only the measurement of one component in equilibrium with cocrystal at various temperatures. Assuming pure cocrystal of known stoichiometry a mass balance can be used to determine the coformer concentration in saturated cocrystal solutions. These concentrations could be used directly to calculate K_{sp} values. For the eutectic involving solid phases of component A and the cocrystal the eutectic concentrations could be calculated from K_{sp} by $K_{sp}=[S_A]^y[B]_{eu}^z$ where S_A is the solubility of component A and y and z indicate the cocrystal stoichiometry of the component A and B. The eutectic concentrations are S_A (assuming no solubilization of A by component B) and $[coformer]_{eu}$. A second method to calculate K_{sp} and K_{eu} values at various temperatures is to measure only equilibrium one component equilibrium concentrations at different initial concentrations of the second component. This method

is commonly used to construct *Bs* type phase diagrams where the concentration of the varied component reflects the initial concentration (not equilibrium). Chapter 3 indicates how K_{eu} and K_{sp} values are calculated. For systems where methods of analysis for coformer concentrations are not readily available, these alternatives could be useful. However, the results in this chapter use direct measurement of both cocrystal component concentrations at the eutectic to calculate K_{sp} and K_{eu}.

4.2.2. High performance liquid chromatography (HPLC)

Solution concentrations of drug and coformer were analyzed by Waters HPLC (Milford, MA) equipped with a UV/Vis spectrometer detector. A C18 Atlantis column (5µm, 4.6 x 250mm; Waters, Milford, MA) at ambient temperature was used to separate the drug and the coformer. A gradient method with a water, methanol, and trifluoroacetic acid mobile phase was used with a flow rate of 1mL/min. Sample injection volumes were between 10-40µL. Absorbance of the drug and coformer analytes was monitored between 210-300nm. Empower software from Waters was used to collect and process the data.

4.2.3. X-ray powder diffraction (XRPD)

XRPD was used to identify crystalline phases in equilibrium with solution. At the eutectic point these were cocrystal and drug. XRPD patterns of solid phases were obtained with a Rigaku MiniFlex X-ray diffractometer (Danvers, MA) using Cu Kα

radiation (λ = 1.5418 Å), a tube voltage of 30 kV, and a tube current of 15 mA. The intensities were measured at 2θ values from 2˚ to 30˚ with a continuous scan rate of 2.5˚/min. Solid phases were analyzed prior to and after equilibration. Results were compared to diffraction patterns reported in literature or calculated from crystal structures published in the Cambridge Structural Database.[3]

4.2.4. Materials

Anhydrous monoclinic form III carbamazepine (CBZ) and sulfamethazine (i.e. SMT) were purchased from Sigma-Aldrich (99+% purity) and used as received. Carbamazepine dihydrate (CBZ(D)) was prepared by stirring CBZ in water for at least twenty-four hours. Hydrates of theophylline and caffeine were prepared in the same manner. The nicotinamide form I (NCT) and benzoic acid (BA) coformers were obtained from Sigma-Aldrich (99+% purity) and used as received. All crystalline drugs and coformers were characterized by XRPD and Raman spectroscopy before carrying out experiments. No impurities in the form of additional peaks were resolved during HPLC analysis of solutions containing the drug or coformer in this study at any of the various temperature conditions. Ethanol (EtOH), and ethyl acetate (EtOAc) were obtained from Fisher Scientific and dried using molecular sieves prior to use. All the cocrystal used for solubility studies were precipitated from coformer solutions by adding solid drug

according to the reaction crystallization method (RCM).[4, 5] Cocrystal of carbamazepine-nicotinamide refers to the form I polymorph.[6]

4.3. RESULTS AND DISCUSSION

4.3.1. Carbamazepine-nicotinamide and sulfamethazine-benzoic acid

The carbamazepine-nicotinamide (CBZ-NCT) cocrystal was previously shown to be thermodynamically stable at 25±1˚C when suspended in several organic solvents at all nicotinamide concentrations studied.[7] The cocrystal had values of $K_{eu} \leq 1$ in these solvents and therefore was thermodynamically stable relative to carbamazepine. CBZ-NCT suspended in water (pure solvent with no coformer added) was shown to be thermodynamically unstable at this temperature and had a corresponding $K_{eu} > 1$. Sulfamethazine-benzoic acid (SMZ-BA) in water was found to be congruently saturating in contrast to CBZ-NCT (incongruent).

Measurements of the CBZ-NCT K_{eu} in water showed values ranging from 330-110 between 4 and 47˚C. Similarly, SMZ-BA in water had K_{eu} values ranging from 0.31 to 0.15 between 23 and 90˚C. These CBZ-NCT and SMZ-BA K_{eu} values represent an approximate two to three-fold change in K_{eu} over the temperatures studied. No temperature dependence was observed for CBZ-NCT in the two organic solvents. These eutectic concentrations along with the K_{eu} values and drug solubilities are listed in Table 4.2.

The aqueous CBZ-NCT K_{eu} values between 4 and 47˚C are shown in Figure 4.1. Based on Equation 4.5 the predicted eutectic behavior using the calculated difference in carbamazepine and cocrystal heat of solution values (19.4 kJ/mol) is indicated by the solid line. The derived model based on heat of solution of the solid phases at the eutectic fits the observed eutectic data (r^2=0.98). The inverse temperature dependence of K_{eu} is observed because temperature increases the solubility of carbamazepine to a greater extent than the cocrystal. K_{eu} decreases with temperature since it reflects the solubility ratio of the cocrystal to drug in pure solvent. Cocrystal is less water soluble relative to carbamazepine because the carbamazepine solubility increase with temperature is greater than the cocrystal increase.

The CBZ-NCT melt (no solvent) eutectic (CBZ and CBZ-NCT) molar ratio (NCT/CBZ) has been reported as approximately 0.7.[8] Because the observed and predicted K_{eu} is decreasing with temperature (Table 4.2) it is approaching this melt eutectic value. This behavior was demonstrated for one other cocrystal and would be interesting to confirm of a wider range of solution temperatures and/or samples.[9] The melt eutectic could serve as and indication for the direction of change with temperature for solution eutectics.

In each solvent the cocrystals showed agreement between the observed temperature dependence of K_{eu} and that calculated from the enthalpy of solution of drug and cocrystal (solid phases at eutectic) according to Equation 4.4. These results demonstrate that Equation 4.4 can be used to determine the stability of cocrystal in

suspension at various temperatures if the cocrystal and drug enthalpies of solution are known.

To determine the temperature dependent stability of cocrystal in these solvents the enthalpy of solution of cocrystal (ΔH_s^{AB}) was calculated from the solubility of cocrystal at different temperatures. The same solubility measurements were performed at different temperatures for sulfamethazine as well as carbamazepine (ΔH_s^{A}) form III in organic solvents and dihydrate in water. These enthalpy and entropy of solution values for drug and cocrystal were calculated graphically from Figure 4.4 using the slope as described by Equation 4.1. Table 4.3 lists the slopes and the corresponding enthalpies of solution. The calculated enthalpies of solution for drug and cocrystal are positive in each solvent. This indicates that dissolution of drug and cocrystal in each solvent are entropy driven processes (i.e. positive entropies of solution). Previously reported aqueous ΔH_s values for carbamazepine dihydrate reported by Yoshihashi (25.2 kJ/mol) and Murphy (~24.3-25.8kJ/mol) are in good agreement with the value determined in this work (24.9 kJ/mol).[10, 11] The measured ΔH_s value (30.7 kJ/mol) for sulfamethazine also agrees with the value reported by Martinez and Gomez (29.46 kJ/mol).

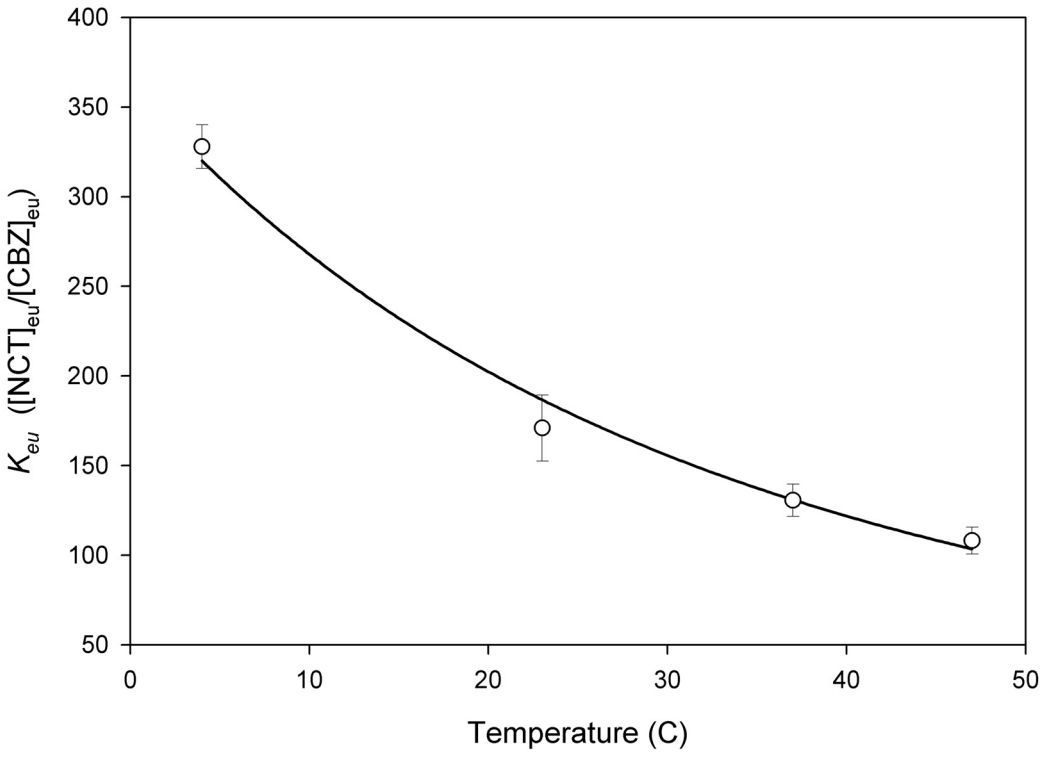

Figure 4.1: Eutectic constant of carbamazepine-nicotinamide in water as a function of temperature. The solid line represents predicted behavior based on Equation 4.5 with $2\Delta H_s^A - \Delta H_s^{AB} = 19.4$ kJ/mol.

Table 4.2: Eutectic concentrations and K_{eu} values for CBZ-NCT and SMZ-BA in aqueous and organic solvents. Concentrations are in mmolal.

	Observed eutectic				
Solvent	K_{eu}	$[drug]_{eu}$	$[coformer]_{eu}$	S_{drug}	Temp (˚C)
CBZ-NCT					
water	332	1.97	652	0.31	4
	173	4.71	817	0.60	23
	133	6.60	875	0.97	37
	110	8.31	912	1.35	47
ethanol	1.01	81.3	81.9	82.1	4
	0.99	140	138	125	23
	0.98	179	176	157	37
	0.92	205	189	207	47
ethyl acetate	0.30	32.7	9.70	30.5	4
	0.29	48.0	13.7	46.0	23
	0.28	63.3	17.8	56.1	37
	0.29	69.2	19.9	61.9	47
SMZ-BA					
water	0.31	1.50	0.47	1.61	23
	0.27	2.24	0.61	2.24	37
				5.11	60
	0.15	16.2	2.4	10.62	90

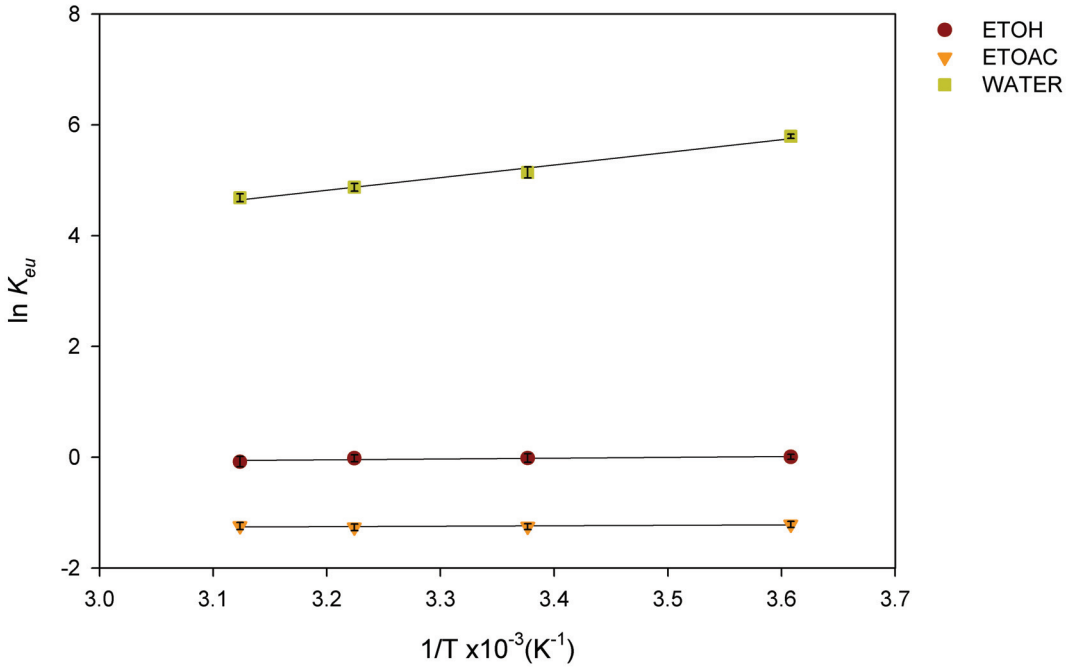

Figure 4.2: CBZ-NCT ln K_{eu} against inverse temperature. Error bars represent the standard error for each measured K_{eu}. Lines represent the best linear fit and the slopes are reported in Table 4.3.

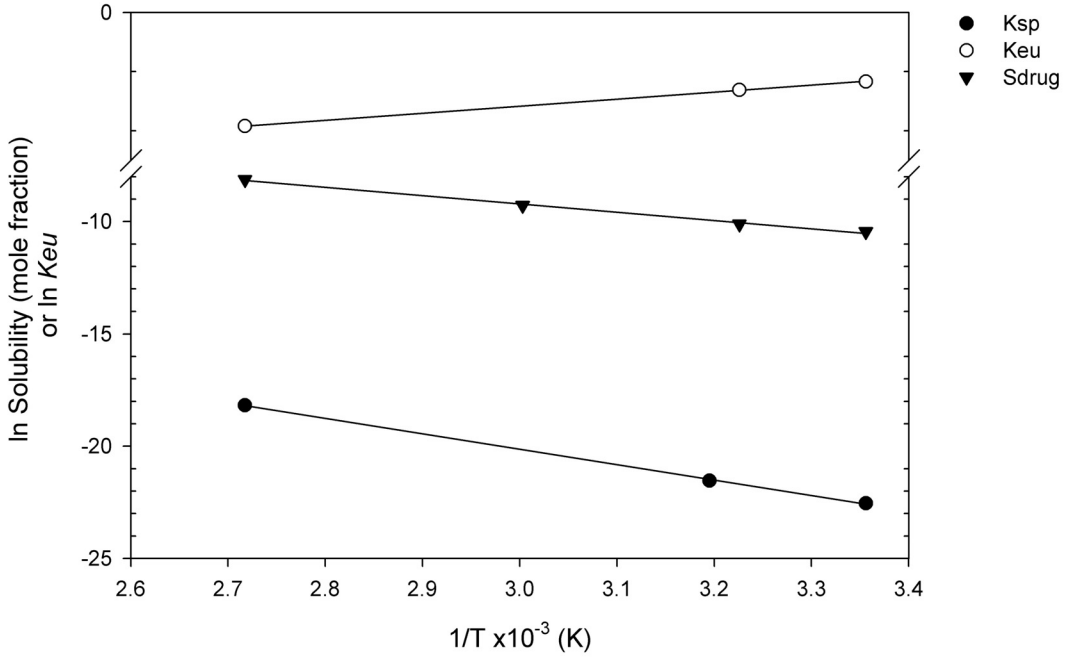

Figure 4.3: Plot of ln SMZ-BA K_{eu} (open circles), K_{sp} (filled circles), and SMZ solubility (triangles) against inverse temperature. Slope and standard error values are listed in Table 4.3.

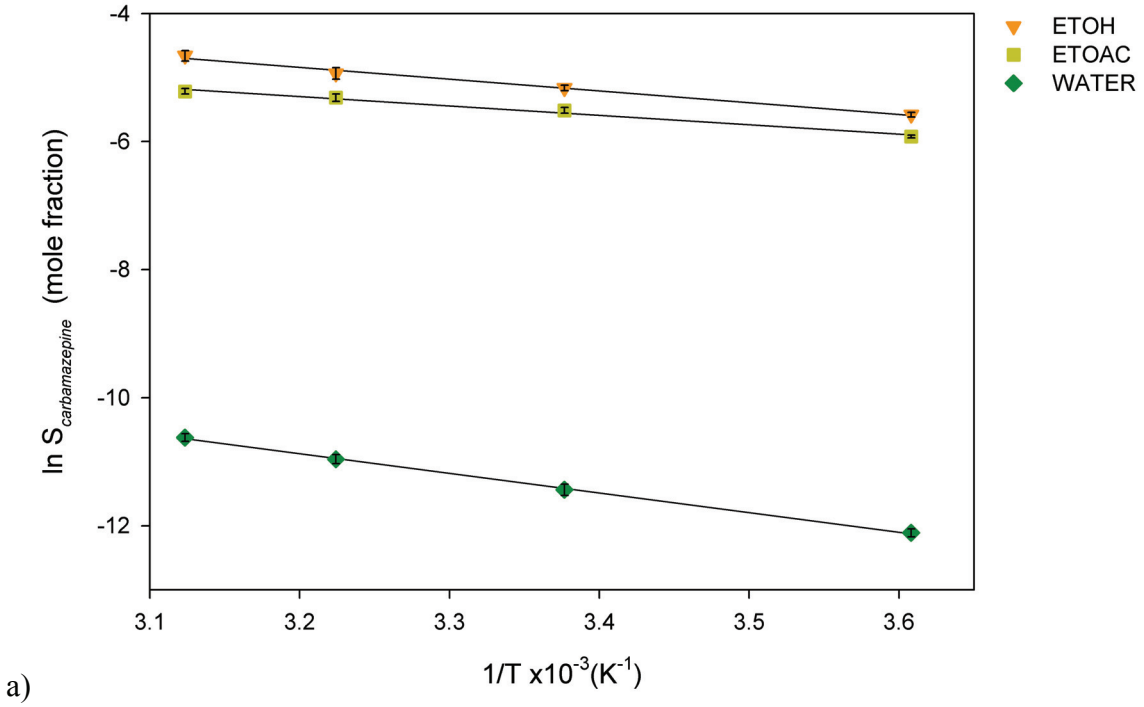

a)

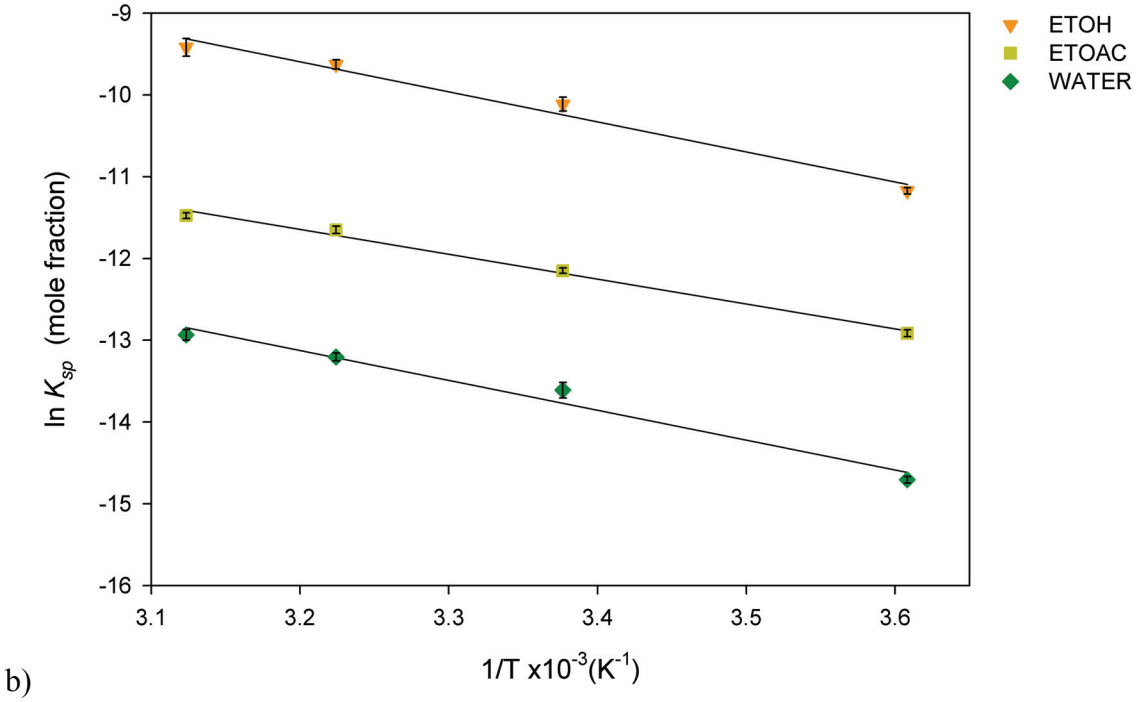

b)

Figure 4.4: Plots of ln solubility against inverse temperature for a) CBZ and b) CBZ-NCT. Error bars represent the standard error for each measured solubility. Lines represent the best linear fit and the slopes are reported in Table 4.3. Solvents: ethanol (triangles), ethyl acetate (squares), and water (diamonds). a) Water: CBZ(D).

Table 4.3: Enthalpy of solution for CBZ, CBZ-NCT, SMZ, and SMZ-BA calculated from Figure 4.4 and Figure 4.2 using the slope indicated. The observed temperature dependence of K_{eu} as well as the predicted value from the enthalpies. All enthalpy values have units of kJ/mol. *CBZ(D)

Solvent	ΔH_s^A ±SE *(slope ±SE)*	ΔH_s^{AB} ±SE *(slope ±SE)*	$2\Delta H_s^A - \Delta H_s^{AB}$ ±SE	R$d\ln K_{eu}/d(1/T)$ ±SE *(slope ±SE)*
	CBZ	*CBZ-NCT*		
water	*24.9 ±0.5	30.4 ±3.3	19.4 ±3.4	19.0 ±1.6
	(2991 ±65.7)	*(3652 ±395)*		*(2285 ±191)*
ethanol	15.3 ±1.3	30.8 ±3.0	0.0 ±3.9	1.2 ±0.6
	(1836 ±162)	*(3669 ±357)*		*(152 ±67)*
ethyl acetate	12.2 ±1.0	25.3 ±1.6	-0.8 ±2.6	0.6 ±0.6
	(1470 ±121)	*(3101 ±198)*		*(77 ±51)*
	SMZ	*SMZ-BA*		
water	30.7 ±1.5	57.3 ±1.3	4.1 ±2.0	9.8 ±0.2
	(3689 ±181)	*(6886 ±156)*		*(1188 ±24)*

CBZ-NCT was not stabilized in pure water by increasing the temperature however, higher temperature required lower $[NCT]_{eu}$ relative to $[CBZ]_{eu}$ to achieve thermodynamic cocrystal stability. For SMZ-BA suspensions there were no observed transformations and the cocrystal was stable in pure water for the temperatures studied (23-90˚C). Equation 4.5 indicates the aqueous transition temperature for CBZ-NCT in water (i.e. $K_{eu}\approx 1$) is approximately >600˚C. This temperature is above the melting temperature of both components. The calculated transition temperature for SMZ-BA in water is approximately <-40˚C. These transition temperatures are calculated from ideal solution behavior according to Equation 4.5 and can provide estimates regarding the extent cocrystal stability changes relative to a component. However, properties of the

solvent can change significantly with temperature and these calculations are only approximations when extrapolating for large temperature changes.

It is evident from the results (Table 4.3) that the temperature effect on K_{eu} is solvent specific. The aqueous K_{eu} temperature dependence of CBZ-NCT is not applicable to other solvents (e.g. ethanol or ethyl acetate) that exhibit different heat of solution values for the cocrystal and components.

The temperature dependence of K_{eu} for a cocrystal-solvent system should not be extended to other solvents unless both the cocrystal has ideal solution behavior in both solvents. For different solvents the nature and strength of solution interactions between solulte-solute, solvent-solvent, and solute-solvent change and therefore the solute activities of cocrystal and its components will exhibit different temperature dependencies. The interactions between solute and solvent can be quantified in terms of the enthalpy of mixing from known heats of fusion and solution. For CBZ in water the enthalpy of mixing has been reported as approximately -11 kJ/mol at 25˚C.[10] From our measured ΔH_s values in ethanol and ethyl acetate and published CBZ (III) ΔH_f data the enthalpies of mixing are approximately -14 and -17 kJ/mol, respectively.[12] Therefore, CBZ has stronger solute-solvent interactions in these organic solvents than in water. The predicted K_{eu} behavior changes with solvent because the nature and extent of the specific solute-solvent interactions influences the heats of solution ($\Delta H_s=\Delta H_f+\Delta H_{mix}$).

The eutectics analyzed were for cocrystal and drug (E1) in equilibrium with solution. The eutectic with coformer (E2) will also have a temperature dependence based

on the cocrystal and coformer enthalpies of solution (Table 4.1). The aqueous heat of solution reported for nicotinamide in water is 19.3 kJ/mol, which gives a calculated change in K_{eu} of ΔH_s^{AB}-$2\Delta H_s^{B}$ of -8.2.[13] This value indicates the E2 K_{eu} value has high $[NCT]_{eu}$ relative to $[CBZ]_{eu}$ at high temperature. Therefore both the E1 and E2 K_{eu} values are becoming richer with respect to the minor solution component and the cocrystal phase stability region is expanding with temperature.

4.3.2. Observed temperature dependence of other cocrystals and racemates

Carbamazepine- isonicotinamide and carbamazepine-3-nitrobenzamide cocrystals

The temperature dependent solubility of (1:1) carbamazepine-isonicotinamide form I (CBZ-INA) and its solubility phase behavior in ethanol were studied by ter Horst and Cains.[14] CBZ-INA form I is indicated as isostructural to CBZ-NCT. CBZ-INA was reported as incongruently saturating in ethanol at 25˚C. The CBZ-INA K_{eu} is 1.55 compared to the CBZ-NCT value we report of 1.0.[14] Therefore, CBZ-NCT is stable in pure ethanol while CBZ-INA is unstable.

van't Hoff plots of CBZ-INA and its components were measured to construct an isothermal phase diagram at 25˚C. The authors made no indications regarding a change in cocrystal stability as a function temperature. Using the published enthalpy of solution data and the eutectic relationships we established (Equation 4.4) for the eutectic (solid cocrystal + CBZ) the calculated value for $2\Delta H_s^{A}$-ΔH_s^{AB} is 3.1. Therefore, the

isostructural cocrystals of CBZ-NCT and CBZ-INA have the same temperature dependence for the eutectic concentrations in ethanol (Table 4.3). The ethanol CBZ-NCT $2\Delta H_s^A$-ΔH_s^{AB} value in Table 4.3 is in agreement (within standard error) with the value calculated from reported data for CBZ-INA. It is unlikely that temperature change can be used to stabilize the cocrystal (K_{eu} =1) in pure solvent because of the very small to zero dependence of K_{eu} on temperature for this system, despite the CBZ-INA K_{eu} value being only slightly greater than one.

The cocrystal of carbamazepine-3-nitrobenzamide (CBZ-NBA) was also reported to be congruently saturating in ethanol between 20 and 40˚C. K_{eu} values extracted from the phase solubility diagrams indicate a range of 0.266 to 0.289.[15] From published van't Hoff data we calculate the change in $2\Delta H_s^A$-ΔH_s^{AB} to be 2.8. The three coformers studied in ethanol (NCT, INA, and NBA) all have similar solubilities relative to CBZ ($S_{coformer}/S_{CBZ}$ ~10). As expected from the component solubility relationships in Chapter 2 they are congruently saturating or only slightly more soluble than the CBZ (K_{eu} ~0.27-1.55). Each cocrystal also showed very little eutectic concentration dependence on temperature in ethanol.

Racemic compounds

The eutectic concentrations of several racemic compounds have also been shown to be dependent on temperature, but in contrast were independent of the solvent.[9, 16-18]

Studies of a investigational phosphodiesterase-4 inhibitor ((+)-3-(2-[(3-cyclopropyloxy-4-difluromethoxy)-phenyl]-2-[5-(2-(1-hydroxy-1-trifluoromethyl-2,2,2-trifluoro)-ethyl)-thiazolyl]ethyl)pyridine *N*-oxide) that was isolated as a racemic compound (referred to as **1** from here on) showed the same eutectic constant and eutectic temperature dependence in both *n*-butyl acetate and dichloroethane.[9] For both solvents the average eutectic constant (solution concentration ratio of the two enantiomers at the eutectic) was 0.08 and 0.06 for 24 and 5˚C, respectively.[19] Therefore lower temperatures have a larger range of solution compositions where the racemic compound is stable in solution ($R d\ln K_{eu}/d(1/T) \approx -1.8$). Although enthalpies of solution were not measured, these results suggest the racemic compound had a higher heat of solution than the pure enantiomers. Presumably, the enantiomer ΔH_s values (not measured) are similar for each solvent and the ΔH_s of the racemic compound does not change significantly with respect to pure enantiomers for an achiral solvent. Similar results for the temperature dependence were shown for racemic malic acid in acetone with slight shifts in K_{eu} values between 20 and 30˚C.[17] In contrast no K_{eu} change was observed for the mandelic acid racemic compound in water between 0 and 60˚C.[18]

From these examples it was seen that racemic compounds can exhibit eutectic concentration changes as a function of temperature but not all systems demonstrate this behavior. If the two enentiomers have the same interaction energies with solvent and if heteromeric (S--R) interactions between the two enantiomers are the same as homomeric

(S--S or R--R) interactions, then they should have equivalent solvation energies. Therefore, it is probable that differences in fusion enthalpies between the racemic compound and the pure enenatiomer contribute to heat of solution differences ($\Delta H_{solution}=\Delta H_{solvation}+\Delta H_{fusion}$). These heat of solution differences between a racemic compound and the pure enenatiomer would lead to the K_{eu} changes observed in some systems mentioned.

Enthalpy of fusion values for racemic compounds have been shown to typically be greater than the pure enantiomer (i.e. negative enthalpy of formation), which in part accounts for the relative stability and formation of the compound.[20] The published example of the racemic compound (**1**) showed higher fusion enthalpy, melt temperature, and presumably enthalpy of solution than the pure enantiomer. The corresponding TPD shows a larger stable region of (**1**) at low temperatures. Based on our review of solubility and enthalpy data for many racemates it is anticipated that this will be the predominant temperature dependence (if any) for most racemic compounds. Conversely, cocrystal enthalpies and temperatures of fusion have no general pattern relative to their components and depend on the solid-state interactions and packing achieved between the two components. CBZ-NCT enthalpy and melt are less than the corresponding carbamazepine values (data presented in chapter 2). For other highly soluble low melting coformers it is more likely that the temperature and enthalpy of fusion (energy/mole cocrystal component) will be below the poorly soluble drug from our literature survey. It

could be expected that these cocrystals according to Equation 4.4 would be more stable in suspensions relative to the drug at higher temperatures. This is opposite of reported and anticipated racemic compound the behavior, however these observations do not account for enthalpy of solvation which are most relevant for cocrystals with chemically/structurally different components.

4.3.3. Eutectic temperature dependence and triangular phase diagrams (TPD)

A schematic TPD shows the behavior for a 1:1 cocrystal with a transition temperature between T_1 and T_2 in Figure 4.5. The K_{eu} is inversely related to the temperature as in the case of CBZ-NCT and SMZ-BA in water. The heating of solution to T_2 corresponds to conditions where cocrystal is congruently saturating in pure solvent (blue point) and stable over a larger range of solution compositions. It is apparent that the stable cocrystal region (central region between the lines extended from the eutectic points to the middle of the triangle base) is lager at T_2. Solution compositions between the two K_{eu} values are stable at T_2 but unstable at T_1. The cocrystal represented is unstable in pure solvent at T_1 and cocrystal dissolution leads to saturation of the drug indicated by the red point.

The relationship provided in this chapter should be considered in the design of solvothermal cocrystal synthetic methods. When solutions are heated or cooled the stability region of the cocrystal defined by the eutectic points can change. For the system

in Figure 4.5, an equimolar solution of the two components at T_2 where cocrystal is the thermodynamically stable phase can lead to crystallization of the stable drug phase at T_1.

In this example, the drug has the highest heat of solution compared to the cocrystal and coformer. Cocrystals with heat of solution values greater than twice that of the drug would exhibit the opposite behavior, where the cocrystal is stable in solution below some transition temperature and unstable at higher temperatures. Therefore it is important to know the enthalpy of solution of cocrystal and its pure components so that stability can be determined for relevant synthesis, processing, storage, and biological conditions.

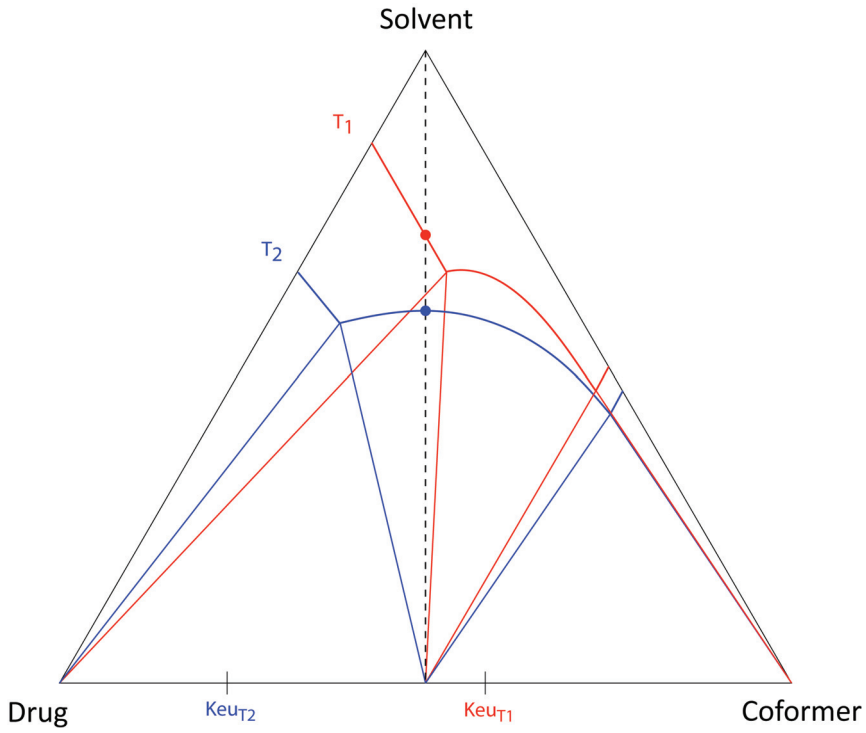

Figure 4.5: Schematic triangular 1:1 cocrystal phase diagram at two temperatures T_1 (low) and T_2 (high). The two points indicate the composition of solvent with equimolar components that is saturated with drug (red/ T_1) cocrystal (blue/ T_2). Cocrystal is stable in pure solvent at T_2 and unstable at T_1. K_{eu} values at each temperature are indicated (K_{eu}>1 at T_1, K_{eu}<1 at T_2).

4.4. CONCLUSIONS

Simple solution calorimetry can be used to calculate the thermodynamic stability of cocrystal in solvent as a function the temperature. Only small amounts of material are required to test the enthalpies of solution and construct solution phase diagrams at a variety of temperature conditions using the derived thermodynamic equations. Cocrystal K_{eu} values were shown to depend on the enthalpy of solution values of the cocrystal and drug. These enthalpy values are specific to a particular solvent and therefore the influence of temperature on cocrystal stability depends on the solvent.

In water the CBZ-NCT K_{eu} changed significantly from 330 to 110 for the temperature range studied (4-47˚C). K_{eu} values decreased with temperatures and therefore heated solvent was more favorable for the stability of cocrystal. CBZ-NCT stability in ethanol and ethyl acetate showed no temperature dependence over this same temperature range. These results were very similar to solubility phase behavior of other structurally similar CBZ cocrystals. The K_{eu} temperature dependence was also determined for SMZ-BA in water and showed that higher temperatures were more favorable to the stability of cocrystal (same trend as CBZ-NCT in water). Notable differences observed with reported racemic compounds were that the temperature dependence, if any, favors stability of the compound at low temperatures and is consistent between different solvents.

4.5. REFERENCES

(1) Mishra, D. S.; Yalkowsky, S. H., Solubility of organic compounds in non-aqueous systems: polycyclic aromatic hydrocarbons in benzene. *Industrial & Engineering Chemistry Research* **1990,** 29, (11), 2278-2283.

(2) Hildebrand, J. H.; Prausnitz, J. M.; Scott, R. L., *Regular and related solutions; the solubility of gases, liquids, and solids*. ed.; Van Nostrand Reinhold Co.: New York, 1970; p 228.

(3) Allen, F. H., The Cambridge Structural Database: a quarter of a million crystal structures and rising. *Acta Crystallographica* **2002,** B58, 380-388.

(4) Childs, S. L.; Rodríguez-Hornedo, N.; Reddy, L. S.; Jayasankar, A.; Maheshwari, C.; McCausland, L.; Shipplett, R.; Stahly, B. C., Screening strategies based on solubility and solution composition generate pharmaceutically acceptable cocrystals of carbamazepine. *Cryst Eng Comm* **2008,** 10, (7), 856-864.

(5) Rodríguez-Hornedo, N.; Nehm, S. J.; Seefeldt, K. F.; Pagan-Torres, Y.; Falkiewicz, C. J., Reaction crystallization of pharmaceutical molecular complexes. *Mol Pharm* **2006,** 3, (3), 362-7.

(6) Porter III, W. W.; Elie, S. C.; Matzger, A. J., Polymorphism in Carbamazepine Cocrystals. *Cryst. Growth Des.* **2008,** 8, (1), 14-16.

(7) Nehm, S.; Rodríguez-Spong, B.; Rodríguez-Hornedo, N., Phase Solubility Diagrams of Cocrystals Are Explained by Solubility Product and Solution Complexation. *Crystal Growth & Design* **2006,** 6, 592-600.

(8) Maheshwari, C.; Rodríguez-Hornedo, N. In *Eutectic behavior of carbamazepine-nicotinamide cocrystal*, The AAPS Journal, 2009.

(9) Wang, Y. L.; LoBrutto, R.; Wenslow, R. W.; Santos, I., Eutectic composition of a chiral mixture containing a racemic compound. *Organic Process Research & Development* **2005,** 9, (5), 670-676.

(10) Yoshihashi, Y.; Yonemochi, E.; Terada, K., Estimation of Initial Dissolution Rate of Drug Substance by Thermal Analysis: Application for Carbamazepine Hydrate. *Pharmaceutical Development and Technology* **2002,** 7, (1), 89-95.

(11) Murphy, D.; Rodríguez-Cintron, F.; Langevin, B.; Kelly, R. C.; Rodríguez-Hornedo, N., Solution-mediated phase transformation of anhydrous to dihydrate carbamazepine and the effect of lattice disorder. *International Journal of Pharmaceutics* **2002,** 246, 121-134.

(12) Rodríguez-Spong, B.; Price, C. P.; Jayasankar, A.; Matzger, A. J.; Rodríguez-Hornedo, N., General principles of pharmaceutical solid polymorphism: A supramolecular perspective. *Advanced Drug Delivery Reviews* **2004,** 56, 241-274.

(13) Kurysheva, A. S.; Sharnin, V. A.; Ledenkov, S. F., The Enthalpies of Solution of Nicotinamide in Aqueous Solutions of Ethanol and Dimethylsulfoxide. *Russian journal of Physical Chemistry* **2004,** 78, (2), 166-170.

(14) ter Horst, J. H.; Cains, P. W., Co-Crystal Polymorphs from a Solvent-Mediated Transformation. *Crystal Growth & Design* **2008,** 8, (7), 2537-2542.

(15) ter Horst, J. H.; Deij, M. A.; Cains, P. W., Discovering New Co-Crystals. *Crystal Growth & Design* **2009,** 9, (3), 1531-1537.

(16) Jacques, J.; Gabard, J., Study of optical antipodal mixtures. 3. Solubility diagrams for several types of racemates. *Bull. Soc. Chim. Fr.* **1972**, (1), 342.

(17) Kaemmerer, H.; Lorenz, H.; Black, S. N.; Seidel-Morgenstern, A., Study of System Thermodynamics and the Feasibility of Chiral Resolution of the Polymorphic System of Malic Acid Enantiomers and Its Partial Solid Solutions. *Crystal Growth & Design* **2009,** 9, (4), 1851-1862.

(18) Lorenz, H.; Seidel-Morgenstern, A., Binary and ternary phase diagrams of two enantiomers in solvent systems. *Thermochimica Acta* **2002,** 382, (1-2), 129-142.

(19) Here we have taken the inverse of the reported K_{eu} values to reflect the fact that these racemic compounds are congruently saturating. This is to be consistent with the K_{eu} definitions presented for cocrystals.

(20) Jacques, J.; Collet, A.; Wilen, S. H., *Enantiomers, racemates, and resolutions*. ed.; Wiley: New York, 1981; p xv, 447 p.

(21) Hildebrand, J. H.; Scott, R. L. The solubility of nonelectrolytes.

(22) Scatchard, G., Equilibria in non-electrolyte solutions in relation to the vapor pressures and densities of the components. *Chem Rev* **1931,** 8, (2), 321-333.

(23) Martin, E.; Yalkowsky, S. H.; Wells, J. E., Fusion of disubstituted benzenes. *Journal of Pharmaceutical Sciences* **1979,** 68, (5), 565-568.

(24) Walden, P., *Z. Elektrochem* **1908,** 14, 713-728.

(25) Yalkowsky, S. H., Estimation of Entropies of Fusion of Organic Compounds. *Industrial & Engineering Chemistry Fundamentals* **1979,** 18, (2), 108-111.

4.6. APPENDIX

Thermodynamic models for K_{eu} from drug and cocrystal fusion properties

Thermodynamic relationships for the calculation of ΔH_s of the eutectic solid phases can be used to determine the temperature dependence of K_{eu} as described in this chapter. An alternative to determining ΔH_s from solution measurements can be achieved using Kirchhhoff's law, which states the energy of a reversible process is equal to a series of irreversible processes between the same points. Therefore, we calculate the irreversible enthalpy of fusion $(\Delta H_f)_T$ of the individual eutectic solid phases at temperature T using the thermodynamic cycle with three processes: (1) heating solid phase to Tm, (2) fusion of solid at Tm, and (3) cooling of liquid to T. Furthermore, the dissolution of a crystalline drug is equivalent to the melting followed by the mixing of the liquid with solvent. The ΔH_s is then calculated as the sum of $(\Delta H_f)_T$ and the enthalpy of mixing between the solvent and solute (ΔH_{mix}):

$$\Delta H_s = (\Delta H_f)_T + \Delta H_{mix} \tag{4.6}$$

For cocrystal (AB) and drug (A) using Kirchhhoff's law we define:

$$\begin{aligned}
(\Delta H_f^{AB})_T &= (\Delta H_f^{AB})_{Tm_{AB}} + \int_T^{Tm_{AB}} C^s_{p_{(AB)}} dT + \int_{Tm_{AB}}^{T} C^l_{p_{(AB)}} dT \\
(\Delta H_f^{AB})_T &= (\Delta H_f^{AB})_{Tm_{AB}} + C^s_{p_{(AB)}} (Tm_{AB} - T) - C^l_{p_{(AB)}} (Tm_{AB} - T) \\
(\Delta H_f^{AB})_T &= (\Delta H_f^{AB})_{Tm_{AB}} - \Delta C_{p_{(AB)}} (Tm_{AB} - T)
\end{aligned} \tag{4.7}$$

$$(\Delta H_f^A)_T = (\Delta H_f^A)_{Tm_A} + \int_T^{Tm_A} C_{p_{(A)}}^s dT + \int_{Tm_A}^T C_{p_{(A)}}^l dT$$
$$(\Delta H_f^A)_T = (\Delta H_f^A)_{Tm_A} + C_{p_{(A)}}^s (Tm_A - T) - C_{p_{(A)}}^l (Tm_A - T) \quad 4.8$$
$$(\Delta H_f^A)_T = (\Delta H_f^A)_{Tm_A} - \Delta C_{p_{(A)}} (Tm_A - T)$$

where Cp refers to the heat capacity of the liquid or solid as indicated. From established ΔH_{mix} relationships that account for the pair potential energies (μ) between drug (A), coformer (B), and solvent (S):[21, 22]

$$\Delta H_{mix}^A = \frac{1}{2}(\mu_{AA} + \mu_{SS} - 2\mu_{AS})$$
$$\Delta H_{mix}^{AB} = \frac{1}{2}(\mu_{AB} + \mu_{SS} - \mu_{AS} - \mu_{BS}) \quad 4.9$$

Combining Equations 4.4, 4.6-4.9 the K_{eu} temperature dependence from thermodynamics of fusion is:

$$\frac{Rd\ln K_{eu}}{d1/T} = \begin{pmatrix} 2(\Delta H_f^A)_{Tm_A} - (\Delta H_f^{AB})_{Tm_{AB}} + 2\Delta C_{p_A}(Tm_A - T) \\ -\Delta C_{p_{AB}}(Tm_{AB} - T) + \mu_{AA} - \frac{3}{2}\mu_{AS} - \frac{1}{2}(\mu_{AB} - \mu_{SS} - \mu_{BS}) \end{pmatrix} \quad 4.10$$

From this equation it is noted that the enthalpies of fusion will contribute to a positive difference between the cocrystal and twice the drug enthalpies of fusion at their Tm will be a positive term if the cocrystal has lower melt temperature than the drug. This relationship is made based on the direct correlation between Tm and ΔH_f which has previously been reported for a variety of organic systems (i.e Walden rule).[23-25] Similarly, the difference between the cocrystal and twice the drug heat capacities can be significant when the temperature studied is far from their Tm values. While the differences in the heat capacities of drug and cocrystal are not predictable, it is apparent

that the crystalline form (A or AB) with the higher Tm will have a greater influence if the ΔCp values are similar for A and AB. Overall heat capacity terms are expected to be low relative to he entropy differences between the drug and cocrystal. The final terms describing the contributions of mixing of the liquid cocrystal components with drug or solvent are typically small (tens of calories per mole) relative to the other terms. An approximation of this equation can be made assuming $\Delta C_p=0$ and $\Delta H_{mix}=0$:

$$\frac{d\ln K_{eu}}{d1/T} = \frac{1}{R}\left[2(\Delta H_f^A)_{Tm_A} - (\Delta H_f^{AB})_{Tm_{AB}}\right] \qquad 4.11$$

This equation is equivalent to 4.4 where the enthalpy of solution is replaced with the enthalpy of fusion. Together these equations indicated the predicted temperature dependence of K_{eu}, which can be calculated from either solution (4.4) or fusion (4.11) measurements of the equilibrium solid phases.

Eutectic solid phases: 2:1 cocrystal and drug

Two equations for the eutectic equilibrium phases:

$$A_s \rightleftharpoons A_{soln}$$
$$S_A = a_A$$

$$A_2B_s \rightleftharpoons 2A_{soln} + B_{soln}$$
$$K_{sp(2:1)} = a_A^2 a_B$$

Therefore the ratio of drug and coformer at the eutectic is:

$$K_{eu} = \frac{a_B}{a_A} = \frac{K_{sp}}{S_A^3}$$

Taking the cube root of this expression give the solubility ratio:

$$(K_{eu})^{1/3} = \frac{S_{AB}}{S_A}$$

To determine the K_{eu} temperature dependence we combine the individual heat of solution equations for the two equilibrium reactions above. These equations are:

$$\frac{d\ln S_A}{dT} = \frac{\Delta H_s^A}{RT^2} \quad \text{and} \quad \frac{d\ln K_{sp}}{dT} = \frac{\Delta H_s^{AB}}{RT^2}$$

Subtracting these equations gives us the K_{eu} temperature dependence:

$$\frac{d\ln K_{eu}}{dT} = \frac{d\ln(\frac{K_{sp}}{S_A^3})}{dT} = \frac{\Delta H_s^{AB} - 3\Delta H_s^A}{RT^2}$$

For graphical determination, we can rewrite this equation as:

$$\frac{R\ d\ln K_{eu}}{d1/T} = 3\Delta H_s^A - \Delta H_s^{AB}$$

Eutectic solid phases: 2:1 cocrystal and 1:1 cocrystal

Two equations for the eutectic equilibrium phases:

$$A_2B_s \rightleftharpoons 2A_{soln} + B_{soln}$$
$$K_{sp(2:1)} = a_A^2 a_B$$

$$AB_s \rightleftharpoons A_{soln} + B_{soln}$$
$$K_{sp(1:1)} = a_A a_B$$

Therefore the ratio of drug and coformer at the eutectic is:

$$K_{eu} = \frac{a_B}{a_A} = \frac{K_{sp(1:1)}^3}{K_{sp(2:1)}^2}$$

Taking the sixth root of this expression give the solubility ratio:

$$(K_{eu})^{1/6} = \frac{S_{(1:1)AB}}{S_{(2:1)AB}}$$

To determine the K_{eu} temperature dependence we combine the individual heat of solution equations for the two equilibrium reactions above. These equations are:

$$\frac{d\ln K_{sp(1:1)}}{dT} = \frac{\Delta H_s^{AB(1:1)}}{RT^2} \quad \text{and} \quad \frac{d\ln K_{sp(2:1)}}{dT} = \frac{\Delta H_S^{AB(2:1)}}{RT^2}$$

Subtracting these equations gives us the K_{eu} temperature dependence:

$$\frac{d\ln K_{eu}}{dT} = \frac{d\ln(\frac{K_{sp(1:1)}^3}{K_{sp(2:1)}^2})}{dT} = \frac{3\Delta H_S^{AB(1:1)} - 2\Delta H_S^{AB(2:1)}}{RT^2}$$

For graphical determination, we can rewrite this equation as:

$$\frac{R\ d\ln K_{eu}}{d1/T} = 2\Delta H_S^{AB(2:1)} - 3\Delta H_S^{AB(1:1)}$$

Eutectic solid phases: 1:1 cocrystal and coformer

Two equations for the eutectic equilibrium phases:

$$B_s \rightleftharpoons B_{soln}$$
$$S_B = a_B$$

$$AB_s \rightleftharpoons A_{soln} + B_{soln}$$
$$K_{sp} = a_A a_B$$

Therefore the ratio of drug and coformer at the eutectic is:

$$K_{eu} = \frac{a_B}{a_A} = \frac{S_B^2}{K_{sp}}$$

Taking the square root of this expression give the solubility ratio:

$$(K_{eu})^{-1/2} = \frac{S_{AB}}{S_B}$$

To determine the K_{eu} temperature dependence we combine the individual heat of solution equations for the two equilibrium reactions above. These equations are:

$$\frac{d\ln S_B}{dT} = \frac{\Delta H_s^B}{RT^2} \quad \text{and} \quad \frac{d\ln K_{sp}}{dT} = \frac{\Delta H_s^{AB}}{RT^2}$$

Subtracting these equations gives us the K_{eu} temperature dependence:

$$\frac{d\ln K_{eu}}{dT} = \frac{d\ln(\frac{S_B^2}{K_{sp}})}{dT} = \frac{2\Delta H_s^B - \Delta H_s^{AB}}{RT^2}$$

For graphical determination, we can rewrite this equation as:

$$\frac{R\ d\ln K_{eu}}{d1/T} = \Delta H_s^{AB} - 2\Delta H_s^B$$

CHAPTER 5

COCRYSTAL ACTIVITY AND SOLVENT EFFECTS ON SOLUBILITY AND THERMODYNAMIC STABIILTY

The cocrystal and component solubility behavior described to this point was based on the assumption that the activity coefficients were constant for dilute solution and concentration ranges considered. In this chapter, we seek to estimate cocrystal solubility and eutectic behavior in different solvents from knowledge of component solubilities in different solvents as well as the measured cocrystal solubility in reference solvent. Component solubilities are used to estimate activity coefficient ratios in different solvents. In the synthesis and screening of pharmaceutical cocrystals from solutions, it is important to understand the effect that different solvents have on thermodynamic stability and solubility. The ability to predict the stable conditions for cocrystals in various solvents can save considerable time and materials in the development and selection process.

Solubility phase diagrams are a critical resource for the design and scale-up of solution cocrystallization processes. Measuring phase solubility behavior in various solvent systems consumes much time and materials. Several methods have been developed to reduce the resources required to generate these diagrams including

calorimetric methods or methods to analyze turbidity of known compositions as a function of temperature.[1-5] These temperature and composition data are then used to calculate the isothermal solubility phase diagrams. It has also been shown that isothermal equilibrium measurements of only the eutectic points can also be used to calculate cocrystal solubility phase behavior.[6, 7] Despite these contributions it still requires considerable resources and time to analyze various solvent systems for the design and selection of solvent and composition for solution processes to synthesize cocrystals. The objectives of this study are to (1) quantify the activity of a series of cocrystals with different physicochemical properties from their ideal solubility values and (2) predict cocrystal solution phase stability in different solvents from activity differences of the cocrystal components. To test these estimations cocrystals of carbamazepine and theophylline were studied whose solubility and thermal analysis were presented in previous chapters.

5.1. THEORETICAL

5.1.1. Ideal cocrystal solubility and activity

Melting temperatures and enthalpies of pharmaceutical crystals have found prevalent utility as indicators of ideal solubility. These are readily measurable properties associated with the crystal lattice energy that must be overcome for dissolution to occur. Among structurally similar pharmaceutical crystalline drug substances, those with high

melt temperatures are generally recognized to possess lower solubility.[8, 9] Equation 5.1 is a fundamental and common thermodynamic model for the relation between solubility and melt properties.[9] For an ideal solution the solubility, X_A^{id} (mole fraction) is a function of the heat of fusion, melt temperature, and solution temperature.

$$\ln X_{AB}^{id} = -\frac{\Delta H_f^{AB}}{R}\left(\frac{1}{T} - \frac{1}{T_m}\right) \qquad 5.1$$

$$\text{with} \quad \Delta H_f \cong \Delta H_s^{id}$$

where ΔH_s and ΔH_f are the enthalpies of solution and fusion, respectively. R is the universal gas constant and T_m is the cocrystal melting temperature. The ideal solubility product (K_{sp}^{id}) of a saturated cocrystal solution can also be calculated from Equation 5.1. For a 1:1 cocrystal $K_{sp}^{id}=(X_{AB}^{id})^2$.

The two main assumptions in Equation 5.1 are that enthalpy of fusion is temperature independent (*i.e.* heat capacity is zero) and is approximately equal to the ideal enthalpy of solution. More involved expressions have been derived to address these assumptions by including additional thermodynamic parameters such as solute heat capacity. The equation 5.1 approximation of ideal solubility, often regarded as an upper solubility limit, provides a good comparison for experimental cocrystal solubilities.[8] For an ideal solution the cocrystal activity coefficient is defined as unity. The cocrystal activity coefficient (γ_{AB}) for the saturated solution can be calculated from the difference between the ideal (X_{AB}^{id}) and observed (X_{AB}) cocrystal solubilities.

$$\ln \gamma_{AB} = \ln X_{AB}^{id} - \ln X_{AB} \qquad 5.2$$

Combining Equations 5.1 and 5.2 gives:

$$\ln X_{AB} = -\frac{\Delta H_f^{AB}}{R}\left(\frac{1}{T} - \frac{1}{T_m}\right) - \ln \gamma_{AB} \qquad 5.3$$

The activity coefficient of a cocrystal in the saturated solution can be calculated from Equation 5.3 using the observed solubility (X_{AB}) and the ideal solubility (X_{AB}^{id}) from thermal analysis. Equation 5.3 enables the quantification of the two independent factors (crystallinity and solvation) that determine the solubility of cocrystals. This relationship between cocrystal solubility and stability can be examined based on the effect of the solvent. Similar equations can be derived for the solubility of the cocrystal components.

It is apparent from these equations that cocrystals can alter drug solubility by both changing interactions of the crystalline solid (ideal solubility) and the solvation properties (activity coefficient). Other methods for improving drug solubility such as cosolvents, additives or surfactants affect only the solvation or activity coefficient.[10-12] Because cocrystals offer the potential to alter the solid-state contribution of the crystal lattice toward solubility they can supplement other solvation approaches.

5.1.2. K_{sp} and K_{eu} predictions for different solvents

If thermal properties are not readily available or measurable it is possible to use a measured solubility product in a reference solvent and the component solubilities to estimate the cocrystal solubility product in a different solvent. First we consider the

cocrystal solubility product in terms on the component activities (denoted throughout this chapter $K_{sp,a}$ by the subscript *a*):

$$K_{sp,a} = a_A^y a_B^z = \gamma_A^y X_A^y \gamma_B^z X_B^z \quad 5.4$$

where *a, γ,* and *X* are the component activities, activity coefficients, and concentrations, respectively. The subscript *a* is used to refer to the K_{sp} in activity not concentration terms. When activity coefficients are assumed to be unity (ideal solution) the cocrystal solubility product in terms of component concentrations is:

$$K_{sp} = X_A^y X_B^z \quad 5.5$$

The solubility product of a 1:1 cocrystal in concentration terms for two different solvents (s1 and s2) with non-ideal solution behavior can be related by the activity coefficients. Combining Equations 5.4 and 5.5 gives:

$$K_{sp}^{s1} \gamma_A^{s1} \gamma_B^{s1} = K_{sp}^{s2} \gamma_A^{s2} \gamma_B^{s2} = K_{sp,a} \quad 5.6$$

Rearranging these activity coefficients gives:

$$K_{sp}^{s2} = K_{sp}^{s1} \frac{\gamma_A^{s1} \gamma_B^{s1}}{\gamma_A^{s2} \gamma_B^{s2}} \quad 5.7$$

Equation 5.7 can be used to calculate the K_{sp}^{s2} from K_{sp}^{s1} when the activity coefficients are known at the corresponding component concentrations for the two solvents. The activity coefficients in a saturated component solution can also be calculated from the ideal and observed solubilities of each component. Concentrations and activity

coefficients that refer to saturated solutions of a pure component are indicated in this chapter using a superscript after the identity (e.g. A^o).

$$\gamma_{A^o} = X_A^{id} / X_{A^o}$$
$$\gamma_{B^o} = X_B^{id} / X_{B^o} \qquad 5.8$$

where X_A^{id} *and* X_B^{id} are the component ideal solubilities. $X_A^{\,o}$ and $X_B^{\,o}$ are the measured component solubility values. K_{sp}^{s2} can be estimated from K_{sp}^{s1} by assuming that the activity coefficients of the saturated component solutions are equal to the activity coefficients of the saturated cocrystal solution ($\gamma_A^{\,o}=\gamma_A$ and $\gamma_B^{\,o}=\gamma_B$). From these assumptions Equation 5.7 and 5.8 are combined to give:

$$K_{sp}^{s2} \frac{X_A^{id^{s2}} X_B^{id^{s2}}}{X_{A^o}^{s2} X_{B^o}^{s2}} = K_{sp}^{s1} \frac{X_A^{id^{s1}} X_B^{id^{s1}}}{X_{A^o}^{s1} X_{B^o}^{s1}} \qquad 5.9$$

The ideal solubility values are independent of the solvent and can be canceled from Equation 5.9:

$$K_{sp}^{s2} = K_{sp}^{s1} \frac{X_{A^o}^{s2} X_{B^o}^{s2}}{X_{A^o}^{s1} X_{B^o}^{s1}} \qquad 5.10$$

This equation provides a simple relationship to predict the cocrystal solubility in various solvents using only measured component solubilities and the K_{sp} in one solvent. It does not require the determination of activity coefficients or ideal solubility values. However, this model assumes that the activity coefficients are constant for all component concentrations. Equation 5.10 uses activity coefficients for saturated component solutions (i.e. $\gamma=\gamma^o$) in place of the actual values for the saturated cocrystal solution and

can exhibit deviations when the concentrations of cocrystal components for the cocrystal solution is very different from the component solubilities. This error would be greatest for cocrystals with large thermodynamic solubility differences relative to one or more of the components. Also, it is assumed for Equation 5.10 that the solutions are sufficiently dilute and that the presence of the second component B in solution does not alter γ_A and vice versa.

This same analysis presented for prediction of K_{sp} values in other solvents (Equation 5.10) can be extended to predict K_{eu} values for a different solvent. $K_{eu,a}$ is the activity ratio of the two cocrystal components at the eutectic.

$$K_{eu,a} = a_{Beu} / a_{Aeu} = \gamma_{Beu} X_{Beu} / \gamma_{Aeu} X_{Aeu}$$

The K_{eu} in concentration terms for two solvents (s1 and s2) are:

$$K_{eu}^{s1} = X_{Beu}^{s1} / X_{Aeu}^{s1}$$
$$K_{eu}^{s2} = X_{Beu}^{s2} / X_{Aeu}^{s2}$$

Substituting K_{eu} in the $K_{eu,a}$ expression shows the difference between the two solvents are the γ values for the two components in each solvent:

$$K_{eu}^{s2} \frac{\gamma_{Beu}^{s2}}{\gamma_{Aeu}^{s2}} = K_{eu}^{s1} \frac{\gamma_{Beu}^{s1}}{\gamma_{Aeu}^{s1}} = K_{eu,a}$$

By substituting the activity coefficients with solubilities as defined by Equation 5.8 the ideal solubility values cancel (solvent independent) to give:

$$K_{eu}^{s2} \frac{X_B^{id} X_{A^o}^{s2}}{X_{B^o}^{s2} X_A^{id}} = K_{eu}^{s1} \frac{X_B^{id} X_{A^o}^{s1}}{X_{B^o}^{s1} X_A^{id}} \qquad 5.11$$

Again, the ideal solubility values are independent of the solvent and can be canceled from Equation 5.11:

$$K_{eu}^{s2} = K_{eu}^{s1} \frac{X_{B^o}^{s2} X_{A^o}^{s1}}{X_{B^o}^{s1} X_{A^o}^{s2}} \qquad 5.12$$

Therefore, the eutectic constants in various solvents can be predicted based on the solubility of the components in each solvent based on the same assumptions that apply for Equation 5.10 just for the case of the eutectic concentrations (i.e. $\gamma_A^o = \gamma_{Aeu}$ and $\gamma_B^o = \gamma_{Beu}$). Changes in K_{eu} with solvent depend on the component solubilities. Under ideal conditions a solvent for which the coformer solubility is high relative to the drug should have a large K_{eu} indicating the cocrystal is more soluble relative to the drug ($K_{eu} = \alpha^{(y+z)/z}$). The influence of coformer solubility on cocrystal solubility was observed in Chapter 2 and 3. Assuming ideal conditions any increase in coformer solubility relative to the drug, by either changing coformer or solvent, is expected to increase the K_{eu} and the cocrystal solubility in pure solvent. This behavior might not be observed for different solvents if $\gamma^o \neq \gamma$ for either component.

These ideal K_{sp} and K_{eu} predictions apply to solvents where a composition exists such that the cocrystal solubility product is less than the product of the component activities (1:1 cocrystal). This criterion establishes that the free energy of cocrystal formation is favored (negative) at some composition. If no such composition exists, for the temperature and experimental conditions, then the cocrystal has a higher chemical

potential than the components and will not be thermodynamically stable and not exhibit a eutectic composition.

5.1.3. Critical coformer activity

The eutectic coformer activity (a_{Beu}) is the critical concentration required to stabilize a cocrystal in contact with a solution or in suspension. a_{Beu} is important because it defines the phase stability regions and is the coformer activity when cocrystal and drug are both in equilibrium with solution. The coformer activity has been calculated by dividing the measured eutectic coformer concentration by the solubility of the coformer in pure solvent.[13] The solute activity coefficient is assumed to be constant in dilute solutions and the solute activity is proportional to its concentration. Therefore, estimation of the eutectic coformer concentration for a solvent can be made from the solubility ratio of cofomer in two solvents:

$$X_{B_{eu}}^{s2} = X_{B_{eu}}^{s1} \frac{X_{B^o}^{s2}}{X_{B^o}^{s1}} \qquad 5.13$$

where X_{Beu} and $X_B{}^o$ refer to coformer concentration at the cocrystal eutectic and to coformer solubility in pure solvent, respectively.

5.2. MATERIALS AND METHODS

5.2.1. Materials

Anhydrous monoclinic form III carbamazepine (CBZ(III)) and anhydrous theophylline form II (THP) were obtained from Sigma-Aldrich (99+% purity) and used as received.[14-16] Carbamazepine dihydrate (CBZ(D)) was prepared by stirring CBZ(III) in water for at least twenty-four hours. The hydrate of theophylline was prepared in the same manner. Cocrystal coformers nicotinamide (NCT) and saccharin (SAC) were obtained from Sigma-Aldrich (99+% purity) and used as received. All crystalline drugs and coformers were characterized by X-ray powder diffraction (XRPD) and Raman spectroscopy before use. No impurities in the form of additional peaks were resolved during HPLC analysis of solutions containing the drug or coformer in this study. Ethanol (EtOH), isopropanol (IPA), and ethyl acetate (EtOAc) were obtained from Fisher Scientific and dried using molecular sieves prior to use. All the cocrystals used for solubility studies were precipitated from coformer solutions by adding solid drug according to the reaction crystallization method (RCM).[17, 18] Cocrystals of carbamazepine-saccharin and carbamazepine-nicotinamide refer to the form I polymorphs.[19]

5.2.2. Solubility analysis of cocrystal, drug, and coformer

Cocrystal and components solubilities and eutectic concentrations were measured adding excess solid to solvent and stirring with magnetic stir bars for 2-5 days. The solubilities of THP-NCT and its components were measured at 23±1˚C as described in Chapter 2. Nicotinamide, theophylline, and THP-NCT aqueous solubilities were measured under non-ionizing conditions between pH 4 and 7. The K_{sp} values of THP-NCT and CBZ-NCT (water) are listed in Chapter 2, and were calculated from the eutectic concentrations. CBZ-SAC and its components were measured at 25±0.1˚C. Saccharin and CBZ-SAC solubilities in water were measured in solutions below pH 1 where saccharin is predominantly unionized. K_{sp} values of CBZ-SAC and CBZ-NCT (organic solvents) are those reported in Chapter 3, and were calculated from multiple points in the phase solubility diagram at and above the eutectic coformer concentration. Solutions were sampled using syringes with 0.2μm filters. Cocrystal component concentrations were analyzed by HPLC. The solid phase(s) of each sample were isolated and analyzed by XRPD to ensure no phase transformation occurred.

5.2.3. High performance liquid chromatography (HPLC)

Solution concentrations of drug and coformer were analyzed by Waters HPLC (Milford, MA) equipped with a UV/Vis spectrometer detector. A C18 Atlantis column (5μm, 4.6 x 250mm; Waters, Milford, MA) at ambient temperature was used to separate

the drug and the coformer. A gradient method with a water, methanol, and trifluoroacetic acid mobile phase was used with a flow rate of 1mL/min. Sample injection volumes were between 10-40μL. Absorbance of the drug and coformer analytes was monitored between 210-300nm. Empower software from Waters was used to collect and process the data. All concentrations in this chapter are reported in mole fraction.

5.2.4. X-ray powder diffraction (XRPD)

XRPD was used to identify crystalline phases in equilibrium with solution. At the eutectic point these phases were cocrystal and drug. XRPD patterns of solid phases were obtained with a Rigaku MiniFlex X-ray diffractometer (Danvers, MA) using Cu Kα radiation (λ = 1.5418 Å), a tube voltage of 30 kV, and a tube current of 15 mA. The intensities were measured at 2θ values from 2° to 30° with a continuous scan rate of 2.5°/min. Solid phases were analyzed prior to and after equilibration. Results were compared to diffraction patterns reported in literature or calculated from crystal structures published in the Cambridge Structural Database.[20]

5.2.5. Differential scanning calorimetry (DSC)

Crystalline samples of 1-3 mg were analyzed by differential scanning calorimetry (DSC) using a TA instrument (Newark, DE) 2910 MDSC system equipped with a refrigerated cooling unit. DSC experiments were performed by heating the samples at a

rate of 10 K per minute under a dry nitrogen atmosphere. Temperature and enthalpy calibration of the instrument was achieved using a high purity indium standard. Hermetic aluminum sample pans were used for all measurements. The mean result of three or more samples is reported for each substance. Cocrystal samples for DSC analysis were comprised of several large crystals grown by slow partial evaporation of solutions containing the components. These crystals were isolated from solution, washed, and characterized by Raman microscopy before being combined to yield an adequate mass for DSC analysis.

5.3. RESULTS AND DISCUSSION

5.3.1. Cocrystal activity from observed and ideal solubility values

To demonstrate cocrystal activity differences in various solvents the K_{sp} of carbamazepine-saccharin (CBZ-SAC), carbamazepine-nicotinamide (CBZ-NCT) and theophylline-nicotinamide (THP-NCT) cocrystals were measured in four solvent systems. Ideal solubility values were calculated for these cocrystals at 25˚C based on the Equation 5.1. The melting temperature and enthalpy of fusion for the cocrystals and components used in these calculations are listed in Table 5.1.

These cocrystals represent cases where the melting temperature is either below (CBZ-SAC) or between (CBZ-NCT and THP-NCT) the melt temperatures of the cocrystal components. The ideal solubility for the CBZ-SAC and CBZ-NCT is between

that of their pure components. The ΔH_f values for these two cocrystals (normalized per mole of component) are slightly above their components. For THP-NCT the ideal solubility is above both THP and NCT and the cocrystal ΔH_f is less than either component. These cocrystals and components represent a small sample although they have different fusion properties and represent a variety of structural and physicochemical properties.

The activity coefficients for CBZ-SAC, CBZ-NCT, and THP-NCT in different solvents were calculated from Equation 5.3 using measured solubilities and the ideal solubilities (mole fraction) listed in Table 5.1. The ideal solubility values represent the solubility limit imposed by the crystallinity of these solid forms. It is the maximum achievable solubility considering the energy required to break the crystalline structure. Interactions between solute-solute, solute-solvent, and solvent-solvent significantly lower the solubilities of these components relative to the ideal solubilities in Table 5.1. This solution nonideality is quantified by the activity coefficients.

Table 5.1: Fusion properties and ideal solubilities (Equation 5.1) of cocrystals and cocrystal components. Solubility and K_{sp} values are in mole fraction.

	Tm (K)	ΔH_f (kJ/mol)	ideal solubility (K_{sp}^{id})[b]
cocrystal			
carbamazepine-saccharin	450.7	27.5[a]	2.36 x10^{-2}
			(5.56 x10^{-4})
carbamazepine-nicotinamide	434.0	27.6[a]	3.08 x10^{-2}
			(9.51 x10^{-4})
theophylline-nicotinamide	448.2	14.6[a]	1.39 x10^{-1}
			(1.92 x10^{-2})
drug			
carbamazepine	465.3	25.6	2.44 x10^{-2}
theophylline	546.8	29.0	4.89 x10^{-3}
coformer			
saccharin	502.8	26.9	1.20 x10^{-2}
nicotinamide	403.8	23.8	8.12 x10^{-2}

[a]The enthalpy of fusion for cocrystals is normalized by moles of component molecules (drug + coformer) per mole of cocrystal. [b] ideal K_{sp} is the square ideal solubility.

Figure 5.1 shows, for each cocrystal and component, a graphic representation of experimental solubility values and the calculated relative contribution of the ideal solubility or activity coefficient (γ) in light and dark grey portions, respectively. The ideal solubility portion is constant for each solvent. This solubility limit is independent of the solvent and purely based on the strength of the solid-state crystalline interactions. The magnitude of the activity coefficient is different for each solvent. γ indicates the extent to which specific interactions limit solubility and is independent of the crystal

lattice strength. The highest component γ values are observed for CBZ and SAC, which are the least soluble in water. The CBZ and SAC solubilities in organic solvents were close to the ideal behavior and γ values were smaller than the aqueous value. Both CBZ and SAC have lipophilic character and are more soluble in the less polar organic solvents. SAC γ values in the organic solvents were close to one and the ideal solubility was close to the measured solubility. A small deviation was observed for carbamazepine in isopropanol, which did not correspond with the polarity of these solvents (EtOH>IPA>EtOAc). For NCT in water the γ value was positive indicating a higher observed solubility relative that the ideal. NCT is reported to exhibit self-association in water and significantly changes the nature of the solvent (i.e. viscosity, conductivity, refractive index) at high concentrations.[21-23] Figure 5.1 also shows the cocrystal activity coefficients and ideal solubilities in each solvent. CBZ-SAC activity coefficients showed a trend similar to that of carbamazepine in these solvents. CBZ-NCT also had a similar activity coefficient trend to that observed for CBZ-SAC in these solvents, however the activity coefficients were slightly higher in the organic solvents and lower in water. This corresponds to the γ values for nicotinamide, which increased in the less polar solvents. NCT and THP are more water-soluble than CBZ-SAC or its components. γ values for THP-NCT and its components in water were lower in each case than CBZ-SAC and its components. Calculated activity coefficients are listed in Table 5.2 along with the observed and ideal solubility data for these cocrystals and components.

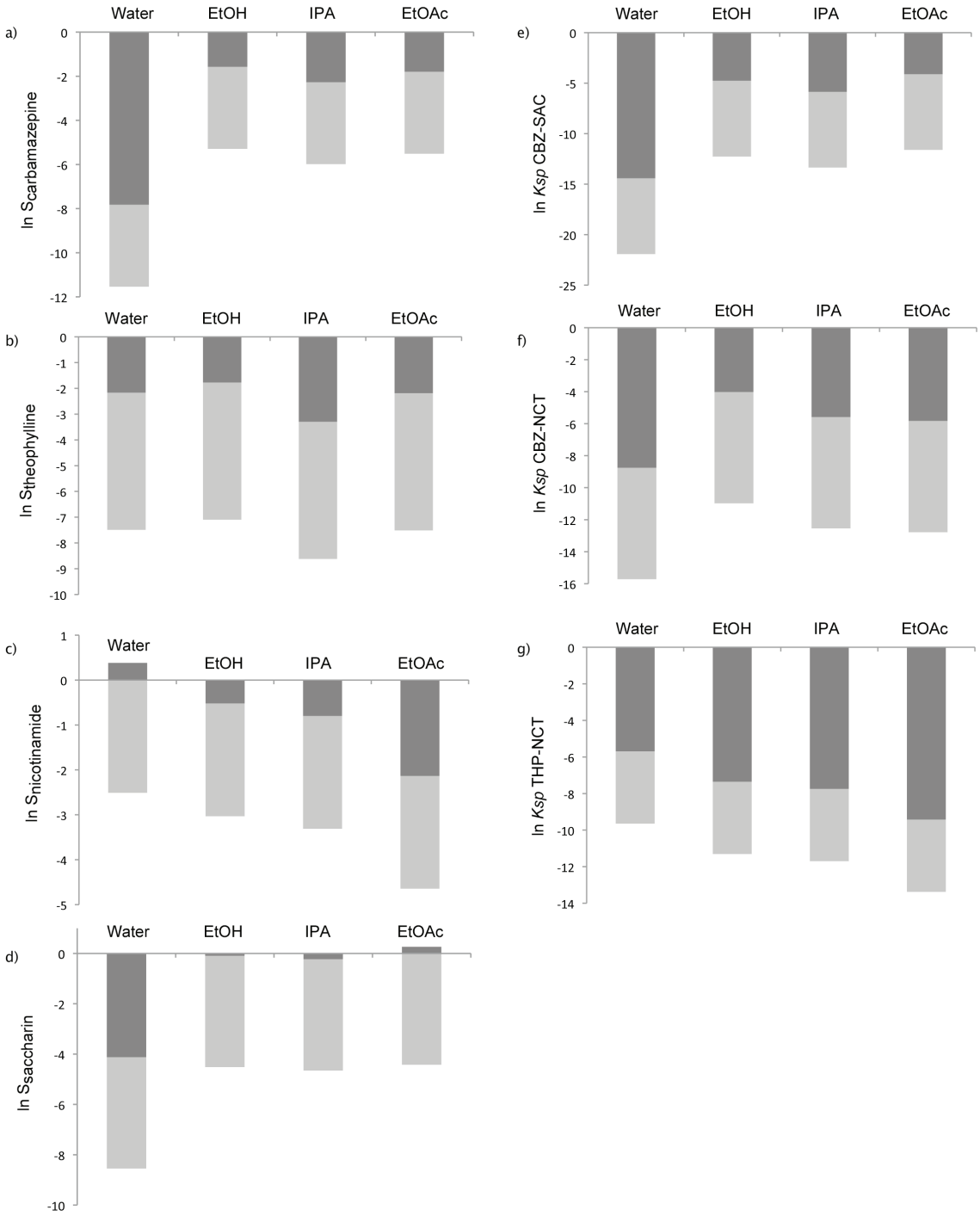

Figure 5.1: ln solubility for a) CBZ and b) THP c) NCT d) SAC e) CBZ-SAC f) CBZ-NCT g) THP-NCT in water, ethanol, isopropanol, and ethyl acetate. The solubilities are split into the ideal solubility/crystal fusion (light grey) and activity coefficient/solvation (dark grey) components according to Equation 5.3. The values of each component are reported in Table 5.2.

Table 5.2: Calculated cocrystal and component γ values from observed and ideal solubilities (Equation 5.3). ln K_{sp} values are based on mole fraction units (K_{sp} from Table 5.1).

solvent (logP)[24]	water (-1.3)	ethanol (-0.3)	isopropanol (0.5)	ethyl acetate (0.7)
carbamazepine-saccharin				
ln K_{sp}	-21.9	-12.3	-13.4	-11.6
ln K_{sp} ideal	-7.50	-7.50	-7.50	-7.5
-ln γ	-14.4	-4.8	-5.9	-4.1
carbamazepine-nicotinamide				
ln K_{sp}	-15.8	-11.0	-12.6	-12.8
ln K_{sp} ideal	-7.0	-7.0	-7.0	-7.0
-ln γ	-8.8	-4.0	-5.6	-5.8
theophylline-nicotinamide				
ln K_{sp}	-9.6	-11.3	-11.7	-13.4
ln K_{sp} ideal	-4.0	-4.0	-4.0	-4.0
-ln γ	-5.6	-7.3	-7.7	-9.4
carbamazepine				
ln K_{sp}	-11.5	-5.3	-6.0	-5.5
ln K_{sp} ideal	-3.7	-3.7	-3.7	-3.7
-ln γ	-7.8	-1.6	-2.3	-1.8
theophylline				
ln K_{sp}	-7.5	-7.1	-8.6	-7.5
ln K_{sp} ideal	-5.3	-5.3	-5.3	-5.3
-ln γ	-2.2	-1.8	-3.3	-2.2
saccharin				
ln K_{sp}	-8.5	-4.5	-4.6	-4.2
ln K_{sp} ideal	-4.4	-4.4	-4.4	-4.4
-ln γ	-4.1	0.1	-0.2	0.2
nicotinamide				
ln K_{sp}	-2.1	-3.0	-3.3	-4.6
ln K_{sp} ideal	-2.5	-2.5	-2.5	-2.5
-ln γ	0.4	-0.5	-0.8	-2.1

5.3.2. Prediction of cocrystal solubility product and stability in other solvents

The cocrystal K_{sp} measured in one solvent can be used to estimate K_{sp} and K_{eu} values in other solvents using Equations 5.10 and 5.12. Estimations were made for CBZ-SAC and THP-NCT using cocrystal component solubilities in each of the four solvents to account for activity coefficient differences. The observed solubility product in each solvent and the estimated values from three other solvents are listed in Table 5.3.

For CBZ-SAC and THP-NCT the percent error (average estimated versus observed K_{sp}) was calculated and ranges from 28-187%. This is similar to other reported cocrystal K_{sp} predictions, which had ≥27% error.[1] Despite the error associated with these K_{sp} estimations, they do provide useful guidance considering the range of solubility values is several orders of magnitude. The K_{sp} for CBZ-SAC in each of the organic solvents (K_{sp} from 1.6×10^{-6} to 9.1×10^{-6}) only slightly under estimated the aqueous K_{sp}. The estimated K_{sp} values ranged from 1.6×10^{-10} to 2.7×10^{-10} compared the observed value of 3.0×10^{-10}. These results demonstrate that good estimations can be made for solvents where the K_{sp} values differ by four orders of magnitude (10^{-6}-10^{-10}). The predictions of aqueous CBZ-SAC and THP-NCT solubilities from organics solubilities showed the best agreement with observed values. This could be from using organic reference solvents where cocrystal components exhibit more ideal behavior (low γ values). It has been suggested that measuring the K_{sp} in a reference solvent where both components have a high solubility (low γ) to can lead to better predictions.[1]

The thermodynamic stability of CBZ-SAC in each solvent was predicted using observed K_{eu} values from the other three solvents and the component solubilities (Equation 5.12). Every cocrystal K_{eu} predicted from a different solvent agreed with the observed cocrystal stability (Table 5.4). All the predicted K_{eu} values for water were greater than one, which agreed with the observation that CBZ-SAC is unstable (incongruently saturating) in water. The predicted K_{eu} values for the organic solvents were all less than one and the cocrystal was observed to be thermodynamically stable (congruently saturating) when suspended in these solvents.

Phase solubility behavior is important when synthesizing cocrystal by solution crystallization and these results demonstrate that it is not necessary to construct phase diagrams for each solvent. Solvent can be chosen based on component solubilities using Equation 5.12 after measuring the cocrystal K_{sp} or K_{eu} in one solvent. If a solvent of interest has an estimated K_{eu} value close to one (for 1:1 cocrystal), a direct measurement of the K_{eu} is reasonable to confirm the stability. The results presented here and in Chapters 3 and 4 show that eutectic constants are useful for estimating the stability and solubility behavior of cocrystals and require limited experimental work.

Table 5.3: Observed (italics) and estimated K_{sp} values for a) CBZ-SAC and b) THP-NCT cocrystals from Equation 5.10 are listed by row according to solvent. Columns list the solvent used for reference in estimating K_{sp} values for the other solvents. The average predicted K_{sp} from the three solvents is listed with the standard deviation and percent error relative to the observed value. All K_{sp} and solubility units are mole fraction.

predicted and observed K_{sp} values

a)	Water	EtOH	IPA	EtOAc	CBZ solubility	SAC solubility	average predicted K_{sp} (Equation 5.10)	standard deviation	percent error
Water	*$3.0x10^{-10}$*	$1.6x10^{-10}$	$1.2x10^{-10}$	$2.7x10^{-10}$	$9.7x10^{-6}$	$1.9x10^{-4}$	$1.9x10^{-10}$	$7.7x10^{-11}$	38
EtOH	$8.8x10^{-6}$	*$4.7x10^{-6}$*	$3.6x10^{-6}$	$8.0x10^{-6}$	$5.0x10^{-3}$	$1.1x10^{-2}$	$6.8x10^{-6}$	$2.8x10^{-6}$	44
IPA	$3.8x10^{-6}$	$2.1x10^{-6}$	*$1.6x10^{-6}$*	$3.5x10^{-6}$	$2.5x10^{-3}$	$9.5x10^{-3}$	$3.1x10^{-6}$	$9.4x10^{-7}$	97
EtOAc	$1.0x10^{-5}$	$5.4x10^{-6}$	$4.1x10^{-6}$	*$9.1x10^{-6}$*	$4.0x10^{-3}$	$1.6x10^{-2}$	$6.5x10^{-6}$	$3.1x10^{-6}$	28

b)	Water	EtOH	IPA	EtOAc	THP solubility	NCT solubility	average predicted K_{sp} (Equation 5.10)	standard deviation	percent error
Water	*$6.5x10^{-5}$*	$2.0x10^{-5}$	$8.4x10^{-5}$	$2.0x10^{-5}$	$5.6x10^{-4}$	$1.2x10^{-1}$	$4.1x10^{-5}$	$3.7x10^{-5}$	36
EtOH	$3.9x10^{-5}$	*$1.2x10^{-5}$*	$5.0x10^{-5}$	$1.2x10^{-5}$	$8.3x10^{-4}$	$4.8x10^{-2}$	$3.4x10^{-5}$	$2.0x10^{-5}$	174
IPA	$6.4x10^{-6}$	$2.0x10^{-6}$	*$8.3x10^{-6}$*	$1.9x10^{-6}$	$1.8x10^{-4}$	$3.6x10^{-2}$	$3.5x10^{-6}$	$2.6x10^{-6}$	58
EtOAc	$5.1x10^{-6}$	$1.6x10^{-6}$	$6.6x10^{-6}$	*$1.6x10^{-6}$*	$5.5x10^{-4}$	$9.6x10^{-3}$	$4.5x10^{-6}$	$2.6x10^{-6}$	187

Table 5.4: Observed (italics) and estimated K_{eu} values for CBZ-SAC from Equation 5.12 are listed by row according to the solvent. Columns list the solvent used for reference in estimating K_{sp} values for the other solvents. The average predicted K_{eu} from the three solvents is listed with the standard deviation.

predicted and observed K_{eu} values

	Water	EtOH	IPA	EtOAc	average predicted K_{eu} (Equation 5.12)	standard deviation	percent error
Water	*3.29*	1.71	1.33	2.88	1.97	0.82	38
EtOH	0.35	*0.19*	0.14	0.31	0.27	0.11	44
IPA	0.60	0.32	*0.25*	0.55	0.49	0.15	97
EtOAc	0.62	0.33	0.25	*0.56*	0.40	0.19	28

5.4. CONCLUSIONS

K_{sp} and K_{eu} are based on the activities of cocrystal components in saturated solutions of cocrystal or cocrystal and drug, respectively and can be used to express the solubility and thermodynamic stability of cocrystals. The results demonstrate that cocrystal component solubilities could be used to estimate the component activity changes in different solvents and to calculate cocrystal solubility and stability based on the measured K_{sp} in one solvent. The assumption of ideal solution behavior and the use of constant activity coefficients for different solution compositions corresponded with high error (28-187%) for estimated K_{sp} and K_{eu} values in four solvents (water, ethanol, isopropanol, and ethyl acetate). Even with the large error of the estimates K_{eu} values the observed stability of CBZ-SAC for each of the four solvents had good agreement with the estimated stability from the other solvents. The observed K_{eu} values in solvents where CBZ-SAC is congruently saturating successfully predicted incongruent behavior (water) and vice versa. Using cocrystal activity coefficients to make stability predictions can save considerable time and materials in solvent selection for synthesis of cocrystals, however for nonideal solutions these estimates have large error and are imprecise approximations of real behavior.

5.5. REFERENCES

(1) Ainouz, A.; Authelin, J. R.; Billot, P.; Lieberman, H., Modeling and prediction of cocrystal phase diagrams. *Int J Pharm* **2009,** 374, (1-2), 82-89.

(2) ter Horst, J. H.; Cains, P. W., Co-crystal polymorphs from a solvent-mediated transformation. *Cryst Growth Des* **2008,** 8, (7), 2537-2542.

(3) ter Horst, J. H.; Deij, M. A.; Cains, P. W., Discovering New Co-Crystals. *Cryst Growth Des* **2009,** 9, (3), 1531-1537.

(4) Kaemmerer, H.; Lorenz, H.; Black, S. N.; Seidel-Morgenstern, A., Study of System Thermodynamics and the Feasibility of Chiral Resolution of the Polymorphic System of Malic Acid Enantiomers and Its Partial Solid Solutions. *Cryst Growth Des* **2009,** 9, (4), 1851-1862.

(5) Lorenz, H.; Seidel-Morgenstern, A., Binary and ternary phase diagrams of two enantiomers in solvent systems. *Thermochimica Acta*\ **2002,** 382\, (1-2\), 129\-142\.

(6) Good, D. J.; Rodríguez-Hornedo, N., Cocrystal Eutectic Constants and Prediction of Solubility Behavior. *Cryst Growth Des* **2010,** 10, (3), 1028-1032.

(7) Good, D. J.; Rodríguez-Hornedo, N., Solubility Advantage of Pharmaceutical Cocrystals. *Cryst Growth Des* **2009,** 9, (5), 2252-2264.

(8) Grant, D. J. W.; Higuchi, T., *Solubility behavior of organic compounds*. ed.; Wiley: New York, 1990; p liii, 600 p.

(9) Yalkowsky, S. H., *Solubility and solubilization in aqueous media*. p.61-77 ed.; American Chemical Society ;Oxford University Press: Washington, D.C. New York, 1999; p xvi, 464 p.

(10) Millard, J. W.; Alvarez, F. A.; Yalkowsky, S. H., Solubilization by cosolvents: Establishing useful constants for the log-linear model. *Int J Pharm* **2002,** 245, (1-2), 153-166.

(11) Miyako, Y.; Tai, H.; Ikeda, K.; Kume, R.; Pinal, R., Solubility Screening on a Series of Structurally Related Compounds: Cosolvent-Induced Changes on the Activity Coefficient of Hydrophobic Solutes. *Drug Development and Industrial Pharmacy* **2008,** 34, (5), 499-505.

(12) Yalkowsky, S. H., *Techniques of solubilization of drugs*. ed.; M. Dekker: New York, 1981; p xii, 224 p.

(13) Zhang, G. G. Z.; Henry, R. F.; Borchardt, T. B.; Lou, X. C., Efficient co-crystal screening using solution-mediated phase transformation. *J Pharm Sci-Us* **2007,** 96, (5), 990-995.

(14) Porter, W. W.; Elie, S. C.; Matzger, A. J., Polymorphism in carbamazepine cocrystals. *Cryst Growth Des* **2008,** 8, (1), 14-16.

(15) Rodriguez-Spong, B.; Price, C. P.; Jayasankar, A.; Matzger, A. J.; Rodriguez-Hornedo, N., General principles of pharmaceutical solid polymorphism: a supramolecular perspective. *Advanced Drug Delivery Reviews* **2004,** 56, (3), 241-274.

(16) Szterner, P.; Legendre, B.; Sghaier, M., Thermodynamic properties of polymorphic forms of theophylline. Part I: DSC, TG, X-ray study. *Journal of Thermal Analysis and Calorimetry* **2010,** 99, (1), 325-335.

(17) Childs, S. L.; Rodriguez-Hornedo, N.; Reddy, L. S.; Jayasankar, A.; Maheshwari, C.; McCausland, L.; Shipplett, R.; Stahly, B. C., Screening strategies based on solubility

and solution composition generate pharmaceutically acceptable cocrystals of carbamazepine. *Cryst Eng Comm* **2008,** 10, (7), 856-864.

(18) Rodríguez-Hornedo, N.; Nehm, S. J.; Seefeldt, K. F.; Pagan-Torres, Y.; Falkiewicz, C. J., Reaction Crystallization of Pharmaceutical Molecular Complexes. *Mol Pharm* **2006,** 3, 362-367.

(19) Porter III, W. W.; Elie, S. C.; Matzger, A. J., Polymorphism in Carbamazepine Cocrystals. *Cryst. Growth Des.* **2008,** 8, (1), 14-16.

(20) Allen, F. H., The Cambridge Structural Database: a quarter of a million crystal structures and rising. *Acta Crystallographica* **2002,** B58, 380-388.

(21) Lim, L. Y.; Go, M. L., Caffeine and nicotinamide enhances the aqueous solubility of the antimalarial agent halofantrine. *European Journal of Pharmaceutical Sciences* **2000,** 10, (1), 17-28.

(22) Sanghvi, R.; Evans, D.; Yalkowsky, S. H., Stacking complexation by nicotinamide: A useful way of enhancing drug solubility. *International Journal of Pharmaceutics* **2007,** 336, (1), 35-41.

(23) Suzuki, H.; Sunada, H., Mechanistic studies on hydrotropic solubilization of nifedipine in nicotinamide solution. *Chemical & Pharmaceutical Bulletin* **1998,** 46, (1), 125-130.

(24) Hansch, C.; Leo, A.; Hoekman, D., *Explonng QSAR*. ed.; American Chemical Society: Washington, DC., 1995.

CHAPTER 6

STABILITY AND PHASE BEHAVIOR OF CARBAMAZEPINE-SARCOSINE ANHYDRIDE

Principles of supramolecular chemistry including hydrogen bond interactions as well as drug and cofomer structural and geometric considerations have been used to successfully engineer many pharmaceutical cocrystals.[1-13] More than fifty cocrystal forms have been identified for carbamazepine.[14] Many of the published carbamazepine cocrystals are with carboxylic acid coformers. Several of these carbamazepine cocrystals were discovered by our group using the reaction crystallization method (RCM) to screen for new cocrystals where non-stoichiometric solution concentrations of the components lead to cocrystal supersaturation and crystallization. Combining supramolecular considerations and RCM, this chapter seeks to discover cocrystals of carbamazepine with sarcosine anhydride and determine their solution phase behavior. Poole and Higuchi reported the formation of molecular complexes between sarcosine anhydride and more than forty various acids, phenols, and alcohols in aqueous solutions. The majority of the solid-state complexes they determined were 2:1 or higher order crystal forms (proton donor-sarcosine anhydride).[15] Aqueous phase diagrams were presented in Chapter 3 (Figure 3.11) for several sarcosine anhydride cocrystals to demonstrate the relationship

between K_{eu} and cocrystal solubility. The use of cofomers of amino acids and their derivatives (e.g. sarcosine anhydride) is attractive because they could prove to be nontoxic and are capable of strong hydrogen bond formation. From the reported sarcosine anhydride complexes, strong interactions were observed with components that have an aromatic nucleus and attached electrophilic groups in positions favorable for making two point attachments with the nucleophilic carbonyl groups of the sarcosine anhydride.[15] Carbamazepine is aromatic and has an amide with two hydrogens anticipated to form hydrogen bonds with the sarcosine anhydride carbonyl groups (Figure 6.1). The established rules of hydrogen bond formation indicate that the most acidic hydrogen atoms will form hydrogen bonds in crystal structures. For carbamazepine these are the amide hydrogen atoms. It was anticipated that these hydrogen atoms would each be capable of forming hydrogen bonds with the carbonyl of sarcosine anhydride. Furthermore it was anticipated these interactions might be preferred over carbamazepine amide-amide homosynthons, which occur in less than ten percent of crystals in the CSD that have only amide and acid functionalities.[16]

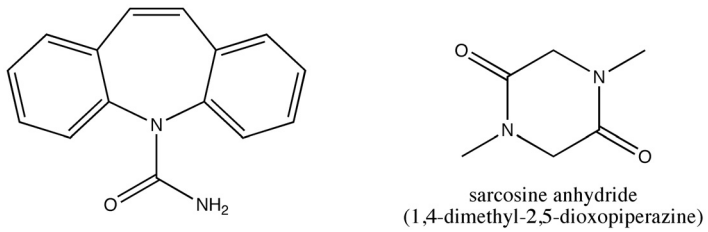

Figure 6.1: Chemical structure of carbamazepine and sarcosine anhydride.

6.1. MATERIALS AND METHODS

6.1.1. Materials

Carbamazepine (CBZ) and sarcosine (SAR) anhydride were purchased from Sigma Chemical Company (St. Louis, MO). Chemicals were used as received without further purification. All chemicals were characterized prior to use by X-ray powder diffraction (XRPD) and infrared (IR) spectroscopy. XRPD of carbamazepine agreed with the Cambridge Structural Database (CSD) simulated X-ray pattern of form III monoclinic CBZ (CSD refcode: CBMZPN01).[16]

6.1.2. Cocrystal synthesis and screening

The synthesis and screening of CBZ-SAR cocrystals was preformed by several methods including RCM, partial solvent evaporation, grinding, or solvent drop grinding. All RCM and solvent evaporation methods were done at 25 ±0.5˚C. A 2:1 cocrystal of carbamazepine-sarcosine anhydride (CBZ-SAR) was discovered by completely dissolving non-stoichiometric amounts (1:2 mole ratio CBZ:SAR) of the two components in acetonitrile and reducing the solvent by half through evaporation over two days. The 1:1 CBZ-SAR cocrystal was isolated from acetonitrile solution (~1:10 molar ratio CBZ:SAR) that was partially evaporated at room temperature. A second 2:1 cocrystal was prepared by RCM from ethanol. Table 6.1 summarizes the conditions for screening and synthesis of CBZ-SAR cocrystals.

Table 6.1: Screening and synthesis methods and conditions for CBZ-SAR cocrystal. All solution methods were done at 25˚C. Solvents are acetonitrile (ACN) and ethanol (EtOH).

Cocrystal	RCM solvent (amount of components added)	Solvent evaporation (amount of components added)	Grinding equimolar ratio (solvent drop)
2:1 CBZ-SAR (I)	ACN (CBZ 60-100mg/g +SAR 20-70mg/g)	ACN (CBZ 30-50mg/g + SAR 50-60mg/g)	-
1:1 CBZ-SAR	ACN (CBZ 40-100 mg/g +SAR 80-120mg/g) EtOH (CBZ 40mg/g +SAR 40-60mg/g)	ACN (CBZ 10-30mg/g + SAR 100mg/g)	ACN
2:1 CBZ-SAR (II)	EtOH (CBZ 40mg/g +SAR SAR 15-35mg/g)	EtOH (CBZ 20mg/g + SAR 30mg/g)	ACN

6.1.3. Eutectic concentrations of drug and coformer

Drug and cocrystal solubilities as well as eutectic concentrations were measured using solutions that were saturated with drug and/or cocrystal by adding excess solid and stirring with magnetic bars at controlled temperature for 2-5 days. Temperature was controlled using a water bath and jacketed beakers set at 25±0.5˚C. Solid drug and/or cocrystal phases were equilibrated with solution for 2-5 days and aliquots of solution were drawn using syringes with 0.2μm cellulose filters for measurement of the component concentrations by HPLC. The solid phase(s) of each sample were isolated and analyzed by XRPD to confirm solid phase(s) at equilibrium. The full method for the determination of eutectic constants is described in chapter 2.

6.1.4. High performance liquid chromatography (HPLC)

Solution concentrations of drug and coformer were analyzed by Waters HPLC (Milford, MA) equipped with a UV/Vis spectrometer detector. A C18 Atlantis column (5µm, 4.6 x 250mm; Waters, Milford, MA) at ambient temperature was used to separate the drug and the coformer. A gradient method with a water, methanol, and trifluoroacetic acid mobile phase was used with a flow rate of 1mL/min. Sample injection volumes were between 10-40µL. Absorbance of the drug and coformer analytes was monitored between 210-300nm. Empower software from Waters was used to collect and process the data. All concentrations in this chapter are reported in molal units unless otherwise noted. The stoichiometry of the sarcosine anhydride cocrystals was initially determined by completely dissolving 3-5mg of each cocrystal in ~2 ml methanol and analyzing the solution concentration ratios by HPLC.

6.1.5. X-ray diffraction

Single crystal

Single crystal X-ray diffraction data for the cocrystal was collected on a Bruker SMART APEX CCD-based X-ray diffractometer (Mo Kα radiation, λ = 0.71073 Å) equipped with a low temperature device. Empirical absorption corrections using SADABS were applied. Structure solution and refinement were performed with SHELXTL. All non-hydrogen atoms were refined anisotropically with the hydrogen

atoms placed in idealized positions except for those involved in hydrogen bonding which were allowed to refine isotropically.

Powder

XRPD was used to identify crystalline phases in equilibrium with solution. At the eutectic point studied, these phases were 2:1 cocrystal I and CBZ III or two cocrystals with different stoichiometry. XRPD patterns of solid phases were obtained with a Rigaku MiniFlex X-ray diffractometer (Danvers, MA) using Cu Kα radiation (λ = 1.5418 Å), a tube voltage of 30 kV, and a tube current of 15 mA. The intensities were measured at 2θ values from 2˚ to 30˚ with a continuous scan rate of 2.5˚/min. Solid phases were analyzed prior to and after equilibration. Results were compared to diffraction patterns reported in literature or calculated from crystal structures published in the Cambridge Structural Database.[16]

6.2. RESULTS AND DISCUSSION

6.2.1. Crystal structure of 2:1 carbamazepine-sarcosine anhydride

Single crystal X-ray analysis revealed a 2:1 CBZ-SAR cocrystal, with structural features that differ from other known CBZ cocrystals. This form is referred to as form I since another 2:1 cocrystal was discovered. Examination of the CBZ-SAR form I crystal structure shows that it is an outlier relative to the three main branches described by Childs *et al.* in the analysis of 50 CBZ crystal structures.[14] The cocrystal does not exhibit the 'translational stack', 'inversion cup' or 'coformer pairing' common to the majority of CBZ structures. Only one other reported CBZ cocrystal (CBZ-10,11-dihydrocarbamazepine) shares the CBZ-SAR space group (CSD refcode: HEMRIB).[16] Figure 6.2 shows the hydrogen bond motif for CBZ-SAR I (2:1). The common CBZ carboxamide dimer is replaced by $R_4^2(8)$ synthon involving four N-H···O hydrogen bonds wherein each sarcosine carbonyl group interacts with two CBZ amides. A second $R_2^2(8)$ synthon involves the C-H···O interaction between the CBZ carbonyl and the SAR ring. This C-H···O interaction can be considered as a hydrogen bond according to the angle and distance (160.1° C-H···O and 2.47 Å H···O).[17, 18] Table 6.2 summarizes the crystallographic properties of the 2:1 cocrystal. Simulated and experimental XRPD patterns are compared in Figure 6.4.

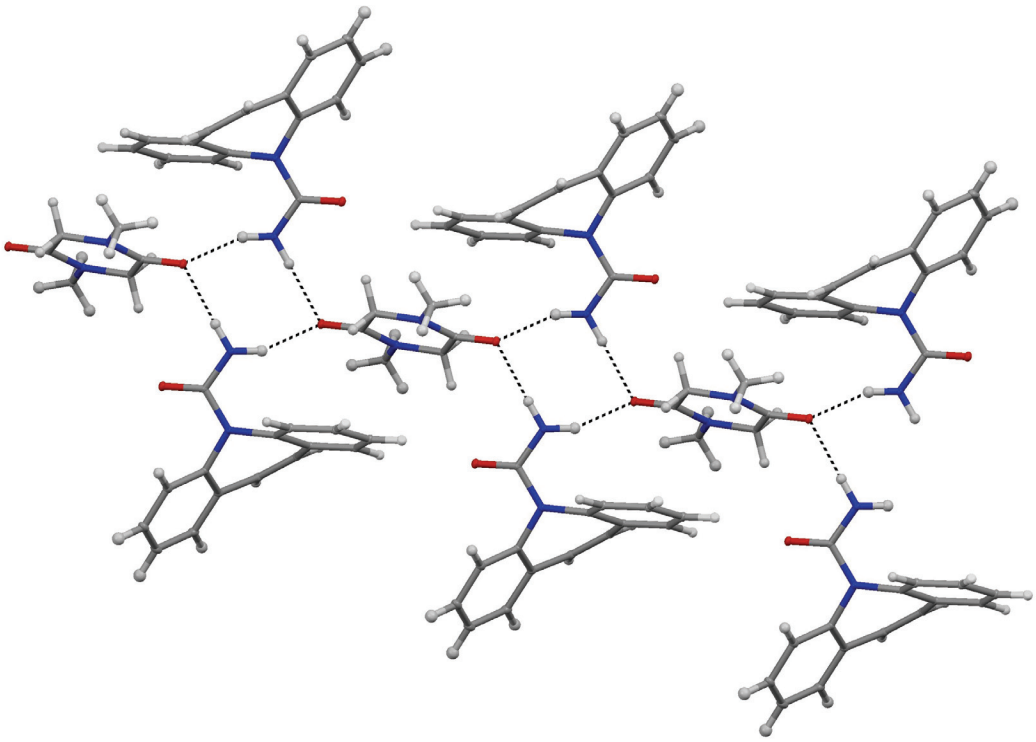

Figure 6.2: Amide-carbonyl heterosynthons in the crystal structure of 2:1 carbamazepine-sarcosine anhydride form I.

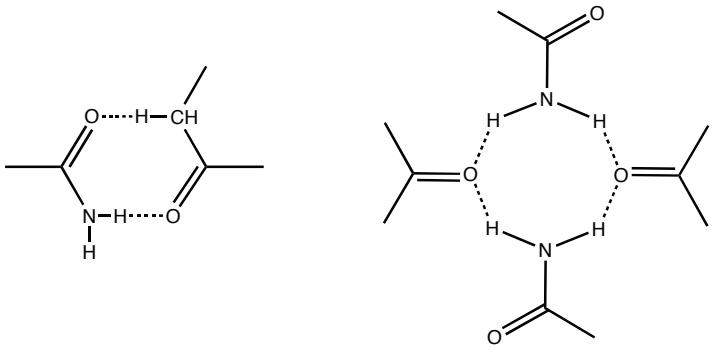

Figure 6.3: Supramolecular synthons in the in 2:1 carbamazepine-sarcosine anhydride form I crystal structure. Left: $R_2^2(8)$, right: $R_4^2(8)$.

Table 6.2: Crystallographic data of 2:1 carbamazepine-sarcosine anhydride form I.

Formula	$2(C_{15}H_{12}N_2O)$, $C_6H_{10}N_2O_2$
Formula weight	614.7
Crystal system	orthorhombic
Space group	Pbca
a (Å)	11.1122(8)
b (Å)	9.2904(6)
c (Å)	29.537(2)
Z	8
V ($Å^3$)	3049.3
ρ_{cal} (g cm^{-3})	2.678
T (K)	85(2)
R-factor	0.0399

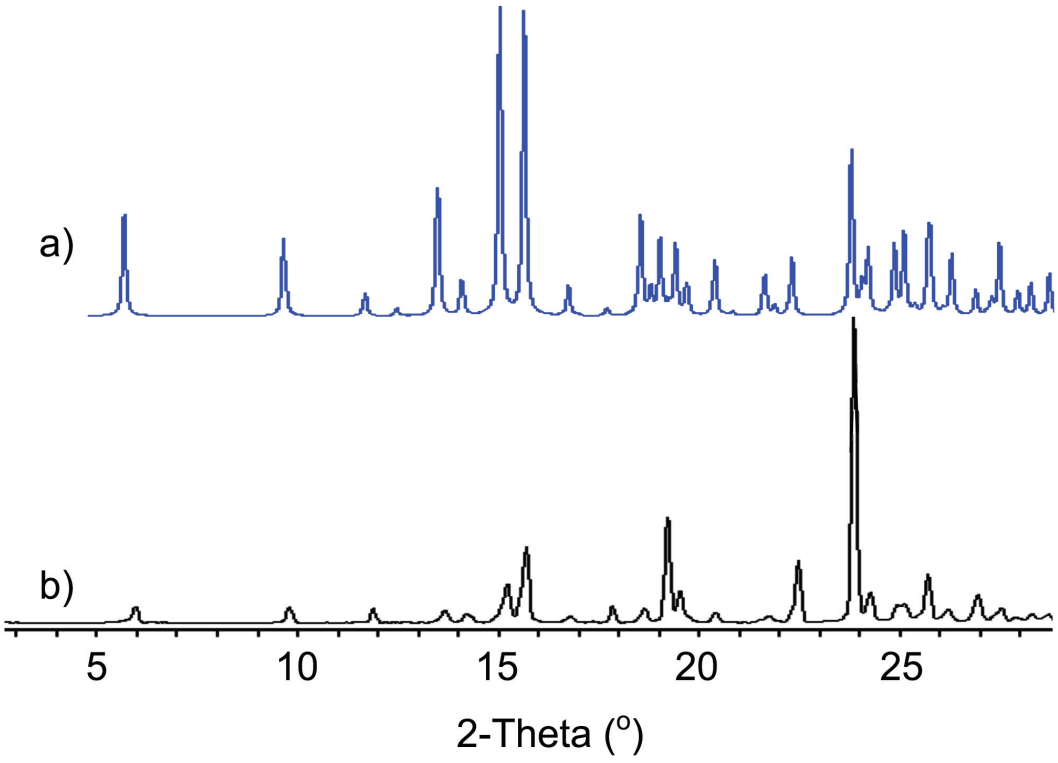

Figure 6.4: Comparison of carbamazepine-sarcosine anhydride cocrystal X-ray patterns a) simulated pattern b) experimental XRPD of 2:1 form I.

6.2.2. 1:1 and 2:1 carbamazepine-sarcosine anhydride cocrystals

Two additional crystal forms of CBZ-SAR were discovered and include a 1:1 cocrystal and another 2:1 cocrystal referred to as form II. The stoichiometry of these cocrystals was determined by dissolution and HPLC analysis. XRPDs are shown in Figure 6.5. These two forms were determined not to be solvates based on thermal analysis (DSC and TGA) shown in Figure 6.6 and 6.7 with the 2:1 form II. The 1:1 cocrystal has a lower melting temperature and a slight endotherm after the melt, which could be from 2:1 cocrystal formed during the melt. Figure 6.7 shows no weight loss before the melt that would indicate a solvate form. The TGA weight loss had two stages after the melt for each cocrystal. The first and second stages of weight loss are likely from chemical degradation of the components after the melt. Melting points of SAR and CBZ are 129 and 191˚C, respectively.

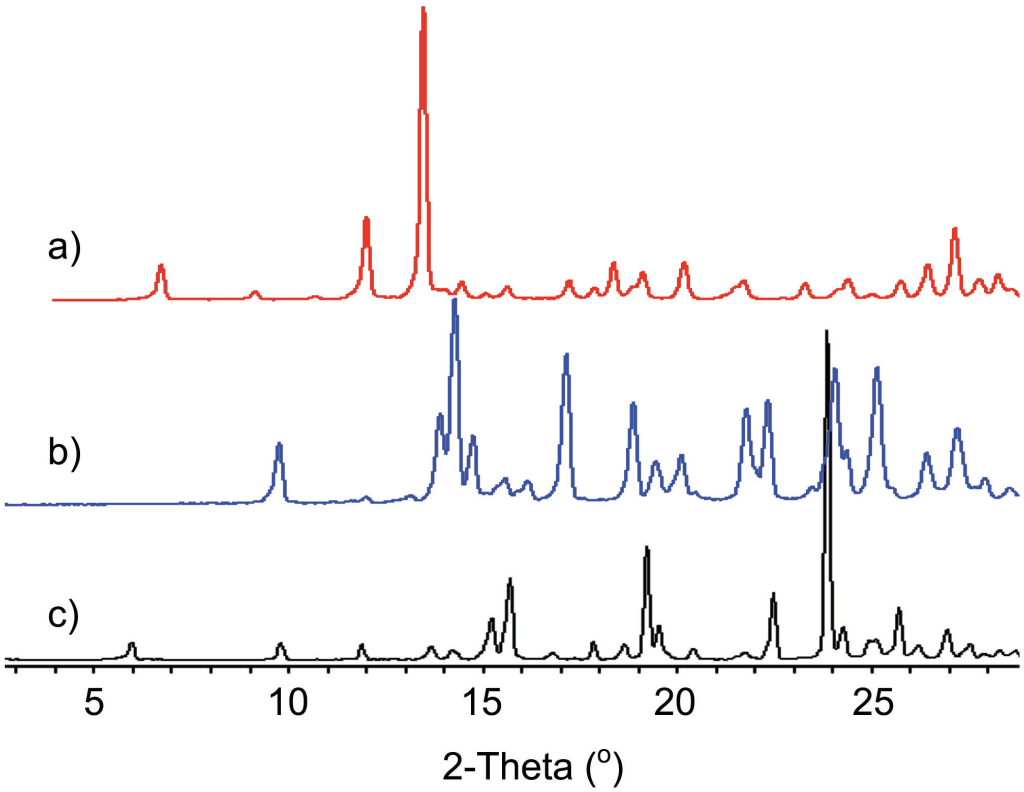

Figure 6.5: Comparison of carbamazepine-sarcosine anhydride cocrystal XRPD patterns a) 1:1, b) 2:1 form II, and c) 2:1 form I.

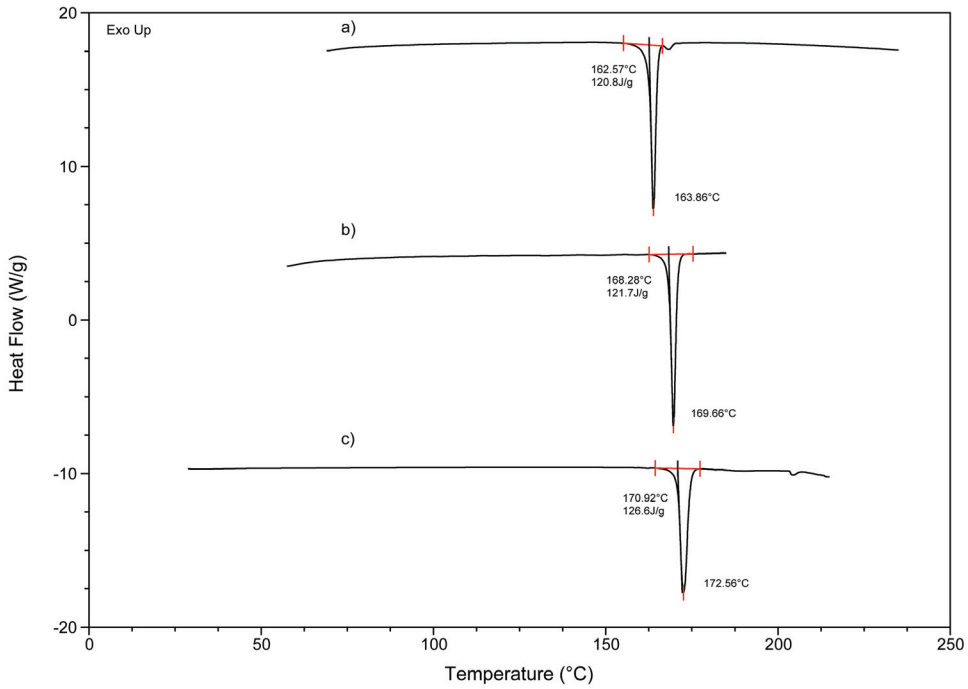

Figure 6.6: DSC of CBZ-SAR cocrystals a) 1:1, b) 2:1 form I and c) 2:1 form II.

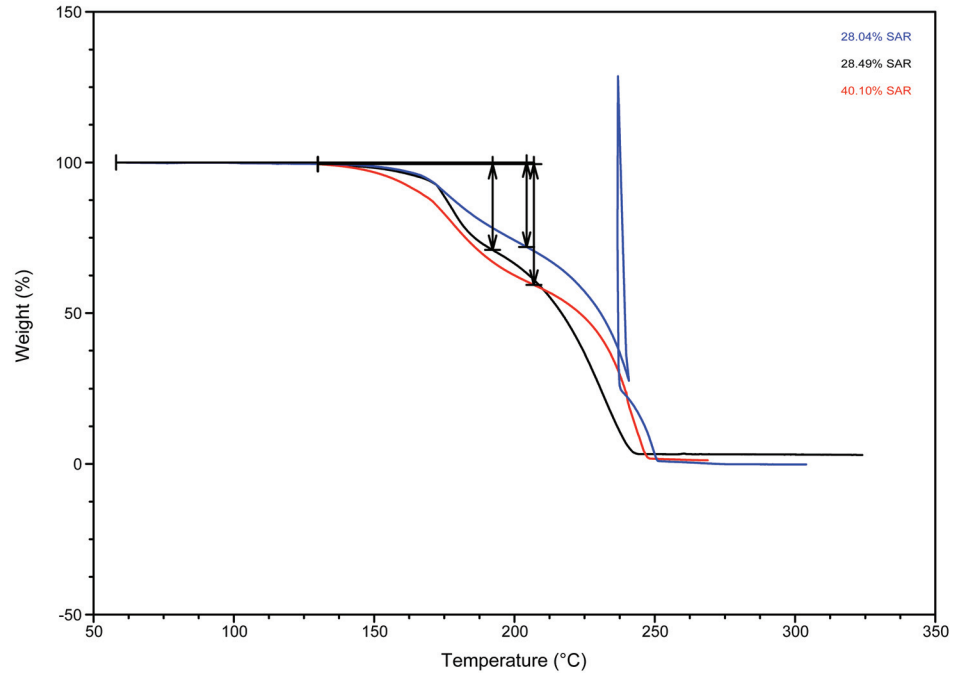

Figure 6.7: TGA of CBZ-SAR cocrystals a) 1:1 (red), b) 2:1 form I (blue) and c) 2:1 form II (black) and the approximate weight loss of the first stage after the melt.

6.2.3. Phase solubility diagram

The discovered CBZ-SAR cocrystal forms were stable in different solvents and concentration ratios of the components (Table 6.1). To understand the solubility behavior of the CBZ-SAC forms, eutectic constants and phase diagrams were measured in acetonitrile.

RCM in acetonitrile generated the 2:1 form I cocrystal at low SAR concentrations and the 1:1 cocrystal in near saturated SAR solutions. Eutectic points were measured to construct the cocrystal phase solubility diagram (Figure 6.8). These eutectic concentrations are listed in Table 6.4. Saturated solutions with concentration ratios of SAR to CBZ between approximately 1 and 3 are thermodynamically stable conditions for the 2:1 form I cocrystal. 1:1 cocrystal is stable in saturated solutions with SAR to CBZ concentration ratios above approximately 3. These eutectic values agree with the concentration ratios used to produce the 2:1 (1:2 CBZ:SAR) and 1:1 (~1:10 CBZ:SAR) cocrystals by partial solvent evaporation. The two instances where different component concentration ratios lead to the formation of these stable cocrystal forms are indicated in Figure 6.8 by dotted lines with arrows extending from the x marks.

Most of the insoluble sarcosine anhydride complexes previously reported and listed in Chapter 3 were 2:1 forms discovered at low sarcosine anhydride concentrations. 1:1 forms were not identified, but if such forms exist they could be expected to form at higher SAR concentrations. For the case of multiple CBZ-SAR cocrystal

stoichiometries, the use of high concentrations of the most soluble component (SAR) to screen for cocrystals is shown to discover a more soluble cocrystal form (1:1) based on the eutectic concentrations and K_{sp} values in Tables 6.3 and 6.4. This behavior has also been reported for carbamazepine-4-aminobenzoic acid (CBZ-4ABA) in ethanol where high concentrations of the more soluble 4-ABD lead to the formation of the more soluble (1:1) cocrystal.[19]

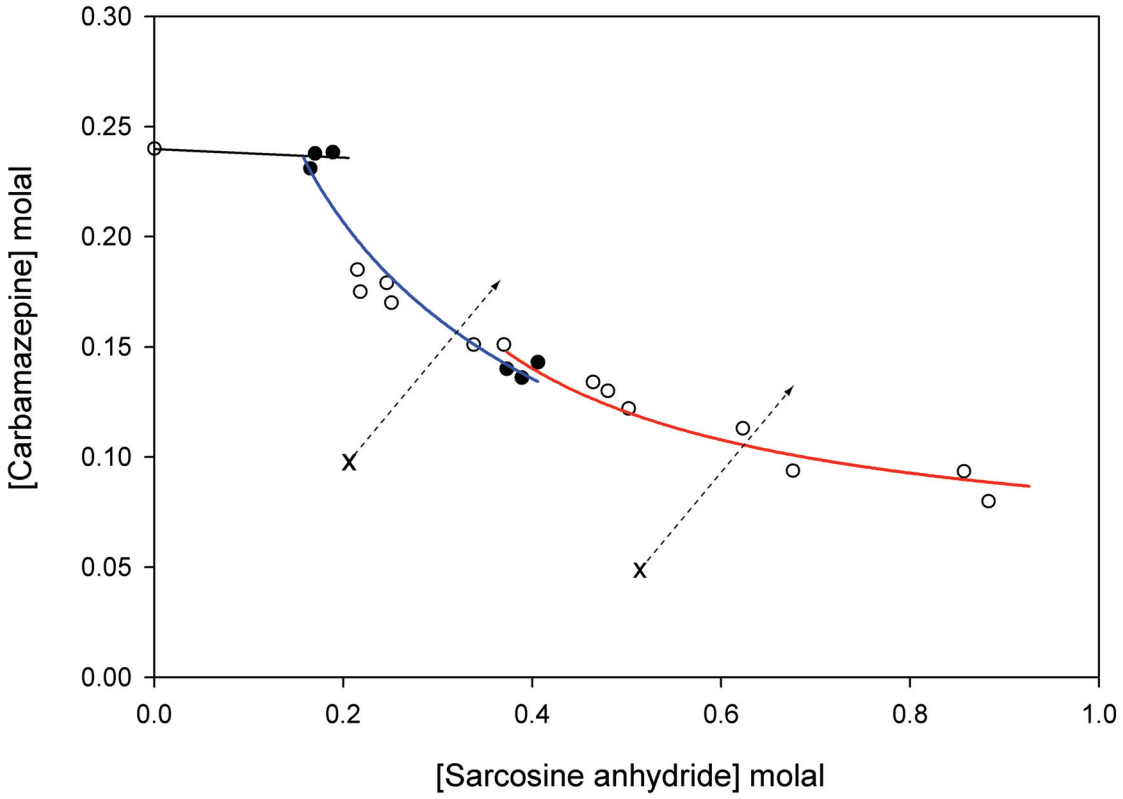

Figure 6.8: Phase solubility diagram of CBZ-SAR in acetonitrile at 25 ±0.5˚C indicating the two eutectic points (filled circles). The K_{sp} of the 2:1 form I cocrystal (blue line) and the 1:1 cocrystal (red line) were calculated by fitting Equations 3.6-3.9. Marks (x) illustrate concentrations ratios that lead to different cocrystal forms when the volume of solvent is reduced.

Table 6.3: Eutectic concentrations for CBZ-SAR in acetonitrile. The solubility of CBZ(III) in acetonitrile was measured as 0.24 ±.008m.

Eutectic	K_{eu}	$[CBZ]_{eu}$ (m)	$[SAR]_{eu}$ (m)
CBZ (III) + 2:1 CBZ-SAR (I)	0.8 ±0.1	0.23 ±8 $x10^{-3}$	0.18 ±2 $x10^{-2}$
2:1 (I) + 1:1 CBZ-SAR	2.8 ±0.3	0.14 ±5 $x10^{-3}$	0.39 ±2 $x10^{-2}$

Table 6.4: Cocrystal solubility products for CBZ-SAR in acetonitrile calculated from data in Figure 6.8 using Equations 3.6-3.9.

Cocrystal	K_{sp}
2:1 CBZ-SAR (I)	1.11 $x10^{-2}$ m^3 ±2.1 $x10^{-3}$
1:1 CBZ-SAR	3.11 $x10^{-2}$ m^2 ±3.6 $x10^{-3}$

RCM in aqueous (pH<1) saturated sarcosine anhydride solutions did not produce any form of the cocrystal. To determine the cocrystal stability and to measure the eutectic concentrations a blend of each of the three cocrystal forms was added to solutions saturated with sarcosine anhydride (no CBZ) as well as to saturated solutions of CBZ (no SAR). XRPD analysis of the solid phases at equilibrium after 2 days showed only the cocrystal components. The results indicate the components have a lower chemical potential in water than any of the cocrystal forms.

6.3. CONCLUSIONS

This chapter presents three new cocrystals of carbamazepine-sarcosine anhydride. These include two 2:1 cocrystals and a 1:1 cocrystal. The phase solubility diagram in acetonitrile is characterized by a eutectic point with two cocrystal phases (2:1 form I and 1:1 forms) as well as the eutectic point between 2:1 form I cocrystal and CBZ III, thus the 2:1 cocrystal was stable at lower coformer concentrations than the 1:1 cocrystal. The 1:1 cocrystal is more soluble and requires high sarcosine concentrations to be stable in solution. This behavior emphasizes the eutectic concentrations and solubility relationships we have previously reported to determine the cocrystal stability.[19-22] The findings of this study have potential applications to efficient cocrystal screening and synthesis.

6.4. REFERENCES

(1) Aakeroy, C. B.; Desper, J.; Fasulo, M.; Hussain, I.; Levin, B.; Schultheiss, N., Ten years of co-crystal synthesis; the good, the bad, and the ugly. *Crystal Engineering Communications* **2008,** 10, 1816-1821.

(2) Aakeroy, C. B.; Salmon, D. J., Building co-crystals with molecular sense and supramolecular sensibility. *Crystal Engineering Communication* **2005,** 7, 439-448.

(3) Anderson, K. M.; Probert, M. R.; Whiteley, C. N.; Rowland, A. M.; Goeta, A. E.; Steed, J. W., Designing Co-crystals of pharmaceutically relevant compounds that crystallize with Z' > 1. *Cryst Growth Des* **2009**, (published online Dec. 2008).

(4) Caira, M. R., Sulfa drugs as model cocrystal formers. *Molecular Pharmaceutics* **2007,** 4, (3), 310-6.

(5) Cheney, M. L.; McManus, G. J.; Perman, J. A.; Wang, Z. Q.; Zaworotko, M. J., The role of cocrystals in solid-state synthesis: Cocrystal-controlled solid-state synthesis of imides. *Cryst Growth Des* **2007,** 7, (4), 616-617.

(6) Childs, S. L.; Chyall, L. J.; Dunlap, J. T.; Smolenskaya, V. N.; Stahly, B. C.; Stahly, G. P., Crystal Engineering Approach to Forming Cocrystals of Amine Hydrochlorides with Organic Acids. Molecular Complexes of Fluoxetine Hydrochloride with Benzoic, Succinic, and Fumaric Acids. *J Am Chem Soc* **2004,** 126, 13335-13342.

(7) Desiraju, G. R., Hydrogen Bridges in Crystal Engineering: Interactions without Borders. *Accounts of Chemical Research* **2002,** 35, 565-573.

(8) Etter, M. C., Hydrogen Bonds as Design Elements in Organic Chemistry. *J Phys Chem-Us* **1991,** 95, 4601-4610.

(9) Fleischman, S. G.; Kuduva, S. S.; McMahon, J. A.; Moulton, B.; Walsh, R. D. B.; Rodríguez-Hornedo, N.; Zaworotko, M. J., Crystal Engineering of the Composition of Pharmaceutical Phases: Multiple-Component Crystalline Solids Involving Carbamazepine. *Cryst Growth Des* **2003,** 3, 909-919.

(10) Nangia, A.; Desiraju, G. R., Supramolecular Synthons and Pattern Recognition. *Topics in Current Chemistry* **1998,** 198, 57-95.

(11) Remenar, J. F.; Morissette, S. L.; Peterson, M. L.; Moulton, B.; MacPhee, J. M.; Guzman, H. R.; Almarsson, O., Crystal Engineering of Novel Cocrystals of a Triazole Drug with 1,4-Dicarboxylic Acids. *J Am Chem Soc* **2003,** 125, 8456-8457.

(12) Walsh, R. D. B.; Bradner, M. W.; Fleischman, S.; Morales, L. A.; Moulton, B.; Rodriguez-Hornedo, N.; Zaworotko, M. J., Crystal Engineering of the Composition of Pharmaceutical Phases. *Chemical Communications* **2003**, 186-187.

(13) Wenger, M.; Bernstein, J., An alternate crystal form of gabapentin: a cocrystal with oxalic acid. *Cryst Growth Des* **2008,** 8, 1595-1598.

(14) Childs, S. L.; Rodríguez-Hornedo, N.; Reddy, L. S.; Jayasankar, A.; Maheshwari, C.; McCausland, L.; Shipplett, R.; Stahly, B. C., Screening strategies based on solubility and solution composition generate pharmaceutically acceptable cocrystals of carbamazepine. *Crystal Engineering Communications* **2008,** 10, 856-864.

(15) Poole, J. W.; Higuchi, T., Complexes Formed in Aqueous Solutions by Sarcosine Anhydride - Interactions with Organic Acids, Phenols, and Aromatic Alcohols. *Journal of the American Pharmaceutical Association* **1959,** 48, (10), 592-601.

(16) Allen, F. H., The Cambridge Structural Database: a quarter of a million crystal structures and rising. *Acta Crystallographica* **2002,** B58, 380-388.

(17) Desiraju, G. R., The C-H...O hydrogen bond in crystals: what is it? *Accounts of Chemical Research* **1991,** 24, (10), 290-296.

(18) Desiraju, G. R., The CH...O Hydrogen Bond: Structural Implications and Supramolecular Design. *Accounts of Chemical Research* **1996,** 29, (9), 441-449.

(19) Jayasankar, A.; Reddy, L. S.; Bethune, S. J.; Rodríguez-Hornedo, N., Role of Cocrystal and Solution Chemistry on the Formation and Stability of Cocrystals with Different Stoichiometry. *Cryst Growth Des* **2009,** 9, (2), 889-897.

(20) Good, D. J.; Rodríguez-Hornedo, N., Solubility Advantage of Pharmaceutical Cocrystals. *Cryst Growth Des* **2009,** 9, (5), 2252-2264.

(21) Good, D. J.; Rodríguez-Hornedo, N., Cocrystal Eutectic Constants and Prediction of Solubility Behavior. *Cryst Growth Des* **2010,** 10, (3), 1028-1032.

(22) Nehm, S.; Rodríguez-Spong, B.; Rodríguez-Hornedo, N., Phase Solubility Diagrams of Cocrystals Are Explained by Solubility Product and Solution Complexation. *Cryst Growth Des* **2006,** 6, 592-600.

CHAPTER 7

HYGROSCOPIC ADDITIVES AND THE MECHANISMS BY WHICH MOISTURE GENERATES COCRYSTALS

The physical and chemical stability of pharmaceutical solids is critically dependent on the presence of water. Solid phase conversions affect the stability, safety, purity, and efficacy of the drug substance and drug product. Pharmaceutical drug products may come into contact with water during production and formulation or at any point through exposure to humid environmental conditions. Drug products that incorporate materials containing water have the potential to transfer it to other components whose stability is affected by water.[1]

Solid phase transformations present significant problems for pharmaceutical drug products when not anticipated during processing and storage. Hydrate formation is a common issue in the selection of solid-state drug forms and cocrystals also have the potential to form hydrates. Hydrate formation is associated with a critical water activity that defines the activity limit below which the anhydrous form is thermodynamically stable. Phase transformations of pharmaceutical solids that have been shown to depend on relative humidity include anhydrous to hydrate, polymorphic, and amorphous to crystalline transformations.[2-10] It appears that identifying the mechanisms for cocrystal

formation when mixed with hygroscopic additives would be of practical importance if cocrystals are to become pharmaceutical products.

The research reported here is based on the premise that mixtures of cocrystal components with hygroscopic additives can lead to cocrystal formation from a solution phase when moisture is sorbed. Earlier reports from our laboratory have shown that cocrystal solubility is a function of the cocrystal components in solution and is described by solubility product and solution speciation.[11-13] Cocrystal solubility decreases as the liquid becomes richer in one of the cocrystal components. The important implication of this mechanism is that supersaturation with respect to cocrystal can be generated by dissolving nonequivalent amounts of its components. Supersaturation is dependent on solution composition and for a binary cocrystal AB is expressed by:[13]

$$\sigma = \left(\frac{[A][B]}{K_{sp}} \right)^{1/2} \qquad 7.1$$

If the required supersaturation for cocrystal nucleation is attained then cocrystals can form. Cocrystal transformation rates have been shown to increase with increasing solution concentration of the more soluble component.[13, 14]

The thermodynamic stability of a cocrystal relative to pure component crystal has been shown to vary with the concentration of components in solution.[11, 13] Solvents in which cocrystal is more soluble than a pure component exhibit a eutectic point where the cocrystal solubility is equal to the solubility of the pure component (for 1:1 cocrystal). At this eutectic point both crystalline forms are at equilibrium. Above the eutectic

concentration cocrystal is the thermodynamically stable form. Rapid transformation of a component to cocrystal has been shown in aqueous media for components that readily transforms to a hydrate in pure water e.g., carbamazepine (CBZ) to carbamazepine-nicotinamide (CBZ-NCT) cocrystal.[13]

This work seeks to determine if cocrystal formation occurs when cocrystal components combined with hygroscopic additives are exposed to conditions where the additive sorbs water. It is hypothesized that dissolution of the cocrystal components in the sorbed water can generate supersaturation and result in nucleation of the cocrystal. CBZ-NCT was selected from previously reported pharmaceutical cocrystals because (1) transformations in aqueous solutions have been observed, (2) the high aqueous solubility of NCT relative to CBZ, (3) carbamazepine is known to form hydrates and (4) more than 40 CBZ cocrystals have been identified. This chapter presents the results of cocrystal formation in ternary mixtures of cocrystal components, comprised of (1) a deliquescent additive (sucrose or fructose), and (2) a hygroscopic additive (PVP). Many additives are hygroscopic and sorb some level moisture, but only certain crystalline materials exhibit deliquescence and have a deliquescent relative humidity (DRH) above which they equilibrate to form solutions that are saturated with respect to the deliquescent substance. Although NCT is deliquescent, its DRH is >94% and studies of mixtures with hygroscopic polymers were carried out at RH<DRH. For amorphous hygroscopic additives the nature of the interaction can vary significantly based on the chemical and physical properties of the material. For PVP is has been shown that sorption of thirty-

weight percent water causes a Tg depression of over 150˚C and the loss of glass properties at ambient temperatures which corresponds to several orders of magnitude increase in molecular mobility.[15] It is desirable to identify the mechanisms by which water sorption of additives with different solid-state forms (crystalline or amorphous) affect cocrystal formation. Finally, factors that influence the kinetics of phase transformations caused by moisture sorption are studied to understand the conditions that are most favorable for cocrystal stability.

7.1. MATERIALS AND METHODS

7.1.1. Materials

All chemicals were obtained from Sigma Chemical Company (St. Louis, MO), and were of USP grade. Chemicals were used as received without further purification. All chemicals were characterized prior to use by X-ray powder diffraction (XRPD) and infrared (IR) spectroscopy. XRPD of carbamazepine agreed with the Cambridge Structural Database (CSD) simulated X-ray pattern of form III monoclinic CBZ (CSD refcode: CBMZPN01).[16] Carbamazepine dihydrate (CBZ(D)) was prepared by stirring CBZ(III) in water for 24-48 hours. Carbamazepine-nicotinamide refers to the form I polymorph.[17] PVP K12, K30, K40, and K90 were obtained from BASF and stored at 0%RH in a P_2O_5 desiccator.

All solids were sieved to collect particle size fractions of <45μm, 45-63μm, and 106-125μm. Large crystals were hand ground prior to sieving. Samples were annealed and characterized again by XRPD and IR prior to using them in these studies. These fractions were used in preparing samples to study deliquescence and hygroscopicity by gravimetric sorption analysis and cocrystal formation in bulk samples at constant RH. The composition of the hygroscopic or deliquescent additives is expressed on a weight percent basis unless otherwise specified.

7.1.2. Eutectic concentrations of drug and coformer

Component solubilities and eutectic concentrations in polymer solutions (PVP additive) were measured using solutions that were saturated with cocrystal and/or drug by adding excess solid and stirring with magnetic bars at controlled temperature for 2-5 days. Temperature was controlled using a water bath and jacketed beakers set at 25±0.1˚C. Equilibration of solid drug and cocrystal phases was reached within 2-5 days and aliquots of solution were drawn with filtered syringes (0.2μm cellulose) for measurement of the component concentrations by HPLC. The solid phase(s) of each sample were isolated and analyzed by XRPD to verify saturation with respect to CBZ (D) and CBZ-NCT for the eutectic or CBZ (D) for the solubility measurements.

7.1.3. Moisture sorption of solid mixtures and cocrystal formation

The effects of the additive deliquescent relative humidity (DRH), storage RH, particle size, and the amount of hygroscopic component on the rate of cocrystal formation was studied using ternary mixtures of CBZ (III), with NCT and a hygroscopic additive (PVP, fructose or sucrose). NCT is deliquescent at RH >94% (25˚C) or in blends with sucrose and fructose at 80% and 55% RH, respectively.[20] RH was selected to produce conditions above and below the DRHs for the mixtures of cocrystal components with sucrose and fructose additives. For mixtures of cocrystal components with PVP several conditions (≤75%RH) were chosen at which NCT would not contribute to the different moisture sorption levels. In these studies an equimolar ratio of cocrystal components (CBZ/NCT) was used with the level of additive in the mixture at 0, 25, or 50 wt%. Raman or infrared spectroscopy was used for real-time monitoring of cocrystal formation and to study cocrystal formation at constant RH and temperature.[13, 18] Sample weight before and after storage were also monitored to determine the mass of moisture sorbed.

Desired RH conditions during storage at 25^{o}C were generated in glass desiccators with appropriate saturated salt solution: K_2CO_3•$2H_2O$ for 43%, NH_4NO_3 for 62%, NaCl for 75%, KCl for 85%, and K_2SO_4 for 98%.[19] An aluminum plate with holes was suspended above the solution to hold samples and a 1/8th inch thick quartz glass lid was used to seal the chamber. The relative humidity in the chambers was confirmed using a

HydroClip SC05 RH probe from Rotronics (Huntington, NY). Probe accuracy is ±1.5%RH / ±0.2^{o}C.

Solid mixtures were stored at 0%RH in P_2O_5 desiccators and analyzed by XRPD and IR prior to introduction into RH chambers. Raman or infrared spectroscopy was used to monitor phase transformations in the mixtures. Raman spectroscopy was used to monitor transformation in all studies of CBZ/NCT mixtures with deliquescent additives. For these studies mixtures with 30-60mg of the components (particle size fraction 45-63μm) were contained in Quartz cuvettes and introduced into the RH chambers.

Infrared spectroscopy was used to monitor all phase transformations of CBZ/NCT mixtures with polyvinylpyrrolidone. Solid mixtures of the components (150mg sieved fraction <45μm) were placed in small crystallization dishes and introduced in the RH chambers. Carbamazepine and nicotinamide mixtures (1:1 mole ratio) with PVP (25 or 50 wt%) were prepared and placed in controlled RH chambers along with equimolar binary mixtures of cocrystal components (no PVP) and pure PVP controls. The composition and storage conditions were: PVP (K12, K90), wt% PVP (25, 50%), and RH (43, 62, 75%). The samples were analyzed with the Quant2 IR calibration method to determine the weight percents of CBZ, NCT, and cocrystal. Samples were analyzed at 24h, 48h, 6 and 9 days.

7.1.4. Raman Spectroscopy

Raman spectra of solid phases were collected with a Kaiser Optical Systems, Inc. (Ann Arbor, MI), RXN1 Raman spectrometer equipped with a 785 nm laser and a fiber optic non-contact probe. Crystallization was monitored *in situ* in bulk (macroscale) with the probe and in microscale using a Leica DMLP (Wetzlar, Germany) Raman microscope. Acquisition conditions were optimized so that the spectra collected for bulk studies had maximum intensity around 30-40k counts. The spectra collected had a spectral resolution of 4 cm^{-1} and were collected between 100 and 3200 cm^{-1}. A non-contact fiber optic probe was used to collect Raman spectra through the quartz chamber lid. Spectra were collected frequently over random areas of the sample for several days. A time course of the change in spectral features was used to monitor cocrystal formation. HoloReact™ software, from Kaiser Optical Systems (Ann Arbor, MI), was used for multivariate curve resolution to plot the change in spectral features correlating to components and cocrystal. The formation of CBZ-NCT was monitored between 924-1182cm^{-1}. Samples were promptly analyzed by XRPD and IR once removed from the chamber.

7.1.5. Polarized Optical Light Microscopy Studies

Particles of cocrystal components and hygroscopic additives were placed in contact with each other on a slide and introduced into a variable relative humidity

microscope stage from Surface Measurement Systems (VGI 2000M. Middlesex, UK). For PVP samples the components were mixed with 50wt% of additive and introduced to the humidity stage. This stage provides temperature and humidity control and measurement capabilities for samples during optical microscopy. The stage is computer controlled and receives a flow of dry nitrogen that is saturated *in situ* with water to the appropriate extent as monitored by internal sensors. Water uptake, deliquescence, dissolution, and crystallization were visually monitored with a Leica DMPL polarizing optical microscope (Wetzlar, Germany). Images were collected with a Spot Insight FireWire 4 Megasample Color Mosaic camera controlled with Spot software (Diagnostics Inc, Sterling Heights, MI). Solid phases crystallized were identified by Raman microscopy.

7.1.6. Gravimetric Vapor Sorption

Vapor sorption studies were conducted at 25˚C by dynamic method to determine DRH or under constant RH to monitor the progress of moisture sorption towards equilibrium moisture content. Both types of gravimetric vapor sorption studies used samples of 5-10mg with particle size of all components between 45 and 63μm unless otherwise noted. All studies were done on an SGA-100 symmetrical gravimetric analyzer from VTI Corp. (Hialeah, FL). The instrument uses a microbalance (CI Electronics, Wiltshire, UK) to monitor sample weight and a chilled dew point analyzer

(Edgetech, Milford, MA) to detect and control humidity in the chamber. Temperature was controlled to within 0.01°C the instrument RH resolution is ±1%.

7.1.7. High performance liquid chromatography (HPLC)

Solution concentrations of drug and coformer were analyzed by Waters HPLC (Milford, MA) equipped with a UV/Vis spectrometer detector. A C18 Atlantis column (5µm, 4.6 x 250mm; Waters, Milford, MA) at ambient temperature was used to separate the drug and the coformer. A gradient method with a water, methanol, and trifluoroacetic acid mobile phase was used with a flow rate of 1mL/min. Sample injection volumes were between 10-40µL. Absorbance of the drug and coformer analytes was monitored between 210-300nm. Empower software from Waters was used to collect and process the data. All concentrations in this chapter are reported in molal units unless otherwise noted.

7.1.8. X-ray powder diffraction (XRPD)

XRPD was used to identify crystalline phases in equilibrium with solution. At the eutectic point these phases were cocrystal and drug. XRPD patterns of solid phases were obtained with a Rigaku MiniFlex X-ray diffractometer (Danvers, MA) using Cu Kα radiation (λ = 1.5418 Å), a tube voltage of 30 kV, and a tube current of 15 mA. The intensities were measured at 2θ values from 2° to 30° with a continuous scan rate of

2.5°/min. Solid phases were analyzed prior to and after equilibration. Results were compared to diffraction patterns reported in literature or calculated from crystal structures published in the Cambridge Structural Database.[16]

7.1.9. Attenuated Total Reflectance Fourier Transform Infrared Spectroscopy

IR spectra of solid phases were collected on a Bruker Vertex 70 FT-IR (Billerica, MA) unit equipped with a DTGS detector. Samples were placed on a zinc selenide (ZnSe) attenuated total reflectance (ATR) crystal accessory, and 64 scans were collected for each sample at a resolution of 4 cm^{-1} over a wavenumber region of 4000-600 cm^{-1}. The Quant2 software in Opus produced a calibration based on the standards of components and cocrystal with cocrystal varying from 0 to 100%. The optimized validation method as determined by Quant2 focused on the following two regions of wavelength: 1600-1750 cm^{-1} and 1300-1450 cm^{-1}. The validation method also applied the vector normalization pre-processing method to obtain the best calibration fit.

Calibration samples (~75mg) were prepared by mixing an equimolar ratio carbamazepine and nicotinamide (sieved particle size <45μm) with 10-90 wt% CBZ-NCT. The samples were mixed and compressed (~200 psi) using a carver press to create uniform discs for ATR-IR analysis. Each standard mixture disc was analyzed three or more different regions to characterize the uniformity of the mixtures. The calibration curve only included cocrystal fractions from 0 to 60% due to variability seen with the

standard mixtures containing high percent cocrystal. The calibration fit based on this 0 to 60% cocrystal range is shown in Table 7.1. Each component of the system showed a high regression value. Plots of the validation sample set for each component are presented in the Appendix 7.5.

Table 7.1: Calibration fit of IR standards (cocrystal and components) from Quant2.

Component	r^2
CBZ	97.84
NCT	97.85
CBZ-NCT	97.85

7.2. RESULTS AND DISCUSSION

7.2.1. Microscopy of vapor sorption and cocrystal formation

Two hygroscopic (PVP K12 and K90) and deliquescent (sucrose) additives were studied to establish the mechanism for cocrystal formation during moisture sorption. Sucrose is deliquescent and sorbs moisture to form a saturated sucrose solution at 86% and in mixtures with NCT the DRH value is lowered to 80% for NCT/sucrose.[20] This lower DRH for the NCT mixture is because NCT is deliquescent (>94% DRH) and combined with sucrose exhibits a eutonic composition.[20] PVP is hygroscopic and sorbs moisture at a wide range of RH conditions. Results presented below in Figures 7.1 and 7.2 show that moisture can generate cocrystals when particulate systems with cocrystal components are exposed to conditions where they sorb moisture. Cocrystal was formed in physical mixtures of components during moisture sorption even when carbamazepine hydrate formation was possible.

The mechanism for deliquescence-induced CBZ-NCT formation was studied by Raman microscopy using a controlled relative humidity stage at 95%RH and 25˚C. Corresponding optical images for a system containing cocrystal components CBZ and NCT with crystalline sucrose additive are provided at multiple time points during this process in Figure 7.1. Sucrose deliquesces rapidly over approximately the first seventy minutes of exposure to 95% RH and concurrent dissolution of carbamazepine and nicotinamide occurs (A-B). The first appearance of cocrystal is on the surface of a CBZ

crystal at about 100 minutes (D). Cocrystal formation propagates for the remainder of the period shown (E-F).

A physical mixture of CBZ and NCT (1:1 mole ratio, <45μm particle size) with 50 weight percent PVP K12 was also studied using a controlled relative humidity stage at 75%RH and 25˚C, as shown in Figure 7.2. The sorption was facilitated by the hygroscopic nature of PVP, not deliquescence, however a similar mechanism of cocrystal formation from solution was observed. The sorption of moisture by PVP created a solution (Figure 7.2) in which cocrystal components dissolved and CBZ-NCT nucleation and growth occurred from the solution. Dynamic vapor sorption of mixtures containing equal weight percent NCT and PVP were analyzed to confirm that NCT (DRH >94%) did not alter the hygroscopic nature of PVP at 75% RH. Figure 7.3 shows that the sorption isotherm of PVP with NCT was very similar to pure PVP. The percent weight change of this PVP/NCT mixture was scaled by the mass fraction of PVP to compare the sorption with pure PVP. The hygroscopicity of the PVP accounts for the moisture sorption of the PVP/NCT mixture at 75% RH. These results indicate that both deliquescent (sucrose) and hygroscopic (PVP) additives could cause the dissolution and solution-mediated transformation of cocrystal components to cocrystal.

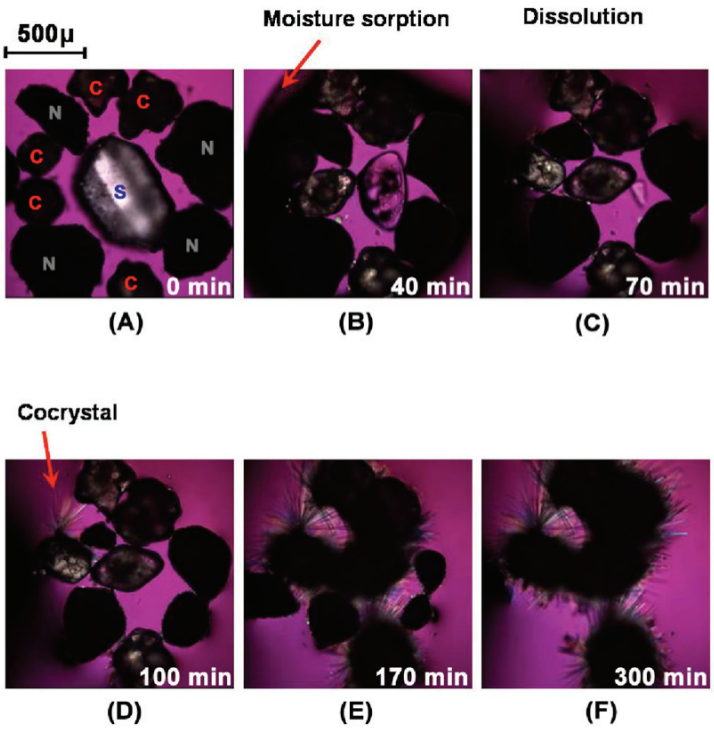

Figure 7.1: Optical microscopy images showing moisture sorption, deliquescence, dissolution and cocrystallization in CBZ/NCT/sucrose at 25°C and 95%RH. Symbols C, N and S represent CBZ, NCT and sucrose respectively. From reference [20].

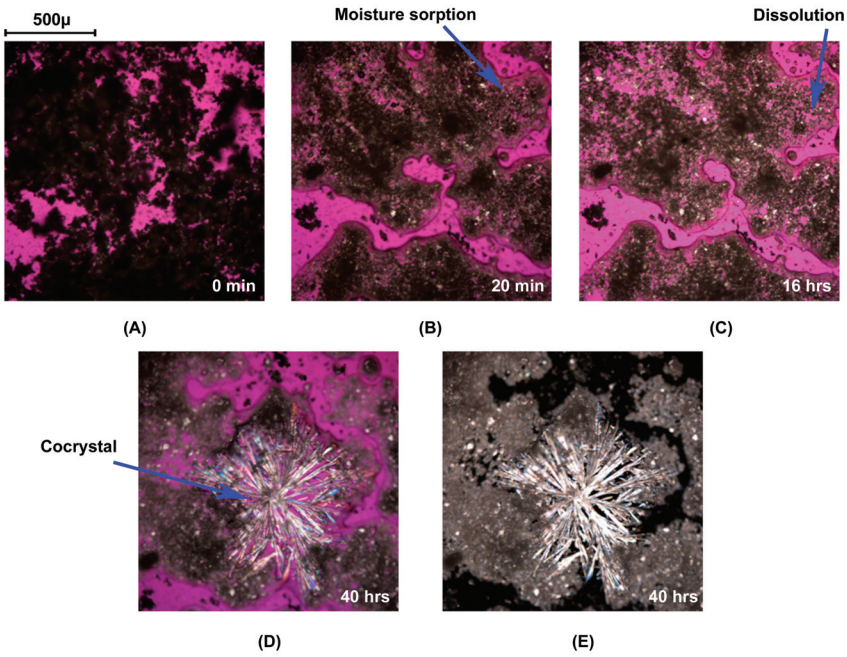

Figure 7.2: Optical microscopy images showing moisture sorption, dissolution and cocrystallization in CBZ/NCT (equimolar) mixture with PVP (50wt%) at 25°C and 75%RH.

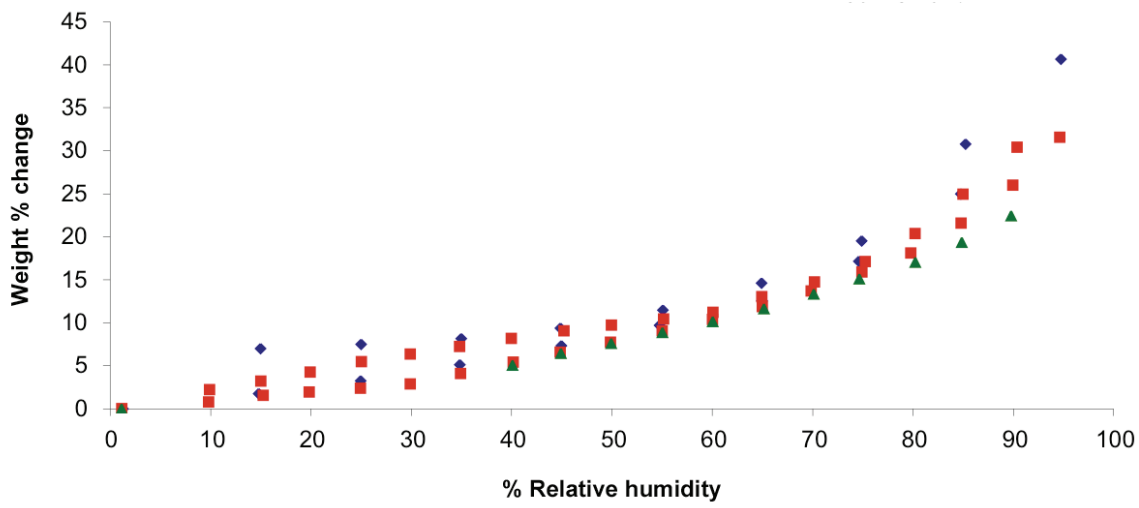

Figure 7.3: Vapor sorption isotherm for K40 (triangles), PVP K30 (squares), and 50/50 weight percent mixture of PVP K30 and NCT (diamonds). The weight percent change of the mixture is scaled by 2x to compare with the pure PVP moisture sorption.

7.2.2. Moisture sorption of solid mixtures and cocrystal formation

Raman and optical microscopy show cocrystal formation from water sorbed by PVP and sucrose and these observed transformations were hypothesized to extend to bulk samples. The formation of CBZ-NCT in bulk samples (ternary mixtures of CBZ and NCT with PVP, sucrose, or fructose) was studied by spectroscopic analysis to monitor factors that affect phase changes.

Samples with deliquescent additives

Sucrose and fructose are deliquescent materials and both exhibit vapor sorption isotherms with sharp inflections at the DRH. In mixtures with NCT the DRH values are 80% for NCT/sucrose and 55% for NCT/fructose at 25˚C.[20] Moisture sorption can lead to cocrystal transformations at conditions above these DRH values. Mixtures of CBZ and NCT with different levels of fructose or sucrose were studied at several RH conditions.

The progress of cocrystal formation in CBZ/NCT/sugar (fructose or sucrose) mixtures at 75% and 85%RH was monitored over a two-day period by Raman spectroscopy. The initial composition of sugar in these mixtures was 10%, 20%, or 50%. It is evident from Figure 7.4 that deliquescence generates cocrystals. Significant cocrystal formation was observed in CBZ/NCT/sugar mixtures above their DRH, while no cocrystal formation was detected in mixtures below their DRH. For instance, cocrystal formation occurred in sucrose and fructose mixtures at 85%RH. In contrast, the samples with sucrose at 75% RH did not form cocrystal during the course of the study

because the RH was below their DRH values (80% for NCT/sucrose mixture).[20] The control sample without sugar also shows no cocrystal formation at 85% RH.

The initial rate of transformation was highest for samples with fructose (NCT/fructose 55% DRH at 25˚C) at all conditions.[20] Comparing these initial transformation rates of fructose samples shows that increased weight fractions of fructose and higher RH conditions lead to more rapid cocrystal formation. The rate of transformation decreases with time. Early time points have the highest transformation rates. Lower rates of cocrystal formation for samples with low sugar composition and/or stored at low RH conditions may be associated with small volumes of water uptake and small domains of supersaturation leading to isolated regions of cocrystal formation in the bulk of the sample. Samples with fructose at 85% RH had higher initial transformation rates than sucrose samples for the same level of sugar and RH. The low DRH of the fructose samples corresponds to more rapid moisture sorption when introduced to the controlled RH chamber. The data in Figure 7.4 highlights the dependence of cocrystal formation rates on the mixture composition and RH.

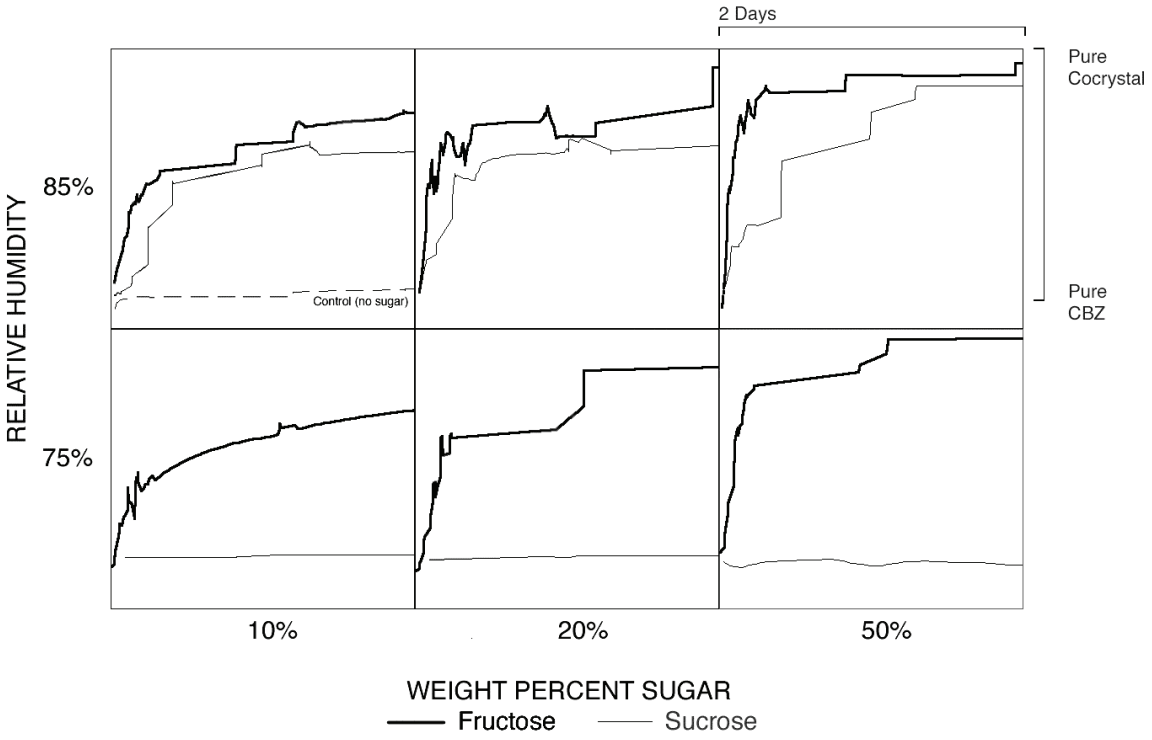

Figure 7.4: Influence of RH and sugar composition on CBZ-NCT cocrystal formation in CBZ/NCT/sugar mixtures. Six separate panes corresponding to two relative humidity conditions and three different sugar compositions are shown. Each pane has the same time and composition axis scaling presented for the top right pane. The maximum of the y-axis corresponds to pure cocrystal, while the minimum corresponds to pure components. From reference 20.

Samples with hygroscopic PVP additives

PVP sorbs moisture across a wide range of RH conditions unlike the deliquescent additives sucrose or fructose. PVP could cause similar transformations observed in the Figure 7.2 at lower relative humidity conditions. For this reason, cocrystal formation from PVP mixtures was studied at lower RH conditions (43% and 62%) than the mixtures with sucrose and fructose. The progress of cocrystal formation in CBZ/NCT/PVP mixtures at 43%, 62% and 75%RH was monitored over a six-day period by infrared

spectroscopy. The initial composition of PVP in these mixtures was 25% or 50% of either PVP K12 or K90 that are low and high molecular weight polymer grades, respectively. Results for the levels of cocrystal formation are listed in Table 7.2 and the corresponding amount of water sorbed for each sample is provided in Table 7.3. PVP K12 and K90 samples sorbed within ±1 wt% for pure PVP control samples at each RH. The average wt% value of the two PVP samples over the six days is indicated in the Table 7.3. Cocrystal formation was observed under all conditions and is associated with a 3-20% weight change due to water sorption. The highest extent of cocrystal formation was observed for CBZ/NCT with 50 wt% PVP K12 at 75%RH. These conditions resulted in 88 wt% cocrystal formation at 6 days with 20 wt% moisture sorption. The lowest extent of cocrystal formation (6-14 wt% CBZ-NCT) was with PVP K12 or K90 samples stored at 43%RH that sorbed 3 wt% moisture. Mixtures with PVP K90 exhibited less cocrystal formation at all RH levels studied. Polymer additives have been shown to inhibit the formation of CBZ(D) from anhydrous CBZ forms in aqueous solutions.[21-23] CBZ(D) formation was not observed in the samples with PVP that sorbed moisture. The main factors for the amount of cocrystal formed were (1) PVP molecular weight, (2) % of PVP, and (3) moisture sorption/RH. The samples with PVP K12 (low molecular weight) showed more cocrystal formation than high molecular weight K90 samples.

Table 7.2: CBZ-NCT formation from CBZ/NCT/PVP stored mixtures as function of RH. Cocrystal composition was quantified by infrared spectroscopy. Values indicate the weight percent cocrystal formed relative the total weight of the initial cocrystal components.

Chamber	43% RH		62% RH		75% RH	
Time point	24 hr	6 day	24 hr	6 day	24 hr	6 day
Control (no PVP)	0	2	1	2	0	2
PVP K12						
50 wt%	26	40	72	77	74	88
25 wt%	5	26	12	72	46	87
PVP K90						
50 wt%	25	23	20	19	8	25
25 wt%	5	6	4	5	3	4

Table 7.3: Moisture sorption by PVP K12/K90 observed over six days as function of RH. Values at 24 hours were within five percent of the six-day average. Scaled values represent the moisture sorption in the mixtures with CBZ and NCT.

	% weight change		
RH%	pure PVP[a]	50 wt% PVP	25 wt% PVP
43	12.92	6.46	3.23
62	26.66	13.33	6.67
75	39.93	19.97	9.98

[a] PVP K12 and K90 showed the same moisture sorption levels (±0.75wt%). Values represent the average for K12 and K90 PVP.

Effect of PVP on solubility and eutectic concentrations

Solubilities of the components and cocrystal were measured in order to determine whether the polymer is affecting kinetic or thermodynamic properties. The solubility of carbamazepine was measured in 10-30 wt% PVP solutions. CBZ(D) solubility increased

approximately 20-fold for 30 wt% PVP solutions as shown in Figure 7.5. Solutions containing PVP could also solubilize cocrystal and affect the stability and extent of cocrystal formation.

Eutectic concentrations were measured to determine CBZ-NCT solubility and stability in 10wt% PVP aqueous solutions using PVP K12, K30, and K90. The K_{eu} of CBZ-NCT in pure water is higher than all of the eutectics measured in PVP solutions. CBZ-NCT eutectic concentrations in water are 0.85 and 5.8×10^{-3}m for NCT and CBZ, respectively. K_{eu} values in 10 wt% PVP solutions ranges from 106-137 (Table 7.4), which is below the value of 147 in pure water (Chapters 2 and 3). This indicates that the addition of PVP increases CBZ-NCT stability relative to the drug, and increases the supersaturation with respect to CBZ-NCT leading to a higher rate of cocrystal formation. Additionally, the K_{eu} values increase with the PVP molecular weight (Figure 7.6a) as a result of the increase in the NCT eutectic concentration. Cocrystal is less soluble in 10 wt% PVP K12 compared to K90. In PVP K12 solutions lower NCT concentrations are required for cocrystal formation. These K_{eu} values could account for the higher level of cocrystal formation seen in K12 mixtures compared to K90 mixtures at 62 and 75% RH. Aqueous solutions with high PVP levels have lower CBZ-NCT K_{eu} values (Table 7.4) because the eutectic concentration of CBZ is increased more than NCT (Figure 7.6b-d). For solutions of the same PVP wt% the $[CBZ]_{eu}$ is similar, however the low molecular weight (K value) polymers have lower $[NCT]_{eu}$ and therefore lower K_{eu} values.

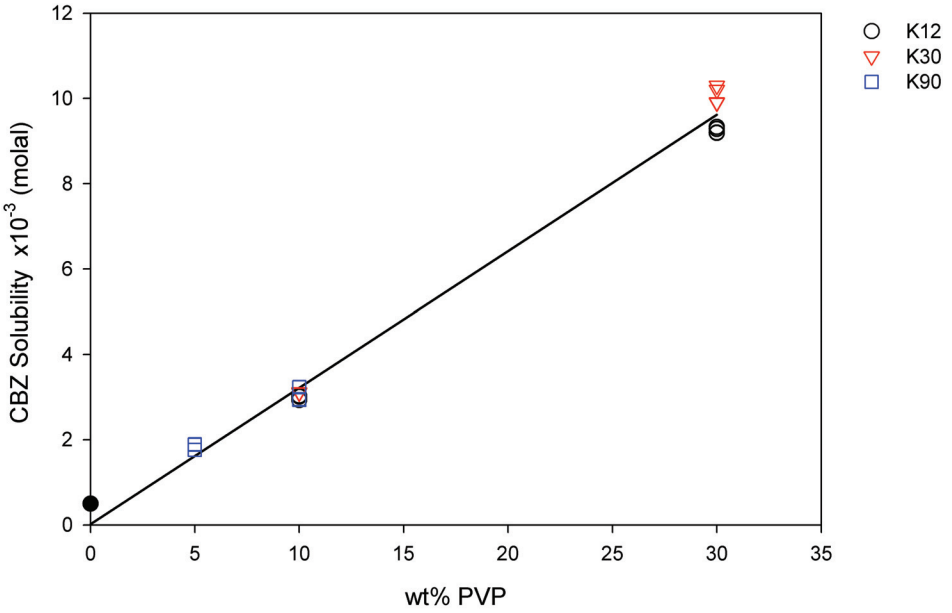

Figure 7.5: Aqueous solubility of carbamazepine against wt% PVP. PVP K12 (circles), K30 (triangles), and K90 (squares). K values are proportional to the polymer molecular weight.

Table 7.4: CBZ-NCT K_{eu} values for aqueous solutions with PVP K12, K30, or K90 at 5-10 wt%. The CBZ-NCT K_{eu} without PVP is 147±9.

	K_{eu} values		
wt%	K12	K30	K90
5	-	-	151±1.4
10	106±1.8	119±0.7	137±3.5
30	57±4.8	61±7.8	-

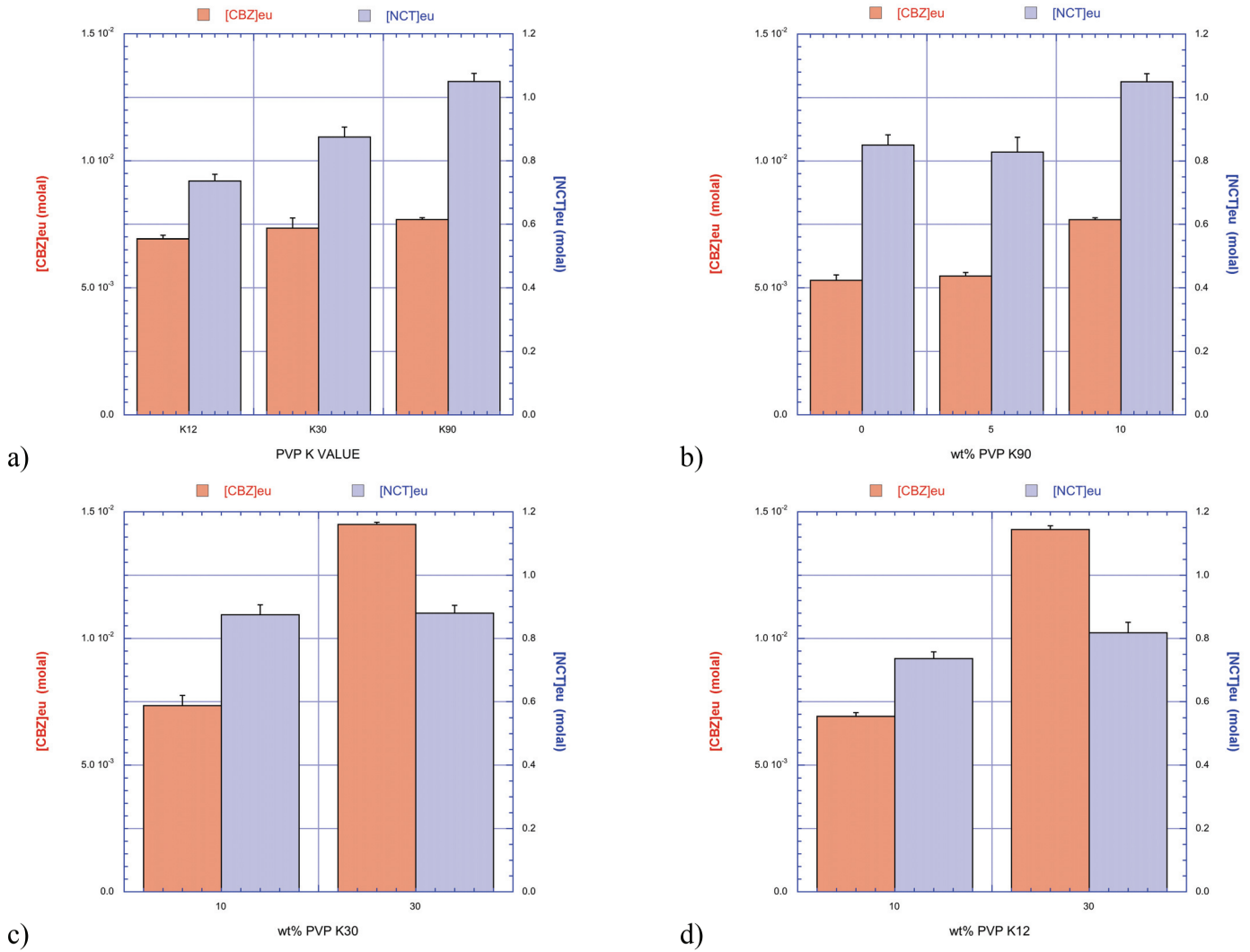

Figure 7.6: CBZ-NCT eutectic concentrations in aqueous a) 10wt% PVP solutions, b) 0, 5, and 10 wt% PVP K90 solutions, c) 10 and 30wt% PVP K30 solutions, and d) 10 and 30wt% PVP K12 solutions.

7.2.3. Discussion of solution-mediated cocrystal formation

Factors that influence the crystalline phase transformation kinetics are nucleation rate, growth rate, and the density and distribution of nucleation sites. Cocrystal nucleation and growth rates will depend on supersaturation. Cocrystal supersaturation is a function of the cocrystal K_{sp} and component concentrations as indicated by Equation 7.1. Supersaturation is determined by cocrystal component dissolution , which will be dictated by the amount and rate of water uptake. Non-stoichiometric concentrations of components in the sorbed moisture result from unequal component dissolution rates, due to different solubilities and/or surface areas. As the solution formed by the sorbed water becomes rich in one of the cocrystal components, the cocrystal solubility decreases. This is indicated by region IV in the phase solubility diagram in Figure 7.7. Cocrystal formation will be initiated when the critical supersaturation for nucleation is achieved. The CBZ and NCT system is particularly interesting since their aqueous solubilities are so different. Due to the higher dissolution rate of the more soluble component (NCT), cocrystal nucleation was observed on the surface or in the vicinity of the less soluble component (CBZ) in mixtures of components with sucrose (Figure 7.1).

The interplay between moisture uptake and dissolution determines the liquid phase composition, supersaturation and subsequent nucleation. This is shown by the rapid initial cocrystal formation rates of CBZ-NCT at both low and high sugar composition when stored at RH above DRH. Low levels of moisture (< 7%) are capable of producing the necessary cocrystal supersaturation to initiate nucleation as shown for the

transformation to CBZ-NCT in mixtures with 10% sucrose or fructose at 85% RH. Also CBZ/NCT/PVP mixtures with 25% PVP at 43%RH showed cocrystal formation with approximately 3% water content. Additives can also influence nucleation by their affects on solution viscosity, molecular associations that precede nucleation, and to the extent that material surfaces serve as catalysts for nucleation. The viscosity range of 10% PVP aqueous solutions is approximately 30-fold between PVP K12 and K90 (~15 and 450 mPa*s at 23˚C).[24-26] The viscosity difference between K12 and K90 becomes great at lower water levels and can influence the nucleation and growth kinetics. It is anticipated that higher viscosity as well as changes in the diffusion and molecular interactions of cocrystal components and PVP in solution may influence nucleation and growth. For low levels of moisture this would suggest a slower rate of cocrystal formation in PVP K90 samples.

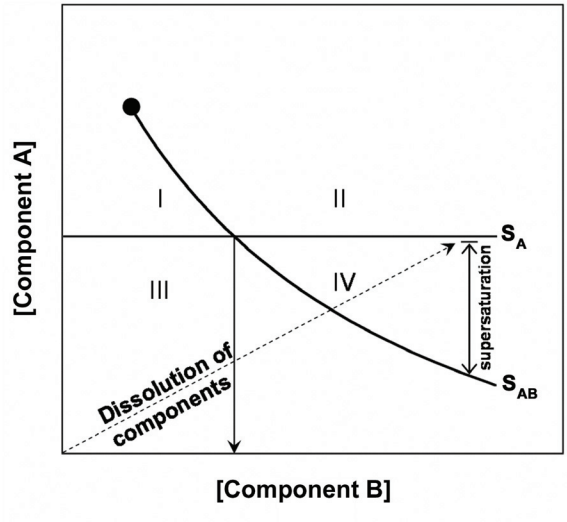

Figure 7.7: Solubility of cocrystal (S_{AB}) as a function of coformer concentration (B). Solubility of pure A is assumed to be independent of coformer concentration. Eutectic concentration and regions of supersaturation and undersaturation are indicated. Cocrystal solubility in pure solvent is represented by a filled circle. Dashed arrow indicates component concentrations due to unequal dissolution rates of components.

Generally one expects the amount of moisture uptake to control the transformation rate based on its temporal and spatial distribution. Low levels of hygroscopic additive and low moisture uptake will have the effect of reducing the regions of moisture sorption. Consequently, small domains of supersaturation can develop in a liquid phase that is not uniformly distributed throughout the sample leading to isolated regions of cocrystal formation. In this case high supersaturation is initially achieved and the transformation rate to cocrystal is initially fast, but the rate will slow or even level off before extensive conversion. This mechanism explains the slower rate and lesser extent of transformation to CBZ-NCT cocrystal at the lower fructose composition (10%) and 75%RH. Also the CBZ-NCT formation for PVP samples at low RH (43 and 63%) increased in the first 24 hours and had little change for the following 5 days.

CBZ/NCT/fructose exhibits faster and more extensive cocrystal formation at 20 and 50% fructose and 85% RH compared to the 10% fructose and 75%RH sample. These results clearly indicate that for low fructose composition at low RH, the transformation is occurring with relatively low moisture uptake where solute transport tends to be limited to small domains of liquid phase. Faster transformation rates with higher fraction of deliquescent additive at RH above DRH were also observed for CBZ/NCT/sucrose. High levels of moisture sorption allow for greater exposure of components to the crystallization medium and to larger extent of cocrystal formation during the initial time period, provided the kinetics and distribution of moisture sorption maintain adequate supersaturation for cocrystal formation. Moisture uptake levels are associated with the hygroscopic nature of the mixture components, the amount of hygroscopic or deliquescent additive, and the RH.

The mechanisms for cocrystal formation reported here are valuable to design stable formulations and predict conditions that will result in cocrystal formation. The amount of hygroscopic additive required to prevent or reverse the transformation to cocrystal can in principle be estimated if one knows the moisture sorption of the mixture at a given composition, temperature and RH, and the eutectic concentrations in the sorbed moisture. For example, the coformer eutectic concentration in water at which the solubility of the CBZ-NCT cocrystal is equal to the solubility of CBZ dihydrate is around 0.8m. If as a first approximation it is assumed that additives do not change eutectic concentrations, levels of moisture sorption that lead to NCT concentrations above 0.8m will favor cocrystal formation and below would favor CBZ(D) and destabilization of the cocrystal (Figure 7.7 regions II/IV stable and I/III unstable).[14] This behavior was also shown for several PVP solutions where $[NCT]_{eu}$ was high for K90 and less CBZ-NCT formation occurred in these samples (Table 7.2). In comparison, PVP K12 had a lower $[NCT]_{eu}$ and a higher level of cocrystal formation.

Moisture sorption and deliquescence of multiple component solid systems are a complex function of phase composition, relative humidity, and temperature.[27-29] The study presented here has focused on identifying the mechanism by which deliquescence induces cocrystal formation and the factors that affect transformation rates.

7.3. CONCLUSIONS

This work demonstrates that moisture sorption by hygroscopic additives can lead to the formation of cocrystals in physical mixtures. Carbamazepine-nicotinamide cocrystal formed from component mixtures in the presence of PVP and deliquescent sugars. Carbamazepine hydrate was not observed under these conditions. The mechanism of cocrystal formation involved moisture uptake, dissolution of components, and cocrystal nucleation and growth. Microscopic studies of these mixtures showed the growth of CBZ-NCT from aqueous solutions produced by moisture sorption of PVP and sucrose. Dissolution can lead to solution compositions above the eutectic concentration where cocrystal is the stable phase. Solutions with hygroscopic additives can also effect the eutectic concentrations and stability of the cocrystals as was demonstrated for CBZ-NCT in PVP solutions. These findings have important implications for the selection of additives in pharmaceutical formulations and establishing conditions where cocrystal is stable.

7.4. REFERENCES

(1) Zografi, G.; Grandolfi, G. P.; Kontny, M. J.; Mendenhall, D. W., Prediction of moisture transfer in mixtures of solids: Transfer via the vapor phase. *International Journal of Pharmaceutics* **1988,** 42, (1-3), 77-88.

(2) Kaneniwa, N.; Yamaguchi, T.; Watari, N.; Otsuka, M., Hygroscopicity of carbamazepine crystalline powders. *Yakugaku Zasshi* **1984,** 104, (2), 184-190.

(3) Salameh, A. K.; Taylor, L. S., Physical Stability of Crystal Hydrates and their Anhydrates in the Presence of Excipients. *J. Pharm. Sci.* **2006,** 95, (2), 446-461.

(4) Kesavan, J. G.; Peck, G. E., Solid-State Stability of Theophylline Anhydrous in Theophylline Anhydrous-Polyvinylpyrrolidone Physical Mixtures. *Drug Dev. Ind. Pharm.* **1996,** 22, (3), 189-199.

(5) Airaksinen, S.; Karjalainen, M.; Kivikero, N.; Westermarck, S.; Shevchenko, A.; Rantanen, J.; Yliruusi, J., Excipient Selection can Significantly Affect Solid-State Phase Transformation in Formulation During Wet Granulation. *AAPS PharmSciTech.* **2005,** 6, (2), E311-E322.

(6) Otsuka, M.; Matsuda, Y., The Effect of Humidity on Hydration Kinetics of Mixtures of Nitrofurantoin Anhydride and Diluents. *Chem. Pharm. Bull.* **1994,** 42, (1), 156-159.

(7) Pirttimaki, J.; Laine, E., The transformation of anhydrate and hydrate forms of caffeine at 100-percent RH and 0-percent RH. *Eur. J. Pharm. Sci.* **1994,** 1, (4), 203-208.

(8) Yoshinari, Y.; Forbes, R. T.; York, P.; Kawashima, Y., Moisture induced polymorphic transition of mannitol and its morphological transformation. *Int. J. Pharm.* **2002,** 247, (1-2), 69-77.

(9) Andronis, V.; Yoshioka, M.; Zografi, G., Effects of Sorbed Water on the Crystallization of Indomethacinfrom the Amorphous State. *J. Pharm. Sci.* **1997,** 86, (3), 346-351.

(10) Tong, P.; Zografi, G., Effects of water vapor absorption on the physical and chemical stability of amorphous sodium indomethacin *AAPS PharmSciTech.* **2004,** 5, (2), Art. No. 26.

(11) Nehm, S. J.; Rodríguez-Spong, B.; Rodríguez-Hornedo, N., Phase solubility diagrams of cocrystals are explained by solubility product and solution complexation. *Cryst. Growth Des.* **2006,** 6, (2), 592-600.

(12) Rodríguez-Hornedo, N.; Nehm, S. J.; Jayasankar, A., Cocrystals: Design, Properties and Formation Mechanisms. In *Encyclopedia of Pharmaceutical Technology*, 2nd ed.; Swarbrick, J., Ed. Marcel Dekker: New York, 2006; pp 615-635.

(13) Rodríguez-Hornedo, N.; Nehm, S. J.; Seefeldt, K. F.; Pagán-Torres, Y.; Falkiewicz, C. J., Reaction Crystallization of Pharmaceutical Molecular Complexes. *Mol. Pharm.* **2006,** 3, (3), 362-367.

(14) Jayasankar, A.; Nehm, S. J.; Rodríguez-Hornedo, N., The Use of Raman Spectroscopy for Real-Time Monitoring of Cocrystal Formation During Wet Granulation. *AAPS J.* **2006**.

(15) Hancock, B. C.; Zografi, G., The Relationship Between the Glass Transition Temperature and the Water Content of Amorphous Pharmaceutical Solids. *Pharmaceutical Research* **1994,** 11, 471-477.

(16) Allen, F. H., The Cambridge Structural Database: a quarter of a million crystal structures and rising. *Acta Crystallographica* **2002,** B58, 380-388.

(17) Porter III, W. W.; Elie, S. C.; Matzger, A. J., Polymorphism in Carbamazepine Cocrystals. *Cryst. Growth Des.* **2008,** 8, (1), 14-16.

(18) Rodríguez-Hornedo, N.; Nehm, S. J.; Jayasankar, A., Process Analytical Technologies to Analyze and Control Cocrystallization. *Am. Pharm. Rev.* **2007***,* 10, 46-55.

(19) O'Brien, F. E. M., The Control of Humidity by Saturated Salt Solutions. *J. Sci. Instrum.* **1948,** 25, 73-76.

(20) Jayasankar, A.; Good, D. J.; Rodríguez-Hornedo, N., Mechanisms by which moisture generates cocrystals. *Molecular Pharmaceutics* **2007,** 4, 360-372.

(21) Tian, F.; Baldursdottir, S.; Rantanen, J., Effects of polymer additives on the crystallization of hydrates: A molecular-level modulation. *Molecular Pharmaceutics* **2009,** 6, (1), 202-210.

(22) Tian, F.; Rades, T.; Sandler, N., Visualizing solvent mediated phase transformation behavior of carbamazepine polymorphs by principal component analysis. *AAPS PharmSciTech* **2008,** 9, (2), 390-394.

(23) Tian, F.; Zhang, F.; Sandler, N.; Gordon, K. C.; McGoverin, C. M.; Strachan, C. J.; Saville, D. J.; Rades, T., Influence of sample characteristics on quantification of carbamazepine hydrate formation by X-ray powder diffraction and Raman spectroscopy. *European Journal of Pharmaceutics and Biopharmaceutics* **2007,** 66, (3), 466-474.

(24) Foroutan, M., Density dependence of the viscosity and excess volume of aqueous solutions of polyvinylpyrrolidone. *Acta Chimica Slovenica* **2006,** 53, (2), 219-222.

(25) Sadeghi, R.; Zafarani-Moattar, M. T., Thermodynamics of aqueous solutions of polyvinylpyrrolidone. *Journal of Chemical Thermodynamics* **2004,** 36, (8), 665-670.

(26) Swei, J.; Talbot, J. B., Viscosity Correlation for Aqueous Polyvinylpyrrolidone (PVP) Solutions. *Journal of Applied Polymer Science* **2003,** 90, (4), 1153-1155.

(27) Salcedo, D., Equilibrium Phase Diagrams of Aqueous Mixtures of Malonic Acid and Sulfate/Ammonium Salts. *J. Phys. Chem. A* **2006,** 110, (44), 12158-12165.

(28) Brooks, S. D.; Wise, M. E.; Cushing, M.; Tolbert, M. A., Deliquescence Behavior of Organic/Ammonium Sulfate Aerosol. *Geophys. Res. Lett.* **2002,** 29, (19), Art. No. 1917.

(29) Wexler, A. S., Second-Generation Inorganic Aerosol Model. *Atmos. Environ.* **1991,** 25A, (12), 2731-2748.

7.5. APPENDIX

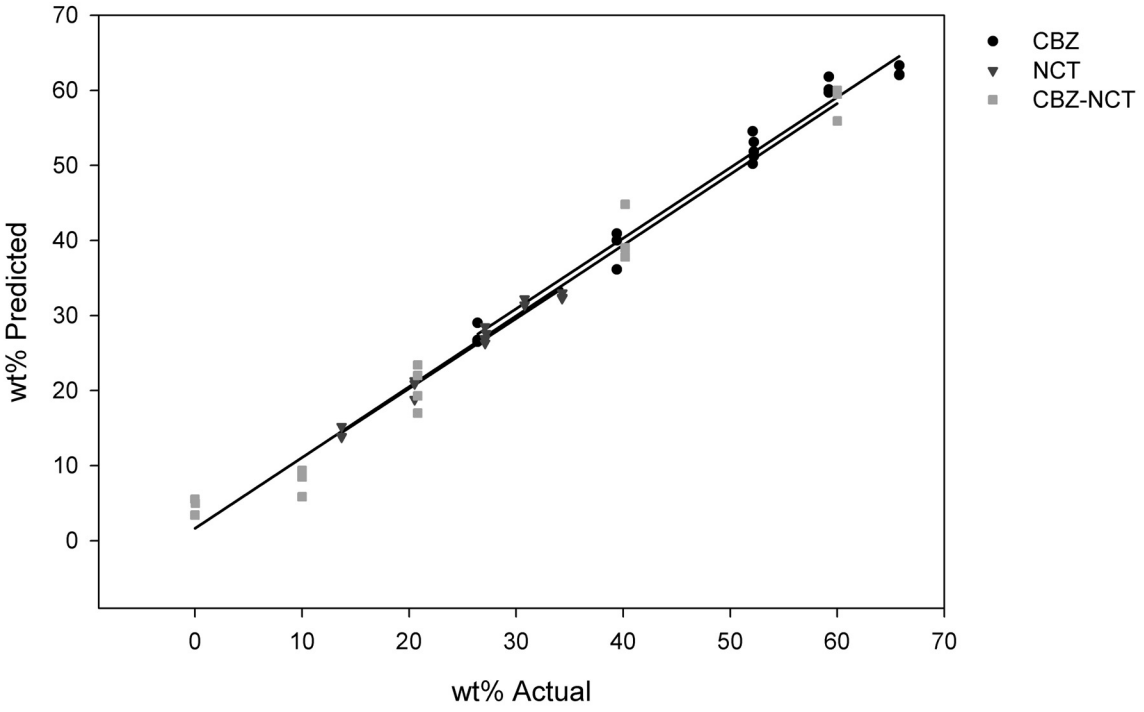

Figure 7.8: Infrared spectroscopy validation data set for Quant2 calibration. CBZ-NCT and component wt% predicted against observed values.

CHAPTER 8

CONCLUSIONS AND FUTURE WORK

This dissertation has focused on the thermodynamic stability and solubility of pharmaceutical cocrystals. The specific goals of this dissertation were to (i) develop methods to measure the thermodynamic solubility of metastable cocrystals, (ii) provide models that describe the equilibrium phase behavior of cocrystals based on component and cocrystal properties, (iii) explain the effect of temperature on cocrystal thermodynamic stability, (iv) estimate solubility and stability for different solvents based on component activity coefficients and measured cocrystal solubility in one solvent, and (v) identify mechanisms by which hygroscopic additives affect the stability of mixtures of solid cocrystal components.

A primary interest in pharmaceutical cocrystals is to improve drug solubility and dissolution kinetics and thereby increase drug absorption and bioavailability. Directly measuring the thermodynamic solubility of many cocrystals may be difficult as their high solubility can lead to supersaturation and subsequent phase transformations to less soluble forms. The work presented in this thesis shows that cocrystal eutectic points are

thermodynamically stable and allow for the measurement of cocrystal solubility and stability relative to their components.

For a three-component system (components A and B and solution) at constant temperature and pressure, any solution composition that contains two solid phases in equilibrium with solution is a eutectic point (Gibbs phase rule). Methods were developed to measure cocrystal eutectic points (i.e. isothermal invariant point) where a solution is in equilibrium with cocrystal and another solid phase (cocrystal component or component solvate, different stoichiometry cocrystal, cocrystal solvate). At the eutectic both solid phases are equally stable and for a 1:1 cocrystal these solid phases at the eutectic have the same solubility.

Methods for analysis of eutectic points and cocrystal solubility were presented for carbamazepine, theophylline, and caffeine cocrystals in four solvents. Fundamental models were established to calculate the equilibrium constants including the solubility product (K_{sp}) and solubilization from these eutectic measurements. The advantage of these methods is that they are accessible and reproducible and they correspond to a thermodynamic equilibrium that is a reference point for describing solution phase behavior. For cocrystals of the same drug, it was shown that the solubility of the cocrystal is proportional to the eutectic coformer concentration. This is because a higher coformer concentration is required to achieve thermodynamic stability between the cocrystal and drug phases. For carbamazepine cocrystals it was shown that more soluble

cocrystals had high eutectic coformer concentrations and were comprised of more soluble coformers.

The contributions of fusion enthalpy and melting temperatures of several cocrystals were compared to the solubility calculated from measured eutectic points. These correlations showed reasonable trends for the organic solvents similar to those described in the literature for ideal solubilities of single component solids. However, aqueous cocrystal solubility values showed considerable deviations from the ideal solubility behavior based on the contributions of crystallinity alone. For this small series of cocrystals solvent-solute interactions, particularly in water, were dominant relative to the ideal solubility estimated from fusion of the crystal lattice.

The solubility of the carbamazepine cocrystals studied was proportional to their component solubilities. These correlations between the solubility of a cocrystal and its pure components do not account for changes in the lattice energy, which likely will cause deviation of these solubility trends. Understanding both the solid-state and solution chemistry of cocrystals is important toward expanding cocrystal-solubility relationships. Future considerations of cocrystal solubility should seek to combine the observed solubility trends and solution models with the contribution of the crystal lattice energy.

A eutectic constant (K_{eu}) was established to extend the utility of cocrystal eutectic concentrations toward describing cocrystal solubility and stability. K_{eu} is the ratio of cocrystal component activities at the eutectic. K_{eu} values are fundamental indicators of

phase behavior and are shown to be a function of the solubility ratio (α) of cocrystal and drug in pure solvent. K_{eu} is shown to depend on solution chemistry including i) solvent, ii) complexation, and iii) ionization, as does the cocrystal solubility. The eutectic solution excess of a cocrystal component is controlled by the relative solubility of the cocrystal and component in pure solvent and was established from the analysis of more than forty observed and predicted K_{eu} values that showed good agreement. When the molecular structure and properties of the components differ it is the solubility of the cocrystal and its components (drug and coformer) that determine the solution eutectic composition. Differences in cocrystal stoichiometry as well as solubility of the components due to ionization and complexation are critical. Therefore in the case of cocrystals the solution composition and stability can be altered by solvent selection. It is indicated that the description of cocrystal solubility using K_{eu} and K_{sp} values greatly improves the ability to discern and compare the true solubility of cocrystals.

Future work can focus on estimating the nature and extend of solubilization or complexation between cocrystal components based on deviations between the observed cocrystal to drug solubility ratio and the predicted ratio from the eutectic concentrations. Additionally it will be useful to apply and expand the eutectic concentrations to predict the solution phase behavior for systems were the cocrystal solubility does not decrease with higher coformer concentrations because of high levels of drug solubilization in concentrated coformer solutions.

Thermodynamic relations were developed that model the temperature dependence of the eutectic concentrations to predict the stability of cocrystals in solutions and suspensions at different temperatures. K_{eu} dependence on temperature is determined by the difference in the enthalpy of solution between the component and cocrystal phases. When there is no difference between cocrystal and component enthalpies of solution K_{eu} will be constant with temperature. K_{eu} and the cocrystal solubility ratio were shown to change with temperature when there were differences between the cocrystal and component enthalpies of solution. Enthalpies of solution were analyzed for sulfamethazine-benzoic acid as well as carbamazepine cocrystals of nicotinamide, isonicotinamide and 3-nitrobenzamide. It was observed that the temperature dependence of the eutectic concentration was predicted from the heats of solution of the cocrystal and components and for carbamazepine-nicotinamide as well as sulfamethazine-benzoic acid in water that K_{eu} decreased with temperature. For carbamazepine-nicotinamide the K_{eu} became closer to the observed composition ratio of binary (without solvent) eutectic for the lowest melting composition of the two components. This observation would be interesting to explore for more systems, because it could enable prediction of temperature dependent solution behavior from thermal melt behavior of the cocrystal components.

The observed change in K_{eu} with temperature was also solvent specific. Carbamazepine-nicotinamide had a significant change in the cocrystal stability region in water and no change in ethanol and ethyl acetate. This is because the cocrystal and component enthalpies of solution were not equal in water, but were equal in the other

solvents. K_{eu} was shown to be independent of temperature when the difference between the cocrystal and component enthalpies of solution was zero. The cocrystal component at the eutectic in water was CBZ dihydrate and for the organics it was anhydrous CBZ III.

Both temperature and solvent considerations are critical to the design of cocrystals synthesis and screening process. Also it has been demonstrated that racemic compounds also have temperature dependent eutectic concentrations, however their behavior is not solvent (achiral) specific. Future work that expands on the observed temperature dependence for both racemic compounds and cocrystals based on their enthalpies of mixing/solvation, fusion, and solution could improve the understanding of the eutectic behavior of cocrystals and their relations to the physicochemical properties of the components and solvent.

The quantification of activity coefficients, based on ideal solution behavior, was carried out to predict solubility and stability in other solvents since the cocrystal chemical potential is independent of solvent. The predicted stability of carbamazepine-saccharin in four different solvent systems corresponded to the observed stability. The success of synthesizing cocrystals is critically dependent on the chemical potential of the cocrystal relative to the components. Cocrystal will be thermodynamically stable at some solution composition if the solubility product ($a_A a_B$ for 1:1 cocrystal AB) of the cocrystal is lower than the product of the component activities. The cocrystal component activity coefficients specific to a cocrystal-solvent system determine whether the cocrystal is

more soluble than either component in pure solvent (incongruently saturating). For carbamazepine-saccharin, the component activity coefficients account for its instability in water while its stable in ethanol, ethyl acetate and isopropanol.

The physical and chemical stability of pharmaceutical solids is critically dependent on the presence of water. Solid phase transformations affect the stability, safety, purity, and efficacy of the drug substance and drug product. Pharmaceutical drug products may come into contact with water during production and formulation or at any point through exposure to humid environmental conditions. Drug products that incorporate materials containing water have the potential to transfer it to other components whose stability is affected by water. Fundamental knowledge of additive interactions with moisture and comprehensive study of solubility behavior of cocrystals and their components is a prerequisite for the development of useful drug products.

Carbamazepine-nicotinamide formed in mixtures with deliquescent (sucrose and fructose) additives even when carbamazepine hydrate formation was possible. Carbamazepine-nicotinamide was also formed in mixtures with polyvinylpyrrolidone (PVP), which is a common pharmaceutical additive that is hygroscopic. The mechanisms responsible for cocrystal formation in cocrystal component mixtures with hygroscopic or deliquescent additives were identified to involve moisture uptake, dissolution of cocrystal reactants, cocrystal nucleation and growth. These mechanisms are important to design formulations and predict conditions that control cocrystal transformations. Cocrystal

solubility dependence on aqueous solution composition and chemistry are good predictors of cocrystal formation in the presence of hygroscopic additives. It is clear from the results that cocrystal formation mechanisms can be solution mediated in the presence of deliquescent or hygroscopic additives or components. The mechanism and potential to influence cocrystal stability has yet to be determined for hygroscopic additives that sorb low levels of moisture, which do not readily form a solution phase. This behavior could be studied at the molecular level to understand the interaction of water with hygroscopic additives and the potential transfer of water to cocrystal components. The equilibrium state of these transformations in the presence of hygroscopic additives could also be confirmed using both cocrystal and components as starting phase(s).

Many cocrystals presented in this work have a higher solubility than one of their components (often drug) and in these cases transformation of cocrystal to a less soluble component can occur. Transformation of cocrystal to a less soluble form can occur until all cocrystal transforms or the eutectic composition is reached. It is beneficial to explore methods to slow transformation kinetics of highly soluble cocrystals that are unstable in solution. The inhibition of solution transformations could be achieved using additives, which prevent the nucleation or growth of the crystalline component(s) thereby maintaining supersaturation for longer periods. This area will be important for transferring the high thermodynamic solubility of incongruently saturating cocrystals to

achieve improved *in vivo* dissolution and performance of cocrystals. Both the kinetic and thermodynamic effects of additives on the cocrystal solubility and dissolution will need to be characterized to optimize cocrystal formulations. Kinetic solubility measurements do not typically serve as good indicators of the solubility of unstable cocrystals because transformations can occur. Eutectic point measurements are indicators of the true solubility of a cocrystal, and can guide cocrystal selection.